TECHNISCHE UNIVERSITÄT MÜNCHEN

Department Chemie

Lehrstuhl für Biotechnologie

Analysis and Modulation of the disease-related Hsp90 machinery

Sandrine Carolina Stiegler

Vollständiger Abdruck der von der Fakultät für Chemie der Technischen Universität München zur Erlangung des akademischen Grades eines

Doktors der Naturwissenschaften (Dr. rer. nat.)

genehmigten Dissertation.

Vorsitzender: Univ.-Prof. Dr. Matthias Feige

Prüfer der Dissertation:

1. Univ.-Prof. Dr. Johannes Buchner
2. Univ.-Prof. Dr. Michael Sattler

Die Dissertation wurde am 3. Mai 2016 bei der Technischen Universität München eingereicht und durch die Fakultät für Chemie am 10. Juni 2016 angenommen.

Summary

This work addresses the disease-related Hsp90 machinery in terms of its modulation by small molecules and mutations. A compound library was screened in order to identify potential new modulators of the interplay between Hsp90 and the co-chaperone Aha1. Aha1 is one prominent co-chaperone that accelerates the progression of Hsp90 through its conformational cycle. Small molecules that inhibit this interplay are promising as new strategies in the treatment of diseases involving Hsp90. As one of the most crucial chaperones in the cell, Hsp90 plays a central role in a variety of cellular processes and its client proteins, such as kinases, are often involved in cancer. A FRET-based screen identified six modulators of the Hsp90/Aha1 interplay, three of them with inhibiting function, three with activatory function. All modulators displayed a micromolar affinity to Hsp90 in the presence of Aha1 and proved efficient not only *in vitro* but also *in vivo*. The maturation of Hsp90 clients, namely the glucocorticoid and mineralocorticoid steroid hormone receptors, was altered by the different compounds, with each giving rise to a unique modulation profile.

The most potent inhibitor 26C8 almost completely abolished the stimulatory potential of Aha1 on Hsp90. Interestingly, this inhibitor did not prevent binding of Aha1 to Hsp90. The binding of Aha1 to Hsp90 in the presence of 26C8 resulted in a highly inefficient complex, in which Hsp90 could no longer be accelerated through its cycle. NMR data suggested potential binding sites for 26C8 at the Hsp90 NTD and MD, which are crucial points of interaction with ATP and Aha1. The binding affinity of ATP to Hsp90 is lowered by 26C8 and this effect is further reinforced in the presence of Aha1. *In vivo*, this results in a highly decreased client processing activity. Degradation of the cystic fibrosis transmembrane receptor, involved in the inherited disease cystic fibrosis, could be slowed down by the inhibitor 26C8. All in all, the identification of modulators for the specific interplay of Hsp90 and Aha1 demonstrates that this could be a promising approach in identifying new, more target-oriented small molecules for a better treatment of diseases.

In the second part of this work, an evolutionary point of view on Hsp90 was taken. Hsp90 from organisms that evolved differently throughout evolution, was analysed bioinformatically. Hsp90 from rather 'unusual' organisms, a thermophilic fungus and a eukaryotic parasite, were analysed. Thermophilic Hsp90 was chosen because of its potential higher stability and eligibility for crystallisation attempts. Hsp90 from a eukaryotic parasite represented a minimal Hsp90 system to provide new insights in basic components of the Hsp90 machinery in lower developed organisms.

Finally, it was addressed how mutations in the ATP binding site of Hsp90 shape its functionality. Phenylalanine residues in the lid and in the ATP binding pocket were mutated to tryptophans. The introduced tryptophans served as photometric probes to further address the mechanism of ATP binding to Hsp90. The *in vitro* ATPase activity of Hsp90 was stimulated by these mutations. The generated lid mutant showed a higher nucleotide affinity compared to wild-type Hsp90. *In vivo*, the mutants were viable and did not show a growth defect at physiological temperatures.

Contents

1 Introduction **1**
- 1.1 Molecular chaperones . . . 1
- 1.2 The molecular chaperone Hsp90 . . . 2
  - 1.2.1 Hsp90 structure . . . 4
- 1.3 Hsp90 co-chaperones . . . 9
  - 1.3.1 The Hsp90 co-chaperone Aha1 . . . 10
  - 1.3.2 Hop/Sti1 . . . 13
  - 1.3.3 p23/Sba1 . . . 14
  - 1.3.4 Sgt1 . . . 15
  - 1.3.5 Other Hsp90 co-chaperones . . . 16
- 1.4 Hsp90 and disease . . . 19
  - 1.4.1 Hsp90 and cancer . . . 19
  - 1.4.2 Cystic Fibrosis . . . 22
- 1.5 Hsp90 inhibitors . . . 23
- 1.6 Objectives . . . 25

2 Results and Conclusions **27**
- 2.1 Hsp90/Aha1 modulators . . . 27
  - 2.1.1 FRET-based screening of a compound library . . . 27
  - 2.1.2 Influence on the ATPase activity of Hsp90 . . . 29
  - 2.1.3 NMR data on the 26C8 inhibitor . . . 35
  - 2.1.4 Effect on ATP binding to Hsp90 . . . 37
  - 2.1.5 Modulator influence on Hsp90/Aha1 complex formation . . . 38
  - 2.1.6 Derivatives of the modulator 26C8 . . . 41
  - 2.1.7 Effects on client maturation . . . 43
  - 2.1.8 Modulation of the CFTR degradation . . . 47
  - 2.1.9 Conclusions . . . 49
- 2.2 'The new 90s' . . . 51
  - 2.2.1 Phylogeny of Hsp90 from different organisms . . . 51
  - 2.2.2 Comparison of different Hsp90 systems . . . 52

2.2.3 Characterisation of thermophilic Hsp90 and Aha1 56
2.2.4 Outlook 63
2.3 Characterisation of Hsp90 tryptophan mutants 65
2.3.1 ATPase activity of Hsp90 Trp mutants 66
2.3.2 Co-chaperone effects 68
2.3.3 Nucleotide affinity of the Trp mutants 70
2.3.4 Trp fluorescence 72
2.3.5 Stopped flow 74
2.3.6 Growth effects of Trp mutants 76
2.3.7 Outlook 77

3 Material and Methods **79**
3.1 Material 79
3.1.1 Media 81
3.1.2 Buffers 83
3.1.3 Strains 84
3.1.4 Plasmids 84
3.1.5 Oligonucleotides 85
3.1.6 Equipment 86
3.1.7 Computer Software 87
3.2 Methods 89
3.2.1 Molecular Biology 89
3.2.2 Site Directed Mutagenesis 90
3.2.3 DNA sequence analysis 91
3.3 Growth and storage of *E. coli* cells 91
3.4 Growth of *S. cerevisiae* 91
3.5 Preparation of competent cells 92
3.5.1 Transformation of *E. coli* cells 92
3.6 Transformation of *S. cerevisiae cells* 92
3.7 Protein Expression and Purification 93
3.7.1 Protein Expression and Cell disruption 93
3.7.2 Protein Purification 93
3.8 Protein Analysis 95
3.8.1 Discontinuous SDS-PAGE 95
3.8.2 Coomassie Staining of SDS gels 96
3.8.3 Immunoblotting (Western Blot) 96
3.8.4 Protein Labelling 98
3.8.5 Analytical Ultracentrifugation 99
3.9 Spectroscopy 100
3.9.1 Circular dichroism 100
3.9.2 Thermal Shift Assay 101
3.9.3 UV absorption spectroscopy 102
3.9.4 ATPase Activity Assay 102
3.9.5 Malachite Green Assay 104
3.10 Fluorescence spectroscopy 104

3.10.1 Fluorescence Resonance Energy Transfer (FRET) 105
3.10.2 Screening for modulators of the Hsp90/Aha1 interaction 106
3.11 Chaperone Assay 107
3.12 Isothermal calorimetry 107
3.13 Surface Plasmon Resonance 108
3.14 *In vivo* Assays 108
3.14.1 Plasmid shuffling 108
3.14.2 β-Galactosidase Assay 109
3.14.3 CFTR Degradation Assay 109

Bibliography **141**

CHAPTER 1

Introduction

1.1 Molecular chaperones

Almost all biological processes in a cell involve the function of proteins. Proteins are one of the most versatile classes of biomolecules and crucial for cellular function. A human cell contains an estimated number of 20,000 to 25,000 different proteins [Kim et al., 2013]. Due to their structural complexity, maintenance of correct protein conformation and assembly is pivotal for a living cell. Given a crowded environment of a cell with protein concentrations of around 300-400 mg/ml [Zimmerman and Trach, 1991], the spontaneous folding of proteins can be error-prone and inefficient [Hoffmann et al., 2010]. Therefore, molecular chaperones assist the folding and transport of various proteins. The concept of molecular chaperones was introduced in 1978 and stimulated rethinking of protein assembly process [Laskey et al., 1978, Ellis and Hemmingsen, 1989]. The concept of spontaneous self-assembly had to be expanded by an assembly which is assisted by molecular chaperones. Per definition, a chaperone is *'a protein that binds to and stabilises an otherwise unstable conformer of another protein - and by controlled binding and release of the substrate protein, facilitates its correct fate of vivo: be it folding, oligomeric assembly, transport of a particular subcellular compartment, or controlled switching between active/inactive conformations'* [Hendrick and Hartl, 1993]. More general, molecular chaperones allow for efficient folding and are an important mediator of protein homeostasis. Partially-folded, newly synthesised proteins expose aggregation-

prone hydrophobic surfaces, normally buried in the core of a fully folded protein [Eichner and Radford, 2011]. The chaperone machinery efficiently counteracts the tendency of non-native proteins to aggregate [Agashe and Hartl, 2000, Walter and Buchner, 2002].
Molecular chaperones can be divided into two major groups: early acting chaperones (like trigger factor or Hsp70) that process the nascent chain, and downstream chaperones, like chaperonins, acting on later folding-stages [Langer et al., 1992, Frydman et al., 1994, Mayer, 2013]. The bacterial trigger factor binds to ribosomes in a 1:1 stochiometry, thereby stabilising short nascent chains [Hesterkamp et al., 1996, Hoffmann et al., 2010]. In the eukaryotic cytosol, this function is carried out by the so called nascent chain-associated complex (NAC) [Beatrix et al., 2000]. Another chaperone of early stages in protein folding is Hsp70 [Bukau et al., 2006]. In bacteria and eukaryotes, it can interact with proteins in, both, a co- and post-translational manner [Sakahira and Nagata, 2002, Mayer and Bukau, 2005, Hartl et al., 2011]. Yeasts and higher eukaryotes possess a variety of specialised Hsp70 homologues to fulfill its complex function in protein folding and regulation [Daugaard et al., 2007].
The name heat shock protein (Hsp) is derived from the initial finding that these proteins are upregulated under heat stress, but also upon other cellular stress conditions, like oxidative stress [Gething and Sambrook, 1992, Ashburner and Bonner, 1979, Wang et al., 2013]. Under stress conditions, the concentration of aggregation-prone proteins increases. Thus, the cell seeks to prevent fatal protein aggregation with the upregulation of heat shock proteins [Tyedmers et al., 2010]. This large class of structurally unrelated proteins can be subdivided into six different groups, according to their molecular weight: small Hsps (sHsps), Hsp40, Hsp60 (chaperonins), Hsp70, Hsp90 and Hsp100. sHsps can function ATP-independently [Jakob et al., 1993], while the other Hsps act in an ATP-dependent manner [Kim et al., 2013]. Hsp70 acts together with the co-chaperone family of Hsp40 (also known as DnaJ) and nucleotide exchange factors (NEFs) [Kampinga and Craig, 2010]. Some proteins are not able to reach a fully folded state through interaction with the Hsp70 machinery. Thus, they are transferred to the Hsp60 or Hsp90 machinery which act on partially folded proteins [Southworth and Agard, 2011, Li and Buchner, 2012]. Steroid hormone receptors are a well-studied examples where the partially folded protein is transferred from the early acting Hsp70 by the co-chaperone Hop to the Hsp90 machinery [Picard, 2006, Taipale et al., 2010]. This in turn activates the receptor in order to fulfill its important cellular function.

1.2 The molecular chaperone Hsp90

Heat shock proteins (Hsps) are a group of molecular chaperones which are upregulated upon cellular stress. As a result, denaturation and aggregation of proteins can be prevented in order to maintain protein homeostasis [Nathan et al., 1997, Tyedmers et al.,

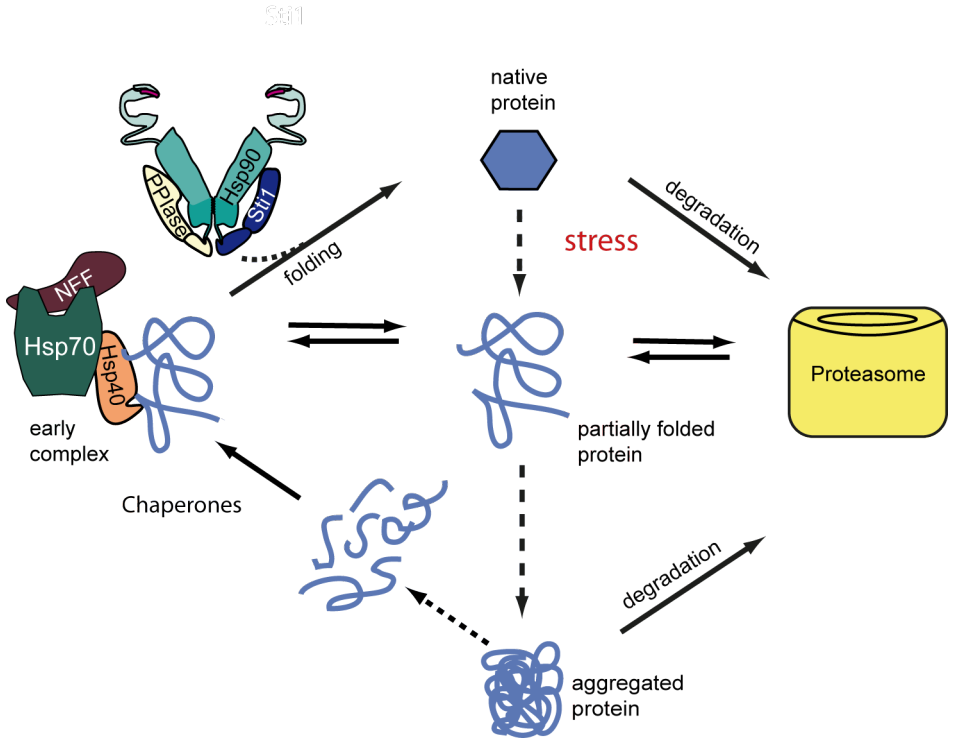

Figure 1.1: Interplay of Hsp70 and Hsp90 A native, functional protein can undergo structural changes due to changes in its cellular environment, e.g. stress conditions. Partially folded proteins are aggregation-prone and can be rescued by chaperone function from proteasomal degradation. Hsp70 does not only chaperone partially folded proteins, but also nascent chains. Together with several co-chaperones, like Hsp40 and NEF, it forms an early complex to stabilise unfolded or partially folded client proteins. Hsp90 acts in a later stage of the folding pathway, together with highly specialised co-chaperones. If a protein fails to be refolded to its native state, it can also be targeted for proteasomal degradation by chaperones.

2010]. However, even under non-stress-related conditions, Hsps carry out important functions for cellular maintenance. As one of the most abundant and evolutionary conserved molecular chaperones, the 90 kDa heat shock protein (Hsp90) plays a key role for cell survival, cell cycle control, cellular stress and hormone signalling [Taipale et al., 2010,Richter and Buchner, 2001]. The Hsp90 chaperone system is highly conserved and present from bacteria to man. To date, there are over hundreds of substrate proteins, termed clients, known to interact with Hsp90 (a regularly updated list of clients can be found at the Picard laboratory website: www.picard.ch/downloads/Hsp90interactors.pdf). It remains somewhat unclear what qualifies a protein for being an Hsp90 client since there is such a broad spectrum of functionally different client proteins. In general, Hsp90 typically interacts with folding intermediates at later folding stages [Jakob et al., 1995, Karagoez et al., 2014]. This is in contrast to other molecular chaperones, like i.e. the Hsp70 chaperone system which acts more on early folding stages of proteins, like nascent polypeptide chains [Bukau et al., 2006]. Hsp70 thereby recognises short hydrophobic motifs exposed in partially denatured or unfolded proteins (as depicted in

figure 1.1) [Rüdiger et al., 1997]. Despite intensive research, structurally common client motifs for Hsp90 client interaction have remained elusive. Since Hsp90's client proteins are highly diverse, it is proposed that a recognition motif per se does not exist. Instead, specificity for client recognition is thought to be mediated by the interplay between Hsp90, co-chaperones and other accessory factors [Taipale et al., 2010]. Each client is hence stabilised and activated by a defined subset of proteins.
The Hsp90 chaperone is not only crucial for client stabilisation but also for viability of a cell in essence. The presence of at least one of the Hsp90 gene family is essential for viability in human, yeast, *C. elegans* and Drosophila [Nathan et al., 1997, Van Der Straten et al., 1997, Yue et al., 1999, Birnby et al., 2000]. However, the bacterial homologue HtpG is typically nonessential [Bardwell and Craig, 1987, Versteeg et al., 1999]. Many eukaryotes feature multiple Hsp90 homologues, including mitochondrial (TRAP1), endoplasmatic reticulum (Grp94), and chloroplast-specific (Hsp90C) isoforms [Sorger and Pelham, 1987, Felts et al., 2000, Taipale et al., 2010, Johnson, 2012]. Cytosolic Hsp90 is the most abundant protein while Hsp90 can also be translocated to the nucleus upon stress and other stimuli [Pratt and Toft, 1997, Akner et al., 1992]. In humans, cytosolic Hsp90 exists as two isoforms, Hsp90α and Hsp90β [Csermely et al., 1998, Chen et al., 2005]. Hsp90β is constitutively expressed and generally more abundant in most tissues whilst Hspα is a stress-inducible form which is often highly overexpressed in cancer cells [Sreedhar et al., 2004, Yano et al., 1996]. In *S. cerevisiae* Hsp90, which displays a 60 % homology to human Hsp90, the cytosolic isoforms are referred to as Hsc82 and Hsp82 [Erkine et al., 1995]. All isoforms share a high degree of sequence similarity (97 % identical in *S. cerevisiae*) [Johnson, 2012], while Hsc82 is constitutively expressed and Hsp90 is the stress-inducible isoform [Erkine et al., 1995, Borkovich et al., 1989].

1.2.1 Hsp90 structure

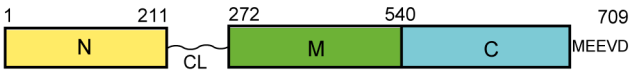

Figure 1.2: Domain structure of Hsp90. Hsp90 consists of three domains: The N-terminal domain (yellow) is connected to the middle domain (green) by a highly flexible, charged linker (CL). The C-terminal domain (blue) contains the MEEVD motif which is important for co-chaperone interaction. The size of each domain in amino acids is depicted and refers to yeast Hsp90.

Hsp90 is as a flexible homodimer consisting of three domains per monomer: The amino-terminal domain (NTD) contains the ATP binding site; the middle domain (MD) has been implicated in client protein and co-chaperone binding; and the carboxy-terminal domain (CTD) is the site of dimerisation [Pearl and Prodromou, 2006, Jackson, 2012, Li and Buchner, 2012]. The dimerisation constant of Hsp90 was found to be about 60 nM [Richter et al., 2001]. All three domains provide interaction sites for client and

co-chaperone interaction with Hsp90 and are depicted in figure 1.3. The *S. cerevisiae* Hsp90 domain structure with the corresponding numbers of residues is summarised in figure 1.2.

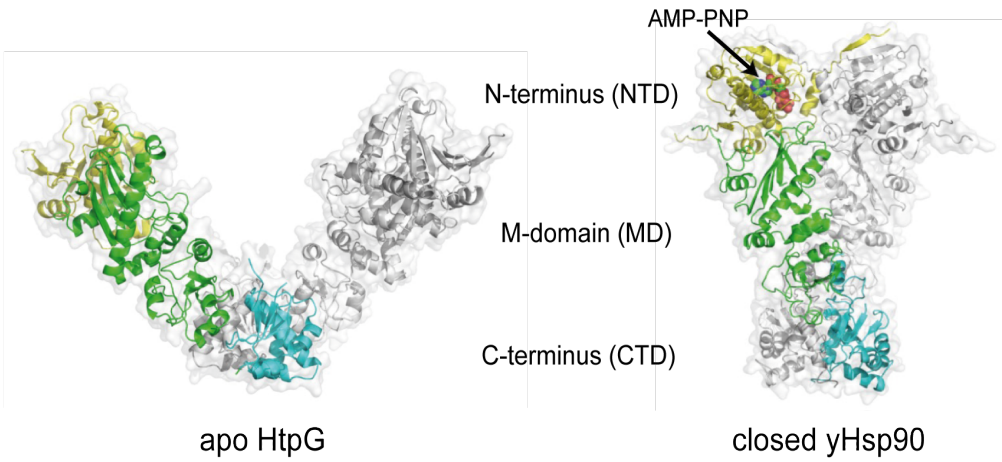

Figure 1.3: Conformations of Hsp90. Crystal structures of bacterial Hsp90 (HtpG) in an open conformation (left, PDB 2IOQ) and nucleotide-bound yeast Hsp90 in a closed conformation (right, PDB 2CG9). The three domains NTD (yellow), MD (green) and CTD (blue) are shown.

The N-terminal domain encompasses the nucleotide-binding site which is crucial for Hsp90's ATP-driven conformational cycle. This highly conserved ATP-binding domain belongs to the superfamily of gyrase, Hsp90, histidine kinase, MutL (GHKL) ATPases. This family is characterised by the use of the conformational energy of ATP-binding and hydrolysis to drive their regulating function in the cell and its members exhibit structurally similar ATP-binding sites [Dutta and Inouye, 2000]. Further, all GHKL family members have an integrated Bergerat ATP-binding pocket which does not display structural similarity to Hsp70 or other kinases [Flaherty et al., 1991,Bergerat et al., 1997]. The Bergerat fold in Hsp90's NTD was revealed by crystallisation (fig. 1.4) [Prodromou et al., 1997]. It is marked by an α/β sandwich structure in which three α helices form a layer over one formed by four β sheets [Prodromou et al., 1997, Dutta and Inouye, 2000]. Direct nucleotide interaction is mediated by Hsp90's amino acid residues Leu34, Asn37, Asp79, Asn92, Lys98, Gly121 and Phe124, whereas Asn37 coordinates a bound Mg^{2+} ion that, in turn, connects phosphates of the nucleotide to the protein through solvent-mediated hydrogen bonds [Prodromou et al., 1997, Dutta and Inouye, 2000].

The most unique feature of the Bergerat fold is a conserved stretch of residues, termed 'lid' motif (residues 100-121 in yeast Hsp90). The Hsp90 lid is a catalytically important loop structure within the N-domain, which closes over the nucleotide binding site upon ATP binding to Hsp90. It remains open in the ADP-bound state of Hsp90. Lid closure is thought to initiate the N-terminal dimerisation reaction [Prodromou et al., 2000, Ali et al.,

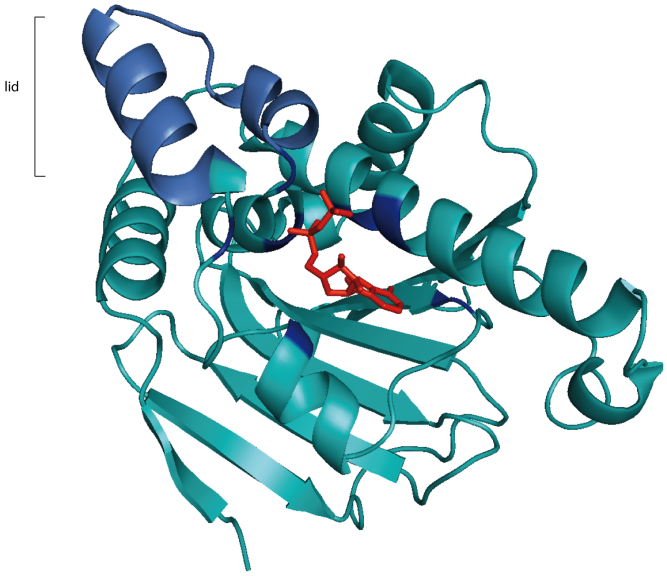

Figure 1.4: ATP binding site in Hsp90. The ATP binding pocket in Hsp90 (cyan) is depicted (pdb file 1am1). ATP (red) shows direct interaction with residues coloured in dark blue. Residues in lighter blue form the lid of Hsp90 (residues 100-121).

2006]. Upon dimerisation of the N-domains, the lid can swing 180 °C to fold over the nucleotide-binding pocket and stabilises the association of the N-domain. [Prodromou et al., 2000]. Thereby, the two N-domains interact with each other via a strand exchange mechanism exchanging the first β-strand between the N-domains. This interaction is crucial for the progression of the ATPase cycle. Removal of the lid was shown to result in an inactive but stimulatory promoter [Richter et al., 2006].

In eukaryotes, the NTD and M-domain are connected by a flexible, charged linker (CL) region which remains structurally undetermined to date. Its length can vary from 56 amino acids in yeast to 95 in the malaria causing parasite *Plasmodium falciparum*. In the *E. coli* Hsp90 homologue HtpG, NTD and MD are connected by a short amino acid stretch of 10 residues [Shiau et al., 2006, Tsutsumi et al., 2009]. Complete deletion of the CL was shown to be lethal in yeast, although most of the CL is dispensable [Hainzl et al., 2009, Tsutsumi et al., 2012]. Recent data underlines that the CL facilitates intramolecular movements between a highly flexible NTD and a state where NTD and MD are tightly connected [Jahn et al., 2014].

The ATPase activity of Hsp90 is rather slow with a rate of 1 ATP/min in yeast Hsp90 and 0.05 ATP/min in human Hsp90 [McLaughlin et al., 2002, Ali et al., 2006]. The isolated N-domain of Hsp90 does not display significant ATPase activity [Obermann et al., 1998]. Minimal ATPase activity requires a sophisticated interplay between N-terminal association and the catalytical loop with the conserved arginine 380 (yeast Hsp90) in the middle-domain. Finally, full ATPase can only be reached in the C-terminally dimerised full-length protein [Richter et al., 2001].

The M-domain is a crucial interaction site for some clients and co-chaperones of Hsp90. It contributes to the Hsp90 ATPase activity and provides the binding site for the co-chaperones Aha1 und p23/Sba1 [Meyer et al., 2004, Lotz et al., 2003, Ali et al., 2006]. The catalytical Arg380 in the yeast Hsp90 MD was identified as being crucial for ATP hydrolysis. It localises nearby the nucleotide-binding pocket and can therefore serve as acceptor of the γ-phosphate of the N-terminally bound ATP molecule [Meyer et al., 2004, Ali et al., 2006]. Mutation of this residue results in a loss of ATPase activity and viability in yeast [Meyer et al., 2003]. Recent studies propose Arg380 as being a stabiliser for the closed conformation of Hsp90, rather than being directly involved in ATP hydrolysis [Cunningham et al., 2012]. The M-domain was further found to provide an interface for substrate-recognition and binding [Vaughan et al., 2006, Park et al., 2011, Street et al., 2012]. The C-domain is the dimerisation site in Hsp90 [Minami et al., 1994]. Dimerisation is essential for Hsp90's chaperoning function in vivo [Wayne and Bolon, 2007]. Moreover, the C-domain plays an important role in co-chaperone interactions since it contains the highly conserved MEEVD (Met-Glu-Glu-Val-Asp) motif at its C-terminal end recognised by tetratricopeptide repeat (TPR) domain-containing co-chaperones [Young et al., 1998, Scheufler et al., 2000, Millson et al., 2008]. The function of Hsp90 involves large conformational changes which are highly dynamic. In the absence of nucleotide, Hsp90 was found to fluctuate between various conformational states, opened and closed [Mickler et al., 2009]. These states were proposed to coexist in a dynamic equilibrium [Southworth and Agard, 2008]. Nucleotide binding occurs to the open, V-shaped conformation of Hsp90 and is kinetically a very fast step [Hessling et al., 2009]. ATP-bound Hsp90 then undergoes a series of conformational rearrangements as described by Hessling *et al.* 2009 (fig. 1.5): The Hsp90 lid closes over the nucleotide pocket with the bound ATP, followed by the dimerisation of the two N-domains. These two states were described as intermediate stages I1 and I2, respectively. Both were described to occur at rather slow kinetic rates and reversibly [Hessling et al., 2009]. Transition from the I2 (closed 1) state then continues to reach a fully closed, twisted conformation (closed 2) where the N- and M-domains rearrange in each protomer to contact each other and form a highly compact state. This step occurs, again, slowly. Transition from closed 2 back to the closed 1 state was found to have to lowest kinetic rate konstant in the whole cycle, which suggested a very unlike transition from closed 2 to closed 1 [Hessling et al., 2009]. The closed 2 state is the ATP hydrolysis competent state. ATP hydrolysis is a fast step in the cycle leading to the return of Hsp90 back to its original open conformation and release of ADP + Pi. Altogether, the rate-limiting steps in the Hsp90 cycle are the conformational rearrangements, not ATP hydrolysis itself [Weikl et al., 2000, Richter et al., 2002, Hessling et al., 2009, Mickler et al., 2009]. Furthermore, the two ATP binding sites showed negative cooperativity, which means that nucleotides do not seem to bind independently to the two Hsp90 monomers [Ratzke et al., 2012a].

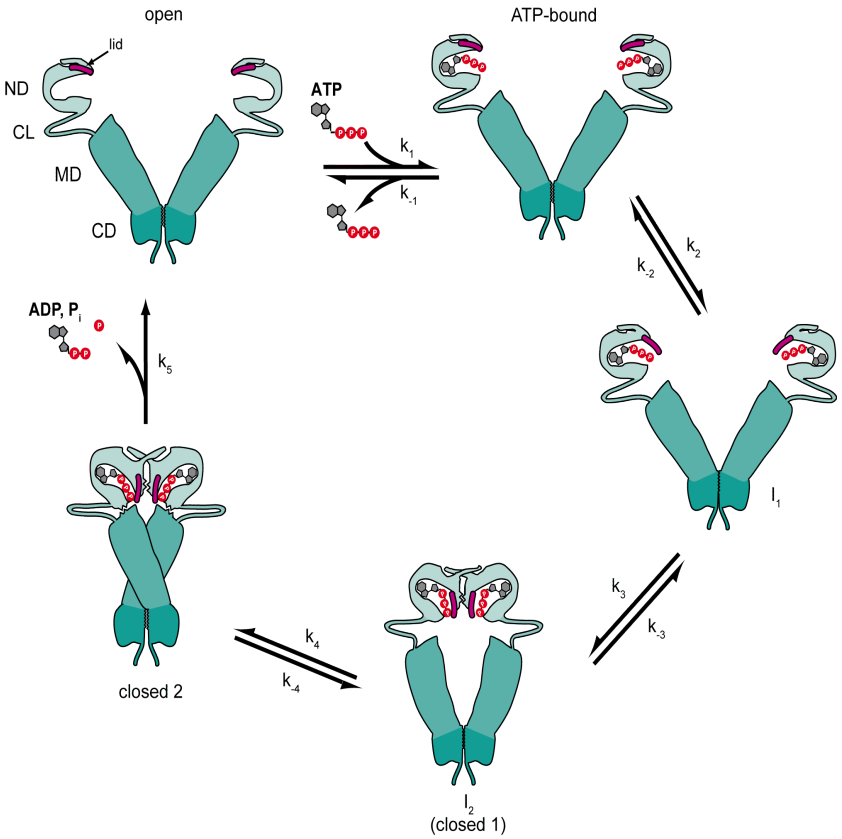

Figure 1.5: Conformational changes of Hsp90. Hsp90 fluctuates between open and closed states. Nucleotide binding induces large conformational changes, leading first to rearrangement of the N-domain (ND) and the lid closing over the nucleotide binding pocket (intermediate state 1, I1). Subsequently, Hsp90 closing is induced with firstly the N-domains making contact to eachother (closed 1, intermediate state I2), followed by complete closing of Hsp90 (closed 2 state). After hydrolysis of ATP to ADP+P_i, Hsp90 returns to the open conformation again. [Hessling et al., 2009]

The Hsp90 cycle can further be influenced by co-chaperones. Some of them, like Aha1, have a stimulatory effect, while others, like Sti1, are inhibitory factors in the progression of the cycle [Röhl et al., 2013]. These influences are thought to mediate a more effective way in chaperoning a client by Hsp90. The client itself can also mediate the progression of the cycle: The well-studied glucocorticoid receptor (GR) is able to slow down the hydrolysis rate of Hsp90 [Lorenz et al., 2014]. Thus, ATPase activity of Hsp90 can be regulated by both, co-chaperones and clients.

1.3 Hsp90 co-chaperones

In order to fulfill its complex cellular tasks, Hsp90 interacts with a variety of cofactors, the so called co-chaperones. Interestingly, co-chaperone support of Hsp90 has not been found in bacterial Hsp90 systems and seems to be eminent in eukaryotes. Co-chaperones are known to perform several tasks: They mediate Hsp90's specificity towards client proteins, recruit clients to Hsp90 or exhibit chaperoning function on their own (reviewed in [Röhl et al., 2013]). Recent studies suggest that each client might have a unique set of chaperones, providing a highly specific regulation despite Hsp90's variety of clients. Over 20 co-chaperones are known to interact with Hsp90. This interaction often involves mediation of Hsp90's ATPase activity which is used to stabilise it in a certain, co-chaperone-specific conformation. Generally, Hsp90 co-chaperones can be divided in two groups: TPR and non-TPR co-chaperones.

Table 1.1: Hsp90 co-chaperones

Co-chaperone	**Type**	**Effect on Hsp90 conformation**	**Literature**
Hop/Sti1	TPR	stabilises open state	Southworth *et al.* 2011, Schmid *et al.* 2012
p23/Sba1	CS	stabilises closed state	Ali *et al.* 2006, McLaughlin *et al.* 2006, Echtenkamp *et al.* 2011
Cdc37		stabilises open state	Vaughan *et al.* 2006, Boczek *et al.* 2015
Aha1		stabilises closed state	Panaretou *et al.* 2002, Meyer *et al.* 2003, Retzlaff *et al.* 2010, Li *et al.* 2013

Cpr6, Cyp40/Cpr7	TPR	unknown	Zuehlke *et al.* 2012, Li *et al.* 2013
PP5/Ppt1	TPR	unknown	Vaughan *et al.* 2008, Wandinger *et al.* 2006
Sgt1	TPR/CS	unknown	Lee 2004 *et al.*, Zhang *et al.* 2008
Cns1	TPR	unknown	Hainzl *et al.* 2004, Johnson *et al.* 2014
Tah1/Pih1	TPR	unknown	Zhao *et al.* 2005, Quinternet *et al.* 2015

Most of the known Hsp90 co-chaperones contain tetratricopeptide repeat (TPR) motifs. This 34-aa consensus sequence mediates binding to the C-terminal MEEVD motif in Hsp90. The TPR-containing co-chaperone Sgt1 provides an exception to this behaviour. Despite its TPR motif, it interacts with the Hsp90 NTD [Zhang et al., 2008]. Together with the similarly conserved EEVD motif of Hsp70, Hsp90's MEEVD motif serves as site of interaction for multiple TPR domains [Scheufler et al., 2000]. Some clients, like SHRs, first interact with the Hsp70 chaperone system, assisted by Hsp40. The client is then transferred by Hsp90 via an intermediate Hsp70-client-Hsp90 complex. For GR, the co-chaperone Hop/Sti1 was shown to mediate this client transfer from Hsp70 to Hsp90 [Pratt et al., 2006, Schmid et al., 2012]. This interplay between the Hsp70 and Hsp90 is also assisted by numerous other co-chaperones [Mayer and Le Breton, 2015]. Recruiting of the respective co-chaperones is dependent on the client. For the extensively studied maturation of GR, the co-chaperones Hop/Sti1, Cpr6 and p23/Sba1 were shown to play crucial, regulatory roles [Lorenz et al., 2014, Kirschke et al., 2014]. Another well-studied Hsp90 client, the oncogenic v-src kinase, was shown to be highly dependent on the co-chaperone Cdc37 [Dey et al., 1996, Boczek et al., 2015].

1.3.1 The Hsp90 co-chaperone Aha1

The Hsp90 co-chaperone Aha1 (activator of the Hsp90 ATPase), together with the homologue Hch1, is one of the most prominent co-chaperones that stimulate the Hsp90 ATPase activity. Initially, Aha1 was found to interact with the vesicular stomatitis virus glycoprotein (VSV-G) and being involved in its transit from the ER to Golgi apparatus [Sevier and Machamer, 2001]. One year later, Aha1 was first described as an Hsp90 co-chaperone by the Pearl and Piper lab [Panaretou et al., 2002]. Hch1 (high copy suppressor of Hsp90 temperature-sensitive mutants) was discovered already in 1999 [Nathan et al., 1999]. Panaretou's study in 2002 revealed a 36% sequence iden-

tity of Hch1 to Aha1's NTD (aa 1-153). Notably, while Aha1 is present in a wide range of organisms, Hch1 seems to be restricted to lower eukaryotes like *C. albicans* and *S. cerevisiae* [Panaretou et al., 2002, Lotz et al., 2003].
Yeast Aha1 is a 39 kDa monomeric protein, divided into two functional domains, the NTD and CTD, depicted in figure 1.6:

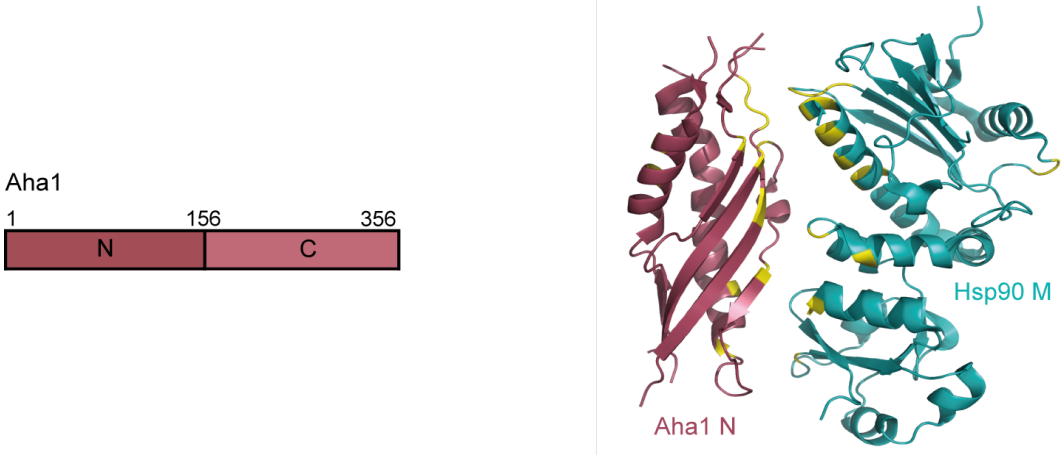

Figure 1.6: Aha1 domain structure and interaction with Hsp90. Aha1 consists of a N-terminal (N) and C-terminal domain (C). In yeast Hsp90, the N-domain consists of 156 aa and the C-domain of 200 aa. Interaction with Hsp90 involves both Aha1 domains: the Aha1 N-domain (raspberry) interacts with the Hsp90 M-domain (teal) and the Aha1 C-domain contacts the NTD of Hsp90.

Up to now, no crystal structure of full-length Aha1 from higher eukaryotes could be obtained. The yeast Aha1 N-domain was successfully crystallised in complex with the yeast Hsp90 MD [Meyer et al., 2004]. This contributed significantly to the understanding of the Hsp90/Aha1 interaction. The binding sites of Aha1 locate within Hsp90's NTD and MD [Meyer et al., 2004, Lotz et al., 2003, Retzlaff et al., 2010]. The Aha1 NTD primarily interacts with the Hsp90 MD. Dimerisation of the Hsp90 N-domains provides a second binding site for the Aha1 C-domain [Meyer et al., 2004, Koulov et al., 2010]. The binding of the Aha1 ND to the Hsp90 MD causes a conformational change in the latter, enabling the residue Arg 380 in the catalytical loop of the MD to access the ATP binding site in the Hsp90 NTD [Meyer et al., 2004]. This contact allows Arg 380 to orient and polarise the γ-phosphate of ATP, an important step for ATP hydrolysis in the Hsp90 NTD [Meyer et al., 2003]. Furthermore, the contact of the Hsp90 N-terminal domains (I_1 state) seems to be stabilised by Aha1, which facilitates a transition to the ATP-hydrolysis competent I_2 state of Hsp90 [Li et al., 2013]. FRET measurements confirmed that binding of Aha1 indeed leads to a faster formation of the I_2 state [Hessling et al., 2009, Li et al., 2013]. Aha1 is able to substantially activate the Hsp90 ATPase activity *in vitro* [Panaretou et al., 2002]. Interestingly, this activation occurs in an asymmetric manner, since one molecule of Aha1 per Hsp90 dimer is sufficient for maximum acceleration of the Hsp90 ATPase rate [Retzlaff et al., 2010]. Interaction between Hsp90 and Aha1 occurs nucleotide-

independently. However, higher binding affinities of Aha1 to Hsp90 were observed in the presence of nucleotide, favouring Hsp90's closed conformation [Retzlaff et al., 2010, Li et al., 2013].
Aha1 can act concerted with the co-chaperone Cpr6 on Hsp90. Their simultaneous binding can cause the exit of Hsp90-bound Sti1. Dissociation of Aha1 from Hsp90 can be triggered by Sba1. A model was proposed by Li *et al.* which puts Hsp90 between inhibitory (Sti1, Sba1) and activatory (Aha1, Cpr6) cofactors. A highly efficient, deterministic system for client processing is hence provided [Li et al., 2013]. Evolutionary, human Aha1 has some additional functions compared to its homologue in yeast. A 22aa N-terminal sequence, only present in human Aha1, was found to act as an autonomous chaperone in order to prevent stress-denatured protein from their aggregation [Tripathi et al., 2014]. Further, hHsp90 shows less stimulation by hAha1, than yHsp90 by yAha1 [Tripathi et al., 2014]. The role of Aha1 in the human system might therefore go beyond the stimulatory co-chaperone of Hsp90. An isoform-specificity for hHsp90α might also play an important role for the Hsp90-Aha1-client interaction in the human system: hAha1 was found to bind to Hsp90α with a higher affinity than to Hsp90β [Synoradzki and Bieganowski, 2015]. Finally, post-translation modifications (PTM) also shape how Aha1 is interaction with Hsp90 and its clients [Walton-Diaz et al., 2013]. Interaction can be affected by phosphorylation, acetylation, and SUMOylation [Mollapour et al., 2014, Mollapour et al., 2011, Xu et al., 2012]. Referring to phosphorylation, the tyrosine residue, Y223, in hAha1 was recently shown to be phosphorylated by the c-Abl tyrosine kinase to promote the association with Hsp90α [Dunn et al., 2015].
In vivo, Aha1 and Hch1 are both not essential. However, they were found to confer thermotolerance in yeast cells under Hsp90 limiting conditions [Lotz et al., 2003]. Nonetheless, deletion of Aha1 results in a dramatic decrease of v-src activity, while Hch1 deletion does not have an effect [Panaretou et al., 2002]. In mammalian cells, Aha1 was found to be involved in Hsp90's interaction with steroid hormone receptors and kinases, such as Raf or c-Abl [Holmes et al., 2008]. The number of Hsp90/Aha1-interactions seems to be far higher than we know these days. A recent study confirmed a variety of interaction partners of Aha1 by a liquid chromatography-tandem mass spectroscopy (LC-MS/MS) approach [Sun et al., 2015]. The spectrum of Aha's cellular tasks ranges from regulation of cell cycle, DNA repair to vesicular transport and protein homeostasis. In the human system, Aha1 was found to interact with all Hsp90 isoforms: Hsp90α/β, Grp94 and TRAP1. Interactions with other molecular chaperones, like Hsp70, Hsp60 and Hsp27, could also be shown [Sun et al., 2015]. Furthermore, Aha1 seems to play a crucial role in the quality control of the cystic fibrosis transmembrane receptor (CFTR) [Wang et al., 2006]. Aha1 promotes the degradation of the disease-related mutant form of CFTR, the misfolded ΔF508. A stabilisation of Δ508 could be achieved by a downregulation of Aha1. Moreover, Aha1 overexpression leads to decrease of Hsp90's ability to activate the kinase Akt [Sun et al., 2012]. These findings underline that the interplay between Hsp90 and Aha1 does not always favour protein activity and folding [Sun et al.,

2012, Holmes et al., 2008].

1.3.2 Hop/Sti1

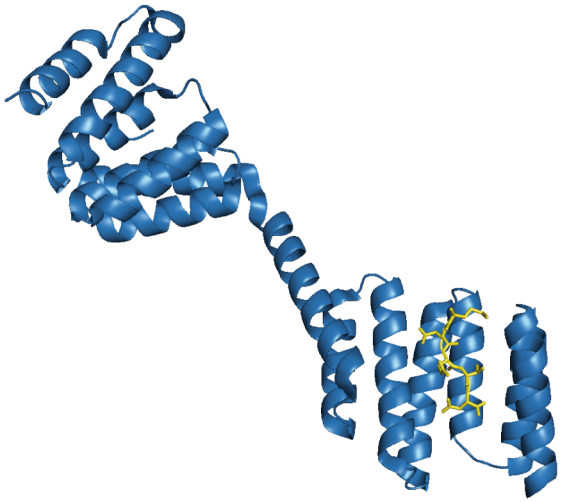

Figure 1.7: Sti1 bound to the Hsp90 MEEVD motif Crystal structure (3uq3) of Sti1 TPR2AB (blue) bound to the Hsp90 MEEVD (yellow) motif. The TPR2A domain binds Hsp90 with high affinity and is connected by a linker to the TPR2B domain.

Hop/Sti1 (Hsp70-Hsp90 organising protein/Stress Inducible Protein 1) is a client-recruiting TPR co-chaperone. It binds and stabilises the open conformation of the Hsp90 dimer [Richter et al., 2003]. Sti1 thereby inhibits the Hsp90 ATPase activity in a non-competitive manner by arresting conformational flexibility of Hsp90 [Richter et al., 2003, Hessling et al., 2009]. Structurally, Sti1 consists of the following domains: TPR1, TPR2A, TPR2B, two DP regions which are rich in aspartate and proline, and a flexible linker between TPR1-DP1 and TPR2A-TPR2B-DP2 [Schmid et al., 2012, Scheufler et al., 2000]. With its three TPR domains, Sti1 is able to act as an adaptor between Hsp70 and Hsp90. By binding to the conserved, C-terminal EEVD motifs of Hsp70 and Hsp90, Sti1 physically connects these two chaperones and provides a scaffold in the client transfer process. The TPR1 and TPR2B domains interact with Hsp70, while the TPR2A domain is highly specific for Hsp90 [Prodromou et al., 1999]. Nonetheless, the TPR2B domain is also involved in inhibition of the Hsp90 ATPase. Together with TPR2A, it was shown to be the central element of Hsp90 inhibition *in vitro* [Schmid et al., 2012]. One Sti1 molecule per Hsp90 is thereby sufficient for ATPase inhibition [Li et al., 2011]. Interaction sites in Hsp90 lie within the C-terminal MEEVD motif, the middle domain and the NTD [Schmid et al., 2012]. The role of the DP domains remains to be clarified, although they seem to contribute to substrate activation [Schmid et al., 2012, Southworth and Agard, 2011].

In vivo, Hop/Sti1 was found to be crucial for activation for the progesterone receptor (PR) and glucocorticoid receptor (GR) [Kosano et al., 1998, Chang et al., 1997].

1.3.3 p23/Sba1

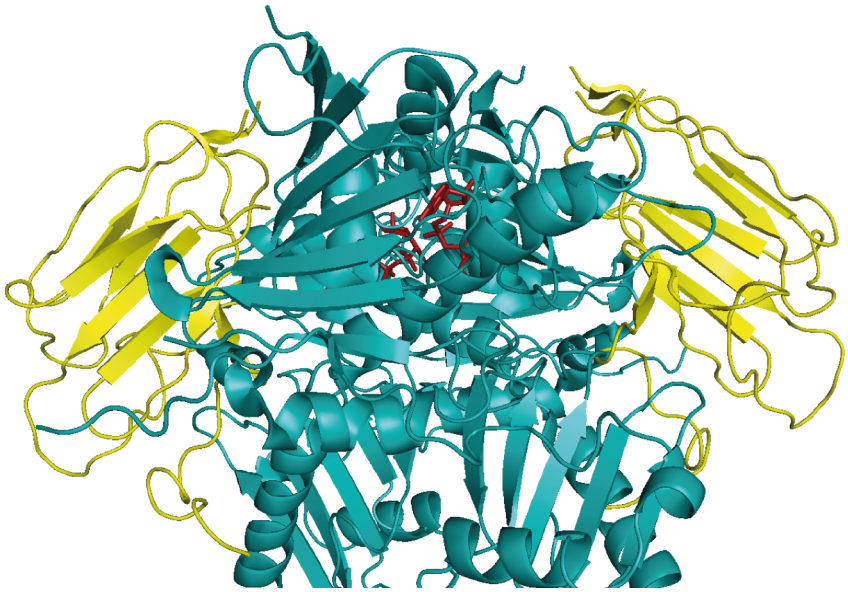

Figure 1.8: Sba1 binds to the Hsp90 NTD. Crystal structure (2cg9) of Sba1 (yellow) bound to Hsp90 (teal) in the closed state (induced by AMP-PNP, red).

The co-chaperone p23 is a small, acidic protein. It was first described in complex together with the avian progesteron receptor and Hsp90 [Johnson et al., 1994]. p23 was named, like many other Hsp90-related proteins, after its molecular weight (of 23 kDa). Its presence is not limited to Hsp90 complexes since it has several other regulatory functions in the cell on its own [Echtenkamp et al., 2011, Prince and Neckers, 2011]. Structurally, p23 can be divided in two domains, an N-terminal domain, containing the Hsp90 binding site, and an unstructured, flexible CTD [Weikl et al., 1999, Ali et al., 2006, Martinez-Yamout et al., 2006]. Functionally, the CTD of p23 exhibits a passive, ATP-independent chaperone activity [Bose et al., 1996, Freeman et al., 1996]. Nevertheless, the absence of the CTD does not hinder p23 binding to Hsp90 [Weikl et al., 1999]. The NTD is highly conserved within the p23 family. Highly homologous p23 domains are also found in small heat shock proteins (sHsps) with a conserved α-crystallin domain, or in the C-terminal CS-domain of the Hsp90 co-chaperone Sgt1 [Garcia-Ranea et al., 2002, Horwitz, 2003]. The Hsp90-p23 interaction is nucleotide-dependent and mediated by the p23 NTD. p23 binds in a late stage of Hsp90's conformational cycle when Hsp90 adopts the N-terminally dimerised closed state [Grenert et al., 1999]. The binding site lies mainly in the Hsp90 NTD, but involvement of the MD was also shown [Ali et al., 2006]. p23 inhibits Hsp90's

ATP hydrolysis rate by trapping Hsp90 in a hydrolysis-competent conformation [Ali et al., 2006]. This, in turn, stabilises the Hsp90-client complex and gives time for client activation [Johnson and Toft, 1995, Richter et al., 2004, Morishima et al., 2003]. The return of Hsp90 to its open confirmation involves release of p23 and the client protein [McLaughlin et al., 2006, Obermann et al., 1998]. Deletion of p23 in yeast only results in minor growth defects, whereas a p23 knockout in mice is perinatally lethal [Grad et al., 2006]. Further roles of p23 involve interaction with steroid hormone receptors (SHR) [Oxelmark et al., 2003, Freeman et al., 2000] and DNA repair [Echtenkamp et al., 2011].

1.3.4 Sgt1

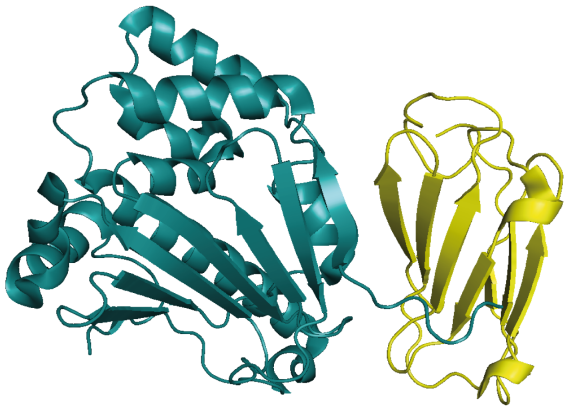

Figure 1.9: The Sgt1 CS domain binds to the Hsp90 NTD Crystal structure (2xcm) of Sgt1 (yellow) bound to Hsp90 (teal). Sgt1 interacts via its CS-domain with the Hsp90 NTD.

Sgt1 (suppressor of the G2 allele of Skp1) is an essential co-chaperone in yeast. It was identified as being involved in both, kinetochore complex assembly and SCF (Skp1-Cul1-F-box)-E3-ubiquitin-ligase-complexes [Kitagawa et al., 1999]. The kinetochore is essential for the cell cycle, more precisely for the control of correct chromosome transmission during cell division [Pesenti et al., 2016]. Sgt1 consists of three domains: The N-terminal TPR-, CS- (CHORD/SGT1 domain) and the C-terminal SGS (Sgt1-specific)-domain, which are conserved from yeast to human. Surprisingly, the interaction with Hsp90 does not seem to occur via the TPR domain, as initially postulated, but via the CS-domain of Sgt1 [Lee et al., 2004, Zhang et al., 2008]. This domain shows structural similarity to the p23 NTD, but exhibits a different mode of interaction with Hsp90. Unlike p23, Sgt1 targets Hsp90 in an open, nucleotide-free conformation and enables client processing via its TPR-domain [Zhang et al., 2008]. Nevertheless, Sgt1 seems to compete with Sba1 and was shown to provoke Sba1-displacement from Hsp90 [Kadota

et al., 2008]. The clients Skp1 and SCF E3 were found to interact with the Sgt1 TPR-domain [Catlett and Kaplan, 2006]. In the case of Skp1 interaction, Sgt1 forms a ternary complex with Hsp90 and Sti1 and is essentially important for the kinetochore assembly in yeasts and humans [Catlett and Kaplan, 2006]. Due to its multidomain structure and the ability to bridge the interaction between Hsp90 and client proteins, Sgt1 acts as a so called 'client adaptor' [Catlett and Kaplan, 2006]. Additionally, homodimerisation of the Sgt1 TPR domain was shown to be required for the assembly of the kinetochore in yeast [Azevedo et al., 2002,Bansal et al., 2004,Steensgaard et al., 2004]. This assembly is an essential step in which Sgt1's role is conserved in yeast and human [Steensgaard et al., 2004].
The important role of Sgt1 in the cell becomes evident when looking at its expression in cancer cells. High expression levels were found in colorectal, gastric, breast, as well as in lung cancers [Ogi et al., 2015, Iwatsuki et al., 2010, Gao et al., 2013]. Thus, overexpression of Sgt1 might be involved in tumorigenesis, possibly by stabilising oncoproteins [Ogi et al., 2015].
Furthermore, nematode Sgt1 of *C. elegans* lacks the TPR-domain while still displaying strong, conformation-independent interaction with Hsp90 [Eckl et al., 2014]. Sgt1 was shown to have chaperone function on its own, similar to p23 and is upregulated upon heat shock [Zabka et al., 2008].

1.3.5 Other Hsp90 co-chaperones

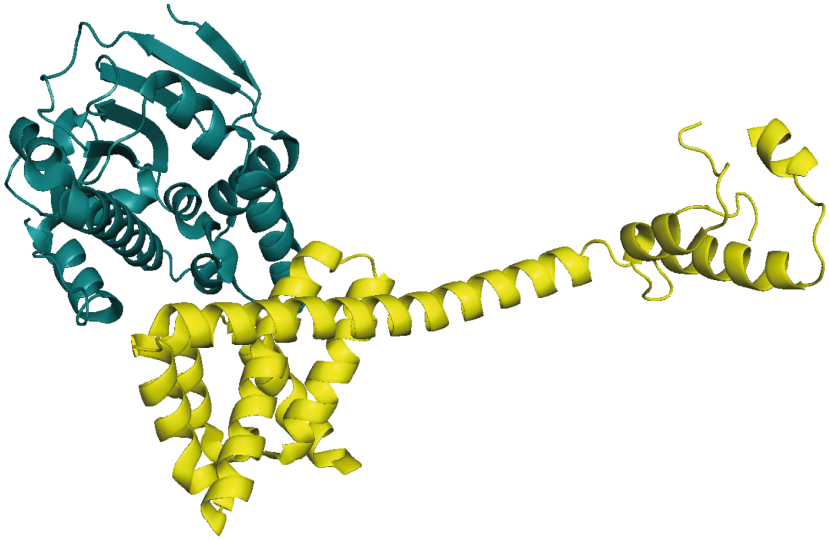

Figure 1.10: Cdc37 bound to Hsp90 Crystal structure (1us7) of Cdc37 (yellow) bound to Hsp90 (teal). Cdc37 interacts via its CTD with the NTD of Hsp90.

Cdc37 (cell division cycle protein 37) is an essential, kinase-regulating co-chaperone. It

was originally identified (as pp50) in mammalians as a component of a protein complex with Hsp90 and the Rous sarcoma-virus (RSV) encoded oncogene pp60v-src [Brugge et al., 1981]. Subsequently, Cdc37 was found together in complex with a vast number of other oncogenic protein kinases, including Cdk4 (cyclin-dependent kinase 4), Raf and erb-b2 receptor tyrosine kinase (ERBB2) [Dai et al., 1996, Stancato et al., 1993, Ghatak et al., 2005]. Interaction with kinases takes place via the Cdc37 N-terminal protein kinase binding domain, whereas interaction with the NTD of Hsp90 occurs via the C-terminal part of Cdc37 (fig. 1.10) [Silverstein et al., 1998, Shao et al., 2003]. Cdc37 has an inhibitory effect on the Hsp90 ATPase. By binding between the Hsp90 N-domains and interaction with the Hsp90 lid, N-terminal dimerisation is hindered and the lid is locked in an open conformation. This leads to ATPase inhibition, mediated by the R167 side chain of Cdc37, which is inserted into the nucleotide binding pocket of Hsp90 and interacts with the catalytically important E33 residue. In this manner, client loading is facilitated, probably through a prolonged interaction between Hsp90 and the client [Roe et al., 2004]. The mechanism of client transfer via Cdc37 to Hsp90, still remains to be elucidated. Also, because the knowledge on Hsp90-Cdc37-kinase complexes remains poor due to only limited structural information [Vaughan et al., 2006]. Although kinases seem to be the preferred target of Cdc37, interactions with targets outside the kinase family were found, such as reverse transcriptase or androgen receptor [Wang et al., 2002, Rao et al., 2001]. Given its striking role in oncogenesis and interaction with oncogenic protein kinases, Cdc37 is an interesting candidate for cancer therapy.

Another important subset of Hsp90 co-chaperones are TPR-containing PPIases (peptidyl-prolyl cis-trans isomerases, also called cyclophilins). This class is represented by **Cpr6**, **Cpr7** (cyclosporin-sensitive proline rotamase 6/7) in yeast and FKBP51, FKBP52 and Cyp40 in mammals [Duina et al., 1996]. These co-chaperones are able to catalyse the interconversion of cis-trans isomerisation of peptide bonds prior to proline residues [Fanghänel and Fischer, 2004]. Most of the PPIases exhibit chaperone activity on their own. In yeast, Cpr6 is the more potent PPIase compared to Cpr7, while Cpr7 is the more potent chaperone [Mayr et al., 2000]. Cpr6 and Cpr7 bind to Hsp90 with a similar affinity, but only binding of Cpr6 results in a slight activation of the ATPase activity of Hsp90 [Panaretou et al., 2002, Mayr et al., 2000]. Both are non-essential proteins in yeast, although a deletion of Cpr7 causes a growth defect. Further, a loss of Cpr7 triggers defective activity of GR and the heat shock transcription factor 1 (HSF1) [Duina et al., 1998, Duina et al., 1996]. A formation of ternary complexes with Hsp90, Cpr6 and Sti1, as well as with Hsp90, Cpr6 and Cpr7 was described in the literature [Li et al., 2011, Li et al., 2013, Zuehlke and Johnson, 2012]. While Cpr6 is also able to form a ternary complex with Aha1 and Hsp90, Cpr7 is not [Li et al., 2013]. Notably, Cpr6 and Cpr7, as well as Cns1 specifically interact with the AMP-PNP or ATP-bound form of Hsp90 [Johnson et al., 2007, Johnson and Toft, 1994]. The fact that Cpr6 and Cpr7 possess chaperone activity on their own [Mayr et al., 2000], leads to the conclusion that they might also play a role in client recruiting. Nonetheless, the role of their PPIase domain is

still puzzling because it seems to be dispensable for client activation [Riggs et al., 2007]. Another TPR-containing PPIase is represented by **Cns1** (cyclophilin seven suppressor). In contrast to Cpr6 and Cpr7, Cns1 is essential in yeast and it can rescue the Cpr7-mediated growth defect [Dolinski et al., 1998, Zuehlke and Johnson, 2012]. Cns1 interacts with both, Hsp90 and Hsp70. It does not alter the Hsp90 ATPase, whereas it activates the ATPase of Ssa1, the yeast Hsp70 homologue [Hainzl et al., 2004]. This stimulatory effect was found to be mediated by the N-terminal TPR-domain of Cns1. Onwards, overexpression of the TPR domain in vivo is sufficient for cell viability at normal temperatures [Tesic et al., 2003], underlining the crucial role of the TPR domain. In yeast, Cns1 can act as a restriction factor of tomato bushy stunt tombusvirus (TBSV) and, together with Cpr6 and Cpr7, it interacts with the intact ribosome [Lin and Nagy, 2013, Tenge et al., 2015]. Moreover, together with Sgt1, it mediates hypersensitivity to co-chaperone overexpression in yeast [Johnson et al., 2014].
The TPR-containing co-chaperone PP5/Ppt1 is a protein serine/threonine phosphatase [Becker et al., 1994, Chen et al., 1994]. Association with Hsp90 is mediated through its N-terminal TPR domain [Chen et al., 1996]. Due to the autoinhibitory function of the Ppt1 TPR domain, the catalytical domain is blocked and the intrinsic phosphatase activity is very low [Chen and Cohen, 1997, Yang et al., 2005]. Binding to Hsp90 leads to abrogation of the intrinsic inhibition of Ppt1 and activates the phosphatase. Ppt1 was shown to mediate dephosphorylation of Hsp90 and Cdc37 [Vaughan et al., 2008, Wandinger et al., 2006]. Ppt1 is not essential in yeast cells, however, a decreased activation of Hsp90 clients was observed in cells lacking Ppt1 [Chen et al., 1994, Wandinger et al., 2006]. Phosphorylation of Hsp90 was shown to inhibit the Hsp90 machinery and its chaperone function [Soroka et al., 2012]. In conclusion, regulating the phosphorylation of Hsp90 is a crucial task Ppt1 fulfills in order to ensure efficient client processing by Hsp90.
The functions of another two Hsp90 co-chaperones, **Tah1** (TPR-containing protein associated with Hsp90) and **Pih1** (protein interacting with Hsp90), are linked to small nuclear ribonucleoprotein (RNP) maturation and chromatin remodelling functions. Tah1 is a TPR co-chaperone, while Pih1 was described as a protein which does not contain any known Hsp90-related motifs [Zhao et al., 2005]. However, recent NMR data suggests that Pih1 contains a CS-domain [Manival et al., 2014, Quinternet et al., 2015]. Tah1 and Pih1 were discovered as Hsp90 co-chaperones in the so called R2TP complex with the essential helicases Rvb1 and Rvb2 [Zhao et al., 2005]. Interaction of Hsp90 with the R2TP complex is important, inter alia, for cytoplasmic assembly of RNA polymerase II [Boulon et al., 2010]. When bound to Hsp90, Tah1 and Pih1 inhibit the Hsp90 ATPase, whereas Tah1 alone causes weak stimulation of the Hsp90 [Millson et al., 2008, Eckert et al., 2010]. Via its N-terminal TPR domain, Tah1 interacts with Hsp90 at the MEEVD motif [Jiménez et al., 2012]. The disordered C-terminal region of Tah1 is at the same time able to recruit Pih1. Upon association with the CS-domain of Pih1, the disordered C-terminal of Tah1 folds [Back et al., 2013, Eckert et al., 2010, Manival et al., 2014, Quinternet et al.,

2015]. Due to this folding event, Tah1, together with Hsp90, stabilises Pih1 which in turn was found to be an unstable protein in both, *in vitro* and *in vivo* [Zhao et al., 2008]. Recent studies even indicate that Pih1 stabilisation might even occur only via Tah1 and Hsp90-independently [Quinternet et al., 2015]. To date, the concerted and closely related interaction of Tah1 and Pih1 is a unique behaviour of Hsp90 co-chaperones.
The list of Hsp90 co-chaperones is dynamic and constantly, new proteins are discovered. The variety of co-chaperones and their diverse mode of interactions underline the complexity of the Hsp90 machinery. Furthermore, it is exactly this complexity which requires specificity. By the formation of unique interaction sites, this specificity might be mediated. An obvious, still remaining question is how the variety of structurally similar co-chaperones achieves transfer of the correct client at the right time, despite competition for binding sites with other co-chaperones.

1.4 Hsp90 and disease

A variety of Hsp90 clients is involved in oncogenic signalling as well as in crucial cellular processes like proliferation, apoptosis and angiogenesis [Neckers and Workman, 2012]. Under normal conditions, these processes maintain the fragile balance of the cellular life cycle. Once hijacked by pathological changes, cancer and other diseases are able to evolve. Besides being an interesting target for cancer, Hsp90 also chaperones clients which are associated in neurodegenerative disorders, like Tau in Alzheimer's disease, and might even be a suitable target for malaria if selective targeting of the malaria parasite Plasmodium falciparum could be achieved [Ramdhave et al., 2013, Paul and Mahanta, 2014, Ou et al., 2014]. Furthermore, Hsp90 has an implicated role in cystic fibrosis [Wang et al., 2006]. Given the tremendous amount of clients, it is not surprising that Hsp90 is of high interest for disease-related research as a promising drug-target [Smith and Workman, 2007, Trepel et al., 2010]. Inhibition of Hsp90 might be the path to follow for gaining control over malignant cells. Promising Hsp90 inhibitors were developed in the last decades. However, none of them have yet reached approval by the FDA (food and drug administration).

1.4.1 Hsp90 and cancer

Hsp90 was found to be upregulated in several types of cancers [Whitesell and Lindquist, 2005, Flandrin et al., 2008, McDowell et al., 2009, Biaoxue et al., 2012, Miyata et al., 2013]. In addition, Hsp90 from tumour cells displays an increased ATPase activity and is much more sensitive to inhibitors, like geldanamycin than Hsp90 from normal cells [Neckers and Workman, 2012]. Furthermore, tumour Hsp90 is mainly present in

multichaperone-complexes, wheras Hsp90 from non-cancerous tissues is usually in an uncomplexed state [Kamal et al., 2003]. This highly active state of Hsp90 is thought to actively stabilise mutant and misfolded oncoproteins. In turn, tumour cell proliferation and malignancy is fostered and tumour growth is promoted. The malignant state of tumour Hsp90 is very sensitive to inhibition and thus provides a suitable, unique target for cancer therapy [Kamal et al., 2003, Neckers and Workman, 2012].
Not only Hsp90, but also its co-chaperones p23, Aha1 and Cdc37 were shown to be overexpressed in cancer cells [McDowell et al., 2009]. Silencing of these co-chaperones resulted in hypersensitivity to the Hsp90 inhibitor geldanamycin in yeast cells [Gray et al., 2007, Forafonov et al., 2008, Smith and Workman, 2009]. Thus, the complexes of Hsp90 and its co-chaperones have a pivotal role in diseases. Consequently, tumour cells overexpressing certain Hsp90 co-chaperones might acquire resistance to Hsp90 inhibitors and thus, targeting of Hsp90 co-chaperones might also provide an efficient approach for the cancer therapy.
The list of oncogenic clients associated with Hsp90 is capacious. Kinases represent the largest class of Hsp90 clients and require Hsp90 due their intrinsic instability [Richter and Buchner, 2001, Taipale et al., 2012, Haupt et al., 2012]. They are essential for regulation of cell growth and proliferation under both, normal and carcinogenic cellular conditions. Cell surface receptor kinases like the EGF (epidermal growth factor) receptor family, IGF-I (insulin-like growth factor I), TGFβ (transforming growth factor β) are known to be associated with Hsp90 [Wrighton et al., 2008, Imamura et al., 1998, Xu et al., 2001]. An EGF receptor family of particular interest is the membrane tyrosine kinase receptor Erb2/HER2 whose overexpression is intimately connected with breast cancer progression [Yarden and Sliwkowski, 2001]. Treatment with the monoclonal antibody drug Trastuzumab (Herceptin) arrests the signalling pathway of Erb2/HER2 and is effective in breast cancer therapy [Arteaga et al., 2012]. A combined 17-AAG Hsp90 inhibition and treatment with Trastuzumab was shown to cause Her2 degradation in this context [Neckers, 2000, Chiosis et al., 2001, Modi et al., 2011b]. Src kinases, like v-src or Abl are another kinase family with Hsp90 dependency. Abl is protein tyrosine kinase and its fusion protein Bcr-Abl (caused by gene translocation) is found in patients suffering from leukemia, for instance chronic myelogenous leukemia (CML) [Goldman and Melo, 2008, An et al., 2000]. Interaction of Abl with Hsp90 is crucial for its stability and correct function. The proto-oncogenic products Raf-1 and B-Raf, both family members of the Raf protein kinase family, are also associated with Hsp90 and play a role in the MAPK (mitogen-activated protein kinases) signalling pathway [Grammatikakis et al., 1999, Stancato et al., 1994]. This pathway is crucial for transmission of extracellular growth signals from cytoplasm to nucleus. Further, Raf-1 and B-Raf have been found as mediators of anti-apoptotic activity demonstrating not only their obvious roles in cancer, but also in inflammatory diseases or pain treatment [Herrera and Sebolt-Leopold, 2002, Dhillon et al., 2007]. Mutated B-Raf kinases are found to a high extent in malignant melanomas and was also shown to play a pivotal role in other cancers, e.g. colorectal cancer [Davies

et al., 2002]. Other cancer-related kinases requiring Hsp90 are cyclin-dependent kinases (Cdk4 in cell cycle control) [Lamphere et al., 1997] and mitotic protein kinases (polo-like kinase, Plk, for cell division) [Lens et al., 2010]. Most of these contemplated kinases also require the Hsp90 co-chaperone Cdc37 for their stability [Mandal et al., 2007].

Steroid hormone receptors (SHR) are another class of Hsp90 clients, closely related to cancer. SHRs are DNA-binding nuclear transcription factors and require Hsp90 to bind to and activate their target proteins. Hsp90 regulates glucocorticoid (GR), estrogen (ER), progesteron (PR) and androgen (AR) receptors which cycle between cytoplasm and nucleus, demonstrating Hsp90's complex role in these cellular compartments [Echeverria and Picard, 2010]. ER is of particular interest in breast cancer, since the majority of these tumours shows a high expression of ER which contributes to tumour progression [Ellmann et al., 2009]. AR is involved in development and progression of prostate cancer [Zhu et al., 2001]. Interestingly, it is one of the non-kinase clients of Hsp90 and Cdc37 [Rao et al., 2001, MacLean and Picard, 2003]. Other SHR clients of Hsp90 are also currently validated as antitumour targets [Ahmad and Kumar, 2011]. Another important nuclear role of Hsp90 involves regulation of the heat shock transcription factor 1 (HSF1) [Anckar and Sistonen, 2011].ß HSF1 has a crucial role inducing the cellular stress response and is thought to facilitate oncogenesis [Chen et al., 2013].

Each cell has a limited number of cell cycles during its life time. These are surveilled by telomeres, which are composed of conserved DNA motifs and located at chromosome ends [Miyata et al., 2013, Gomes et al., 2010]. In contrast, cancer cells possess an unlimited replicative potential. Telomerases are reverse transcriptases which use their catalytical hTERT subunit for telomere synthesis [Nakamura et al., 1997]. Hsp90 and p23 were shown to be associated with hTERT and active telomerase complexes in cells [Aisner et al., 1999].

The tumour suppressor p53 is a crucial protein in the surveillance of cellular growth [Vousden and Lane, 2007, Brady and Attardi, 2010]. Genomic instability of p53 is exploited by tumour cells to circumvent apoptosis, despite their high accumulation of mutations and genetical damage. Once downregulated, p53 can't fulfill its crucial task of arresting the cell cycle for DNA repair or sending mutated cells off to apoptosis. The anti-proliferative function is suppressed and tumour growth is promoted [Roemer et al., 2006]. Hsp90 binds to the DNA-binding domain of p53 and stabilises it [Hagn et al., 2011, Rudiger et al., 2002]. Tumour p53 was shown to interact in a more stable manner with Hsp90, being more dependent on Hsp90 due to its instability. This is another example were tumour proteins heavily rely on Hsp90's function, which sometimes is also described as tumour addiction to Hsp90.

1.4.2 Cystic Fibrosis

Cystic Fibrosis is an inherited disease caused by a misfolded CFTR (cystic fibrosis transmembrane conductance regulator) [Gadsby et al., 2006]. This membrane protein is a multidomain cAMP-regulated chloride channel and maintains the cellular ion balance [Quinton, 2007]. CFTR is located in the apical membrane of secretory epithelia which surround many types of tissues, e.g. lungs or pancreas. Structurally, CFTR consists of two transmembrane domains (TMD1, TMD2), two cytosolic nucleotide-binding domains (NBD1, NBD2) and a regulatory (R-) domain [Riordan et al., 1989, Lewis et al., 2004]. This R-domain is phosphorylated by protein kinases which in turn activates the CFTR [Picciotto et al., 1992, Riordan, 2005]. The regulatory function of CFTR includes chloride ion transport and thereby regulation of the water content in mucus to ensure the normal functions of a variety of organs [Frizzell and Hanrahan, 2012]. In the respiratory system, a mutant CFTR causes a thick, sticky mucus which obstructs the airways and leads to cystic fibrosis [Rowe et al., 2005].The most prevalent mutant form of CFTR is the ΔF508. The mutation causes misfolding and a failure in delivery of the CFTR to the plasma membrane. A correctly folded CFTR is exported by the COPII machinery from the ER to the Golgi apparatus for glycosylation, followed by transfer to the cell surface by endocytic pathways [Wang et al., 2004]. The misfolded CFTR is recognised by the endoplasmatic reticulum (ER) quality control machinery and targets it for proteasome-mediated degradation [Amaral and Farinha, 2013]. In the fairly complex biosynthetic pathway of CFTR, chaperones assist and regulate the folding. The Hsp70 system, the ER-specific chaperone Calnexin, as well as Hsp90 can promote folding of CFTR in different stages, but are also able to target misfolded proteins for degradation [Pind et al., 1994, Farinha and Amaral, 2005, Amaral, 2006]. Interestingly, the interplay of Hsp90 and its co-chaperone Aha1 seems to be a crucial process for degradation of the misfolded Δ508 CFTR by the ER-association degradation (ERAD) pathway. siRNA silencing of Aha1 resulted in stabilisation, trafficking and restoration of the Δ508 channel activity [Wang et al., 2006]. Even though a variety of therapeutics with different modes of action for cystic fibrosis exist [Ma et al., 2002, Muanprasat et al., 2004, Derichs, 2013], the search for better medication is ongoing [Quon and Rowe, 2000]. None of the currently approved drugs is directly targeting the basic folding problem of the mutant CFTR by interacting with one of the involved chaperones. Although it is by far not the only chaperone involved in CFTR folding, inhibition of Hsp90 and Aha1 interaction might be a new approach for development of new therapeutics for cystic fibrosis.

1.5 Hsp90 inhibitors

Geldanamycin (GA) is a naturally occurring benzoquinone ansamycin antibiotic and is the first Hsp90 inhibitor that was discovered [Whitesell et al., 1994]. It was originally isolated from *Streptomyces hygroscopicus*, a bacterium that also produces the immunosuppressant macrolide rapamycin [DeBoer et al., 1970]. The inhibitory effect of GA was initially described as interruption of the src-Hsp90 heteroprotein complex, identifying GA as putative tyrosine kinase inhibitor, but soon it became clear that the mode of action is due to interaction with Hsp90 [Whitesell et al., 1994, Smith et al., 1995]. GA binds to the ATP binding pocket of Hsp90, adopting a compact structure and forming hydrogen bonds within the binding pocket. Thereby, GA mimicks and competes with ATP, and potently inhibits ATP hydrolysis [Stebbins et al., 1997, Grenert et al., 1997]. In turn, not only the essential chaperoning function of Hsp90 is inhibited, but also complex formation between Hsp90 and its clients. The latter are subsequently depleted through ubiquitin-mediated proteasomal degradation [Schneider et al., 1996, Mimnaugh et al., 1996]. GA exhibits anti-cancerous effects, like cell cycle arrest or apoptosis, but it proved too toxic for clinical development [Supko et al., 1995]. Especially its high liver toxicity remains problematic. The better-tolerated GA derivative 17-AAG (17-allylamino-17-demethoxygeldanamycin, tanespimycin) was the first Hsp90 inhibitor to enter clinical trials. The most promising results were seen in patients suffering from HER2 (human epidermal growth factor receptor 2) overexpressing breast cancers, due to the high dependence of the oncogene HER2 on Hsp90 [Modi et al., 2011a, Modi et al., 2007]. Furthermore, 17-AAG proved a prolonged disease stabilisation in various tumour types. However, no complete or partial tumour responses could be observed, which finally lead to discontinuation of the development [Neckers and Workman, 2012]. In contrast, the soluble stabilised hydroquinone form of 17-AAG, IPI-504 (retaspimycin hydrochloride), is still in clinical development [Neckers and Workman, 2012] and showed promising results in therapy of non-small cell lung cancers (NSCLC) [Sequist et al., 2010].
Radicicol (RD) is a resorcinol lactone, originally isolated from *Monosporium bonorden* in 1953 [Delmotte and Delmotte-Plaque, 1953]. In 1998, it's role as Hsp90 inhibitor became evident [Schulte et al., 1998, Sharma et al., 1998]. As GA, radicicol also binds to the Hsp90 binding pocket and thus inhibits Hsp90's function [Roe et al., 1999]. RD binds with an affinity of 19 nM to Hsp90, whereas GA has a lower affinity of 1.2 µM [Duerfeldt et al., 2009]. However, the use of radicicol as a drug is, as for GA, associated with low solubility and high instability in plasma [Soga et al., 1999, Jhaveri et al., 2014]. So RD never advanced into clinical trials. Hence, development of radicicol derivatives was pushed forward in the last decades. Unlike for geldanamycin derivatives, radicicol derivatives are structurally highly heterogenous and only loosely related to each other. They commonly carry the resorcinol core of radicicol which mediates the interaction with Hsp90 [Trendowski, 2015]. The inhibitors NVP-AUY922 (luminespib), AT-13387,KW-2478 and STA-9090 (ganetespib) contain a resorcinol core of radicicol and have been evaluated in

the clinics [Eccles et al., 2008, Lin et al., 2008, Brough et al., 2008, Woodhead et al., 2010, Nakashima et al., 2010]. STA-9090 is the most promising Hsp90 inhibitor so far and was evaluated in a phase III trial for the treatment of NSCLC [Jhaveri et al., 2014].

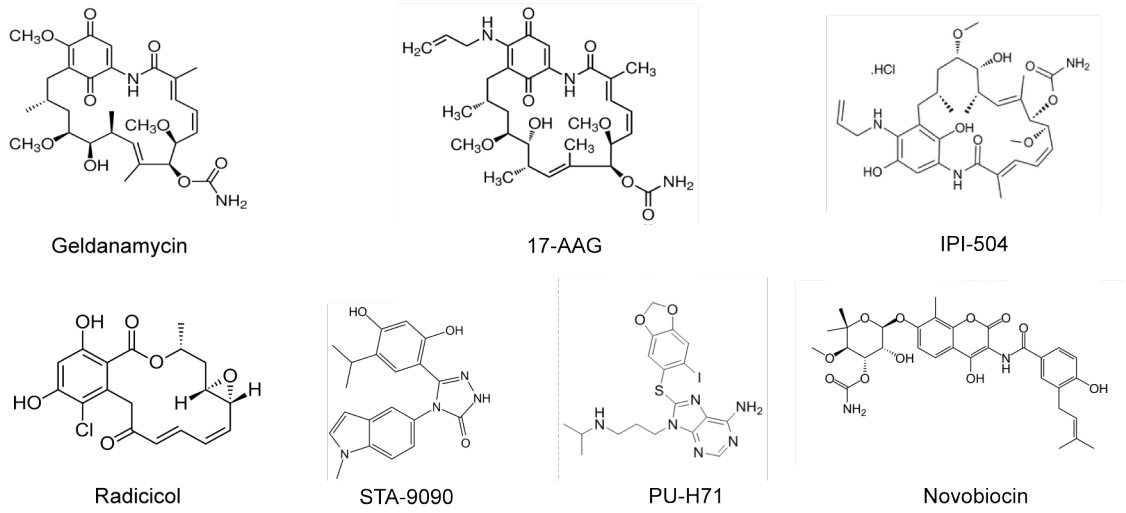

Figure 1.11: Structures of Hsp90 inhibitors.

In addition to the natural products GA and RD, synthetic small molecules were developed to target Hsp90. Generally, crystal structures of GA and RD bound to Hsp90 helped in developing a strategy for rational drug design. Purine-based Hsp90 inhibitors were designed by using the purine moiety of ATP as a template to mimick ATP binding to Hsp90 [Chiosis et al., 2002]. From this purine scaffold series, the inhibitor PU-H71 demonstrated the most potent, antineoplastic effect in a variety of cancers, and a high specificity towards malignant cells [He et al., 2006, Trendowski, 2015]. PU-H71 showed good preclinical results, however, it has to prove itself in clinical trials.
In general, Hsp90 inhibitors that target the ATP binding side were shown to induce the heat-shock response (HSR) in cells with highly upregulated levels of both Hsp90 and Hsp70 [Chiosis et al., 2003]. Consequently, the dosage of these inhibitors needs to be chosen carefully. Alternatively, other interaction sites in Hsp90 than the ATP binding pocket have been tried to be modulated by inhibitors. The aminocoumarin antibiotic novobiocin binds to the C-domain of Hsp90 [Burlison and Blagg, 2006]. Novobiocin and its analogues seem to result in less activation of the HSR and showed promising results in prostate cancer cells [Eskew et al., 2011]. Interestingly, inhibitors for the C-domain of Hsp90 seem to have, besides the role in HSR activation, another important advantage: Their efficacy might not be dependent on co-chaperone expression in the cell. Overexpression of the co-chaperone p23 in tumour cells decreases the efficacy of N-terminal Hsp90 inhibitors, whilst C-terminal inhibitors seemed to remain unaffected by p23 levels [Cox and Miller 3rd, 2004, McDowell et al., 2009].

Another concept for the inhibition of Hsp90 was demonstrated by Zierer *et al.* (2014). The identification of Hsp90 accelerators lead to the conclusion that an acceleration of the Hsp90 cycle can result in an inhibition of client processing. By not giving enough time for the contact of Hsp90 and its clients, stimulatory molecules are able to perturb the efficiency of the Hsp90 machinery.
In conclusion, Hsp90 inhibitors seem to be a promising anti-cancer strategy and might be beneficial for the treatment of other chaperone-related diseases. Several inhibitors reached a clinical trial stage and showed promising results. However, none of them has gained approval by the FDA, so far. The challenge to develop an inhibitor with high specificity and efficacy remains.

1.6 Objectives

This work focuses on the screening for a new generation of Hsp90 inhibitors. As already mentioned, Hsp90 inhibitors gained interest due to Hsp90's regulatory function in a variety of diseases, especially in cancer. Targeting the Hsp90 machinery promises new options in the treatment of diseases. Hsp90's specificity can be mediated by the interplay between its co-chaperones and clients [Mayer and Le Breton, 2015]. The diversity of Hsp90 clients might therefore be regulated by a defined, fine-tuned interplay of Hsp90 and its co-chaperones. Modulation of this interplay might provide an even more selective targeting of only specific components of the Hsp90 machinery. This work focused therefore on Hsp90 and the co-chaperone Aha1 to achieve a more selective targeting of the Hsp90 machinery. Modulators for this system were identified and characterised for their modulating properties.
Furthermore, an evolutionary point of view on the Hsp90 system was taken. Yeast and human Hsp90 systems have evolved throughout evolution and provide a highly potent quality control system for cellular proteins. An evolutionary analysis of Hsp90 machineries in organisms, evolved in different evolutionary branches, was undertaken. A thermophilic fungus and an eukaryotic parasite were addressed in order to access differences between chaperone systems in different organisms.
Another comprehensive approach to understand the Hsp90 machinery better, was undertaken by the analysis of Hsp90 mutants. Tryptophan residues were introduced as photometric probes at crucial ATP interaction sites, namely the Hsp90 lid and the ATP binding site. Effects of these mutants on ATP binding, hydrolysis and the interplay with co-chaperones were addressed. This approach sheds light on the interaction of Hsp90 with nucleotides and which alterations are caused when tryptophans are introduced at crucial functional sites.

CHAPTER 2

Results and Conclusions

2.1 Hsp90/Aha1 modulators

Modulation of the Hsp90 machinery by chemical compounds is a promising approach for the treatment of various diseases. The development of Hsp90 inhibitors has advanced during the last years. However, the discovered inhibitors have to prove their efficacy in the clinic as discussed in the introduction section. To further contribute to the research on Hsp90 modulators, this work aimed to take Hsp90 modulation one step forward: by finding specific modulators of the interplay between Hsp90 and its co-chaperones. The focus was laid on the Hsp90 accelerating co-chaperone Aha1. A small molecule library was screened for the identification of potential new, highly specific modulators of the Hsp90/Aha1 interaction. Promising compounds were further characterised *in vitro* and *in vivo* to elucidate their mode of action.

2.1.1 FRET-based screening of a compound library

A previously established FRET-system [Li $\mathrm{et\ al.}$, 2013] was used to screen for modulators of the Hsp90/Aha1 interaction. The principle of the Hsp90/Aha1 FRET assay is depicted in figure 2.1.

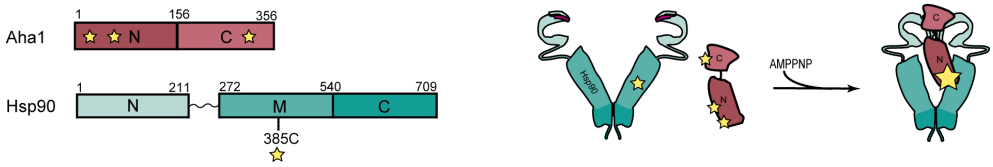

Figure 2.1: Principle of the Hsp90/Aha1 FRET system. In the Hsp90/Aha1 FRET system, Aha1*Alexa488 (red) serves as donor, while Hsp90 385C*Atto550 (blue) is the acceptor. The domain structure with the respective labelled residues is depicted.

Even though Aha1 was shown to interact with Hsp90 in the absence as well as in the presence of nucleotide [Li et al., 2013], the applied FRET system requires the presence of nucleotide to monitor kinetic traces of Aha1 binding to Hsp90. Since the conformational changes of Hsp90 in the presence of ATP are not leading to a stable closed conformation of Hsp90, the non-hydrolysable ATP-analogue AMP-PNP was used. When AMP-PNP binds to Hsp90, the closing reaction of Hsp90 is induced, leading to the fully closed state of Hsp90 and a reduced distance between Hsp90 and Aha1. Thereby, binding which translates into an increase in the FRET signal can be followed by excitation of the donor (Atto488-labelled Aha1) and measurement of the acceptor (Hsp90 385C Atto550-labelled) fluorescence. In close proximity, according to the principle of FRET, the donor transmits its energy in an emission-free manner and acceptor fluorescence increases. Since the small molecules of the screened compound library were dissolved in DMSO, DMSO served as a negative control for the FRET measurements. The Hsp90 inhibitor geldanamycin (GA) was applied as a positive control. GA inhibits the chaperoning-function of Hsp90 by binding to the ATP binding site. Binding of ATP to Hsp90 is essential for Hsp90's function, especially with clients like cell signalling kinases or steroid hormone receptors [Whitesell et al., 1994]. Thus, the progression through the Hsp90 conformational cycle is stopped. Binding of Hsp90 to Aha1 can be blocked by GA which was why GA was chosen as positive control for this assay [Sun et al., 2012]. 1 mM AMP-PNP was added to the Hsp90/Aha1 FRET complex to induce conformational changes. The concentration of tested compounds was 50 µg/ml and FRET kinetics were traced for 18 min.

Figure 2.2 depicts kinetic traces of the most promising hits from the screen. The small molecule 2A03 showed a highly potent inhibition of the Hsp90 Aha1 interplay similar to the GA positive control (data not shown). This compound was not investigated further, since it belongs to the group of purine derivatives and is already described as an Hsp90 inhibitor [Chiosis et al., 2002]. Nevertheless, identifying this compound as a positive hit shows the reliability of the applied screening method. Some modulators, namely 26C8 (green), 51E8 (lavender) and 87H7 (navy blue) had inhibitory effects on the Hsp90/Aha1 interaction, manifested in a slower FRET kinetic. Some other modulators surprisingly also displayed a stimulatory effect (27F4 (lilac), 67A9 (blue), 98F1 (red)). Hits were re-screened twice to exclude false positive hits. Out of 10,000 small molecules screened,

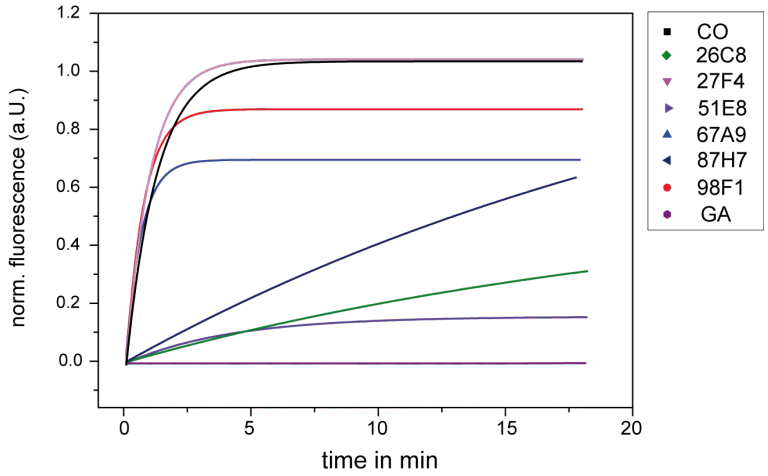

Figure 2.2: FRET Screening of a compound library. FRET kinetics of the Hsp90/Aha1 FRET screening are depicted. Kinetics were recorded after addition of 1 mM AMP-PNP. GA served as positive control (GA, purple), Hsp90/Aha1 + DMSO as negative control (CO, black). Recorded kinetics were normalised relatively to the DMSO control and fitted exponentially. Fitted curves are depicted.

40 showed effects on the Hsp90/Aha1 interaction.

2.1.2 Influence on the ATPase activity of Hsp90

The compounds have impact on the Hsp90 stimulation by Aha1

A regenerative ATPase assay was applied for further evaluation of the potential Hsp90/Aha1 modulators. Initially, all compounds were tested for unspecific effects on the regenerative enzyme system used in this assay (figure 2.3B). None of the compounds showed interaction with the enzyme system. DMSO, the solvent for the small molecules did not influence the assay system either (data not shown). As Aha1 is an accelerator of the Hsp90 ATPase cycle, a higher ATPase activity of Hsp90 can be observed when Aha1 is present. At high Aha1 concentrations, the maximum stimulation of the Hsp90 ATPase activity is up to 20-fold. 40 compounds (final concentration: 50 µg/ml) were tested for their effects on Aha1 stimulation of the Hsp90 ATPase activity. Six compounds showed significant effects on the Hsp90 ATPase activity in the presence of Aha1 (figure 2.3A).

In concordance with the FRET screening, three compounds (26C8, 51E8 and 87H7) were identified as inhibitors of Hsp90/Aha1, while another three (27F4, 67A9 and 98F1) could be classified as activatory modulators. The inhibitor 26C8 had the most dramatic effect on the stimulatory potential of Aha1: Even at saturating Aha1 concentrations (20 µM), 26C8 caused a 93 % decrease of the Hsp90 activity to a k_{cat} of 0.8/min. This

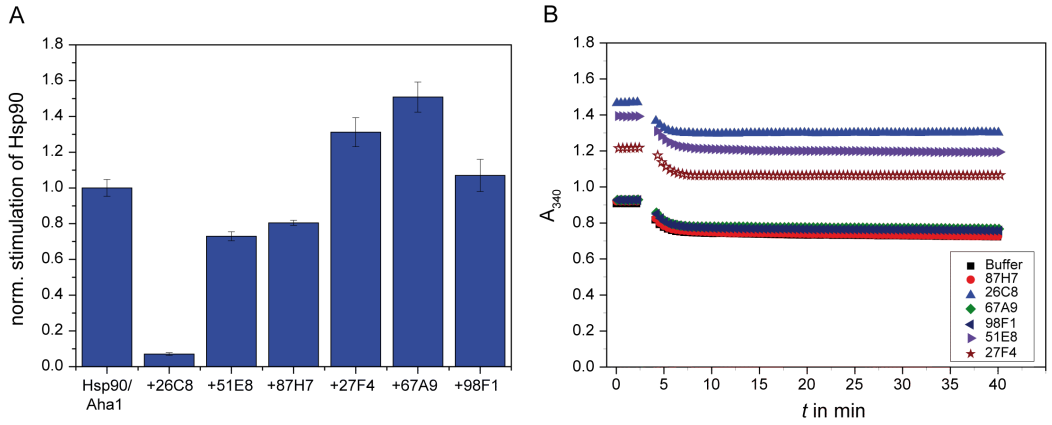

Figure 2.3: Modulator effects on the stimulation of the Hsp90 ATPase by Aha1. A: Aha1 mediated stimulation of the Hsp90 ATPase activity was measured in the presence of the identified modulators. The stimulation of Hsp90 by Aha1 without modulator influence was normalised to 1 and compared to the Hsp90 stimulation under modulator influence. B: Modulator effects on the regenerative enzyme system. The ATPase assay was performed with the modulators, but without Hsp90 and Aha1 to investigate if the modulators have an impact on the regenerative enzyme system.

resembles Hsp90's activity in the absence of Aha1. Thus, the highly stimulatory effect of Aha1 on Hsp90 is abolished by 26C8. Compound 51E8 inhibited Aha1 stimulation of Hsp90 by 23 %, while the compound 87H7 caused a 20 % inhibition of the Hsp90 ATPase activity in the presence of Aha1. The activating small molecules 27F4 and 67A9 increased the stimulatory potential of Aha1 on Hsp90 1.3- and 1.5-fold, respectively. Another compound, 98F1, showed a less pronounced activatory effect with a 1.1-fold stimulation of Hsp90 in the presence of Aha1.

The structures of the six modulators are represented in figure 2.4. 26C8, 51E8 and 87H7 are inhibitors of the Hsp90/Aha1 interplay, whereas 27F4, 67A9 and 98F1 classify as activators. 98F1 was not commercially available, thus the study was continued with a modified version (98F1 mod) which also proved to be active as an accelerator of Hsp90/Aha1 to the same extent as 98F1.

The compounds bind with a micromolar affinity to the Hsp90/Aha1 complex

To further clarify the compounds' modulating properties on the Hsp90/Aha1 interaction, compound titrations were performed to determine the binding constants of each modulator to the Hsp90/Aha1 complex. Therefore, the modulators were titrated at concentrations of 0-500 μM to a complex of 1 μM Hsp90 and 20 μM Aha1. Enzyme kinetics were recorded, using the regenerative ATPase assay system. Catalytical activi-

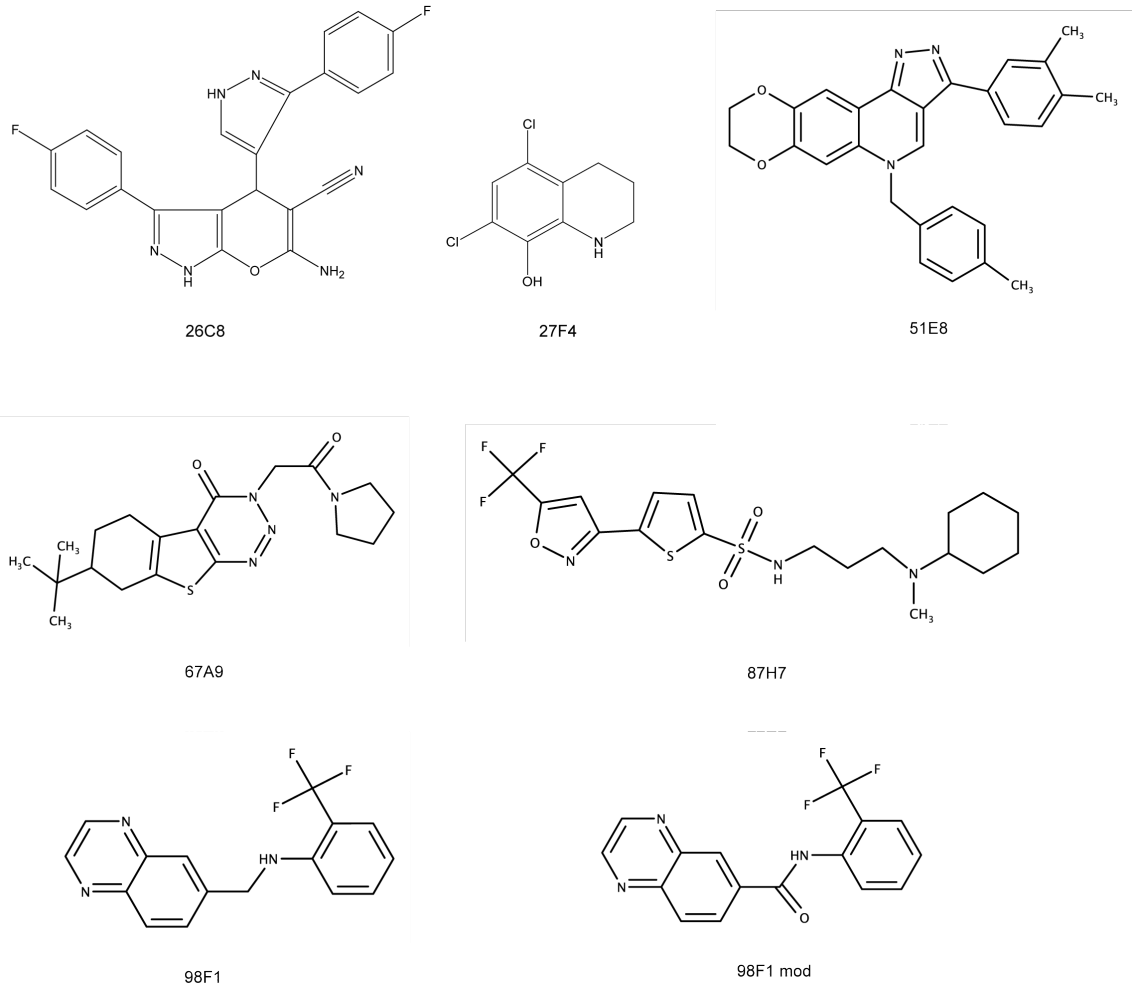

Figure 2.4: Structures of modulators for the Hsp90/Aha1 interaction. As 98F1 was not commercially available, a highly similar derivative (98F1 mod) was used for continuation of the study.

ties were plotted as function of substrate (compound) concentraton and fitted with the Michaelis-Menten model to obtain apparent binding constants of each modulator to the Hsp90/Aha1 complex. All compounds display affinities in the micromolar range as shown in table 2.1.

Table 2.1: **Binding affinities of the modulators to the Hsp90/Aha1 complex.**

Type	**Compound**	**kD (μM)**
Inhibitor	26C8	23.5 $\pm$ 1.7
	51E8	40.3 $\pm$ 5.2
	87H7	> 100
Activator	27F4	163 $\pm$ 42
	67A9	145.2 $\pm$ 70
	98F1	> 100

26C8 has the highest affinity for Hsp90/Aha1 with a kD of 23.5 $\pm$ 1.7 μM. The titration curve is shown in figure 2.5A. For 51E8, a kD of 40.3 $\pm$ 5.2 μM could be determined (figure 2.5B). The inhibitor 87H7 and the activator 98F1, respectively, show an affinity higher than 100 μM. For these molecules, even at concentrations of up to 500 μM saturation could not be reached. The affinity was therefore estimated to be greater than 100 μM. The activators, 27F4 and 67A9 show kDs of 163 $\pm$ 42 μM and 145.2 $\pm$ 70 μM, respectively (figure 2.5D and C, respectively).

Effects of the modulators on the Hsp90 ATPase without Aha1

Despite some clear effects on the Aha1 stimulation of Hsp90, a remaining question was if the modulator effects are only resulting from an altered Hsp90 ATPase activity. Thus, the Hsp90 ATPase activity, without Aha1, was measured in the presence of each modulator (c_{final} = 50 μg/ml). Figure 2.6A shows the effects of the modulators on the Hsp90 ATPase in the absence of Aha1. The catalytic activity was normalised to the ATPase activity of Hsp90 in the absence of compounds. The inhibitor 26C8 showed only a slight inhibition of the Hsp90 ATPase. In the presence of this modulator, the catalytic activity (k_{cat}) of Hsp90 decreased by 33 % from 0.67 min^{-1} to 0.45 min^{-1}. This inhibition of the Hsp90 ATPase might point to a mechanism wherein 26C8 alters the Hsp90 activity, but needs the presence of Aha1 to unfold its strong inhibitory potential.

Surprisingly, the inhibitor 51E8 activates the Hsp90 ATPase by 2-fold, when Aha1 is

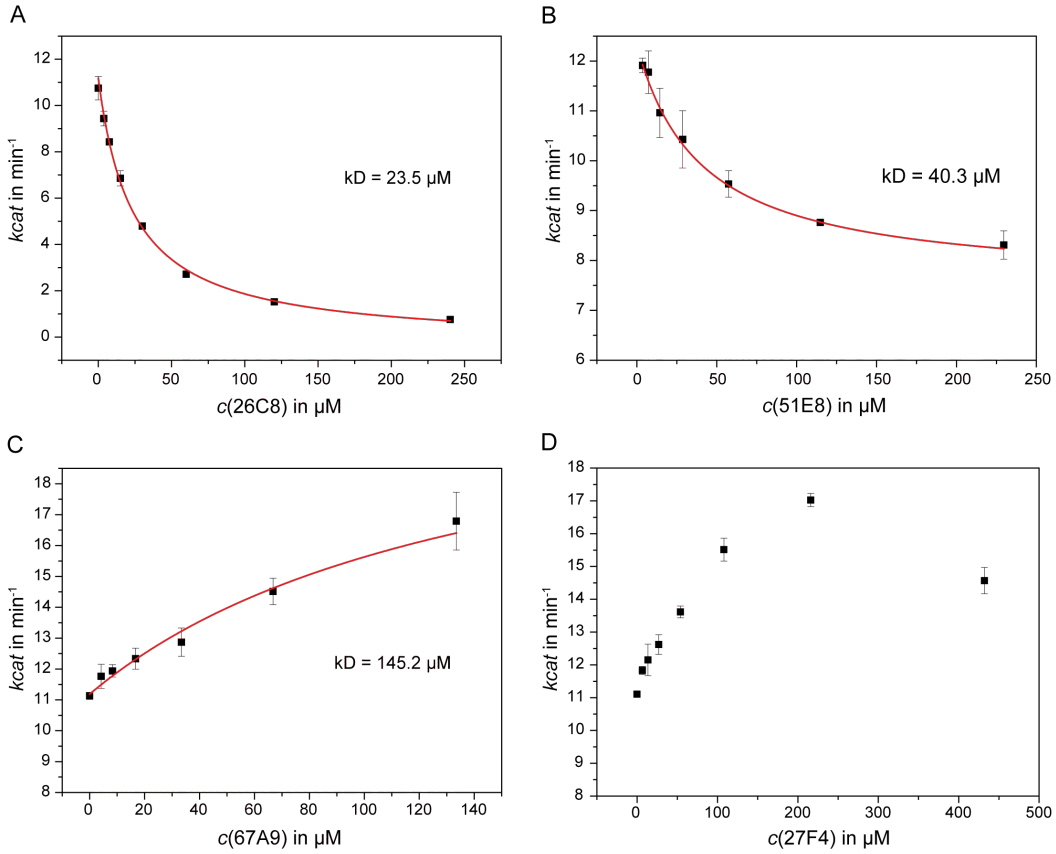

Figure 2.5: Modulator affinities to the Hsp90/Aha1 complex. ATPase rates (k_{cat}) of Hsp90 in the presence of Aha1 are depicted. Modulators were titrated to Hsp90/Aha1. 1 µM of Hsp90 was saturated with 20 µM Aha1 and ATPase activity was measured in low salt buffer at 30 °C. Apparent affinities (kD_{app}) were determined by non-linear regression using the Michaelis Menten fit.

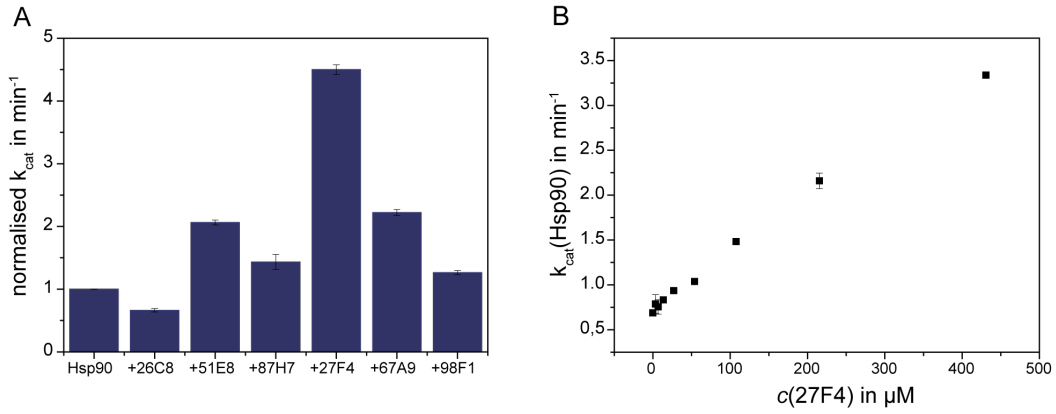

Figure 2.6: Modulator effects on the Hsp90 ATPase in absence of Aha1. A: ATPase rates (k_{cat}) of Hsp90 were determined in absence and presence of the modulators (c_{final} = 50 µg/ml). B: Titration of the activator 27F4 (0-500 µM) to Hsp90 in the absence of Aha1. The apparent binding affinity of 27F4 to Hsp90 in absence of Aha1 was determined applying the Michaelis Menten fit. The ATPase activity of 3 µM Hsp90 was measured in standard assay buffer at 30 °C.

not present. In the presence of Aha1, this modulator shows an inhibitory effect (28 % inhibition). This implies that 51E8 features a unique type of interaction with Hsp90. It shows a distinct mechanism, depending on whether Hsp90 is in complex with a co-chaperone or not. The inhibitor 87H7 does not show an alteration of the ATPase of Hsp90 and thus qualifies as a highly specific Hsp90/Aha1 inhibitor. The activator 27F4 exhibits a 4.5-fold activation of the Hsp90 ATPase activity, when Aha1 is not present. The effect on Hsp90 alone is much stronger than for the Hsp90/Aha1 complex. The observed activation of the Hsp90/Aha1 interaction in the initial FRET-based screening was therefor probably rather due to an activation of Hsp90. Interestingly, a 27F4-stimulated Hsp90 seems to be still able to be stimulated by Aha1 to a high extent, as seen in the ATPase data on Hsp90/Aha1 in the presence of 27F4. Due to its high activatory effect on the Hsp90 ATPase, 27F4 was titrated to Hsp90 to determine its apparent binding affinity (figure 2.6B). Even for concentrations up to 500 μM, no saturation with 27F4 could be reached, thus the kD could not be determined.
Compound 67A9 was initially screened as an activator of the Hsp90/Aha1 interaction - with a 1.5-fold stimulatory potential. On Hsp90, without co-chaperone, 67A9 displayed also a 2-fold activatory effect. The same behaviour was observed for the activator 98F1. Taken together, these results suggest that some of the characterised modulators do not specifically alter the interaction of Hsp90 and Aha1. In fact, most of the six compounds showed altering properties on the Hsp90 ATPase. All activatory compounds displayed stimulatory effects on Hsp90 alone. 67A9 and 98F1 showed a 2-fold activation of the Hsp90 ATPase, while 27F4 displayed a strong 4.5-fold activation of Hsp90. Surprisingly, 51E8, initially screened as an inhibitor for Hsp90/Aha1, displayed a 2-fold stimulation of the Hsp90 ATPase alone. This points to a rather unique mechanism of this modulator. Depending on the conformational or complexed state Hsp90 is in, 51E8 displays different modulatory properties. A stimulatory effect on Hsp90 alone, or an inhibitory effect on Hsp90 together in complex with Aha1. The only modulator not showing an effect on Hsp90 alone is the inhibitor 87H7. Thus, it is speculated that this inhibitor is highly specific for the Hsp90/Aha1 interaction. The strongest inhibitor 26C8 also altered the Hsp90 activity alone. Its presence resulted in a 30 % inhibition of Hsp90. Nonetheless, the inhibitory effect on Hsp90 alone is much weaker compared to the initially observed effect together with Aha1 (93 % inhibition). The inhibition of Hsp90 alone might result in a conformation of Hsp90, which hinders Aha1 interaction or binding. The primary site of interaction seems to be Hsp90 for this inhibitor. Nevertheless, the presence of 26C8 causes a much weaker stimulation of Aha1, pointing towards either an inhibition of the Hsp90-Aha1 interaction or holding Hsp90 in a conformation that hydrolyses ATP much slower. This induced conformation cannot be revoked by Aha1, thus no Aha1 stimulation can occur.
A closing remark in this section refers to the ATPase assay itself which was used for further characterisation of the identified compounds. By testing the 40 initially positive screened hits, 34 modulators were rejected due to the fact that they did not display

altering effects on the Hsp90 ATPase activity under Aha1 influence. The crux in this screening approach lies in the inability to detect specific Aha1 effects. By application of the ATPase assay, the focus lies on the Hsp90 activity itself. Measuring the Hsp90 activity under the influence of Aha1 can only give an indirect read-out on modulating properties of the Hsp90/Aha1-interaction. Thus, it might be possible that some of the 34 rejected small molecules were highly specific Aha1 inhibitors, with no effect on the Hsp90 ATPase activity. By mischance, except for the Hsp90/Aha1 FRET assay, no specific assay for yeast Aha1 exists to date since this protein does not display an ATPase or chaperoning activity by itself (in contrast, human Aha1 has indeed a chaperoning function due to a N-terminal 22 amino acid sequence which is absent from yAha1) [Tripathi et al., 2014]. Furthermore, the given binding affinities of the compounds are only apparent affinities due to the nature of the applied assay. For a direct kD value, other methods, like ITC or SPR should be applied. These approaches were tried in the context of this work. However, they failed due to feasibility or solubility issues of the small molecules. The presented apparent affinities are thus an estimation for the interaction of the modulators with the Hsp90/Aha1 complex. The low micromolar range affinity of 26C8 is a good starting-point for further optimisation of this compound and will be further described in the chapter 2.1.6 - Derivatives of the modulator 26C8. A desirable binding affinity would be in the submicromolar range, e.g. a nanomolar affinity as it is the case for geldanamycin and its derivatives [Stebbins et al., 1997, Neckers and Workman, 2012].

2.1.3 NMR data on the 26C8 inhibitor

Most Hsp90 inhibitors bind to the Hsp90 N-terminal domain and thereby inhibit ATP binding to Hsp90 (reviewed in [Neckers and Workman, 2012]). Thus, Hsp90 cannot fulfill its role as a potent chaperone. Since chaperoning function is also crucial for general cellular processes and important for cell survival, it would be desirable to target the Hsp90 machinery in a more specific way. The identified modulators are promising in interfering with the Hsp90/Aha1 interaction. NMR data in collaboration with the group of Prof. Michael Sattler (TU Munich) could identify residual shifts in the Hsp90 MD upon binding of the inhibitor 26C8. Residues shifted in this region could be identified as essential participators of the interaction with Aha1 (depicted in fig. 2.7).

No direct binding of 26C8 to Aha1 was observed. Thus 26C8 seems to target Hsp90 and thereby alters the mode of interaction of Hsp90 with Aha1. Furthermore, NMR data on the Hsp90 NTD revealed a second interaction site of 26C8. The interaction site lies near the ATP binding pocket [Prodromou et al., 1997]. Figure 2.8 visualises the affected residues in the NTD (coloured in red) upon 26C8 binding. In total, 26 residues of the NTD shifted strongly in the recorded NMR spectra under the influence of 26C8. Affected residues cluster near the nucleotide binding pocket of Hsp90: The helices 28-50 and 85-

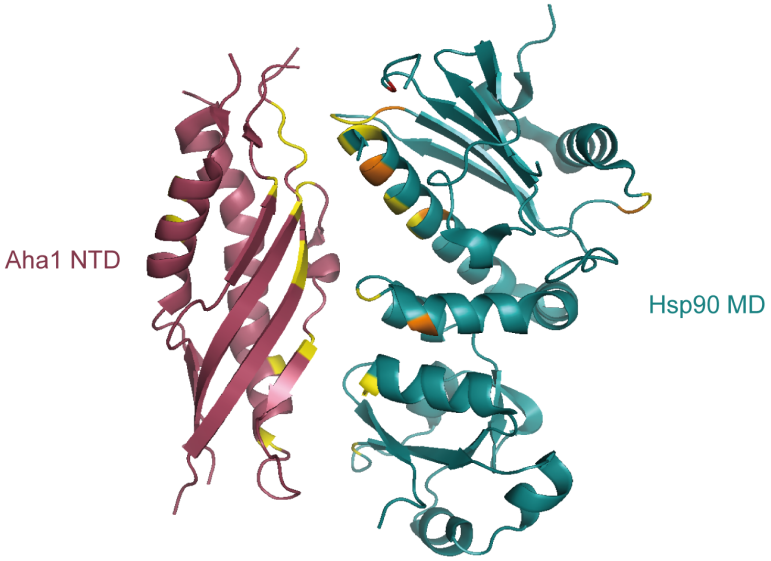

Figure 2.7: Affected residues in the Hsp90 MD upon binding of 26C8. ^{15}N spectra of the Hsp90 MD (teal) and Aha1 NTD (rasberry) were measured and affected residues were mapped onto the crystal structure 1usu of yeast Hsp90 in complex with Aha1. Shifted residues which overlap with the Hsp90/Aha1 interface are depicted in orange. Residues forming the Hsp90/Aha1 interface are coloured in yellow.

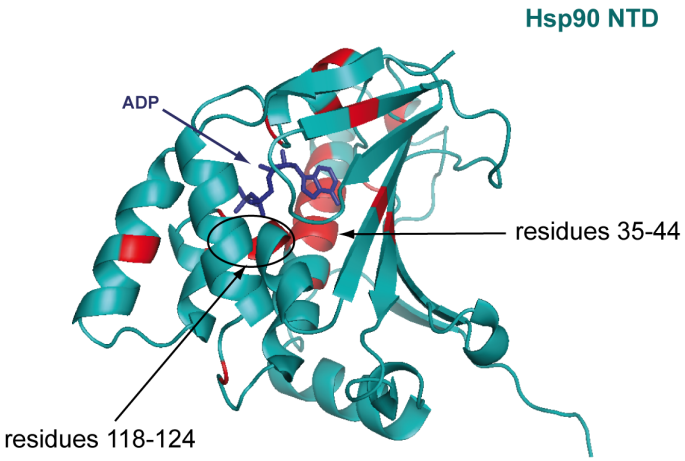

Figure 2.8: Affected residues in the Hsp90 NTD upon binding of 26C8. ^{15}N spectra of the Hsp90 NTD were recorded and affected residues were mapped onto the crystal structure 1am1 of yeast Hsp90. ATP is depicted in blue, while shifted residues are coloured in red.

94 which are part of the Hsp90 nucleotide binding pocket are highly affected [Prodromou et al., 1997]. Another two loop structures of the nucleotide binding pocket, 81-85 and 117-124, also strongly shift. This might explain the inhibition of the Hsp90 ATPase. 26C8 might trigger conformational rearrangements that disfavour nucleotide binding to Hsp90 and thus impede nucleotide binding. However, the ATPase activity is only inhibited by about 30 % as seen from the ATPase assay data. Hindered ATP binding might be the explanation for this. However, ATP binding is not completely abolished since the ATPase activity of Hsp90 is not entirely inhibited by 26C8. Interestingly, the α-helix spanning the residues from E28 to L50 is a helix motif which can also be found in gyrases [Prodromou et al., 1997], implicating that this inhibitor might also be potent in inhibiting other enzymes of a cell.

2.1.4 Effect on ATP binding to Hsp90

Titrations of ATP and 26C8 to Hsp90 by NMR showed that 26C8 is able to compete with ATP and even to displace ATP from the Hsp90 binding pocket (data obtained by Martin Ruebbelke, Chair of Biomolecular NMR Spectroscopy, Prof. Michael Sattler). Considering this, we tested whether 26C8 influences ATP binding of Hsp90 (figure 2.9). ATP titrations with 0-3 mM ATP in the presence and absence of the inhibitor, and also in the presence and absence of Aha1 were performed. As shown in figure 2.9C, the ATP affinity of Hsp90 is not altered in the presence of Aha1 (kD = 0.28 mM and kD = 0.23 mM in the absence and presence of Aha1, respectively). In the presence of the inhibitor 26C8, the ATP affinity of Hsp90 is dramatically decreased to a kD of 4.34 mM (fig. 2.9B). However, ATP affinity of Hsp90 in complex with Aha1 is even further increased by 26C8 (kD = 11.09 mM) as depicted in fig. 2.9D.

In conclusion, the inhibitor 26C8 possesses altering properties on Hsp90's affinity to ATP. As seen in the NMR experiments, a competition with ATP binding is confirmed in the ATPase assay. Nonetheless, the Hsp90 affinity to ATP is even further decreased, when Aha1 and the inhibitor are present. Thus, it is speculated that the competition with ATP binding is not the only possible underlying mechanism for 26C8. 26C8 binds to the Hsp90 NTD and modulates Hsp90's chaperoning function by competing with ATP. This would classify it as an 'ordinary' Hsp90 inhibitor. Nonetheless, the binding site of Aha1 to Hsp90 lies within the MD as well as in the NTD. The Aha1 CD was shown to interact with the Hsp90 NTD [Retzlaff et al., 2010], while Aha1's NTD packs against the Hsp90 MD [Meyer et al., 2004]. Interaction of 26C8 with the Hsp90 NTD, might prevent the Aha1 CD from binding to or interacting with the Hsp90 NTD. Thus the ATPase activity of Hsp90 cannot be fully stimulated, as it was shown that for complete stimulation of Hsp90, the presence of full-length Aha1 is pivotal [Panaretou et al., 2002, Retzlaff et al., 2010]. The Aha1 ND has, however, a slightly activating potential of Hsp90, but for complete

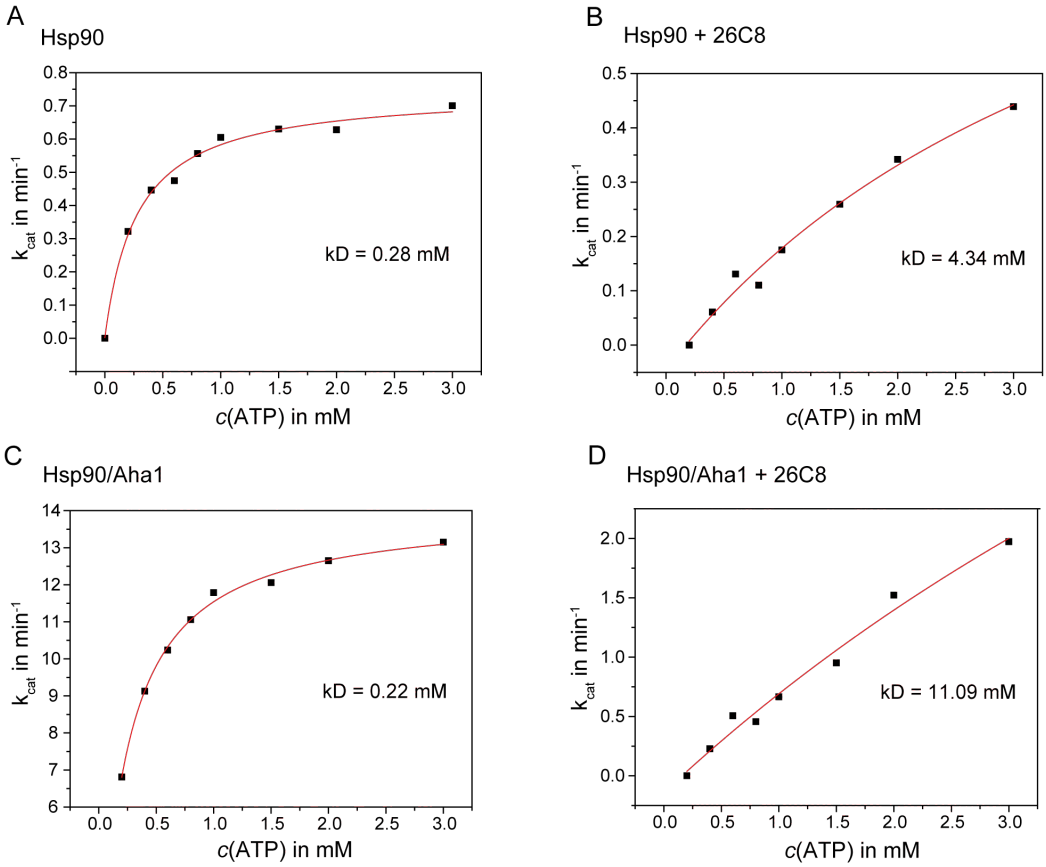

Figure 2.9: Influence on the Hsp90 ATP affinity by the inhibitor 26C8. ATP titrations (0-3 mM ATP) to Hsp90 (3 µM) and the Hsp90/Aha1 (1 µM/20 µM) complex with and without 26C8 (120 µM) were performed. Assays were carried out in low salt buffer at 30 °C. The obtained curves were fitted with the Michaelis-Menten kinetics fit to obtain the apparent binding affinity (kD_{app}.)

stimulation of Hsp90, full-length Aha1 is required [Lotz et al., 2003, Retzlaff et al., 2010].

2.1.5 Modulator influence on Hsp90/Aha1 complex formation

Analytical ultracentrifugation (aUC) was applied to address the question if an altered stimulation of Hsp90 by Aha1 is derived from a disruption of Hsp90/Aha1 complex formation. First, fluorescence aUC was carried out. Alexa488-labelled Aha1, as also used in the Hsp90/Aha1 FRET system, was traced. Complex formation with Hsp90 was observed in a nucleotide-dependent manner, with a higher efficiency in the presence of AMP-PNP (as published in [Li et al., 2013]). The modulators were tested at different concentrations for complex disruption between Hsp90 and Aha1 (figure 2.10). Unfortunately, all measurements suffered from high quenching at high modulator concentrations. Since the peak for unbound Aha1 does not increase when the amount of the Hsp90/Aha1 complex decreases, quenching events must be present. Even at low inhibitor concentra-

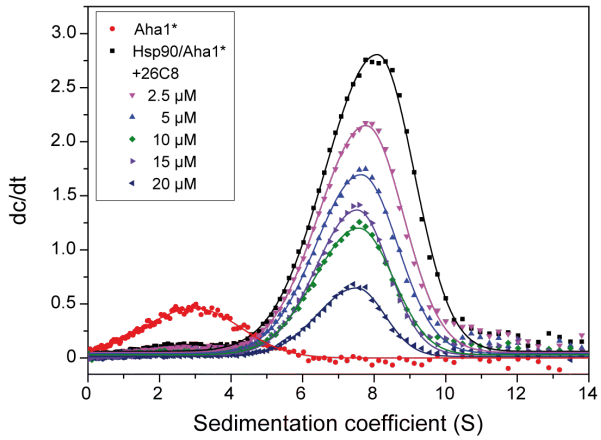

Figure 2.10: Titration of 26C8 to Hsp90/Aha1. Fluorescence aUC measurements on complex formation of Hsp90 and Aha1 (Alexa488 labelled, indicated by an asterisk) in absence and presence of the inhibitor 26C8 were performed. 400 nM of Aha1*Alexa488 and 4 µM of Hsp90 were used. Measurements were performed in the presence of 2 mM AMP-PNP and the indicated concentrations of 26C8.

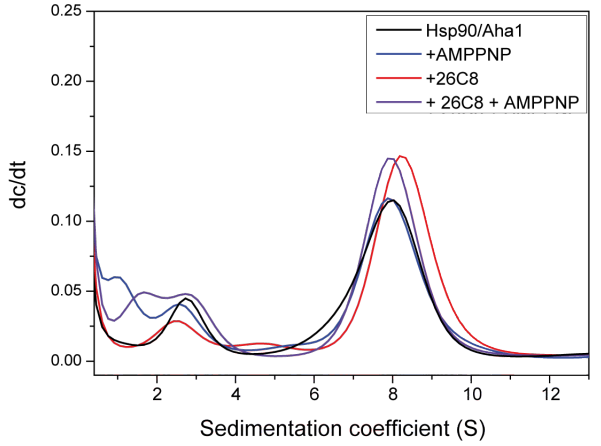

Figure 2.11: Effect of 26C8 on the Hsp90/Aha1 complex. Absorbance aUC measurements on complex formation of Hsp90 and Aha1 in the absence and presence of the inhibitor 26C8 were performed. Absorbance at 280 nm and 3 µM of each protein was measured. Where indicated 0.5 mM of AMP-PNP and 120 µM of 26C8 were added. Samples were corrected for buffer absorbance and, where applicable, nucleotide and compound absorbance.

tions, quenching effects were observed. Following this, a label-free method was used for compound testing: absorbance aUC. There, unlabelled protein complexes are detected at wavelengths of 230 or 280 nm. Prior to these measurements, compound spectra were recorded. 26C8 shows absorbance maxima at 230 nm and 250 nm. Thus, a wavelength of 280 nm was chosen to perform the absorbance aUC runs. Hsp90 and Aha1 were incubated to allow complex formation and 0.5 mM of AMP-PNP was added. As figure 2.11 indicates, complex formation of Hsp90 and Aha1 is highly efficient in equimolar ratios since the addition of AMP-PNP does not increase the complex fraction (black and blue curves). The addition of 26C8 in saturating concentrations results in a shift of the complex to a higher S value (red curve). This shift points towards a higher compaction of Hsp90. Furthermore, the fraction of unbound Aha1 (around 3 S) is decreased upon addition of 26C8. This indicates that the proportion of Hsp90-bound Aha1 is increased by 26C8. The addition of 0.5 mM AMP-PNP to Hsp90/Aha1/26C8 results in a shift back to a lower S value which is identical to the S value of the Hsp90/Aha1 complex. This observation was rather unexpected since one would have guessed that an inhibitor like 26C8 might prevent complex formation of Hsp90 and Aha1. In fact, complex formation seems to be promoted. The impaired stimulation of Hsp90 by Aha1 in the presence of 26C8 might therefore not be the result of a repressed complex formation, but more due to formation of a highly ineffective complex: Even when bound to Hsp90, Aha1 cannot fulfill its role of a potent ATPase stimulator in the presence of 26C8. Presumably, Hsp90 is trapped in a state which hinders progression through the ATP cycle.

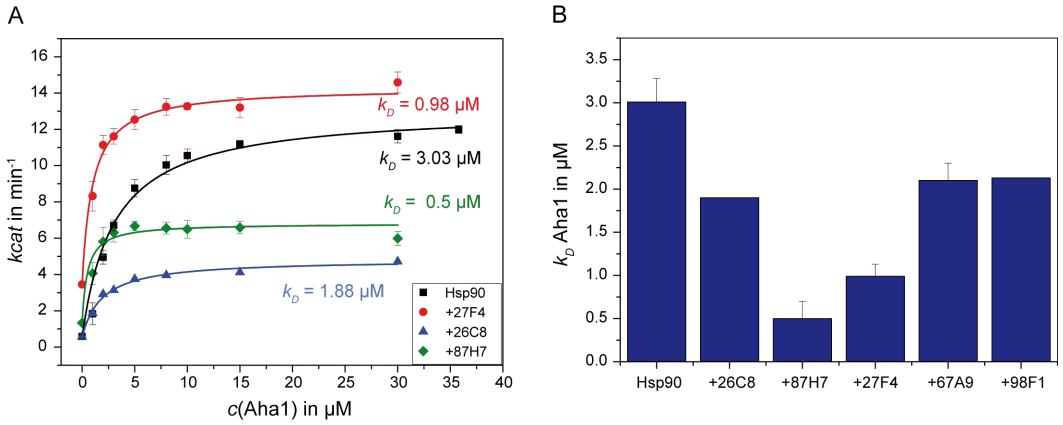

Figure 2.12: Affinity of Hsp90 to Aha1 under the influence of different modulators. Titrations of Aha1 in the absence and presence of different modulators of the Hsp90/Aha1 interaction (26C8, 87H7, 27F4, 67A9, 98F1) were performed. A: Affinity of Aha1 to Hsp90 (black) under influence of 26C8 (blue), 27F4 (red) and 87H7 (green), respectively. B: Binding affinities obtained by Aha1 titrations to the Hsp90/compound influence. 1 µM of Hsp90 was saturated with the respective compound. 1-30 µM Aha1 was titrated to the complex using the regenerative ATPase assay.

Since 26C8 seems to trigger complex formation of Hsp90 with Aha1, affinity titrations

were performed. As depicted in figure 2.12, all tested modulators seem to increase the affinity of Hsp90 to Aha1 (affinities summarised in fig. 2.12B). This is in agreement to the results from the aUC measurements for 26C8.

2.1.6 Derivatives of the modulator 26C8

The inhibitor 26C8 showed the strongest effects of all the tested modulators *in vitro* . Thus, we were wondering if a derivatisation of 26C8 might improve its potency even further. In collaboration with the chair of organic chemistry of Prof. Stephan Sieber (TU Munich), derivatives of 26C8 were generated. The structures of these derivatives are presented in figure 2.13.

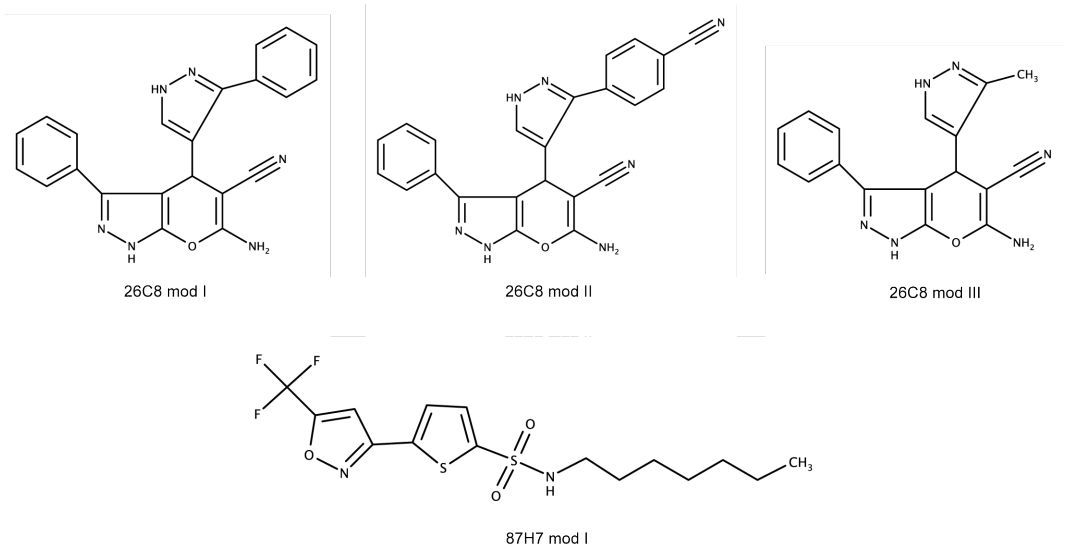

Figure 2.13: Derivatives of the inhibitors 26C8 and 87H7. Derivative structures of the inhibitor 26C8 used in this work are shown. One derivative of 87H7 was also tested but was not effective in modulating the Hsp90/Aha1 interaction.

All derivatives were tested for their potential to alter the Hsp90 ATPase activity under the influence of Aha1 (fig. 2.14A). Therefore, the derivatives' effects were compared to the effects of the unmodified compounds. 87H7 mod. lost its effect of modulating the Hsp90 ATPase in the presence of Aha1 (data not shown). Thus, this compound was not suitable for further experiments. The derivatives of the inhibitor 26C8 still showed modulating properties of the Hsp90 ATPase as presented in figure 2.14A. Modulator 26C8 mod I and 26C8 mod III lead to an almost complete depletion of the Hsp90 ATPase activity. Titrations of these derivatives were performed to further assess the mode of interaction of these molecules with Hsp90. A titration with 26C8 mod III revealed a very weak interaction, showing a kD of 179.2 μM. 26C8 mod I bound with a much higher

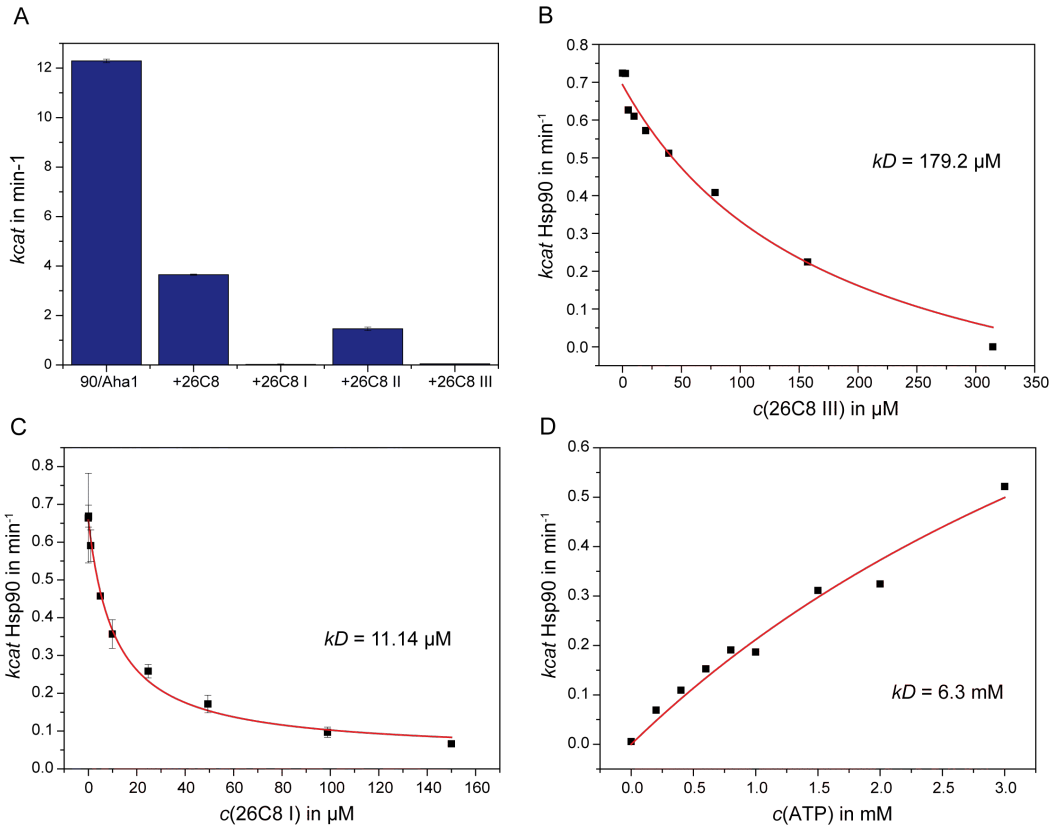

Figure 2.14: Effects of the 26C8 derivatives on the Hsp90 activity. A: Effects of the 26C8 modulator series on the stimulatory potential of Aha1 on Hsp90. 120 µM of each modulator were applied to Hsp90/Aha1 (1 µM/20 µM) and their effects on the k_{cat} of Hsp90 were assessed. Measurements were performed in low salt buffer at 30 °C. B/C: Titrations of 26C8 mod III (B) and 26C8 mod I (C) to 3 µM Hsp90. D: Titration of ATP to the Hsp90/26C8 mod I (3 µM/120 µM) complex. Measurements B-D were performed in standard assay buffer at 30 °C. Kinetics were fitted by non-linear regression using the Michaelis Menten fit.

affinity (kD 11.14 μM) to Hsp90 and abolished Hsp90's catalytical activity completely at a concentration of 150 μM. This effect on Hsp90 is more pronounced for this derivative than for the unmodified version of 26C8. To further address if the depletion of the Hsp90 activity is due to competition with ATP, ATP titrations to an Hsp90/26C8 mod I complex were performed. The affinity of ATP to Hsp90 is decreased around 20-fold in the presence of 26C8 mod I (kD 6.3 mM). This drastic decrease in ATP affinity points to a mechanism where 26C8 mod I competes with ATP for Hsp90's ATP binding pocket. This would be another example for a modulator interacting with the ATP binding pocket of Hsp90, similar to mechanisms of the established Hsp90 inhibitors radicicol or GA.
26C8 mod II is the most potent molecule of the tested derivatives in terms of specific modulation of the Hsp90/Aha1 interaction, since it still hinders Aha1 stimulation of Hsp90. However, the Hsp90 ATPase activity is more decreased in the presence of 26C8 mod II, than in the presence of 26C8. Therefore it seems that 26C8 mod II acts more on Hsp90 alone than specifically on the interplay of Hsp90 and Aha1.

2.1.7 Effects on client maturation

In the next step, the *in vivo* effects of the identified modulators on Hsp90 clients were examined. Effects on the activity of steroid hormone receptors (SHR), an important class of Hsp90 clients, were investigated. In particular, the glucocorticoid receptor (GR) and the mineralcorticoid receptor (MR) activities were addressed. As already mentioned, GR is a widely studied client of Hsp90. GR is highly dependent on Hsp90 and the interplay of the Hsp70-Hsp90 machinery [Lorenz et al., 2014, Kirschke et al., 2014]. Inhibition of Hsp90 with radicicol, but also with GA showed a reduced GR activity *in vivo* and demonstrated the importance of Hsp90 chaperoning of GR [Bamberger et al., 1997, Rosenhagen et al., 2001]. MR showed reduced activity in ΔAha1 yeasts and is thus dependent on the presence and function Aha1 (Dissertation Priyanka Sahasrhabudhe). To this end, an alteration of MR activity by the identified modulators was expected. To monitor GR and MR activity, respectively, in yeast, a β-galactosidase reporter assay was applied. A hormone-inducible (Aldosterone for MR, DOC for GR) expression plasmid for GR and MR, respectively, and a coupled, inducible β-galactosidase (β-Gal) reporter system allows functional examination of SHRs in yeast cells. Each measurement was performed in triplicates and repeated at least three times. Modulators were added to the cells in concentrations of 0-1000 μM. For each modulator concentration, a DMSO control was included. DMSO did not change the SHR activity in yeast. The normalised data of the SHR (MR and GR, respectively) activity is shown in figure 2.15.
GR activity remains almost unaffected by the Hsp90/Aha1 inhibitor 26C8 (fig. 2.15C). Even at high concentrations, the GR activity remains on a high level of around 90 %. Compared to the modulation of GR activity, the effect for 26C8 is much stronger on MR activity (depicted in fig. 2.15A, red bars). In the presence of 26C8, MR activity is

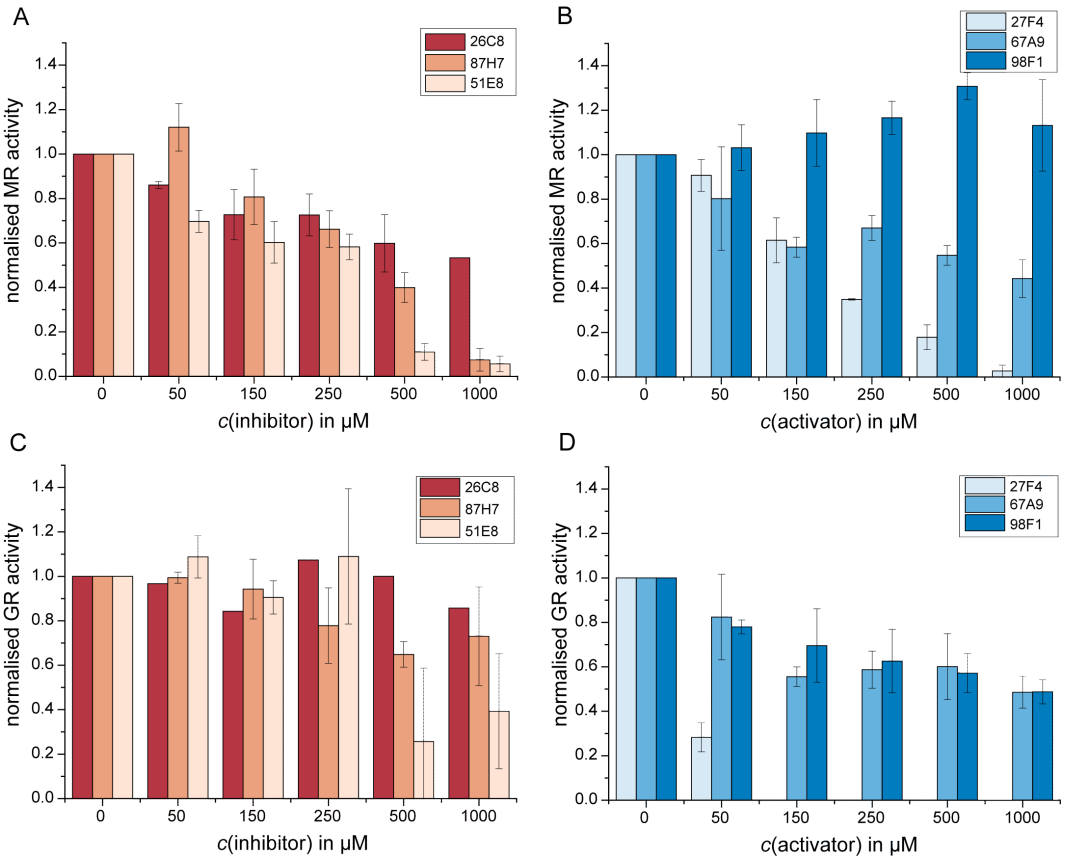

Figure 2.15: Effects of the Hsp90/Aha1 modulators on SHR activity in yeast. SHR activity in yeast was monitored at different modulator concentrations (0-1000 µM) using the β-Gal reporter assay. A+B: Effects of the Hsp90/Aha1 modulators on MR activity. C+D: Effects of the Hsp90/Aha1 modulators on GR activity. Each measurement was performed in triplicates and repeated at least three times. For each concentration, a DMSO control was included. Activities were normalised and the standard deviation was calculated.

decreased by up to 40 %. These findings show the high potency of 26C8 not only *in vitro*, but also *in vivo*. The alteration of MR, but not of the GR activity implies a selective targeting of the Hsp90/Aha1 interplay.
Modulator 51E8 displayed 40 % of inhibition on the MR activity without influencing the GR activity up to a concentration of 250 μM 51E8 (fig. 2.15A and C, orange bars). At higher compound concentrations, the inhibitory effect on MR was even higher (up to 90 %). However, a slower growth and lower OD of the yeast cells was observed at such high concentrations so that this inhibition might be due to general toxicity effects of 51E8.
The inhibitor 87H7 showed the strongest inhibition of MR activity *in vivo* (fig. 2.15A, salmon bars). There was no effect on GR activity up to a concentration of 150 μM. At higher concentrations of 87H7, GR activity was inhibited around 30 %. Surprisingly, modulator 67A9, screened as an *in vitro* activator, had a pronounced inhibitory effect on SHR activity *in vivo* (fig. 2.15B, medium blue bars). MR activity, as well as GR activity were both decreased by 50 %. This compound was shown to be an activator of the Hsp90 ATPase activity when Aha1 is present *in vitro*. This activation of Hsp90 seems to alter the potential of Hsp90 to activate or at least maintain the cellular function of GR and MR, respectively. The modulator 98F1 shows an activation of MR activity in the β-Gal assay up to 30 %, while in turn, the GR activity is decreased to 50 % (fig. 2.15 B+D, dark blue bars). The activator 27F4 is a highly potent modulator of SHR activity in yeast (fig. 2.15 B+D, light blue bars). For MR, an almost completely abolished activity was observed, while for GR, no activity could be detected for 27F4 concentrations higher than 100 μM. Titrations of 27F4 were thus performed at lower concentrations to assess the potency of this modulator (fig. 2.16).
These titrations confirmed the high efficacy of 27F4 to inhibit SHR activity in yeast. For MR, 300 μM 27F4 lead to almost complete inhibition, while GR was even more sensitive to 27F4. At a concentration of 150 μM 27F4, there was no detectable GR activity.

These experiments considered that an Aha1-specific effect of the compound should manifest in a higher modulation of the MR activity. MR was found to be more dependent on Aha1 in yeast than GR (Dissertation Priyanka Sahasrhabudhe) However, this is a rather indirect way for showing a specificity of modulators for the Hsp90/Aha1 interplay. For the most promising inhibitor 26C8, titrations were performed not only in a wt yeast strain, but also in a △Aha1 strain. This approach identified a much more pronounced effect of 26C8 in wt yeast cells on MR activity than in the △Aha1 strain as depicted in figure 2.17.

As expected, DMSO does not alter MR activity, neither in the wt strain, nor in the △Aha1 strain (black curve, fig. 2.17). The shown DMSO controls represent triplicates from four independent experiments (error bars are included, but on this scale negligibly small). In △Aha1 cells, 26C8 does not reduce MR activity significantly (blue line, fig. 2.17), whereas a decrease in MR activity of up to 40 % can be seen in wt yeast cells. In conclusion, this confirms that the effect of decreased MR activity by 26C8, is mediated by a

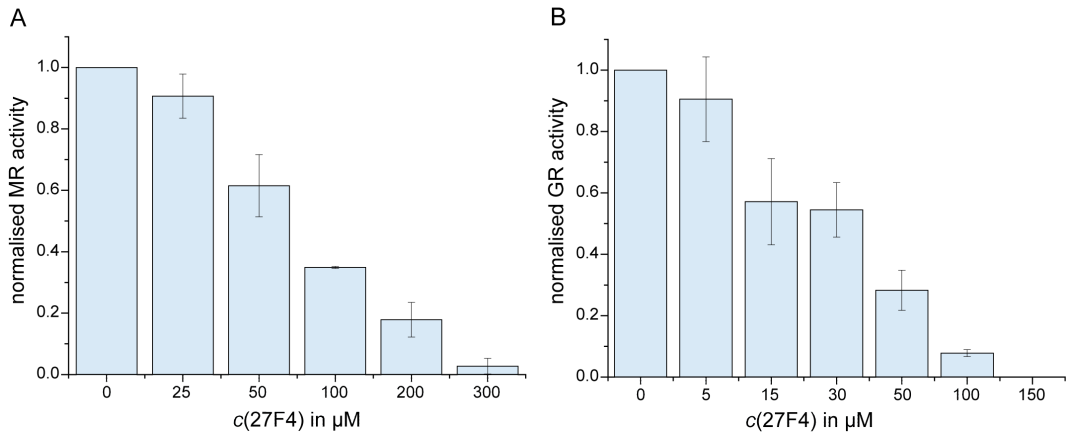

Figure 2.16: Effects of 27F4 on SHR activity in yeast. SHR activity in yeast was monitored in the presence of the modulator 27F4. A: Effects of 27F4 on MR activity. B: Effects 27F4 on GR activity. Each measurement was performed in triplicates and repeated at least three times. For each concentration, a DMSO control was included. Activities were normalised, averaged and the standard deviation was calculated.

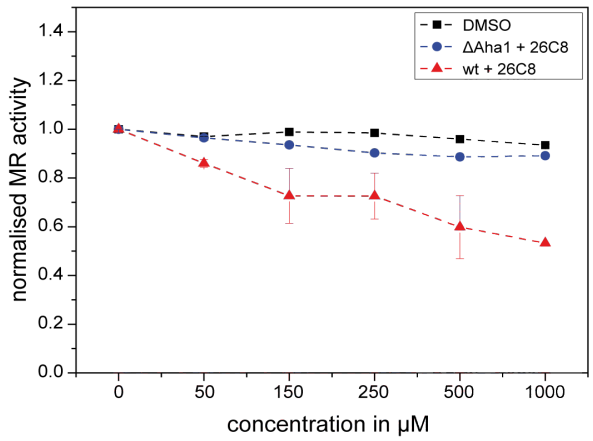

Figure 2.17: Effect of 26C8 on MR activity in wt and Aha1 yeast cells. The MR activity in wt and ΔAha1 yeast cells was determined at different concentrations of 26C8. Activities were normalised relative to the DMSO control. Measurements were performed in triplicates and repeated twice.

specific interaction of 26C8 with the Hsp90/Aha1 interplay.
Taken together, these results suggest that the screened compounds are highly potent modulators of the Hsp90 interaction with steroid hormone receptors *in vivo*. The selective alteration of MR activity, but not GR activity for 26C8, 87H7 and 51E8 indicates a specificity of the inhibitors towards the Hsp90 co-chaperone Aha1. The fact that activation of the Hsp90-Aha1 interaction *in vitro* results in an inhibitory effect on SHR activity *in vivo* denotes a unique mechanism for the identified compounds. For the activators 27F4, 67A9 and 98F1, it seems that an increased Hsp90 ATPase activity does not provide enough time for client processing/folding and therefore leads to reduced client activity *in vivo*. An acceleration of the Hsp90 chaperone cycle was already shown to lead to a decreased client processing *in vivo* [Zierer $\mathrm{et\ al.}$, 2014]. This approach might be another strategy for the intervention of the Hsp90 chaperone system.

2.1.8 Modulation of the CFTR degradation

As mentioned earlier, the co-chaperone Aha1 is important in the CFTR folding pathway [Wang $\mathrm{et\ al.}$, 2006]. The disease-related mutant form of CFTR, $\triangle$F508 CFTR, is a misfolded protein which is degraded before it is able to reach incorporation into the plasma membrane [Van Goor $\mathrm{et\ al.}$, 2011]. Thus, its function as ion channel is made impossible and causes cystic fibrosis, a severe sickness in humans [Riordan $\mathrm{et\ al.}$, 1989,Qu $\mathrm{et\ al.}$, 1997]. Studies on $\triangle$F508 CFTR showed that the misfolded protein would even be functional, although less efficient than the wild-type form of CFTR [Wang $\mathrm{et\ al.}$, 2006]. Degradation of $\triangle$F508 CFTR was shown to be triggered, amongst others, by the Hsp90/Aha1 machinery. Thus, the effect of the Hsp90/Aha1 inhibitor 26C8 on CFTR degradation was investigated. As Wang *et al.* (2006) demonstrated, a downregulation of Aha1 levels was able to rescue $\triangle$F508 CFTR from degradation. Following this, treatment with the Hsp90/Aha1 inhibitor 26C8 should have a similar effect. Since it disrupts the stimulatory effect of Aha1 on Hsp90, it might be comparable to a knockdown of Aha1 and result in stabilisation of the $\triangle$F508 CFTR.
First, wild-type and $\triangle$Aha1 yeast strains were transformed with a CFTR plasmid, encoding either the wt or the mutant, $\triangle$F508 CFTR (constructs were a kind gift from Jeff Brodsky, University of Pittsburgh, USA). CFTR levels were analysed by Western blotting using an HA antibody, since the CFTR constructs were HA-tagged. CFTR was only detectable in significant amounts during the log phase of yeast growth. Figure 2.18 depicts the amount of CFTR in both, wt and $\triangle$Aha1 yeast cells. As expected and in agreement with published results, the stability of $\triangle$F508 CFTR is enhanced in the $\triangle$Aha1 strain. It is also expressed to a lower extent in wt yeasts than the wt CFTR. However, it was surprising that the amount of wt CFTR is decreased in $\triangle$Aha1 yeasts. It would have been expected that the amount of wt CFTR at least stays at the same level and is not dramatically dependent on the presence of Aha1, as supposed by Wang *et al.* (2006).

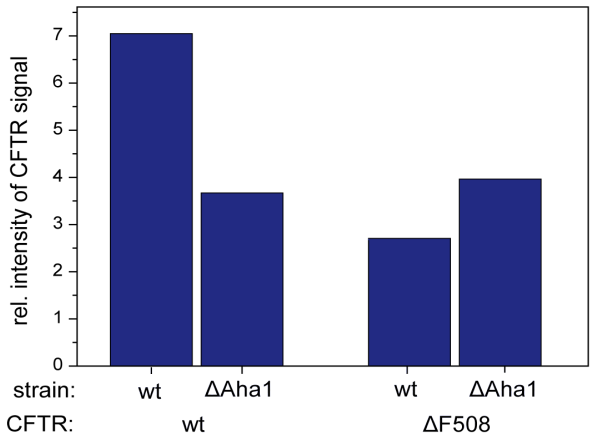

Figure 2.18: CFTR levels in wt and △Aha1 yeast cells. The amount of CFTR expressed in wt and △Aha1 yeast cells was determined by Western Blot. Intensities were corrected for the PGK loading control.

Effects of the inhibitor 26C8 were subsequently addressed. The wt yeast strain expressing either wt CFTR or the △F508 variant were treated with cycloheximide. This results in a general inhibition of translation and thus also of CFTR. CFTR levels were followed over a time span of 40 min. PGK served as a loading control. Since PGK levels did not remain the same throughout the experiment, CFTR levels were corrected for the PGK controls to balance differences in loading. Figure 2.19 shows a representative blot and its quantification for the degradation of wt (A) and △F508 CFTR (B), respectively. After 5 min, a significant amount of CFTR was already degraded: 60 % of wt CFTR and 65 % of △F508. wt CFTR showed a slower degree of reduction during the time course than △F508, confirming that it has a higher stability than △F508. After 40 min, only 4 % of the initial amount of △F508 CFTR was present, while about 20 % of wt CFTR can still be detected. In the presence of the inhibitor 26C8, the CFTR life span was extended (dark red bars, fig. 2.19). After 5 min, levels of each, wt and △F508 CFTR, are only reduced by 20 %, whereas without modulator, a reduction of 60 % was observed for both CFTR forms. Degradation of CFTR could not be completely prevented by 26C8, but the data implies that degradation is progressing slower. After 25 min, 40 % of the △F508 CFTR was still detectable (only 5% without inhibitor). In case of the wt CFTR, the detected levels were similarly high as for the △F508 variant. However, the relative difference in stabilised amounts was less dependent on the modulator for wt than for △F508. The detectable CFTR wt amount after 25 min was 20 % in absence of modulator, while in the presence of modulator, 40 % could still be detected. For △F508, after 25 min, 8 % of the initially detected CFTR was detected in the absence of 26C8. In its presence, 40 % of △F508 was detected.

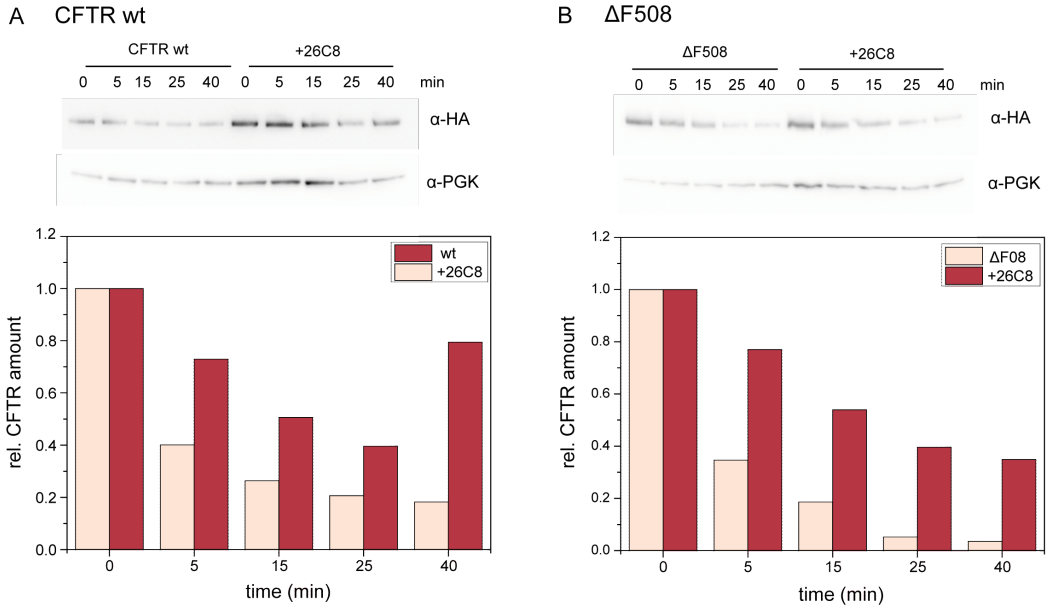

Figure 2.19: CFTR degradation in the presence of the inhibitor 26C8. Cycloheximide chases of wt (A) and ΔF508 CFTR (B) in the presence and absence were performed with yeast cells expressing CFTR wt and ΔF508, respectively. CFTR was detected using an HA-antibody, PGK served as loading control. CFTR signals were determined relatively to the PGK loading controls.

2.1.9 Conclusions

A screening of a 10,000 compound library using an Hsp90/Aha1 FRET assay, resulted in the identification of different modulators for the Hsp90 machinery. Six compounds showed promising effects and characteristic activity profiles. In addition to the Hsp90/Aha1 FRET and ATPase assays, the effects of the identified modulators were addressed in more detail. Effects on the Hsp90 ATPase activity in the absence of co-chaperones revealed that not all of the six compounds are specifically modulating the Hsp90/Aha1 interplay. Indeed, with 27F4, a strong activator of the Hsp90 ATPase (6-fold activation) was found. This activatory effect causes a dramatic decrease of GR client activity *in vivo*. The principle of a strong acceleration of the Hsp90 ATPase might initially sound contradictory. However, a high Hsp90 activity results in a change of the progression of the conformational cycle and most likely in less time for the contact with the client protein. The client might be released before complete activation can take place, which results in less active client proteins [Zierer $\mathrm{et\ al.}$, 2014].
With the inhibitor 26C8, another promising modulator was discovered. 26C8 showed a pronounced effect on the stimulation of Hsp90 by Aha1. Stimulation of Aha1 was decreased by 93 % in the presence of 26C8. Affinity titrations with 26C8 revealed a micromolar binding affinity (23.5 $\pm$ 1.7 μM) to Hsp90/Aha1. The effect on the Hsp90 ATPase in the absence of Aha1 was rather moderate (30 % inhibition). Surprisingly, the complex formation of Hsp90 and Aha1 seems to be promoted by 26C8 as seen from

aUC data. Affinity titrations confirmed that the kD for Aha1 to Hsp90 is increased by 26C8. However, this complex seems to be highly ineffective in terms of the progression through the ATPase cycle. Even when bound, Aha1 is not able to potently stimulate Hsp90 when 26C8 is present. Considering the NMR data, 26C8 interacts with the Hsp90 MD, which is the primary site for the Aha1 interaction [Meyer et al., 2004]. Additionally, strong shifts of residues from the Hsp90 NTD could be detected in the presence of 26C8. These residues cluster in and close to the nucleotide binding pocket of Hsp90. Given the interaction of 26C8 with these two crucial sites, the NTD for ATP binding and the MD for Aha1 binding, the observed modulating effects on Hsp90 can be explained. Interaction of 26C8 with the Hsp90 NTD causes a 30 % decrease of the ATPase activity, but seems to have an additional effect: Preventing the Aha1 CD from its correct association with the Hsp90 NTD. The observed shifts of Hsp90 residues in the MD point towards a slight alteration of the Aha1 binding site, which would further explain why Aha1 is not able to stimulate Hsp90 to an extent normally observed. Figure 2.20 outlines a possible mechanism of the effect of 26C8 on the Hsp90/Aha1 interplay.

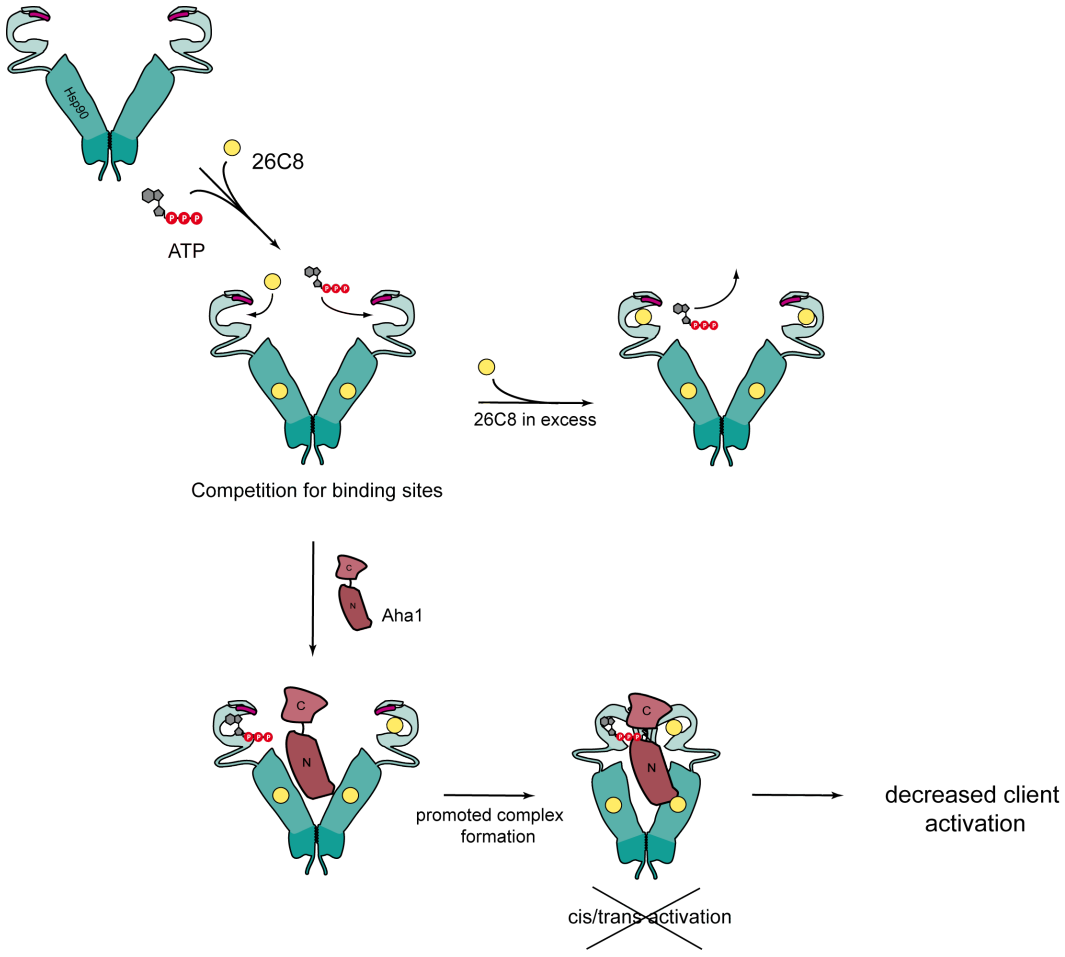

Figure 2.20: Model for 26C8 interaction with Hsp90/Aha1.

2.2 'The new 90s'

Hsp90 is a highly abundant protein in the cell and can be found in all organisms from bacteria to man. The only kingdom which does not possess an Hsp90 system, are the archaea [Johnson, 2012]. Some parts of Hsp90, e.g. the nucleotide binding pocket, are highly conserved and even lower eukaryotic organisms feature an Hsp90 system with a variety of co-chaperones. To elucidate the evolutionary pathway of Hsp90, a closer look at somehow uncommon Hsp90 systems was taken: Hsp90 from the thermophilic fungus *Chaetomium thermophilum* and from the eukaryotic parasite *Encephalitozoon cuniculi*. We characterised parts of the Hsp90 system with a focus on Hsp90 and its co-chaperone Aha1.

2.2.1 Phylogeny of Hsp90 from different organisms

The phylogenetic analysis of Hsp90 in a variety of organisms was performed using the amino acid sequences of Hsp90 from higher eukaryotes to bacteria and parasites. A phylogenetic tree was generated by aligning several representative Hsp90 family members using the ClustalO algorithm [Sievers $\mathrm{et\ al.}$, 2011]. The evolutionary relation of Hsp90 proteins from different organisms is depicted in figure 2.21. For higher eukaryotic organisms which possess two isoforms of Hsp90, Hsp90α was chosen to perform the alignments. The following organisms were included in this study: *Homo sapiens*, *Pan troglodytes* (chimpanzee), *Sus scrofa* (pig), *Oryctolagus cuniculus* (rabbit), *Gallus gallus* (chicken), *Rattus norvegicus* (rat), *Mus musculus* (mouse), *Drosophila melanogaster* (fruit fly), *Danio rerio* (zebrafish), *Salmo salar* (salmon), *Saccharomyces cerevisiae* (baker's yeast), *Chaetomium thermophilum* (thermophilic fungus), *Cyanidioschyzon merolae* (red alga), *Encephalitozoon cuniculi* (eukaryotic parasite) and *Monosiga brevicollis* (unicellular choanoflagellate).
M. brevicollis was included in this study since the group of choanoflagellates (eukaryotic flagellates) are thought to represent the closest unicellular relatives to metazoans (eukaryotic, multicellular organisms) [King $\mathrm{et\ al.}$, 2008]. Another interesting feature of *M. brevicollis* is its highly elaborated tyrosine kinase network which was found to be more diverse than in any known metazoa [Manning $\mathrm{et\ al.}$, 2008].

The red alga *C. merolae* was included because this organism represents one of the oldest groups of eukaryotic algae. It is furthermore an ultrasmall unicellular organism living in an extreme environment of sulfur hot springs (pH 1.5, 45 °C) [De Luca $\mathrm{et\ al.}$, 1978, Misumi $\mathrm{et\ al.}$, 2005].
Another 'extreme' organism is the thermophilic fungus *C. thermophilum*. It lives at opti-

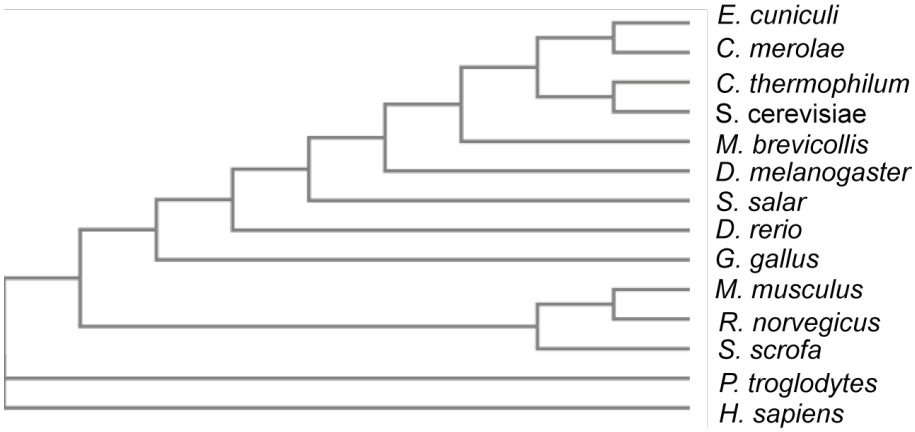

Figure 2.21: Phylogeny of Hsp90 proteins. Selected Hsp90 family members were aligned with the ClustalO algorithm [Sievers et al., 2011]. The phylogenetic tree was generated based on these alignments with the ClustalO tool.

mal growth temperatures of 50-55 °C and has a genome size of 28.3 Mb [Amlacher et al., 2011]. *C. thermophilum* belongs to the phylum *Ascomycota* and helped researchers already to discover the nuclear pore complex structure in more detail [Amlacher et al., 2011]. Neudegger *et al.* crystallised the human HSF1 paralogue Skn7 from *C. thermophilum* [Neudegger et al., 2016].
The eukaryotic parasite *E. cuniculi* is another somehow uncommon representative of organisms featuring an Hsp90 system. It belongs to the class of intracellular microsporidians and infects a range of vertebrate hosts, like humans, rabbits or birds [Katinka et al., 2001, Pelin et al., 2016]. *E. cuniculi*, with a remarkably small genome of about 2.9 Mb, is a widely accepted model organism to study reduction and adaptation [Katinka et al., 2001, Keeling and Fast, 2002]. Parasites are normally seen as minimal protein systems and thus one might conclude that Hsp90 is not present at all in these organisms. However, *E. cuniculi* proves differently since it possesses, despite a very small genome, an Hsp90 system (addressed in the section 2.2.2 - Comparison of different Hsp90 systems). Organisms from human to baker's yeast are 'classical' Hsp90 systems which are widely studied. *M. brevicollis*, *C. merolae*, *C. thermophilum* and *E. cuniculi* represent 'new' Hsp90 systems which might provide new insights in the evolutionary history of Hsp90. Yet, they have not been studied.

2.2.2 Comparison of different Hsp90 systems

The focus of this evolutionary study on Hsp90 was laid on the comparison of yeast Hsp90 with thermophilic and parasite Hsp90. The thermophilic Hsp90 was cloned from cDNA of the thermophilic fungus *Chaetomium thermophilum* (a kind gift of Ed Hurt, BZH Heidelberg), while the parasite Hsp90 was derived from the eukaryotic parasite *Encephalitozoon cuniculi*. The *E. cuniculi* Hsp90 (EcHsp90) displays a 41 % homology to yeast

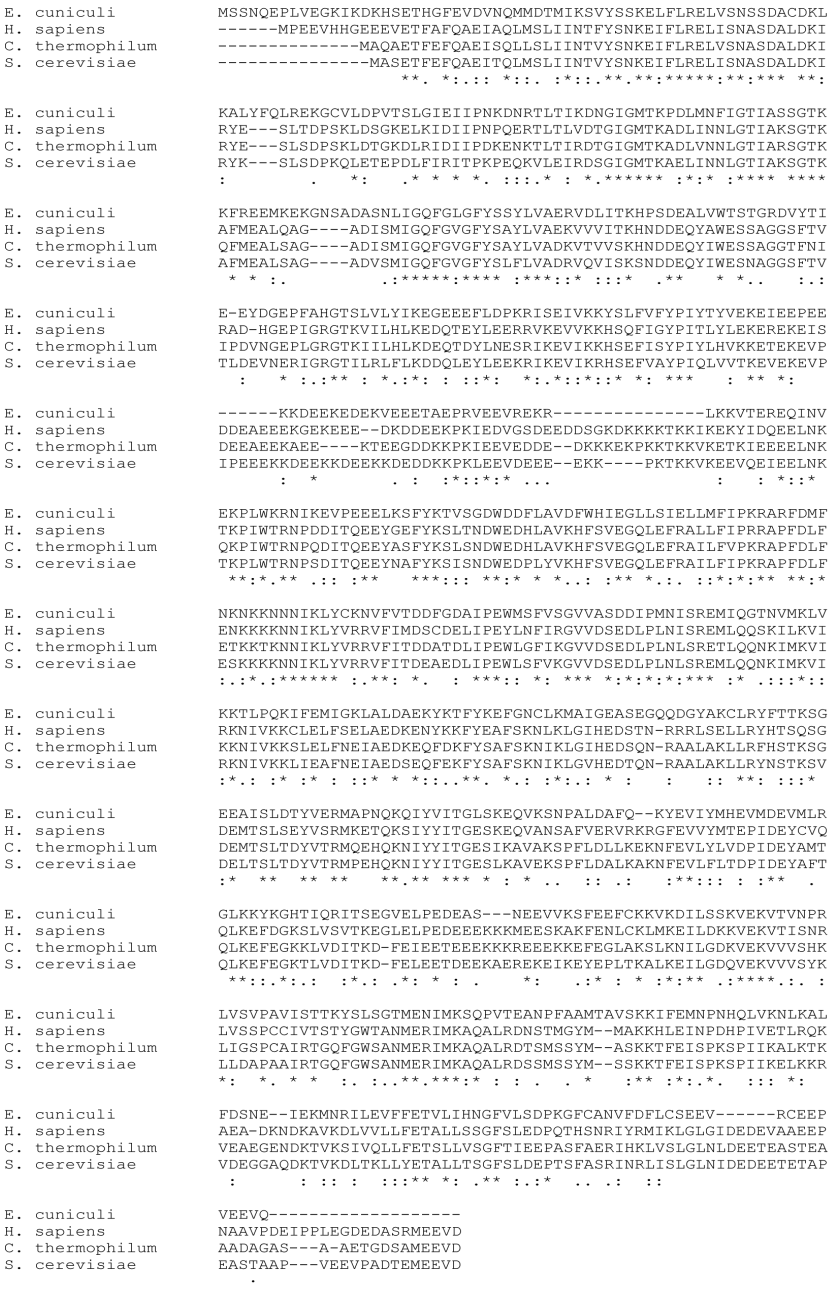

Figure 2.22: ClustalO alignment of full-length Hsp90 from different organisms. A multiple sequence alignment, produced by ClustalO, of Hsp90 protein sequences from *E. cuniculi*, *C. thermophilum*, *S. cerevisiae* and *H. sapiens*. Conserved residues (*), semi-conservative mutations (.) and conservative mutations (:) are shown.

Table 2.2: **Hsp90 systems from *E.cuniculi* and *C. thermophilum*.** PSI-BLAST (*E. cuniculi*) (A) and BLAST (*C. thermophilum*) (B) algorithm-based sequence alignments of proteins from the Hsp90 machinery.

A

E. cuniculi

Protein	Existence	Seq. Identity	Query cover	Name	NCBI Ref. Seq.
Hsp90	+	41%	93%	Heat-shock protein Hsp90 Homolog	NP_584635.1
Hop/Sti1	+	38%	20%	Hypothetical protein ECU09_1180	XP_955669.1
Aha1	+	27%	38%	Hypothetical protein ECU07_1300	NP_586059.1
Cpr6	+	50%	46%	Peptidyl-prolyl cis-trans Isomerase	NP_597176.1
Cns1	?	20%	61%	Hypothetical protein ECU09_1180	XP_955669.1
Sgt1	?	48%	12%	Hypothetical protein ECU05_1160	NP_597459.1
Pih1	?	24%	27%	Hypothetical protein ECU02_0390	NP_584566.1
Tah1	?	37%	65%	Hypothetical protein ECU09_1180	XP_955669.1
Cdc37	?	44%	4%	Hypothetical protein EC07_0640	NP_585992.1
PP5/Ppt1	+	39%	57%	Ser/Thr Protein Phosphatase 2-A	NP_584753.1
p23/Sba1	?				

B

C. thermophilum

Protein	Existence	Seq. Identity	Query Cover	Name	NCBI Ref. Seq.
Hsp90	+	73%	99%	Heat shock protein hsp90-like protein	XP_006697122.1
Hop/Sti1	+	50%	99%	Putative heat shock protein	XP_006695859.1
Aha1	+	37%	98%	Putative chaperone binding protein	XP_006694758.1
Cpr6	+	33%	99%	Putative cis-trans-protein	XP_006694995.1
Cns1	+	33%	97%	Hypothetical protein	XP_006694288.1
Sgt1	+-	34%	61%	Hypothetical protein	XP_006697210.1
Pih1	?	?	?	unclear	
Tah1	?	35%	63%	Hypothetical protein	XP_006694049.1
Cdc37	+	31%	89%	Hypothetical protein	XP_006693078.1
PP5/Ppt1	+	44%	99%	Ser/Thr Phosphatase-like protein	XP_006693273.1
p23/Sba1	+	40%	78%	Putative cochaperone protein	XP_006691093.1
Hch1	?	36%	99%	Putative chaperone binding protein	

Hsp90 (table 2.2A). With a molecular mass of 79 kDa it is only slightly smaller than its yeast homologue (82 kDa). *E. cuniculi* is particulary noteworthy due to its small genome of only 2.9 Mbp. In comparison, the genome of *C. thermophilum* is 28.3 Mbp, the human genome is estimated to be around 3.2 Gbp [Venter et al., 2001, Amlacher et al., 2011]. Peroxisomes and mitochondria are not present in *E. cuniculi* [Vávra and Lukeš, 2013, Keeling and Fast, 2002]. It seems surprising that a small parasite like *E. cuniculi* contains an Hsp90 system including the co-chaperones Sti1, Cpr6, Ppt1 and Cdc37. Sba1 seems absent from *E. cuniculi*. The co-chaperones Aha1, Cns1, Pih1 and Tah1 could not be identified with the blastp algorithm. The blastp algorithm can align proteins which are highly related, but will give negative results, when the proteins do not share a high similarity [Altschul et al., 1990] (see also BLAST factsheet at NCBI online 'How to BLAST guide'). To this end, alignments with the PSI (position-specific iterative)-BLAST algorithm were performed. PSI-BLAST is suitable to identify distant proteins which do not share a common evolutionary relationship. Identified *E. cuniculi* co-chaperones by PSI-BLAST were Aha1, Cns1, Pih1 and Tah1. Hence, it is concluded that these four co-chaperones seem to be quite different from their counterparts in yeast.
The thermophilic Hsp90 was of particular interest, since we wanted to elucidate stability and *in vitro* function of this thermophilic protein. *C. thermophilum* Hsp90 (CtHsp90) is highly homologous (73 % homology) to yeast Hsp90 and it might show thermophilic adaptation not found in *S. cerevisiae*. Furthermore, thermophilic proteins might be easier to crystallise due to their higher thermodynamic stability. Thus, we attempted crystallisation trials to elucidate the structure of Hsp90 in this thermophilic organism. The Hsp90 system from *C. thermophilum* is summarised in table 2.2B. *C. thermophilum* features an almost complete Hsp90 system. Except for Pih1: alignments with the yeast counterpart failed and did not show clear, positive results. Tah1 retrieved a bad alignment score running the blastp algorithm, however, the PSI-BLAST algorithm, indicated not a close relationship between yTah1 and CtTah1, but showed a positive result.
An alignment of Hsp90 from *E. cuniculi*, *C. thermophilum*, *S. cerevisiae* and *H. sapiens* is depicted in figure 2.22. To identify homologous regions in Hsp90 from these different organisms, a multiple sequence alignment was performed by applying the Clustal Omega (ClustalO) algorithm [Sievers et al., 2011]. Identical amino acids in the analysed sequences are marked with an asterisk (*), semi-conservative residue mutations are marked with a point (.) and conservative mutations are marked with a colon (:). As expected, crucial sites, important for the functionality of Hsp90, are highly conserved between these differing organisms. The NTD which contains the ATP binding pocket, the charged linker, as well as the MEEVD motif in the CTD are highly conserved parts of Hsp90 in human, yeast and *C. thermophilum*. EcHsp90 differs from those three organisms, since it does neither contain a charged linker sequence, nor a MEEVD motif. The CTD of EcHsp90 ends with a EEVQ motif. Sequence alignments of the EcHsp90 system with the yHsp90 machinery predict Sti1 and other TPR co-chaperones in the *E. cuniculi* system. These TPR co-chaperones show a 38 % identity in the case of EcSti1 and only

20 % identity for Cns1 (compared to its homologues from yeast).

2.2.3 Characterisation of thermophilic Hsp90 and Aha1

Thermal stability

The structure and thermal stability of CtHsp90 as well as of CtAha1 was addressed by CD measurements and TSA assays. Recorded spectra were compared to yHsp90 and yAha1 spectra (data not shown) to observe possible differences in secondary structure and protein stability. Far-UV CD spectra were recorded at 25, 55 and 95 °C to investigate the secondary structure of the different proteins at different temperatures. As depicted in figure 2.23, a high alpha helical content could be observed for CtHsp90. Upon a change in temperature, no changes in secondary structures could be detected. This is consistent with recorded CD spectra of yeast Hsp90. Spectra of CtAha1 revealed a mixed content of alpha helical and beta sheet structures. However, the signal of CtAha1 decreased at a temperature of 95 °C. Again, this is consistent with CD spectra obtained for yAha1.

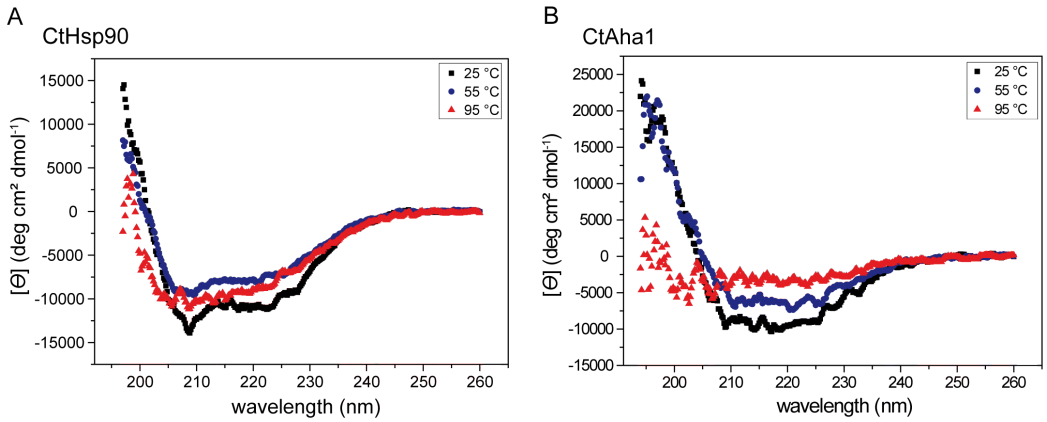

Figure 2.23: Secondary structure of Hsp90 and Aha1 from different organisms. CD spectra for CtHsp90, EcHsp90 and yHsp90 (A). Spectra of yAha1 and CtAha1 (B). Measurements were performed in 10 mM sodium phosphate buffer in 1 mm cuvettes. Far-UV spectra of 2 mg/ml of each protein were measured at 25, 55, 95 °C and buffer-corrected. Mean residue molar ellipticity was then calculated.

For both thermophilic proteins, CtHsp90 and CtAha1, thermal transitions were recorded. No thermal transition could be detected, which is, again, consistent with thermal transition measurements for yeast Hsp90 and yeast Aha1. TSA assays which address the tertiary structure of a protein were performed. The fluorescent dye Sypro Orange was applied since it is interacting with hydrophobic areas from proteins, which are exposed during thermal denaturation. This interaction can be followed by an increasing fluorescence of Sypro Orange. After complete unfolding of a protein, the Sypro Orange - pro-

tein interaction is weakened and a decrease in the fluorescence signal can be observed. Bleaching of Sypro Orange is also occurring and contributes additionally to a decrease in fluorescence. Figure 2.24 summarises the TSA measurement of yHsp90, CtHsp90, EcHsp90 (fig. 2.24A) and yAha1, CtAha1 (fig. 2.24B). Obtained data was fitted with a Boltzmann fit with the Origin software to determine the melting temperature for each sample. Melting temperatures are summarised in table 2.3

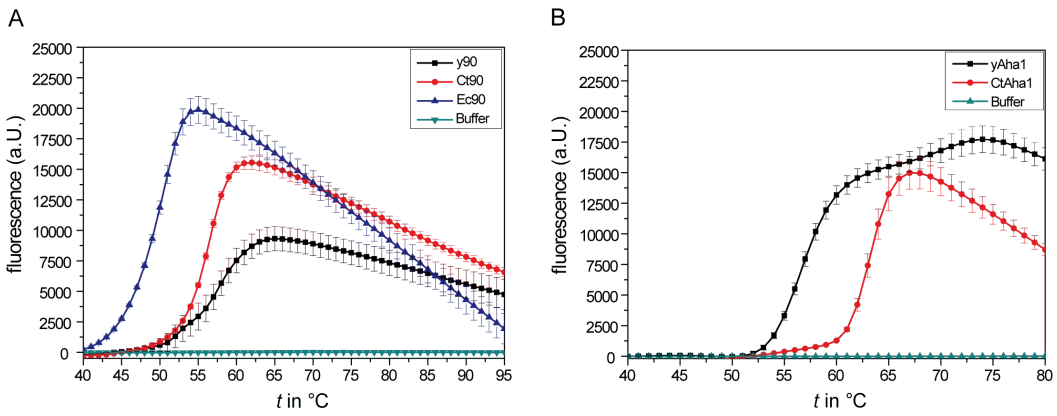

Figure 2.24: Thermal stability of Hsp90 and Aha1 from different organisms. TSA assays using Sypro Orange as reporter dye were performed. Melting temperatures of Hsp90 from each of *S. cerevisiae*, *C. thermophilum* and *E. cuniculi*, and of Aha1 from both *S. cerevisiae* and *C. thermophilum* were determined. 2 µg of protein were measured in standard assay buffer in each case. Data was fitted with a Boltzmann fit in Origin to obtain the melting temperature (T_M).

Table 2.3: **Melting temperatures of Hsp90 and Aha1 from yeast and *C. thermophilum***

Protein	**T_M (°C)**
yHsp90	56.7 ± 1.1
CtHsp90	58.2 ± 0.7
EcHsp90	49.3 ± 0.3
yAha1	56.7 ± 0.2
CtAha1	63.6 ± 0.4

For CtHsp90 a melting temperature of of 58.2 ± 0.7 °C was measured. yHsp90 has a melting temperature of 56.7 ± 1.1 °C, while EcHsp90 had the lowest melting temperature of 49.3 ± 0.3 °C. CtHsp90 is thus slightly more thermostable than yHsp90. CtAha1 melted at 63.6 ± 0.4 °C, while yAha1 showed a melting temperature of 56.7 ± 0.2 °C. Thus, CtAha1 displays a higher thermal stability than its homologue from yeast. Nevertheless, these differences in thermal stability between proteins from *S. cerevisiae* and *C. thermophilum* are not as prominent as one would expect. The low melting temperatures of the two investigated *C. thermophilum* proteins were somehow surprising. It would

have been expected that a thermophilic protein displays a significantly higher melting temperature than its counterpart from *S. cerevisiae*. By definition, a thermophilic system is able to cope with temperatures from 50 to 90 °C (moderate thermophiles) [Bitton, 2002]. Data from the thermal stability leaves doubt on the functionality (due to stability) of CtHsp90 and CtAha1 at temperatures over 60 °C *in vitro*.
The question what makes a thermophilic organism thermophile now arises. Is the ability of surviving extreme temperatures mediated on the protein level, and if so which proteins are crucial for thermophiles? It does not seem that Hsp90 is the most important, maybe not even any mediator of protein stability in *C. thermophilum* when it is itself not stable, or at least: not more stable than Hsp90 from *S. cerevisiae* which lives at optimum temperatures of only 30 °C. Other protein systems, like sHsps might be more crucial in the mediation of thermophilicity. A look into the literature on thermophilic organisms also suggests that thermophilic proteins display significant changes in their thermodynamic stability and amino acid sequence [Berezovsky et al., 2005]. Thermophilic proteins might possess a highly decreased entropy when it comes to protein unfolding [Razvi and Scholtz, 2006]. As kinetically expected, some amino acids contribute more to protein stability than others. Alanine, for example, is thought to be the best helix-forming residue and might thus contribute to stability [Sriprapundh et al., 2000]. Proline is highly limited in the conformations it can engage with and displays a very low conformational entropy. Subtle changes in amino acid composition might therefore make a thermophilic protein out of its mesophilic counterpart. However, proteins often have to undergo conformational changes which are coupled to their functionality. An interesting observation in this context is that an increase in protein stability could also cause an suppression of protein function as speculated by Gliakina *et al.* 2007. Other factors which might be essential for thermophiles are a higher number of salt bridges, an increased hydrophobicity and a higher content of aromatic, high desolvation energy-possessing, residues [Robinson-Rechavi et al., 2006, Spassov et al., 1995, Perl and Schmid, 2002].
An interesting example for protein stability is the hyperthermophilic eubacterium *Thermotoga maritima* [Huber et al., 1986]. Its HU DNA binding protein has a melting temperature of 101.9 °C, whereas the glutamate dehydrogenase domain II displays a melting temperature of only 69.5 °C [Ruiz-Sanz et al., 2004, Consalvi et al., 2000]. That said, proteins from thermophilic organisms can differ quite strongly in their corresponding melting temperatures. The isopropyl malate dehydrogenase from *E. coli* has a melting temperature of 107 °C, which is another example that melting temperature cannot be the only determining factor for the general protein stability in organisms. Proteins from thermophilic organisms, as well as from their mesophilic counterparts seem to have in some cases surprisingly high or surprisingly low melting temperatures, as the examples above demonstrate.

Activity of thermophilic Hsp90 at higher temperatures

The ATPase activity of Hsp90 is important for its functionality. Activity of thermophilic Hsp90 was investigated and the stimulatory potential of CtAha1 on CtHsp90 was assessed. The ATPase activity of CtHsp90 was measured using a regenerative ATPase assay. Temperatures from 30-60 °C were tested to address the function of CtHsp90 also at elevated temperatures. The catalytic rate of CtHsp90 was slightly lower to the one of yHsp90 in the regenerative ATPase assay. At 30 °C, CtHsp90 shows a catalytic activity of 0.35 min^{-1}, while the k_{cat} of yHsp90 is 0.68 min^{-1}. At 40 °C, CtHsp90's k_{cat} is 0.78 min^{-1} compared to a k_{cat} of 1.80 min^{-1} for yHsp90. For temperatures of 50 °C and above, the regenerative ATPase assay was not suitable, since it contains LDH and PK. At 55 °C, the whole assay system showed very low numbers of catalytical activities, even for thermophilic Hsp90. The ATPase activity was thus measured with different ATPase assay systems, whereby the malachite green (MLG) assay was suited best for determining the potential of Hsp90 to hydrolyse ATP. The MLG assay detects free phosphate in aqueous solutions. In this assay, the free orthophosphate, cleaved from ATP, forms a complex with malachite green molybdate under acidic conditions. The molybdophosphoric acid complex can be measured at 630 nm and directly relates to the free phosphate [O'Toole et al., 2007]. The hydrolysis reaction can be carried out at different temperatures with the endpoint determination at room temperature. Due to its high sensitivity and thermal stability, the MLG assay was the method of choice for the determination of ATP hydrolysis rate of CtHsp90 at higher temperatures. ATPase rates of CtHsp90 were compared to yHsp90 and EcHsp90 (figure 2.25).

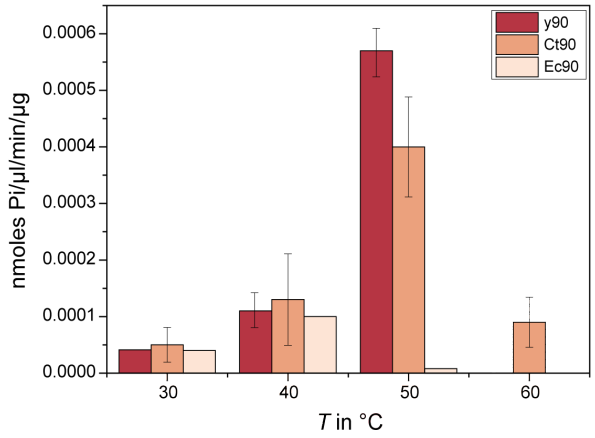

Figure 2.25: ATPase rates of thermophilic Hsp90 compared with its yeast and parasite counterparts. The ATPase activity at from 30-60 °C for Hsp90 from different organisms was determined using a MLG assay system. Reactions were performed for 20 min at the respective temperature and the amount of free phosphate was calculated.

At 30 °C and 40 °C, all three Hsp90s have a comparable rate of ATP hydrolysis. The potency for ATP hydrolysis of EcHsp90 is dramatically decreased at temperatures over

40 °C, with a strong depletion at 50 °C and no measurable ATP hydrolysis of EcHsp90 at 60 °C. CtHsp90 has an activity maximum at 50 °C with 0.0004 nmoles phosphate/µl/ min/µg protein. At 60 °C, CtHsp90's turnover is decreased 4-fold to 0.0001 nmoles phosphate/µl/min/µg protein. At higher temperatures than 60 °C, no activity of CtHsp90 was detectable with the MLG assay. For yHsp90, the catalytic potential for ATP hydrolysis was increasing from 30 to 50 °C from 0.5 to 0.55 nmoles phosphate/µl/min/µg protein. At a temperature of 60 °C, non-reproducible activities of Hsp90 were detected. In three independent measurements negative hydrolysis rates were detected twice, while a high hydrolysis rate was detected once. Thus, no value for 60 °C is presented for yHsp90 in figure 2.25. Surprisingly, CtHsp90 seems to be less active than yHsp90 at 50 °C. Nevertheless, a stable ATP hydrolysis rate could be observed for CtHsp90 at 60 °C, while yHsp90 showed high fluctuations in the MLG assay. This might point to a more stable ATPase function of CtHsp90 at temperatures above 50 °C compared to yHsp90.
To further address the *in vitro* function of CtHsp90, the stimulatory potential of CtAha1 was addressed. This high homology between Aha1 in these two different organisms, suggests also a high similarity in their stimulatory potential of the Hsp90 ATPase activity. To this end, binding affinities of CtAha1 to CtHsp90 were determined in the regenerative ATPase assay system at different temperatures. As already mentioned, the regenerative assay system is not accurate above temperatures of 50 °C. To this end, measurements were performed at 30 and 40 °C. For temperatures higher than 50 °C, the MLG assay was applied. However, this assay was not suitable for determining binding affinities. The stimulatory potential of CtAha1 on CtHsp90 was compared to the yeast Hsp90 system as summarised in table 2.4.
Generally, the kD of CtAha1 to CtHsp90 is significantly lower than the one of yAha1 to yHsp90. yAha1 binds to yHsp90 with a kD between 3.23 and 3.67 µM (30 and 40 °C), respectively. The kD of CtAha1 to CtHsp90 is around 4-times lower with 12.93 and 10.88 µM (30 and 40 °C), respectively. Furthermore, the potential of CtAha1 to stimulate CtHsp90's ATPase rate is far lower than yAha1's stimulation of yHsp90 (summarised in fig. 2.26).

Table 2.4: **Binding affinities of CtAha1 to CtHsp90**

Protein	**kD (µM)**	**T (°C)**
CtHsp90/CtAha1	12.93	30
yHsp90/yAha1	3.23	30
CtHsp90/CtAha1	10.88	40
yHsp90/yAha1	3.67	40

Yeast Aha1 seems to have a rather unique feature in stimulating Hsp90's ATPase activity up to even 30-fold at 40 °C. As figure 2.26 shows, this stimulation seems to require both,

yHsp90 and yAha1. yAha1 is also able to stimulate CtHsp90 (blue line). However, this stimulation is, even at high yAha1 concentrations, limited by CtHsp90's ATPase activity. The stimulation of CtAha1 by CtHsp90 also results in a 16-fold stimulation. yAha1 is able to stimulate CtHsp90 around 13-fold. In comparison, hAha1 seems to have the weakest stimulatory potential on its hHsp90 complement (cyan curve). Even with 30 μM hAha1, no saturation of the hHsp90 ATPase activity could be observed. These findings underline the unique, high stimulation of yHsp90 by yAha1, but also that hHsp90 is only weakly activated ATPase by Aha1.

A

Protein	kD (μM)	T (°C)
y90/yAha1	3.67	40
h90/hAha1	16.18	37
Ct90/CtAha1	10.88	40
Ct90/yAha	2.66	40

B

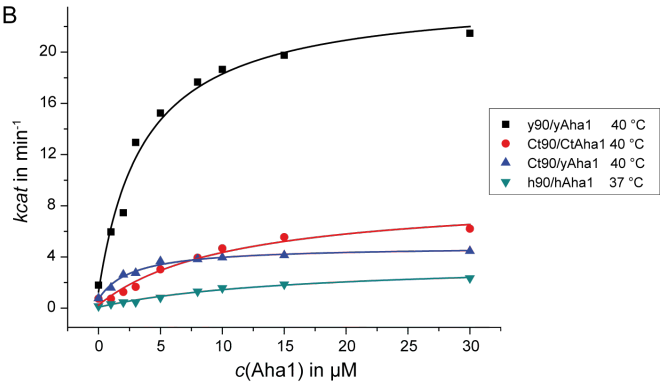

Figure 2.26: Hsp90 stimulation by Aha1 in Hsp90 systems from different organisms. A: kDs for Aha1 to Hsp90 are summarised for the respective proteins. The stimulatory potential of Aha1 on Hsp90 was addressed by titrating 0-30 μM Aha1 to 2 μM Hsp90 (B). Titrations were performed at 40 °C (for hHsp90/hAha1 at 37 °C) using a regenerating ATPase assay system.

Going back to *C. thermophilum*, CtAha1 seems to be homologous to yAha1 in terms of its stimulatory potential on Hsp90. However, much weaker affinities for Hsp90 were observed in the thermophilic Hsp90 system (fig. 2.26A). Interestingly, the Hsp90 systems can cross-react with each other (fig. 2.27). CtHsp90 can be stimulated by yAha1 and yHsp90 is stimulated by CtAha1. This finding demonstrates the high similarity of these two proteins systems *in vitro*. Nonetheless, the activation of yHsp90 by yAha1, resulting in high k_{cat} values is significantly stronger than the one of CtHsp90 by yAha1 (visualised in fig. 2.27A). Stimulation of CtHsp90 by yAha1 does not result in a comparably high k_{cat} than for yHsp90. Furthermore, CtAha1 is able to stimulate yHsp90, but again not to the same extent as yHsp90 is activated by yAha1. Thus, the Aha1 stimulation of Hsp90 seems to be not only dependent on the potency of Aha1 to stimulate Hsp90, but also on the potency of Hsp90 to be stimulated.

Surprisingly, CtHsp90 was not significantly more active than yHsp90 at higher temperatures. A difference in activity would have been expected since CtHsp90 is considered as a thermophilic protein from an organism adapted to temperatures from 50-70 °C [Amlacher et al., 2011]. At 70 °C, no activity for CtHsp90 could be detected in the MLG green assay, which points out that isolated CtHsp90 is not more stable than its non-thermophilic counterpart from yeast. One can speculate that thermophilic mechanisms

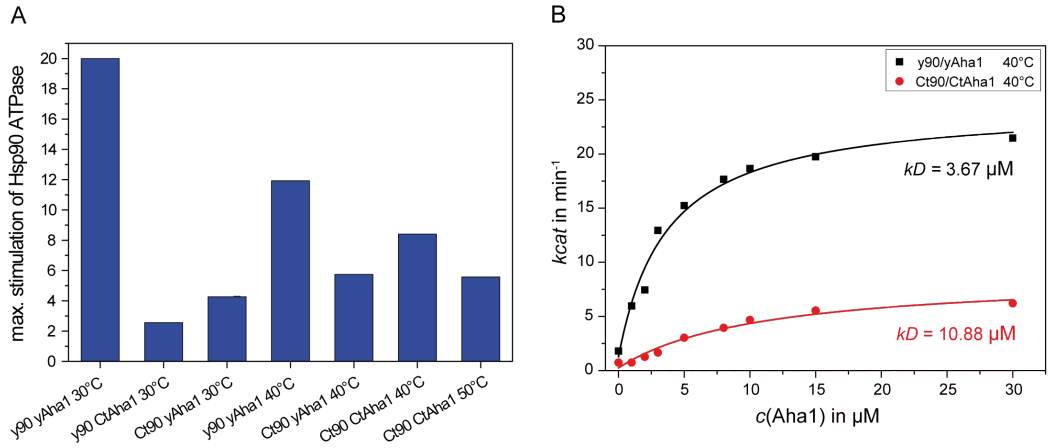

Figure 2.27: Stimulation of Hsp90 by Aha1. Titrations of 0-30 µM Aha1 to 2 µM Hsp90 were performed using a regenerative ATPase system. A: Maximum stimulation of Hsp90 by Aha1. Data for yHsp90/yAha1 was obtained at 30 and 40 °C. CtHsp90/CtAha1 was measured at 30-50 °C. Furthermore the potential of yAha1 to cross-stimulate CtHsp90 was assessed at 30 and 40 °C. B: Titrations of yAha1 to yHsp90 (black) and CtAha1 to CtHsp90 (red) at 40 °C.

in vivo are much more complex than only a more thermostable protein. In summary, the thermophilic Hsp90 does not seem dramatically different from its yeast homologue in terms of ATPase activity and its stimulatory potential of Aha1. *In vitro* data does not suggest a functional difference of these two Hsp90s.

Chaperone function of thermophilic Hsp90

The chaperoning function of Hsp90 is one of its crucial tasks in the cell to contribute to client stability and activation. To this end, the chaperoning potential of CtHsp90 and EcHsp90 were compared to yHsp90 (fig. 2.28A.) CS was used as model substrate. CS aggregation was followed at 350 nm at 42 °C. 1:5 and 1:10 ratios (CS:Hsp90) were tested. All Hsp90s were able to suppress aggregation of CS. EcHsp90 thereby seems to be the weakest chaperone, since a 1:5 ratio still resulted in a slight aggregation of CS. This was not the case for yHsp90 or CtHsp90 in a 1:5 ratio.

The observed weaker chaperoning activity of EcHsp90 might result from the lower stability or activity of EcHsp90 at elevated temperatures. As seen in the ATPase assays, EcHsp90's activity is already decreased at temperatures above 30 °C (see also figure 2.25). Thus, it is not surprising that a slightly lower chaperoning activity for EcHsp90 is observed in the CS aggregation assay at 42 °C.
Furthermore, the chaperoning potential of CtAha1 was addressed (fig. 2.28B). yAha1 does not possess any chaperoning function. In contrast, human Aha1 was shown to have a chaperoning activity on its own [Tripathi et al., 2014]. As shown in figure 2.28B, CtAha1 is more similar to yAha1 than to hAha1 because even at ratios of 1:20 (CS:CtAha1), no

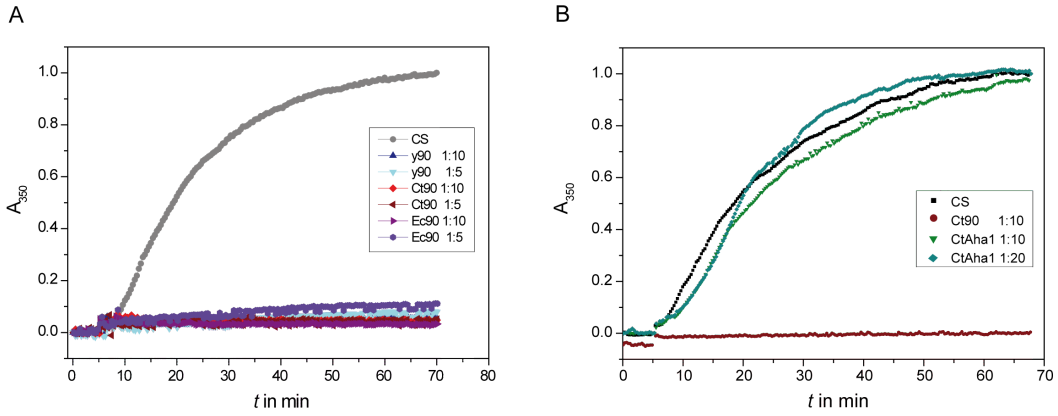

Figure 2.28: Chaperone activity of different Hsp90s. Aggregation of CS as model substrate was measured at a wavelength of 350 nm at 42 °C. A: Different ratios of yHsp90, CtHsp90 an EcHsp90 were applied to investigate the potential of these Hsp90s to suppress CS aggregation. Ratios of 1:5 and 1:10 (CS:Hsp90) were tested. B: CtHsp90 (1:10 ratio CS:CtHsp90, pos. control) and CtAha1 (1:10 and 1:20 ratio, CS:CtAha1) were tested for their chaperoning potential.

chaperoning activity of CtAha1 can be detected. This demonstrates another analogy of CtAha1 with yAha1.

2.2.4 Outlook

In this project, the evolutionary relation of Hsp90 from different organisms was addressed bioinformatically. Alignments of Hsp90 sequences from commonly investigated organisms, like Drosophila, yeast or rabbit were aligned with each other to generate a phylogenetic tree on the evolution of Hsp90. Furthermore, rather 'unusual' organisms like the thermophilic fungus *C. thermophilum* and the eukaryotic parasite *E. cuniculi* were included. Even though *E. cuniculi* has a highly reduced genome [Keeling and Fast, 2002, Corradi, 2015], sequence analysis revealed an Hsp90 machinery, consisting of Hsp90, Sti1, Cpr6, Cdc37 and Ppt1. For other members of the Hsp90 family, low alignment scores were obtained, implying that they do not exist in *E. cuniculi*. However, this small Hsp90 system is rather surprising since one could have suggested that *E. cuniculi* does not harbour any Hsp90. The existence of this protein family in *E. cuniculi* seems to confirm studies which entitled *E. cuniculi* as a highly specialised organism and not as simple as initially supposed [Keeling and Fast, 2002].
C. thermophilum was of particular interest since it naturally lives at temperatures up to 60 °C [Bock et al., 2014]. Studying proteins from this fungus might provide new insights into thermophilic adaptation of organisms. Biochemical assays for testing *in vitro* characteristics of CtHsp90 and CtAha1 were applied. Surprisingly, this protein is neither significantly more stable, nor more active at higher temperatures *in vitro*. Mediation of thermophilicity might not occur via Hsp90. From another point of view, these experiments also demon-

strated the high stability and thermal tolerance of yeast Hsp90. Since ATPase activities at temperatures over 40 °C are still measurable and thermal stability is not very different from its thermophilic counterpart, yeast Hsp90 seems highly tolerant to a variety of conditions. Even though the *in vitro* studies did not reveal significant differences of CtHsp90 and yHsp90, other co-chaperones of *C. thermophilum* were cloned into expression vectors and purified. The purified proteins were sent for crystallisation trials in collaboration with the chair for crystallography (Prof. Michael Groll, TU Munich). Furthermore, an Hsp90 MC construct was generated to allow crystallisation trials of Hsp90 in complex with Sti1 and other TPR-co-chaperones. Crystal structures, especially full-length, from this Hsp90 system might provide new insights into the Hsp90 machinery.

2.3 Characterisation of Hsp90 tryptophan mutants

Hsp90 is a highly dynamic protein, able to adopt different, functionally distinct conformations. It cycles from the open to the closed state via intermediates [Mickler et al., 2009, Hessling et al., 2009]. ATP is a crucial inducer of conformational changes, which can also be seen when the non-hydrolysable ATP-analogon AMP-PNP is added to Hsp90 *in vitro*. AMP-PNP induces a fully-closed state of Hsp90, making is able to study interactions of closed Hsp90 with its partners [Ali et al., 2006, Hessling et al., 2009, Ratzke et al., 2012b]. Some co-chaperones, like p23/Sba1 only interact with the fully closed state of Hsp90 [Grenert et al., 1999]. A variety of Hsp90 mutants was already studied *in vitro* and *in vivo*. Some point mutations in Hsp90 lead to a reduced ATPase activity, while others trigger a complete loss. The Hsp90 mutant D79N is not able to bind ATP anymore and thus Hsp90's function is lost [Prodromou et al., 1997]. Other mutants, like E33A or R380A are still able to bind ATP, however, they cannot hydrolyse it. [Panaretou et al., 1998]. As these examples demonstrate how crucial the interaction of nucleotides with Hsp90 is, surprisingly little is known on the nucleotide binding process itself. Structural rearrangements like lid closure over the ATP binding pocket are well-known [Prodromou et al., 2000]. Other studies investigated the Hsp90 subunit communication with regard to nucleotide binding. Hsp90 dimers where one subunit lacks an NTD are deficient for ATP hydrolysis [Richter et al., 2001]. Single molecule studies imply that ATP binding in one subunit does not promote nucleotide binding in the second subunit [Ratzke et al., 2012a], which points towards negative cooperativity [Acerenza and Mizraji, 1997]. Another study states that ATP binding has only a weak impact on conformational preferences of Hsp90 [Mickler et al., 2009]. Nonetheless, a crystallographic study indicates that ATP-binding induces N-terminal dimerisation and a possible cooperativity of ATP binding to the Hsp90 subunits [Ali et al., 2006]. However, comprehensive studies on ATP binding with regard to its possible cooperative mechanism are missing. An *in vivo* study revealed an asymmetric ATPase-driven mechanism of Hsp90 *in vivo*, whereby ATP binding to both subunits is required, but ATP hydrolysis of at least one subunit supports viability [Mishra and Bolon, 2014].

In order to elucidate the binding mechanism of ATP to Hsp90, mutants with modifications in crucial ATP-interacting sites were studied. Therefore, tryptophans were introduced in yeast Hsp90 at the positions 104 (lid) and 124 (ATP binding site) (figure 2.29). The Trp residues were chosen since they can serve as photometrically probes. Trp absorbs light at 280 nm and emits fluorescence [Edelhoch, 1967]. Measurements of Trp fluorescence can give information about structural changes upon nucleotide binding. Due to their size, an introduction of tryptophan residues might be critical for protein structure and thus functionality. For that reason, phenylalanin residues were mutated to tryptophans since their sizes are comparable and should not cause structural defects in the protein.

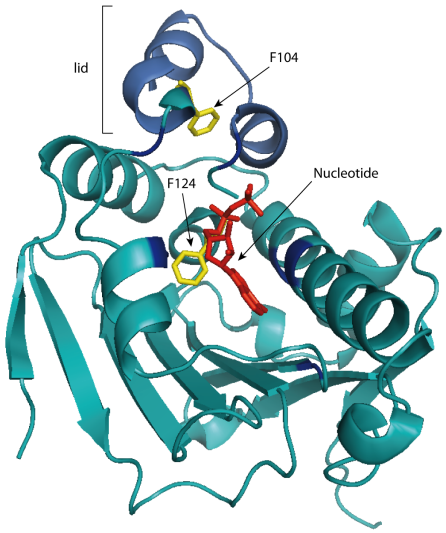

Figure 2.29: Location of the mutated residues. Residues which form the nucleotide binding pocket of Hsp90 are coloured in dark blue. Tryptophans were introduced at the positions 104 and 124 (yellow). F124 directly interacts with nucleotide (red) and forms the core of the ATP binding pocket, while F104 is part of the lid.

ATPase, FRET assays, stopped-flow and others were applied to characterise the Hsp90 Trp mutants. Growth effects in yeasts were further addressed.

2.3.1 ATPase activity of Hsp90 Trp mutants

The mutation of residues at crucial sites of Hsp90 might result in inactive variants of Hsp90, as the earlier given examples demonstrate. The positions 104 (lid) and 124 (ATP-binding site) are directly coupled to the progression of the Hsp90 ATPase cycle [Hessling et al., 2009, Mickler et al., 2009]: ATP binds to the ATP binding pocket of Hsp90 in an open state and induces structural rearrangements of Hsp90. The lid is closing over the nucleotide binding pocket (I_1 state), Hsp90 cycles to the closed state and ATP hydrolysis occurs, followed by the release of ATP + P_i. Hsp90 returns then again to the open state [Hessling et al., 2009, Mickler et al., 2009]. Mutation of amino acids at switch points known to drive the ATPase cycle of Hsp90 is a critical endeavour since it can lead to a complete loss of function. Point mutations at, for example, the positions 41, 83, or 380 result in a loss or dramatic decrease of Hsp90's ATPase activity [Nathan and Lindquist, 1995, Meyer et al., 2003, Hawkins et al., 2008]. Since introduction of tryptophans at the positions 104 and 124, respectively, might disrupt the functionality of Hsp90, ATPase activities of the generated Hsp90 variants, F104W and F124W, were assessed. A regenerative ATPase assay system was applied to test the ATPase activity. The co-chaperones

Aha1 and Sti1 were also added to the Hsp90 mutants to test for the ability of stimulation and inhibition, respectively. Catalytical activity of Trp mutants was measured at 30 °C and kinetics were fitted with the Michaelis-Menten model to determine the kD_{app}. A comparison of the ATPase activities for Hsp90 wt and the Trp mutants is shown in figure 2.30.

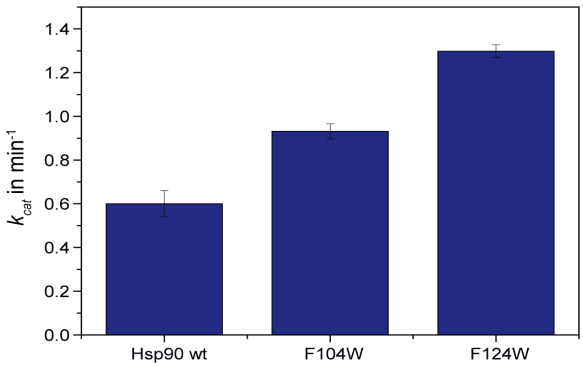

Figure 2.30: ATPase activity of Hsp90 Trp mutants. ATPase activity of Trp mutants and Hsp90 wt were measured at 30 °C in standard assay buffer. 2 mM ATP was added to 3 µM of Hsp90. Kinetics were recorded for 60 min and fitted with a Michaelis Menten fit (implemented in the Origin Software).

The F124W mutant showed a 2-fold increased catalytical activity (k_{cat} = 1.30 ± 0.03 min^{-1}) compared to yHsp90 wt (k_{cat} = 0.6 ± 0.06 min^{-1}). The lid mutant F104W displayed just a slightly higher ATPase activity compared to yHsp90 wt (k_{cat} = 0.93 ± 0.03 min^{-1}). Thus, introduction of tryptophans at crucial switch points, 104 and 124, of the Hsp90 ATPase cycle does not decrease the catalytical activity.

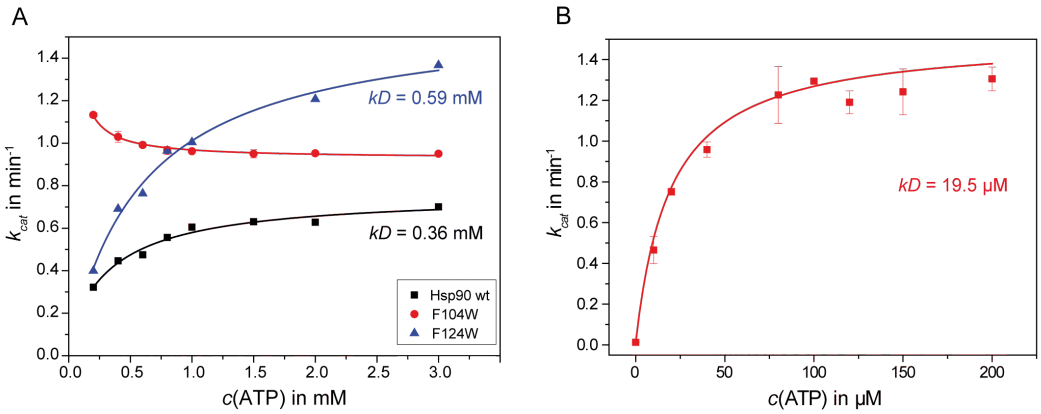

Figure 2.31: ATP affinity of Hsp90 Trp mutants. A: ATP titrations were performed at 30 °C in order to determine the affinity for ATP. ATPase activity of 3 µM Hsp90 wt (black), F104W (red) and F124W (blue) were measured in standard assay buffer with 0.2-3 mM ATP. B: ATP titration to Hsp90 F104W. ATPase activity under ATP concentrations of 0.01-0.2 mM ATP were measured in standard assay buffer at 30 °C.

To further test for the ATP affinity of the Hsp90 mutants, titration of ATP in a concentration range from 0.2-3 mM were performed. Titrations are depicted in figure 2.31A. The F124W mutant showed an ATPase activity profile similar to titrations of ATP to wt Hsp90. A lowered affinity for ATP to F124W (0.6 mM) could be determined (ATP affinity wt Hsp90: 0.3 mM). ATP titration for the lid-variant F104W resulted in a surprising behaviour: the ATPase activity was slightly inhibited upon the addition of ATP (fig. 2.31A). The inhibition of the ATPase activity by ATP in the case of the F104W mutant is an unusual behaviour of Hsp90, also given that the F104W ATPase activity of 0.93 min^{-1} does not differ dramatically from wt Hsp90. For F104W, ATP titration in the applied range of 0.2-3 mM, resulted in a fast saturation. Thus, titrations with ATP concentrations lower than 0.2 mM were performed. For Hsp90 wt, such low concentrations do not result in a detectable change in the Hsp90 activity with the used regenerative assay system. This is due to its rather low ATP affinity. Surprisingly, we could observe an increase in the ATPase activity of the F104W mutant at ATP concentrations from 10 to 200 µM ATP (fig. 2.31B). The activity of this variant is highly increased from 0-80 µM ATP (max. k_{cat} 1.3 min^{-1}) and reaches a plateau from 80-200 µM ATP. Addition of higher concentrations of ATP results again in a slight decrease of the catalytical activity (figure 2.32).

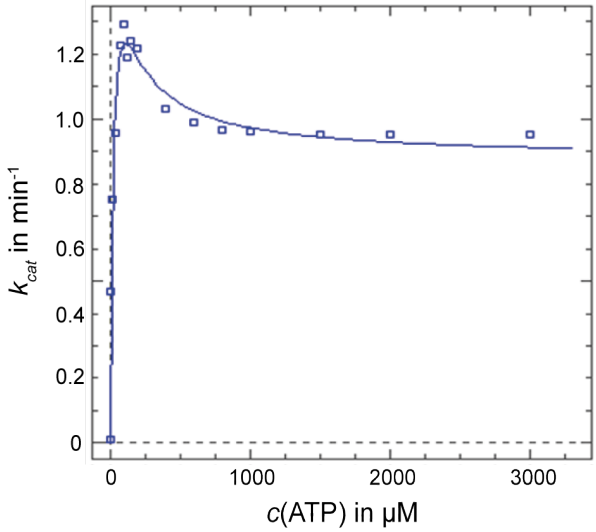

Figure 2.32: ATP affinity of Hsp90 F104W. ATP titrations were performed at 30 °C in order to determine the affinity for ATP. ATPase activity of 3 µM Hsp90 F104W was measured in standard assay buffer with 0.01-3 mM ATP. Obtained data was fitted with the programme Dynafit using a two site binding model for Hsp90.

2.3.2 Co-chaperone effects

An altered ATPase activity of Hsp90 might also result in altered co-chaperone effects. Affinities of Hsp90 and its mutants were tested for the co-chaperones Aha1 and Sti1 (fig-

ure 2.33). For Aha1, wt Hsp90 has an affinity of 3.23 μM. Both, the F124W and F104W mutant, showed slightly higher affinities for Aha1 (fig. 2.33A). F124W has an affinity of 1.21 μM, while F104 binds Aha1 with an affinity of 1.9 μM. Interestingly, stimulation of Aha1 resulted for all Hsp90 variants in almost the same catalytical activities as wt Hsp90. Especially for F124W, it might have been possible that a saturation with Aha1 leads to an even higher catalytical activity. This mutant showed a 2-fold increase in ATPase activity compared to Hsp90 wt. Overall, slightly higher ATPase rates where observed for F124W upon Aha1 titration compared to wt or F104W. At Aha1 concentrations of 30 μM, F124W showed a maximal k_{cat} of 14 min^{-1}, whereas Hsp90 wt and F104W had a k_{cat} 12 min^{-1}.

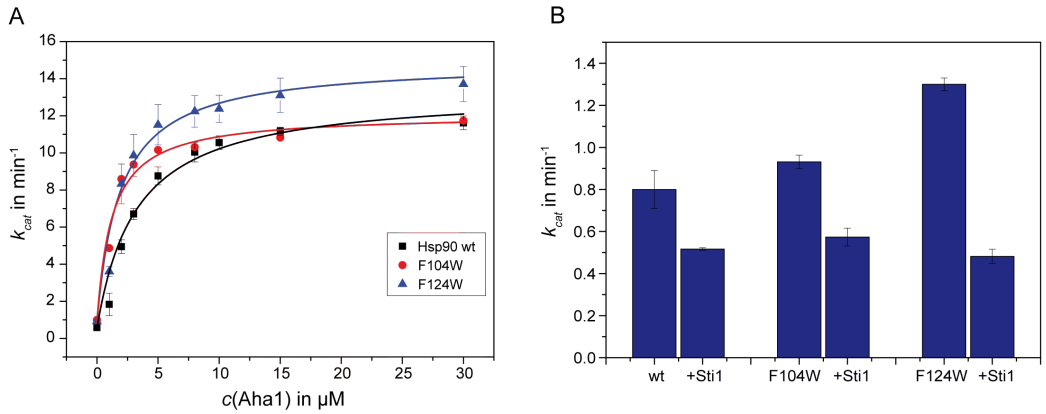

Figure 2.33: Co-chaperone influence on Hsp90 Trp mutants. A: Influence of Aha1. ATPase activity of 1 μM of Hsp90 was measured in the presence of 2 mM ATP and varied concentrations of Aha1 (0-30 μM). B: Influence of Sti1 on Hsp90. The influence of Sti1 on Hsp90 wt and on the Trp variants was measured. The Hsp90 ATPase activity in equimolar ratios with Sti1 was determined (1 μM Hsp90, 1μM Sti1). Measurements were performed at 30 °C in low salt buffer (Aha1) and HKM (50-75-5, pH 7.5) assay buffer (Sti1).

The effect of Sti1 on wt Hsp90 and the Trp mutants was also addressed (fig. 2.33B). For Hsp90 wt and its variants, an expected inhibitory effect of Sti1 could be observed. For Hsp90 wt, a 36 % inhibition upon the addition of Sti1 at equimolar concentrations was observed. F104W showed a Sti1-mediated inhibition of 39 %, whereas the strongest Sti1 effect was observed for F124W: The ATPase activity was decreased by 63 % (k_{cat} 0.48 min^{-1} in the presence of Sti1, compared to a k_{cat} of 1.30 min^{-1} without Sti1). Interestingly, all variants showed an almost complete inhibition upon Sti1 addition at saturating conditions (data not shown). The kD of Sti1 to Hsp90 wt and its mutants was determined to be around 0.5 μM, consistent with previously published results [Schmid et al., 2012]. Again, the co-chaperone influence of the Trp variants does not differ dramatically from Hsp90 wt. The only exception is the higher inhibition of F124W at equimolar Sti1 concentrations. Sti1 can inhibit F124W twice as strongly at such concentrations than Hsp90 wt or F104W. Nonetheless, saturating Sti1 concentrations result in the same complete inhibition of the Hsp90 ATPase for the Trp mutants as well as for Hsp90 wt.
In summary, co-chaperones do not influence the Hsp90 Trp variants in a dramatically

different way than Hsp90 wt. Affinities of both, Aha1 and Sti1, are also not significantly different between Hsp90 and the mutants. It seems that only the intrinsic ATPase activity without co-chaperones is altered in these mutants.

2.3.3 Nucleotide affinity of the Trp mutants

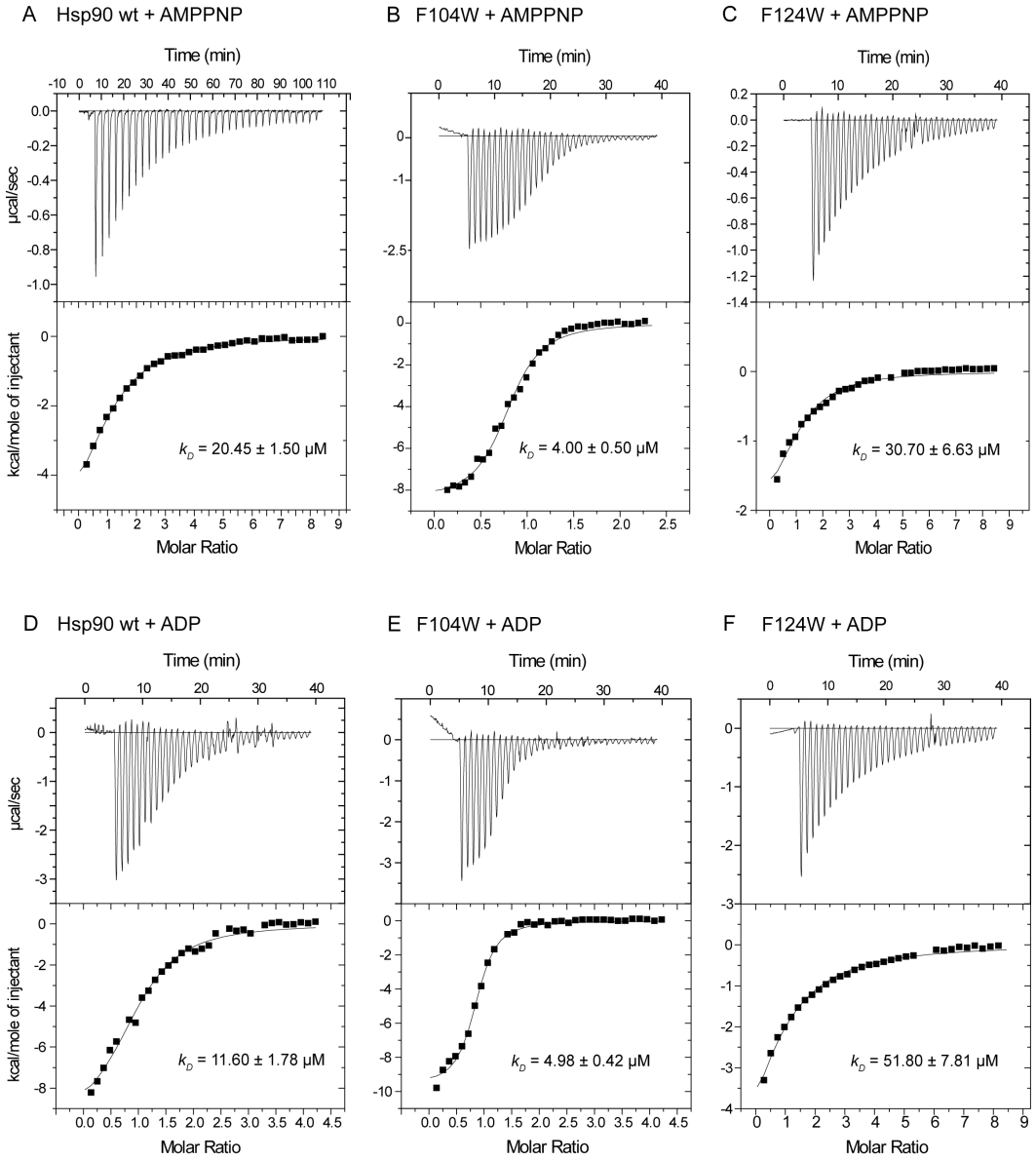

Figure 2.34: Nucleotide affinities to the Hsp90 NTD. A-C: AMP-PNP was titrated to Hsp90 NTD wt (A), F104W (B) and F124W (C). D-F: ADP was titrated to 50 µM Hsp90 NTD. Titration curves were fitted by a one set of sides model with the Origin software. Measurements were performed in standard assay buffer at 20 °C.

As observed in the ATPase assay, the Trp mutants display an altered affinity for ATP.

To further characterise the nucleotide affinity of the mutants, ITC measurements were performed. Since mutations of Hsp90 were introduced in the NTD, only the NTD domain was used in the ITC. The nucleotides ADP (open state of Hsp90) and AMP-PNP (fully closed state of Hsp90) were titrated to the wt and mutant Hsp90 NTD, respectively. AMP-PNP titrations to the different NTD variants were performed in different ratios of NTD to AMP-PNP (figure 2.34 D-F). All measurements were fitted with a 'one set of sides' binding model. Also, measurements with different ratios of NTD to nucleotide that resulted in a fast or no saturation of the NTD with nucleotide were fitted, which resulted in reproducible binding affinities for ATP to each tested construct.
1 mM ADP titrated to 50 μM of Hsp90 NTD (wt and F104W, respectively), did not result in saturation for 50 μM of the F124W NTD. Thus, measurements were repeated with 2 mM ADP. Results are summarised in figure 2.34. Binding studies of AMP-PNP to Hsp90 revealed an affinity of 20.45 $\pm$ 1.50 μM. F104W showed a 5-fold higher affinity for AMP-PNP (kD = 4.00 $\pm$ 0.50 μM), while the AMP-PNP affinity of F124W was decreased (kD = 30.70 $\pm$ 6.63 μM) (fig. 2.34A-C). Titrations of the Hsp90 NTD with ADP resulted in similar results than for AMP-PNP (fig. 2.34D-F). The y90 wt NTD binds ADP with an affinity of 11.60 $\pm 1.78 \mu$M. Again, F104W displayed a much higher affinity with 4.98 $\pm$ 0.42 μM. The titration of ADP to F124W revealed a kD of 51.80 $\pm$ 7.81 μM, which is almost 5-fold lower than the ADP affinity to Hsp90 NTD wt.
These measurements confirm data obtained by the ATPase assay. F124W shows the weakest affinity to nucleotides. Binding affinities for ADP and AMP-PNP are in an equal range for F124W. The F104W variant shows again the highest nucleotide affinity for both, AMP-PNP and ADP. Hsp90 wt has an around 2-fold higher affinity for ADP than for AMP-PNP. Interestingly, this difference does not hold true for the F104W variant. It has similar binding affinities for both, AMP-PNP and ADP. However, it is still surprising that a mutation in the highly important lid region of Hsp90 does result in an improved nucleotide affinity and an elevated ATPase activity. In the case of F124W, there is even an inverse ratio of the affinities to AMP-PNP and ADP in comparison to wt Hsp90: F124W shows a higher AMP-PNP affinity (kD = 30.70 $\pm$ 6.63 μM) than for ADP (kD = 51.80 $\pm$ 7.81 μM). The introduced Trp residue at position 124 might hinder nucleotide binding due to steric hindrance. Since the naturally occurring Phe at position 124 at wt Hsp90 is smaller in size than a Trp, this possible steric hindrance would not be surprising. However, the observed 2-fold higher ATPase activity is somewhat contradictory to this lowered nucleotide affinity. Intramolecular FRET measurements can be applied to investigate conformational closing rates and the influence of different nucleotides for a variety of conformational Hsp90 states. Unfortunately, the data set on the Hsp90 FRET for the Trp variants was not complete at the time this thesis was written. The preliminary data will thus not be presented.

2.3.4 Trp fluorescence

The introduction of strategically placed tryptophans into a protein can be used as a probe to monitor nucleotide binding [Weber et al., 1994, Kumar et al., 2009]. Hsp90 wt contains five tryptophans which are distributed over the whole protein sequence and do not specifically accumulate within a certain region (uniprot protein sequence of Hsp82, entry number: P02829). Tryptophan fluorescence spectra were recorded in order assess if the generated Hsp90 Trp variants are suitable as fluorescent probes and show a specific change in signal upon nucleotide binding. The different Hsp90 variants were excited at 295 nm and emission was recorded from 310-380 nm. For nucleotide titrations, the emission wavelength was set to 338 nm. The fluorescent signal was corrected for the inner filter effect of nucleotides as described in the Materials and Methods section. Prior to the measurement, Hsp90 Trp mutants were incubated with increasing amounts of AMP-PNP (0-2 mM) in standard assay buffer at RT. Figure 2.35 shows the recorded emission spectra of Hsp90 wt (A), F104W (B) and F124W (C).

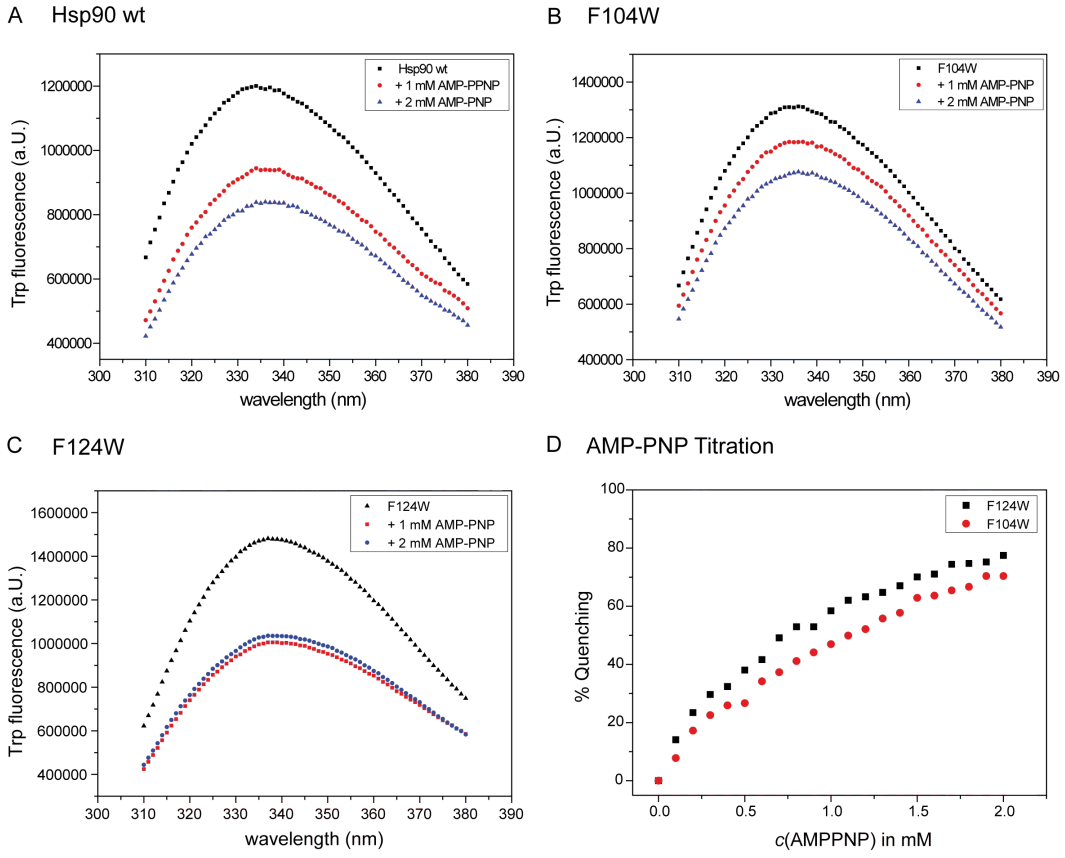

Figure 2.35: Trp fluorescence of Hsp90 wt and the Trp mutants. A-C: Trp fluorescence spectra of Hsp90 in absence and presence of AMP-PNP. Emission spectra were recorded from 310-380 nm. D: 0-2 mM AMP-PNP were titrated to F104 and F124W, respectively, and Trp fluorescence was recorded at a wavelength of 338 nm. All measurements were performed in standard assay buffer. Samples were excited at 295 nm.

As expected, the Trp mutants display a higher intrinsic tryptophan fluorescence (up to 20 % higher fluorescent signal), implying that the introduced tryptophans are accessible and not buried inside any hydrophobic pockets. Addition of 1 mM AMP-PNP resulted in quenching of the Trp fluorescence for all Hsp90 variants and the wild-type. The strongest quenching (34 %) was observed for F124W, confirming that position 124 is directly involved in nucleotide binding. Trp fluorescence of Hsp90 wt was quenched by 20 % upon introduction of AMP-PNP. A further addition of nucleotide (final concentration of 2 mM AMP-PNP) did not result in any further quenching of F124W's fluorescence (fig. 2.35C). F104W's fluorescence signal was reduced by only 15 %. This implies that the introduced Trp at position 104 in the lid segment remains mostly accessible upon addition of nucleotide and is not quenched by AMP-PNP. This is not surprising in terms of the lid function in wt Hsp90: After nucleotide binding, the lid repositions and closes over the Hsp90 nucleotide binding pocket. The introduced tryptophan residue might remain on the outer side of Hsp90 and not be repositioned into the nucleotide binding pocket.
Furthermore, AMP-PNP titrations (0-2 mM) to the Hsp90 Trp variants were performed (figure 2.35D). Emission was recorded at a wavelength of 338 nm, while protein samples were excited at 295 nm. AMP-PNP caused a maximal quenching of the fluorescence signal by 78 % of the F124W variant, while the Trp fluorescence of the F104W mutant was quenched by 70 %.

2.3.5 Stopped flow

Stopped flow measurements were performed to assess the association of Hsp90 with nucleotides. The rate constants for each Trp variant were determined by taking advantage of the change in tryptophan fluorescence upon binding of nucleotides. 4 μM of Hsp90 were mixed with nucleotide in a stopped flow device and the signal in tryptophan fluorescence was recorded. Figure 2.36 summarises the results of the stopped flow fluorimetry measurements (performed by Jochen Reinstein, MPI for medical research Heidelberg, Germany). 200, 400 and 600 μM of ADP and ATP, respectively, were added to 4 μM of F124W (fig. 2.36A and B, respectively). For MABA-ATP, concentrations of 7 and 15 μM were applied (fig. 2.36C).

Table 2.5: **Kinetic constants for nucleotide binding to F124W**

F124W + ADP	**F124W + ATP**
k_{on} = 0.72 $\mu M^{-1}s^{-1}$	k_{on} = 0.098 $\mu M^{-1}s^{-1}$
k_{off} = 11.7 s^{-1}	k_{off} = 33.5 s^{-1}
kD_{calc} = 16.2 μM	kD_{calc} = 340 μM

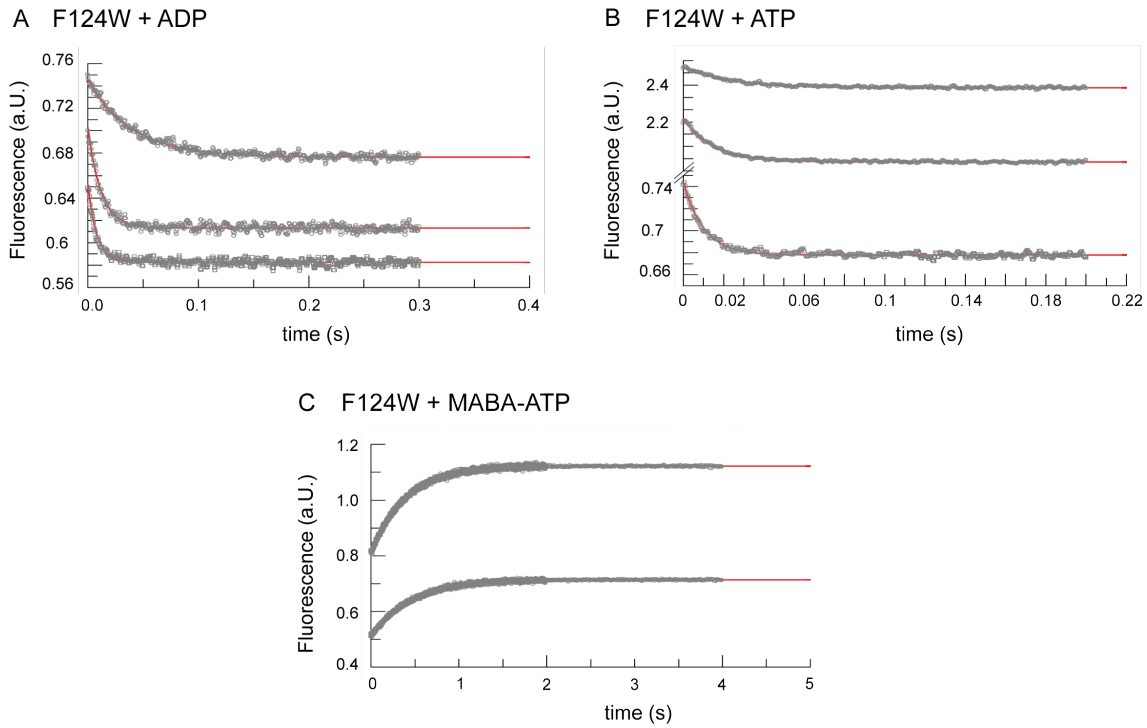

Figure 2.36: Pre-steady state nucleotide binding kinetics. The change in tryptophan fluorescence after mixing Hsp90 F124W with different nucleotides ADP (125, 350, 700 μM) (A), ATP (125, 350, 700 μM) (B), MABA-ATP (7.5 and 15 μM)(C) was measured by stopped flow fluorimetry. Measurements were performed at 25 °C in 40-50-5, pH 7.5 assay buffer. 4 μM of F124W were used for each measurement.

Table 2.5 summarises the kinetic rate constants of nucleotide binding for F124W. For both, ADP and ATP binding, the limiting factor is the k_{on} rate. For ATP binding to F124W, a k_{on} of 0.098 $\mu M^{-1}s^{-1}$ and a k_{off} rate of 33.5 s^{-1} were determined. ADP binding gave a k_{on} of 0.72 μM^{-1} and k_{off} rate of 11.7 s^{-1} were determined. The affinity for ADP to F124W was determined as 16.2 μM and the ATP affinity was calculated as 340 μM. This is in consistency with a high affinity for ADP and low affinity for ATP, which was also measured by ITC and ATPase assays. Kinetic rates for the binding of MABA-ATP were estimated: k_{off} = 1.9 s^{-1}, k_{on} = 0.04 $\mu M^{-1}s^{-1}$ with a kD of around 47 μM. This data is consistent with previous data for Hsp90 wt (data not shown). In case of ATP binding, there is no tight binding detectable, which might point to a mechanism where ATP binding occurs in a non-cooperative manner. However, it is not clear if the introduced reporter Trp is able to sense both, binding of nucleotides and structural rearrangements of Hsp90. Due to five other tryptophans in Hsp90, it cannot be excluded that changes in Trp fluorescence represent mixed signals, from the introduced Trp at position 124 and the naturally occurring wt Trp residues.
For the F104W variant, stopped flow measurements were also performed. Surprisingly, signals obtained for nucleotide binding were rather weak for this mutant. The signal for ATP binding was about 1.3-1.5 % of the protein and not dependent on the ATP concentration. No amplitudes or rate constants could be determined. ADP does also not produce any observable signal, only a fast phase (k_{on} 1.35 s^{-1}) with only a minor amplitude, which may be an artifact. Measurements with MABA-ATP produced a good signal, comparable to wt Hsp90, but slower and much stronger. From single binding and chase experiments, the binding constant for MABA-ATP to F104W can be estimated to about 1 μM. However, this signals were rather unexpected and might be considered carefully due to a high possibility that only artifacts were observed. F104W thus does not seem to be suitable as probe for nucleotide binding.

2.3.6 Growth effects of Trp mutants

Hsp90 is essential for yeast cells and its deletion results in lethality [Nathan $\mathrm{et\ al.}$, 1997]. Two isoforms, encoded by the HSP82 and HSC82 genes, exist in yeast [Borkovich $\mathrm{et\ al.}$, 1989]. At least one isoform is necessary to support viability. In order to address if an altered ATPase activity of Hsp90 results in altered growth, the Hsp90 variants were shuffled into yeast cells. Viability as well as sensitivity to different environmental conditions can be addressed. An established shuffling system [Nathan $\mathrm{et\ al.}$, 1997] was applied. This system makes use of a shuffling strain that has a deletion of the naturally occurring two Hsp90 genes and an Hsp90 gene on a URA-plasmid with a constitutive GPD promoter. By transferring this strain to 5'FOA plates, the URA-plasmid displays a high toxicity and keeping this plasmid would result in death of the cells. This circumstance can be used to supply the cells with a modified version of Hsp90. A p423 HIS-plasmid

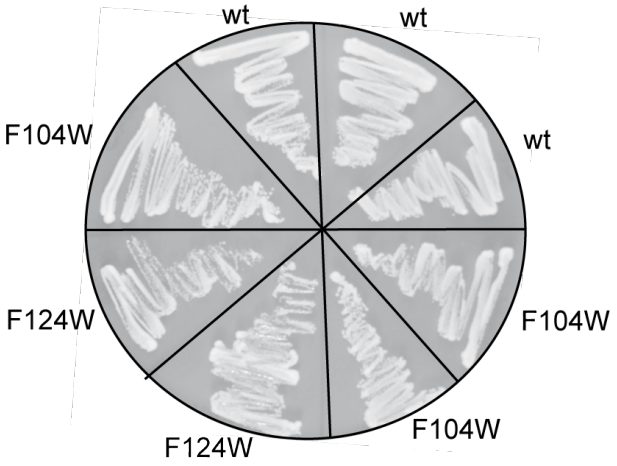

Figure 2.37: Viability of Trp variants in yeast cells. The tryptophan variants F104W and F124W were shuffled into yeast cells and grown at 30 °C. A p423 plasmid with Hsp90 wt was used as control. Cells were grown on 5'FOA plates for two days and then transferred to FOA-free His plates.

was chosen as vector for the Hsp90 Trp variants and wt. The shuffling strain was transformed with the plasmids of the different Hsp90 variants and grown on -Ura -His selective medium. Subsequently, cells were transferred to FOA-plates in order to cause loss of the URA-Hsp90 plasmid. Cells were transferred afterwards onto -His plates. As shown in figure 2.37, the two Trp mutants, F104W and F124W, support viability in yeast. No difference in growth could be observed between wt Hsp90 and the Trp variants.

2.3.7 Outlook

Tryptophans at the positions 104 and 124 in yeast Hsp90 were introduced as potential spectroscopic probes to elucidate the events that occur upon nucleotide binding to Hsp90. First, it was confirmed that the engineered Hsp90 variants, were still active concerning the ATPase activity and co-chaperone interaction. Interestingly, the two mutants showed an elevated ATPase activity compared to Hsp90 wt. F124W showed a two-fold higher ATPase actvity, while the activity of F104W was slightly elevated (k_{cat} = 0.93 min^{-1}) compared to Hsp90 wt. F124W was stimulated slightly more than the wild-type by the co-chaperone Aha1, whereas stimulation of F104W resulted in the same activity as Hsp90 wt. However, both mutants had an increased affinity to Aha1 (F104W kD = 1.9 μM , F124W kD = 1.21 μM , wt kD = 3.23 μM). The co-chaperone Sti1 could inhibit both mutants, resulting in the same activity as for the wild-type. However, the relative inhibition by Sti1 was higher for the Trp variants than for the wild-type. Generally, the co-chaperone influence on the Trp variants differs only slightly from Hsp90 wt. Interaction with the conformation sensitive co-chaperone Sba1 was not tested so far. Since

Sba1 only binds to closed Hsp90, this co-chaperone can be used to investigate if the Trp mutants are still able to reach a fully closed state. If the interaction with Sba1 is altered, a possible conclusion might be that the mutants cannot reach the closed state and thus, interaction with Sba1 is impaired. Especially for the F104W lid mutant, it might be possible that it cannot completely close due to the bulky Trp residue in the lid structure.
Both, F104W and F124W, variants were characterised further for their changes in tryptophan fluorescence upon nucleotide binding. Trp fluorescence spectra implied that the signal of both mutants can be quenched upon binding of AMP-PNP. However, the fluorescence of both mutants could not be completely quenched since Hsp90 naturally contains five tryptophans which are also contributing to the fluorescent signal. Quenching of F124W was more efficient than that of F104W. This might be due to the position of the introduced tryptophans: Position 124 was shown to be the binding site for ATP, which means that most of the 124W fluorescence might be quenched upon nucleotide binding. Position 104, part of the lid structure, is repositioned after nucleotide binding to close over the nucleotide binding pocket and stabilise the closed state of Hsp90 [Hessling $\mathrm{et\ al.}$, 2009]. Fluorescence of this tryptophan might not be quenched completely since the lid is not buried inside a hydrophobic pocket. This could also be seen in the stopped flow fluorimetry measurements, which could not rule out that the observed changes in tryptophan fluorescence might not be specific for the position 124. Sensing only the binding event of nucleotides at the Trp reporter position 124 might be unlikely. The question remains if these two artificially introduced tryptophans are suitable for reporter residues for dissecting the nucleotide binding mechanism of Hsp90. In case of the well-characterised chaperone GroEL, reporter tryptophans were also introduced and could help in elucidating the cooperative mechanism of ATP binding [Yifrach and Horovitz, 1995]. Nonetheless, GroEL wt does not contain any tryptophans leading to a highly specific signal for Trp fluorescence of the engineered Trp residue. In Hsp90, this is rather complicated and might require a deletion of all the naturally occurring tryptophans which would result in a highly artificial scenario and probably also a non-functional Hsp90 protein. *In vivo* data on the Trp variants, suggest viability of these two mutants.
Nucleotide binding studies for the Trp mutants revealed a much higher affinity of F104W for nucleotides. Nucleotide binding to this mutant seems promoted and a kD of 19.5 μM was determined. This is an extraordinary high ATP affinity. F124W overall shows a decreased nucleotide affinity compared to Hsp90 wt. A study on the human Hsp90β lid mutant I123T (which corresponds to the position V114 in yeast Hsp90) revealed that this mutation causes a highly active Hsp90 *in vitro* and at the same time causes 17-AAG inhibitor resistance in yeast cells [Zurawska $\mathrm{et\ al.}$, 2010]. Subsequently, this allowed for the selection of inhibitor-tolerant HEK293 cells [Zurawska $\mathrm{et\ al.}$, 2010]. This might be a possible scenario as well for the Trp mutants and will be addressed further with *in vivo* experiments on inhibitor tolerance. Growth of F104W as well as of F124W yeast cells did not seem to be affected, however, growth under heat stress or other stress conditions was not addressed. Observing viability of the Trp mutants *in vivo* might support

the mutational study of Zierer *et al.* (Dissertation Bettina Zierer, TU Munich) which does not necessarily link an altered ATPase activity with lethal effects of Hsp90 mutants *in vivo*. Under normal conditions, mutants with no ATPase activity *in vitro*, like the E33A mutant, but also mutants with a higher ATPase (e.g. T22I) are viable *in vivo* [Nathan and Lindquist, 1995, Panaretou $\mathrm{et\ al.}$, 1998]. However, those mutants show a severe growth defect under heat stress. Furthermore, for a complete data set of the herein addressed Trp mutants, closing kinetics applying the intramolecular Hsp90 FRET system and client activation (e.g. GR, v-Src) *in vivo* will be determined.

CHAPTER 3

Material and Methods

3.1 Material

Chemicals	Manufacturer
Acrylamide solution (38 % with 2 % bisacrylamide)	Roth, Karlsruhe, Germany
Adenosin-5'-diphosphate	Roche, Mannheim, Germany
Adenosine 5'-O-(3-thiotriphosphate)	Roche, Mannheim, Germany
Adenosin-5'-triphosphate, disodium salt	Roche, Mannheim, Germany
Adenosyl-imidodiphosphate	Roche, Mannheim, Germany
Agarose, disodium salt, ultrapure	Roth, Karlsruhe, Germany
Albumin from bovine serum	Sigma, St. Louis, USA
Amino acids	Sigma, St. Louis, USA
^{15}N Ammoniumchloride	Euriso-top, Au, Germany
Ammoniumperoxodisulfate (APS)	Serva, Heidelberg, Germany
Ammoniumsulfate	Merck, Darmstadt, Germany
Ampicillin	Roth, Karlsruhe, Germany
Bacto Agar	Difco, Detroit, USA
Bacto Peptone	Difco, Detroit, USA
Bacto Tryptone	Difco, Detroit, USA
Bromphenol blue S	Serva, Heidelberg, Germany
Chloramphenicol	Sigma, St. Louis, USA
Coomassie Brilliant Blue G-250	Serva, Heidelberg, Germany
Coomassie Protein Assay Reagent	Pierce, Rockford, USA

D_2O (60 %, >99 %)	Euriso-top, Au, Germany
Deoxyribonucleoside triphosphates (dNTPs)	Roche, Mannheim, Germany
Dimethylsulfoxid (DMSO)	Merck, Darmstadt, Germany
1,4-Dithiothreitol (DTT)	Roth, Karlsruhe, Germany
1-Ethyl-3-(3-dimethylaminopropyl) carbodiimide hydrochloride (EDC)	GE Healthcare, Uppsala, Sweden
ECL WesternBright Detection Spray	advansta, Menlo Park, USA
Ethanol, p.a.	Merck, Darmstadt, Germany
Ethanolamine hydrochloride-NaOH	GE Healthcare, Uppsala, Sweden
Ethidiumbromide	Sigma, St. Louis, USA
Glycerol, 99 %	Roth, Karlsruhe, Germany
Guanidinium hydrochloride, p.a.	ICN, Irvine, USA
Imidazol	Roth, Karlsruhe, Germany
Isopropyl-D-1-thiogalactopyranoside (IPTG)	Merck, Darmstadt, Germany
Isopropanol	Merck, Darmstadt, Germany
Kanamycin	Roth, Karlsruhe, Germany
LB_0	Serva, Heidelberg, Germany
2-β-Mercaptoethanol, pure	Roth, Karlsruhe, Germany
Malachite Green chloride	Sigma, St. Louis, USA
β-Nicotinamide adenine dinucleotide	Roche, Mannheim, Germany
N-(2-Hydroxyethyl)-piperazine-N'-2-ethan-sulfonic acid (HEPES)	Roth, Karlsruhe, Germany
N,N,N',N'-Tetramethylethylendiamin (TEMED)	Roth, Karlsruhe, Germany
N-Hydroxysuccinimide (NHS)	GE Healthcare, Uppsala, Sweden
Phosphoenolpyruvic acid, monopotassium salt	Sigma, St. Louis, USA
Polysorbate 20 (Tween 20)	Merck, Darmstadt, Germany
Protease inhibitor mix G	Serva, Heidelberg, Germany
Protease inhibitor mix HP	Serva, Heidelberg, Germany
Radicicol	Sigma, St. Louis, USA
Salmon Sperm DNA	Sigma, St. Louis, USA
Sodiumdodecylsulfate (SDS)	Serva, Heidelberg, Germany
Stain G	Serva, Heidelberg, Germany
Tris-(hydroxymethyl)-aminomethan (Tris)	Roth, Karlsruhe, Germany
Titriplex (EDTA)	Serva, Heidelberg, Germany
Yeast Extract	Serva, Heidelberg, Germany
Yeast Nitrogen Base (YNB)	Difco, Detroit, USA
YPD	Sigma, St. Louis, USA

Antibodies/Enzymes	**Manufacturer**
Citrate synthase from pig heart	Roche

Monoclonal IgG-POD conjugate against rabbit IgG (goat)	Sigma
Monoclonal IgG-POD conjugate against mouse IgG (sheep)	Sigma
Monoclonal anti-hemagglutinin (HA) antibody, clone HA-7 (mouse)	Sigma
Polyclonal sera against Hsp90 co-chaperones (rabbit)	Dr. Pineda, Berlin, Germany
Restriction enzymes	Promega, Mannheim, Germany
Thrombin	Serva
DNA Ligase T4	Promega
DNA Polymerase Pfu	New England Biolabs (NEB), Frankfurt, Germany
DNA Polymerase Phusion	NEB
DNA Polymerase Q5	NEB
DpnI	NEB
Pyruvate Kinase	Roche
Lactat Dehydrogenase	Roche

Kits and Size Markers	**Manufacturer**
BiaCore Amine Coupling Kit	GE Healthcare Life Sciences
Wizard® Plus SV Mini-Preps DNA purification	Promega
Wizard® SV Gel and PCR Clean-Up System	Promega
Low range molecular weight marker	Biorad, Munich, Germany
PeqGold 1 kb DNA ladder	peqlab, Erlangen, Germany
Protein Marker IV, prestained	peqlab

3.1.1 Media

Medium	
dYT medium:	5 g/l NaCl, 10 g/l yeast extract, 16 g/l pepton/trypton
LB medium:	20 g/l LB_0 powder
for plates:	2 % agar agar
M9 medium:	7.52 g/l Na_2HPO_4, 3 g/l KH_2PO_4, 0.5 g/l NaCl, pH 7.3
Antibiotics	
Kanamycin	35 μg/ml
Ampicilin	100 μg/ml

Chloramphenicol	50 μg/ml

Depending on the plasmid-mediated antibiotic resistancy of the *E. coli* cells, cells were grown in LB medium supplemented with the respective antibiotic.

Yeast medium:

YPD	20 g/l YPD powder

Drop Out Mix:

Amino acid	**Amount**
Adenine	0.5 g
Arginine	2.0 g
Aspartic Acid	2.0 g
Histidine	2.0 g
Leucine	10.0 g
Lysine	2.0 g
Methionine	2.0 g
Phenylalanine	2.0 g
Threonine	2.0 g
Tryptophan	2.0 g
Tyrosine	2.0 g
Uracil	2.0 g
	Σ = 30.5 g

Selective amino acid mix

YNB	6.7 g
Selective amino acid mix	0.87 g
Glucose/Raffinose/Galactose	20 g
H_2O	ad 1 l
for plates: 2 % agar agar (Serva)	

3.1.2 Buffers

Quick Ligation Buffer	
Tris-HCl, pH 7.5	50 mM
$MgCl_2$	10 mM
ATP	1 mM
DTT	10 mM

TAE Buffer	50x
Tris/acetate, pH 8.0	2 M
EDTA, pH 8.0	50 mM

Standard assay buffer	
HEPES	40 mM
KCl	150 mM
$MgCl_2$	5 mM
pH 7.5	

Low salt assay buffer	
HEPES	40 mM
KCl	20 mM
$MgCl_2$	5 mM
pH 7.5	

Laemmli Loading Buffer (5x)	
TrisHCl	300 mM
SDS	10 % (w/v)
Glycerol	50 % (w/v)
Bromphenol blue	0.05 % (w/v)
β-Mercaptoethanol	5 % (v/v)

SDS-PAGE Buffer (10x)	
TrisHCl	250 mM
Glycine	2 M
SDS	1 % (w/v)

Agarose Gel Loading Buffer	
Glycerol	50 % (v/v)
EDTA, pH 8.0	10 mM
Bromphenol blue	0.2 % (w/v)
Xylencyanole	0.2 % (w/v)

3.1.3 Strains

Strain	Genotype	Origin
E. coli		
E. coli MACH1	Δ*rec*A1398 *end*A1 *ton*A Φ80ΔlacM15 Δ*lac*X74 *hsd*R(rk- mk+)	Invitrogen, Darmstadt, Germany
E. coli BL21 (DE3)	F-*ompT hsdS*(rB- mB-) *dcm*+ Tetr *gal endA* Hte [*arg*U *ile*Y *leu*W CamR]	Stratagene, La Jolla, USA
E. coli XL1 blue	*rec*A1 *end*A1 *gyr*A96 *thi*-1 *hsd*R17 *sup*E44 *rel*A1 *lac*	Stratagene, La Jolla, USA
S. cerevisiae		
BY4741	MATa; his3Δ1; leu2Δ0; met15Δ0; ura3Δ0	Euroscarf, Frankfurt, Germany
BY4741 ΔAha1	MATa; his3Δ1; leu2Δ0; met15Δ0; ura3Δ0; YDR214w::kanMX4	Euroscarf, Frankfurt, Germany

3.1.4 Plasmids

Expressionplasmid	Cloning Site	Origin
pET11 Hsp82 N210	NdeI/BamHI	Klaus Richter
pET11 N210 F104W	NdeI/BamHI	this work
pET11 N210 F124W	NdeI/BamHI	this work
pET28 Hsp82	NdeI/XhoI	Klaus Richter
pET28 Hsp82 F104W	NdeI/XhoI	this work
pET28 Hsp82 F124W	Nde/XhoI	this work
pET28 Hsp82 D61C	Nde/XhoI	Martin Hessling
pET28 Hsp82 Q385C	Nde/XhoI	Martin Hessling
pET28 Hsp82 D61C F104W	NdeI/XhoI	this work
pET28 Hsp82 D61C F124W	NdeI/XhoI	this work
pET28 Hsp82 Q385C F104W	NdeI/XhoI	this work
pET28 Hsp82 Q385C F124W	NdeI/XhoI	this work
pET28 Hsp82 MD	NdeI/XhoI	Marco Retzlaff
pET28 CtHsp90		GeneArt
pET28 ySgt1	NdeI/NotI	this work
pET28 Sba1	NdeI/BamHI	Klaus Richter
pETSUMO Hsp82	BamHI/XhoI	Alina Röhl
pET28 hHsp90β	BamHI/XhoI	Oliver Lorenz
pETSUMO Sti1	BamHI/XhoI	Andreas Schmid
pET28 yAha1	NdeI/BamHI	Klaus Richter
pET28 yAha1 N-domain	NdeI/XhoI	Marco Retzlaff
pET28 yAha1 C-domain	NdeI/XhoI	Marco Retzlaff

pET28 hAha1	BamHI/XhoI	Klaus Richter
pETSUMO Hsp82 NM	BamHI/XhoI	Alina Röhl
pETSUMO CtHsp90	BamHI/XhoI	this work
pETSUMO CtHsp90 MC	BamHI/XhoI	this work
pETSUMO CtAha1	BamHI/XhoI	this work
pETSUMO CtSti1	BamHI/XhoI	this work
pETSUMO CtCdc37	BamHI/XhoI	this work
pETSUMO CtCpr6	BamHI/XhoI	this work
pETSUMO CtSba1	BamHI/XhoI	this work
pET28 EcHsp90	BamHI/XhoI	Jing Li
pRSET A Cpr6		C. Prodromou
pRSET A Cpr7		C. Prodromou

Yeast vectors	**Origin**
pSM1152 CFTR wt PGK	Jeff Brodsky
pSM1152 CFTR $\triangle$F508 PGK	Jeff Brodsky
p423 GPD empty vector	ATCC, Manassas, USA
p423 GPD Hsp82	Alexandra Rehn
p423 GPD Hsp82 F104W	This work
p423 GPD Hsp82 F124W	This work
p416 CtAha1	This work
p413 GPD hGR	Priyanka Sahasrhabudhe
p413 GPD hMR	Priyanka Sahasrhabudhe
p426 GPD βGal	Andreas Schmid
pUC$\triangle$s 26X	Brian Freeman

3.1.5 Oligonucleotides

Oligonucleotides were synthesised by MWG Eurofins (Ebersberg, Germany). Primers for the QuikChange Mutagenesis were designed in accordance with the manufacturer's protocol. Primers for SLIC cloning were designed with the NEBuilder® Assembly Online Tool (NEB).

Construct	**Sequence**
Hsp82 F104W fwd	TACTAAAGCTTGGATGGAAGCTCTATCTGCT
Hsp82 F104W rev	GAGCTTCCATCCAAGCTTTAGTACCAGACTTA
Hsp82 F124W fwd	GGTGTTGGTTGGTACTCTTTATTCTTAGTTG
Hsp82 F124W rev	ATAAAGAGTACCAACCAACACCGAATTGACC
hHsp90β F113W fwd	ACTAAAGCATGGATGGAGGCTCTTCAGGCTG
hHsp90β F113W rev	CAGCCTGAAGAGCCTCCATCCATGCTTTAGTAC

hHsp90β F129W fwd	ATTGGGCAGTGGGGTGTTGGCTTTTATTC
hHsp90β F129W rev	AATAAAAGCCAACACCCCACTGCCCAATC
CtHsp90 MC fwd	tcacagagaacagattggtggatccAAGCAAAAGCCCATCTGG
CtHsp90 MC rev	agtggtggtggtggtggtgctcgagTTAGTCAACCTCCTCCATAG
CtAha1 fwd	tcacagagaacagattggtggatccATGGTTCTGCACAATCCC
CtAha1 rev	agtggtggtggtggtggtgctcgagTTATCCAAAAGTAGCCTTGATG
CtSti1 fwd	cagagaacagattggtggatccATGTCGACTGCCGAAGAG
CtSti1 rev	cagtggtggtggtggtggtgctcgagCTACCGGCCAACCCTAATG
CtCdc37 fwd	cagagaacagattggtggatccATGCCGGTTGATTACAGC
CtCdc37 rev	cagtggtggtggtggtggtgctcgagTCACTCCGGGTCGTCAAT
CtCns1 fwd	tgtgctggaattctgcagatatcATGTCCGACAAAGTCGAAG
CtCns1 rev	agtggtggtggtggtggtgctcgagCTACTTGCTCTCCCTCTTAG
CtCpr6 fwd	cagagaacagattggtggatccATGACCGCTGAGGAGAAC
CtCpr6 rev	cagtggtggtggtggtggtgctcgagTCATAGCTCAAAGAACTTCTTG
CtHsp70 fwd	tcacagagaacagattggtggatccATGGCTCCCGCCGTCGGC
CtHsp70 rev	agtggtggtggtggtggtgctcgagTTAGTCGACCTCCTCGACGGTC
CtSba1 fwd	cagagaacagattggtggatccATGGCCACCGATACTGTC
CtSba1 rev	cagtggtggtggtggtggtgctcgagTTACGAGACAACCACCTC
CtSgt1 fwd	cagagaacagattggtggatccATGTCTGGAACAACGGCG
CtSgt1 rev	cagtggtggtggtggtggtgctcgagTCAACTCTCCCACTTCTTAGG

3.1.6 Equipment

Analytical balances	
BP 121S	Sartorius, Göttingen, Germany
BL310	Sartorius, Göttingen, Germany
Analytical Ultracentrifuge	
Beckman ProteomeLab XL-A (Ti-50 rotor)	Beckman, Fullerton, USA
Centrifuges	
Avanti J25 (JA-10, JA-25.50 rotor)	Beckman, Fullerton, USA
Eppendorf Centrifuge 5415C	Eppendorf, Hamburg, Germany
Rotina 420R Centrifuge	Hettich, Tuttlingen, Germany
Chromatographic devices	
Äkta FPLC	GE Healthcare Life Sciences
Jasco HPLC system	Shimadzu, Munich, Germany
Chromatographic material	
HiLoad FF Ni-NTA 6 ml	GE Healthcare Life Sciences
Homogeniser Ultra Turrx DIAX900	Heidolph, Schwabach, Germany
Hydroxyapatite column	Biorad, Munich, Germany
PD10 desalting column	GE Healthcare Life Sciences
Resource Q 6 ml	GE Healthcare Life Sciences

Superdex 75/200 prep grade (16/600)	GE Healthcare Life Sciences
Superdex 75/200 prep grade (26/600)	GE Healthcare Life Sciences
Gel electrophoresis	
Hoefer Mighty Small II Gelelectro-phoresis device	GE Healthcare Life Sciences
Power amplifiers	
LKB-GPS 200/400 Power Amplifier	GE Healthcare Life Sciences
Pharmacia EPS 3500, 301 1001	GE Healthcare Life Sciences
Spectroscopic devices	
Biotech Ultrospec 3000 UV-Vis Spectrometer	Amersham, Uppsala, Sweden
FluoroMax III Spectrofluorimeter	Jobin Yvon, Edison, USA
Fluorescence detection system (aUC)	Aviv Biomedical, Lakewood, USA
Jasco J715 with PTC 343 Peltier Device	Jasco, Groß-Umstadt, Germany
Varian Cary 50/100 Bio UV-VIS-Spectrometer	Varian, Palo Alto, USA
Surface plasmon resonance	
Biacore X100	GE Healthcare Life Sciences
CM5 sensor chip research grade	GE Healthcare Life Sciences
Other equiment	
Amicon Centrifugal Filter Units	Amicon, Witten, Germany
Cell disruptor Basic Z	Constant Systems, Warwick, UK
Dialysis Tube Spectra/Por (6-8 kDa)	Spectrum, Houston, USA
Eppendorf Thermomixer	Eppendorf, Hamburg, Germany
Image Quant 4000 detection device	GE Healthcare Life Sciences
Incubator	Haake, Karlsruhe, Germany
Cellulose Acetate Filters, 0.45 μm	Sartorius, Göttingen, Germany
Mixer Mill MM 400	Retsch, Haan, Germany
Pipet tips	Sarstedt, Nümbrecht, Germany
pH Meter	WTW, Weilheim, Germany
Quartz Cuvettes	Hellma, Müllheim, Germany
Slide-A-Lyser® Dialysis Cassette	Thermo Scientific
Thermocycler Primus	MWG, Ebersberg, Germany
Vortex MS2	IKA, Staufen, Germany

3.1.7 Computer Software

Software	Developer
Adobe Creative Suite	Adobe Systems Inc., San Jose, USA
Clustal W/O alignment tool	[Sievers et al., 2011]
ImageJ 1.48v	Wayne Rasband, NIH, Bethesda, USA

Origin 8	OriginLab Corp., Northhampton, USA
LaTex	www.latex-project.org
PDB database	www.rcsb.org ([Berman et al., 2000])
Prot Param Tool	www.expasy.ch
Pymol	Schrödinger LLC, New York, USA
Saccharomyces genome database	[Cherry et al., 2012]
SedView	[Hayes and Stafford, 2010]
Serial Cloner 2.5	Franck Perez, Serial Basics
SWISS-MODEL	[Arnold et al., 2006]
UniProt	www.uniprot.org

3.2 Methods

3.2.1 Molecular Biology

DNA Amplification

Polymerase Chain Reaction (PCR) was applied for amplification of DNA for cloning and subcloning purposes, respectively. The Quik Change ® Mutagenesis Method (Stratagene, LaJolla, USA), a site-directed mutagenesis approach, was used for the introduction of point mutations in existing constructs. The sequence- and ligation-independent cloning (SLIC) method [Jeong $\mathrm{et\ al.}$, 2012] was applied to clone the thermophilic Hsp90 system into a pET SUMO vector.

Standard PCR Mix:	
Template DNA	1 µl
10x Pfu buffer	5 µl
dNTP mix (10 mM each)	1 µl
Primer forward (100 pmol/µl)	1 µl
Primer reverse (100 pmol/µl)	1 µl
Pfu Polymerase	1 µl
H_2O	ad 50 µl

Standard PCR Programme:	
95 °C	2 min
95 °C	30 s
50-60 °C	30 s - 1 min
72 °C	30 s
	35 Cycles
72 °C	3 min
8 °C	forever

SLIC cloning	
Primer Mix:	5 µl fwd Primer
	5 µl rev Primer
	20 µl ddH_2O
Template: 1:100 dilution	c_{final} = 0.5 - 1 ng

SLIC cloning Mix:	
Q5 Polymerase Buffer	10 µl
Primer Premix	5 µl
dNTP	1 µl
Q5 Polymerase	0.4 µl
ddH_2O	32.6 µl
Σ =	50 µl

SLIC cloning PCR:	
98 °C	1 min
98 °C	10 s
55-65 °C	20 s
72 °C	30 s
35 Cycles	
72 °C	3 min
4 °C	forever

The annealing temperatures were chosen accordingly to the applied primers. PCR constructs were analysed on a 1 % agarose gel supplemented with 0.002 % stain G to visualise DNA (120 V, 30 min). A 1 kb DNA ladder served as size standard. Successfully amplified constructs were purified with a PCR clean-up Kit following the manufacturer's instructions (Promega, Madison, USA). DNA was stored at -20 °C.

3.2.2 Site Directed Mutagenesis

Site Directed Mutagenesis was applied to introduce point mutations into the Hsp90 wild-type construct. The optimised QuikChange® protocol (Stratagene, LaJolla, USA) was followed. For this method, primers with the point-mutation of choice were generated and the wild-type template was amplified as stated above (see DNA Amplification). After successful PCR, 1 µl of the restriction enzyme DpnI was added to the PCR product (1h, 37 °C). DpnI cuts hemimethylated, parental DNA and can therefore separate the mutated PCR product from the template DNA which does not harbour any mutations. 10 µl of the PCR mixture was transformed into 100 µl of XL1 cells following the standard

transformation protocol (described in the section 3.3). Clones were picked, prepped and the purified DNA was send for sequencing (MWG Eurofins, Ebersberg, Germany).

3.2.3 DNA sequence analysis

All constructs were sent for sequencing with MWG Eurofins, Ebersberg, Germany or GATC Biotech, Konstanz, Germany. pET 28b vectors were sequenced with T7 and T7 term/pET Rb primers for forward and reverse sequencing, respectively. Yeast vectors were sequenced by using the GPD forward and CYCterm reverse primers.

3.3 Growth and storage of *E. coli* cells

E. coli cells were grown at 37 °C in LB liquid medium or on LB plates. To select for the harbouring plasmids, the respective antibiotics (Kanamycin, Ampicilin, Chloramphenicol) were added to the medium. Liquid cultures were inoculated with a single colony from a plate or in a 1:100 dilution from an overnight culture. Cell growth was monitored photometrically at 600 nm. An OD of 1 equals approximately $5 \cdot 10^8$ to $1 \cdot 10^9$ cells per ml of medium [Sambrook $\mathrm{et\ al.}$, 1989]. To allow for long-term storage of *E. coli* cells, glycerol stocks were prepared by adding 600 µl of 87 % sterile glycerol to 300 µl of *E. coli* culture, flash frozen and stored at -80 °C.

3.4 Growth of *S. cerevisiae*

S. cerevisiae was grown in liquid media or on media plates at 30 °C. Wild-type and ΔAha1 knock-out strains were grown in YPD, while other strains were selected by drop-out media with a lack of the appropriate amino-acids. The selection of plasmids in yeasts is dependent on the lack of a single (or several) nutrient which allows to select for cells harbouring the particular plasmids that allow for auxotrophy. An OD_{600} of yeast cells equals approximately 3 x 10^7 cells/ml [MacDonald, 2001]. For long-term storage of *S. cerevisiae*, glycerol stocks were prepared as described in the section 3.3 - Growth and storage of *E. coli* cells.

3.5 Preparation of competent cells

Solution A: 40 mM Sodium-acetate, 100 mM $CaCl_2$, 70 mM $MnCl_2$
Solution B: 69 ml Solution A, 31 ml 87 % (v/v) Glycerol

Chemically competent cells were prepared by following the protocol of [Sambrook $\mathrm{et\ al.}$, 1989]. Briefly, *E. coli* cells were grown over night without antibiotics to an OD_{600} of 0.5 to 1, supplemented the next day with 2 ml of 1 M $MgCl_2$ and incubated for 10 min at 37 °C under agitation. Cells were cooled down on ice for 1 h and harvested at 4500 rpm, 5 min. Pellets were resuspended in 20 ml of solution A and incubated for 1 h on ice. Cells were pelleted again and resuspended in 2 ml of Solution B. 100 µl aliquots were flash frozen in liquid nitrogen and stored at -80 °C.

3.5.1 Transformation of *E. coli* cells

100 µl of competent *E. coli* cells were transformed with 1 µl of plasmid and incubated for 20-30 min on ice. Cells were heat shocked for 45 s at 42 °C. 600-800 µl of LB_0 medium was added and cells were incubated at 37 °C at 800 rpm for 45-60 min. Cells were spun down at 8000 rpm for 1 min and plated on LB plates with the appropriate antibiotic. Plates were incubated at 37 °C over night.

3.6 Transformation of *S. cerevisiae cells*

Plate Mix:	
45% PEG 4000	90 ml
1 M LiOAc	10 ml
1 M Tris/HCl, pH 7.5	1 ml
0.5 M EDTA	0.2 ml

Transformation of *S. cerevisiae* was performed by using the lithium acetate method [Ito $\mathrm{et\ al.}$, 1983]. Briefly, a single colony of *S. cerevisiae* was inoculated in 5 ml medium over night at 30 °C. The next day, 200 µl of the culture was spun down at 5000 rpm for 3 min, cells were decanted and left with approximately 100 µl of supernatant. 0.67 µl of carrier DNA (salmon sperm ssDNA) and 100 ng of plasmid were added and cells were resuspended. 150 µl Plate Mix and 6 µl of a 1 mM DTT stock solution were added, cells were gently vortexed and incubated at RT for 16-22 h. Cells were heat shocked for 30 min at 42 °C and spun down for 3 min at 5000 rpm. The supernatant was discarded, the

cell pellet resuspended and cells were plated with glass beads on the respective media plates, YPD and selective medium, respectively. Cells were allowed to grow for two days at 30 °C.

3.7 Protein Expression and Purification

3.7.1 Protein Expression and Cell disruption

All recombinant proteins were expressed in *E. coli* BL21 cod$^+$ RIL cells. Expressed constructs contained a His6-tag or a SUMO-His6-tag. The SUMO tag is generally recommended to increase the solubility of the protein of interest [Panavas $\mathrm{et\ al.}$, 2009]. Protein expression was performed in four times two liters dYT medium. Expression flasks were inoculated with an overnight preculture in 1:100 or 1:50 dilutions. The cells were grown at a temperature of 37 °C with the respective antibiotics. Growth was monitored at OD_{600}. Expression was induced with 1 mM IPTG when cells had reached an optical density of OD_{600} 0.6 - 0.8. Hsp90 was expressed for 4 h at 37 °C. Hsp90 co-chaperones were expressed at 18 °C overnight. Cells were harvested by centrifugation (10 min, 7000 rpm, Beckman centrifuge, JA-10 rotor) and pellets resuspended in the corresponding purification buffer with protease inhibitor mix HP. Storage of resuspended pellets occurred at -80 °C after flash-freezing. After addition of DNase I, cells were disrupted with a cell disrupter at 2.1 kbar and centrifuged for 45 min at 20,000 rpm (Beckman centrifuge, JA 25-50 rotor). The proteins purified in this work, were soluble and therefore the pellet was discarded. The supernatant was injected on a Ni-NTA (full-length proteins and Aha1 domains) and DEAE (untagged Hsp90-domain constructs) column, respectively.

3.7.2 Protein Purification

The progress of the protein purification was followed via analysis of the protein fractions with SDS-PAGE. All proteins were purified over an Äkta FPLC system (GE Healthcare, Life Sciences, Freiburg, Germany) at a temperature 8 °C. Hsp90 and its cochaperones were purified over a Ni-NTA, ResQ and SEC column. Aha1 was purified by two runs over a Ni-NTA column, followed by a size exclusion run over a Superdex75 (26/600). According to the size of the protein, Superdex200 or Superdex75 columns were used for the last purification step. Hsp90 domain constructs were purified without a tag and therefore purified over DEAE, ResQ and SEC. Proteins were stored in standard buffer: 40 mM HEPES, 150 mM KCl, 5 mM MgCl2, pH 7.5. Aha1 and Sgt1 were stored in low salt buffer: 40 mM HEPES, 20 mM KCl, 5 mM $MgCl_2$, pH 7.5. All proteins were

snap frozen and stored at -80 °C. Column specifications and purification procedures in this section were adapted from the GE Healthcare Life Sciences Protein Purification Handbook (GE Healthcare Life Sciences, Freiburg, Germany).

Ni-NTA affinity chromatography

Buffer A: 50 mM $NaHPO_4$, 300 mM NaCl, 20 mM Imidazol, pH 7.8
Buffer B: 50 mM $NaHPO_4$, 300 mM NaCl, 300 mM Imidazol, pH 7.8

Affinity chromatography allows purification and enrichment of the protein of interest from cell lysates or other samples (GE Healthcare Life Sciences, Protein Purification Handbook). This method makes use of a specific, reversible interaction between the protein of interest and its binding partners. Those interactions can be either biospecific, like antibodies binding to their partner proteins, or non-biospecific as binding of a tagged protein with its immobilised ligand. Maltose-binding protein (MBP), Glutathione S-transferase (GST) and Histidine (His_6) tag are commonly used protein tags. In this work, proteins were tagged with six histidines which allowed interaction with a Ni^{2+} ion charged chelating ligand immobilised to a highly cross-linked agarose column (HisTrap FF column, GE Healthcare Life Sciences, Freiburg, Germany). This column is characterised by a high loading capacity of around 40 mg/ml medium (GE). The soluble fraction of the cell lysate was loaded on the HisTrap column and washed with 35 column volumes. The protein was eluted with 300 mM imidazole and fractions were diluted in Resource Q Buffer A to a final volume of 150 ml.

Anion Exchange Chromatography

Buffer A: 40 mM HEPES, 20 mM KCl, 1 mM EDTA, pH 7.5
Buffer B: 40 mM HEPES, 1 M KCl, 1 mM EDTA, pH 7.5
(Buffers supplemented with 1 mM DTT where applicable.)

Ion exchange chromatography is capable of separating proteins by only minor differences in their net surface charge properties. The net surface charge of a protein can be estimated by its isoelectric point (pI) resulting from its charged amino acid residues. Depending of the protein's net charge, a positively charged matrix or negatively charged matrix can be used. Hsp90's pI is estimated to be 4.9 (www.expasy.ch, Prot Param Tool) which is suitable for purification by anion exchange chromatography. Therefore, the protein fractions obtained after the Ni-NTA run were loaded onto a Resource Q column, washed with Resource Q Buffer A for 35 column volumes. For elution, the salt concentration (KCl) was first increased in 10 ml to 100 mM, followed by a linear gradient over

150 ml to 500 mM KCl. Elution of Hsp90 usually occurred at 100-200 mM KCl.

Size Exclusion Chromatography

Buffer: 40 mM HEPES, 150 mM KCl, 5 mM $MgCl_2$, pH 7.5
(supplemented with 1 mM DTT where applicable)

Size Exclusion Chromatography (SEC) is used to separate proteins according to their molecular weight. Protein fractions obtained after anion exchange were pooled and concentrated to a volume of 5 and 10 ml for the Superdex 16/600 and Superdex 26/600, respectively. Amicon devices with a defined filter size (3,000 - 30,000 MWCO) depending on the size of the respective protein were used to concentrate the purified protein. The concentrated protein was loaded to the Superdex column, concentrated to the desired concentration and, were necessary, dialysed in standard assay buffer. Aliquots were snap frozen and stored at -80 °C.

Cleavage of protein tags

To cleave off affinity tags, proteins were digested with Thrombin over night in dialysis buffer (NiNTA buffer A). 100 U Thrombin were added to 15 mg of protein. Constructs for NMR analysis that were cloned in a pET 28b vector with a MBP solubility tag contained a tobacco etch virus (TEV) protease cleavage site. For the cleavage with TEV protease, proteins fractions after the Ni-affinity purification step were dialysed in NiNTA A Buffer. TEV protease was added in a ratio of 1 OD_{280} of TEV protease per 100 OD_{280} of substrate and incubated at 4 °C over night in NiNTA A dialysis buffer. SUMO protease was added to constructs cloned in a pET 28b SUMO vector over night at 4 °C to cleave off the tag. Successful tag cleavage was verified with an SDS-PAGE and tag removal occurred over a Ni-NTA run, whereby the cleaved tag bound to the column and the protein of interest could be collected from the flow through.

3.8 Protein Analysis

3.8.1 Discontinuous SDS-PAGE

Separation gel buffer (2x):	1.5 M Tris-HCl, pH 8.8, 0.8 % SDS (w/v)
Stacking gel buffer (4x):	0.25 M Tris-HCl, pH 6.8, 0.4 % SDS (w/v)

Discontinuous sodium dodecyl sulfate polyacrylamide gel electrophoresis (SDS-PAGE) was carried out to separate protein samples according to their molecular weight [Berg et al., 2012]. The anionic detergent SDS forms complexes with proteins through hydrophobic interactions. Proteins treated with SDS display a uniform negative charge since its intrinsic charges are masked by SDS. By boiling the protein sample with SDS and DTT or β-Mercaptoethanol (to disrupt of disulfide bonds), the tertiary structure can be disrupted and denatured, linear proteins are formed. The migration of proteins in an electric field is then only dependent on their molecular weight since SDS-coated proteins have the same charge to mass ratio. Proteins were run on 7.5-15 % acrylamide/bisacrylamide 19:1 (40 % w/v) SDS-gel according to their molecular weight. Stacking gels were casted to a final concentration of 5 % acrylamide/bisacrylamide 19:1 (40 % w/v). Polymerisation was induced by the addition of APS (10 % (w/v) in H_2O) and TEMED. 5x Lämmli buffer was added to the protein samples and proteins were boiled for 5 minutes at 95 °C. For the estimation of protein size, a low molecular weight protein marker (biorad, Munich, Germany) was used. For *in vivo* experiments with protein isolated from yeast cells, samples were boiled with 5x Lämmli buffer for 10 min at 95 °C. When SDS-PAGE was followed by a Western Blot, a prestained protein Marker (Protein Marker IV; peqlab, Erlangen, Germany) was loaded on a gel. Gels were run at 35 mA for 40-60 min.

3.8.2 Coomassie Staining of SDS gels

Detection of proteins in polyacrylamide gels was carried out after the Fairbanks staining protocol [Fairbanks et al., 1971]. Gels were brought to a short boil in Fairbanks A solution (25 % (v/v) isopropanol, 10 % (v/v) acetic acid, 0.05 % (w/v) Coomassie Blue R250) and incubated on a shaker at room temperature for a few minutes. Destaining occurred in Fairbanks D solution (10% acetic acid). The detection limit of the Fairbanks protocol lies at around 50 ng of protein [Fairbanks et al., 1971].

3.8.3 Immunoblotting (Western Blot)

For a more specific and more sensitive detection of proteins, immunoblotting can be applied [Kurien and Scofield, 2006]. This method is based on the interaction of an antibody with its antigen, e. g. the protein of interest in the given sample. After separation by SDS-PAGE, proteins were electrophoretically transferred to a polyvinylidene difluoride membrane (PVDF membrane, 0.45 μm pore size) by semi dry blotting. A constant current of 72 mA per blot was applied for 1 hour. After protein transfer, the membrane was incubated in 5 % milk in PBS-T for 1 hour at room temperature or over night at 4

°C. Incubation with 5 % milk (in PBS-T) blocks unreacted binding sites on the PVDF membrane and prevents unspecific interaction of the antibody with the membrane. The primary antibody was diluted in PBS-T supplemented with 1 % milk powder and incubated for one hour at room temperature under agitation. After washing the membrane with PBS-T (three times, 15 min), incubation with the secondary antibody was performed for 1 hour at RT. After washing the membrane again, detection was performed by chemiluminescence. The secondary antibodies used in this work are bound to horseradish peroxidase (HRP). After addition of the Western Blot detection ECL spray (Western-Bright ECL Spray, Advansta, Menlo Park, USA), a luminescent substance is oxidised by HRP and will cause luminescence, which was detected with an Image Quant 4000 detection device (GE Healthcare Life Sciences, Freiburg, Germany).

Standard protocol for Western Blotting:		
Block	5% milk in PBS-T	60 min, RT or o/N, 4 °C
Primary antibody	in 1% milk in PBS-T	60 min, RT or o/N, 4 °C
Wash	PBS-T	3 x 15 min, RT
Secondary antibody	in 1% milk PBS-T	60 min, RT
Wash	PBS-T	3 x 15 min, RT
Detection	ECL detection kit	

Western Blot Transfer Buffer	
Glycine	36 g
TrisHCl	7.6 g
Methanol	500 ml
SDS	0.3 % (w/v)
H_2O	ad 2.5 l

PBS-T	
NaCl	5.84 g
Na_2HPO_4	11.5 g
NaH_2PO_4	2.96 g
H_2O	ad 1 l
Tween-20	1 ml

Dilutions of antibodies:	
α-Hsp82	1 : 40 000
α-Ssa1	1 : 20 000
α-HA	1 : 5 000
α-PGK	1 : 5 000
α-rabbit	1 : 20 000
α-mouse	1 : 20 000

All other antibodies (antibodies against Hsp90 co-chaperones) were diluted 1 : 5 000 (except for α-Cpr7 (o/N incubation, 4 °C)). All antibodies were incubated for 1 h, RT under agitation.

3.8.4 Protein Labelling

Proteins containing cysteines were labelled via maleimide chemistry using Alexa and Atto fluorophores, respectively. Since yeast Hsp90 naturally does not contain any cysteines, 61C and 385C engineered variants were used for the labelling. Hsp90 was labelled with Atto fluorophores: Measurements with the Hsp90 intramolecular FRET system were performed after the protocol from Hessling *et al.* 2009. Aha1 was labelled with Alexa488 Fluor® C5 maleimide (invitrogen, Carlsbad, USA). For the Hsp90/Aha1 FRET system, Aha1*Alexa488 served as a donor while Hsp90*Atto550 was the acceptor [Li $\mathrm{et\ al.}$, 2013]. For the labelling procedure, the manufacturer's manual was followed. Briefly, disulfide bonds were reduced with 1 mM DTT. Since DTT interferes with the labelling reaction, DTT was subsequently removed over a PD10 desalting column. A threefold molar excess of fluorescent dye was incubated with the respective protein for 1 h, RT under stirring and protected from light. The reaction was quenched by the addition of 10 mM DTT to the protein-label mixture. Free-label was removed over a PD10 desalting column, over HPLC or through dialysis over night. Concentration of the labelled protein and the degree of labelling (DOL) were determined according to the following equations:

$$c_{Protein} = \frac{A_{280} - (A_{max} \cdot cf)}{\epsilon_{Protein} \cdot dilution factor} \tag{3.1}$$

$$DOL = \frac{A_{max} \cdot dilution factor}{\epsilon_{dye} \cdot c_{Protein}} \tag{3.2}$$

$c_{Protein}$ = concentration protein in M

A_{280} = absorbance at 280 nm

A_{max} = absorbance maximum of dye

cf = correction factor of the dye

ϵ_{dye} = molar extinction coefficient dye in cm^{-1} M^{-1}

Table: Fluorophores

Fluorophor	**Manufacturer**
Alexa Fluor 488 maleimide	Invitrogen, Carlsbad, USA
ATTO488-maleimide	ATTO-TEC, Siegen, Germany
ATTO550-maleimide	ATTO-TEC, Siegen, Germany
5-(and-6)-Carboxyfluorescein-NHS	Invitrogen, La Jolla, USA

3.8.5 Analytical Ultracentrifugation

Analytical ultracentrifugation (aUC) allows to investigate interaction and complex formation of proteins by analysing their time of sedimentation [Laue and Stafford, 1999]. Experiments were performed in a Beckman XL-A analytical ultracentrifuge (Beckman Coulter, Brea, USA). For fluorescence aUC runs, a AVIV-FIS fluorescence detection system (Aviv Biomedical, Lakewood, USA) was applied, for absorption aUC a standard interferometer attached to a UV/VIS detection system (Beckman Coulter, Brea, USA) was applied. Protein samples were analysed for their conformational states at 42,000 rpm in standard assay or low salt buffer. For monitoring complex formation in fluorescence aUC, 3 μM of unlabelled protein and 400 nM of fluorescently labelled protein were analysed. For analysis for sedimentation velocities in the absorption aUC, 5-10 μM of protein was applied. Generally, an absorption between 0.3 and 0.8 was aimed for the absorption aUC experiments. The Beer-Lambert-law ($A = \epsilon \cdot c \cdot d$, with A = absorption, ϵ = extinction coefficient of the respective protein, d = pathlength of cuvette) was applied for the estimation of the concentration to be used for these measurements. Nucleotides were used in a final concentration of 2 mM. Scans were recorded at excitation wavelength of the used fluorophore in 90 s intervals. Sedimentation raw data was converted into dc/dt profiles by subtracting nearby scans and converting the difference into dc/dt plots using the programme SEDVIEW. dc/dt profiles were analysed by applying bi-Gaussian functions to determine the $s_{20,w}$ values.

3.9 Spectroscopy

All spectroscopically obtained data were corrected against the respective assay buffer. For UV/VIS spectra and determination of the protein concentration, a buffer baseline was recorded and subtracted.

3.9.1 Circular dichroism

Circular dichroism (CD) allows for determination of secondary and tertiary structures of polypeptides and proteins [Kelly $\mathrm{et\ al.}$, 2005, Greenfield, 2007]. Optically active molecules have the ability to absorb clock-wise (right) and counter-clock-wise (left) linear polarised light differently. A CD spectrometer is supplied with a monochromator which polarises light at the wavelength λ which is then further polarised right-handed or left-handed through a modulator in a high frequency alternating field. A synchronous detector measures alternately the light intensities I_L/I_R. In the chiral protein solution, I_L/I_R is absorbed differently at different wavelengths and the light's polarisation level will be turned to a certain extent. This ellipticity Θ quantitatively describes the circular dichroism. The molar ellipticity can be calculated as follows:

$$\Theta_{MRW} = \frac{\Theta \cdot 100}{c \cdot d \cdot N_{AS}} \tag{3.3}$$

Θ_{MRW} = mean molar ellipticity in deg cm^2 dmol^{-1}
Θ = measured ellipticity in deg
d = cell length in cm
c = protein concentration in M
N_{AS} = number of the amino acid residues of the protein

Proteins contain a high number of asymmetrically carbon atoms which are optically active. CD spectroscopy in the far-UV range (170-250 nm) allows for the characterisation of a protein's secondary structure. α-helical structure show two characteristic minima at 208 and 222 nm in the CD spectrum, whereas β-sheet structures are characterised by a minimum at 218 nm. Taking the shape and the amplitude of the recorded CD spectrum into account, proportions of α-helices and β-sheets can be calculated [Creighton, 1989, Bohm $\mathrm{et\ al.}$, 1992]. CD spectroscopy in the near-UV range (250-300 nm) allows to characterise for a protein's specific tertiary structure fingerprint. Recorded CD spectra within this region are characterised by phenylalanines (250-270 nm), tyrosines (270-290 nm) and tryptophans (280-300 nm). Disulfide bonds can also contribute to the intensity

of near-UV CD spectra.
The table 'Parameters for CD spectroscopy' summarises experimental conditions for CD spectroscopy:

Table: Parameters for CD spectroscopy

Parameter	**Far-UV CD**	**Near-UV CD**
Start	260 nm	320 nm
End	195 nm	250 nm
Resolution	0.2 nm	0.2 nm
Accumulations	20	20
Scanning Speed	20 nm/min	20 nm/min
Path length of cuvette	0.1 cm	0.5 cm
Temperature	15-20 °C	15-20 °C
Protein Concentration	0.1-0.3 mg/ml	1.5 mg/ml

In this work, CD spectra in the far-UV range were recorded to assess protein folding states and thermal stability. For the assessment of protein stability, thermal transitions were recorded. Thereby, a change in the CD signal can occur when a protein's native structure undergoes denaturation. A Peltier PTC343 Temperature Element (Jasco, Groß-Umstadt, Germany) was used to increase the temperature step-wise at a constant heating rate of 20 °C per hour in CD assay buffer. The wavelength for the thermal transition was determined from the minima in the CD spectra of the native protein. To determine the melting temperature from the thermal transition curves, a Boltzmann fit, implemented in the Origin 8G software, was applied.

3.9.2 Thermal Shift Assay

The protein Thermal Shift Assay (TSA) can be applied to investigate the stability of a protein's tertiary structure. The combination of a real-time melt experiment with a real-time PCR device results in a protein specific fluorescence melting profile [Matulis $\mathrm{et\ al.}$, 2005]. Unfolding of a protein leads to exposure of hydrophobic surfaces. The fluorophore Sypro Orange (Molecular Probes, Leiden, Netherlands) interacts with exposed hydrophobic side chains. Sypro Orange does not show fluorescence in aquaeous solutions but in nonpolar environments. This, in turn, can be followed by an increase in fluorescence of this dye (excitation: 490 nm, emission: 575 nm). The melting temperature T_M can be calculated from the recorded melting profiles applying a Boltzmann fit. In this work, 5 µg of protein was used for the Thermal Shift Assay. Changes in the fluorescent signal upon increasing temperatures (25-95 °C) was recorded in a M 3000P qPCR System

(Agilent/Stratagene, Waldbronn, Germany). The temperature was increased by 1 °C per cycle.

3.9.3 UV absorption spectroscopy

UV absorption spectroscopy was applied to determine protein concentration. Proteins and peptides absorb UV-light in aquaeous solutions with a maximum absorbance at around 200-280 nm according to their amino acid contents [Layne, 1957, Stoscheck, 1990]. Aromatic amino acid side chains (e.g., tryptophan, tyrosine, phenylalanine) show a strong absorption of UV-light between 240-300 nm. Peptide bonds absorb UV-light in the far UV-range (180-230 nm) due their carbonyl groups. Disulfide bonds exhibit absorption at around 260 nm. With regard to a protein's characteristic composition of amino acids, molar extinction coefficients can be calculated which in turn, can be used for calculation the protein concentration. To obtain the molar extinction coefficient, the amino acid sequence of the given protein was inserted into the ExPASy ProtParam Web Tool provided by the Swiss Institute of Bioinformatics (SIB) (http://web.expasy.org/protparam/). Applying the Beer-Lambert law, the protein concentration can be determined as follows:

$$A_{280} = \epsilon \cdot c \cdot d \tag{3.4}$$

Whereas A is the measured absorbance at 280 nm, ϵ the molar extinction coefficient of the protein (M^{-1} cm^{-1}), c protein concentration (mol l^{-1}), d pathlength of the cuvette (cm).
UV absorption measurements were performed in UV quartz class cuvettes with a pathlength of 1 cm in a final volume of 120 μl. All proteins were diluted to obtain absorption values between 0.2 and 1 the ensure the linearity of the Lambert-Beer law. Spectra were recorded between 240 and 340 nm in a Cary 50 UV-VIS spectrophotometer. Prior to the absorption measurements, the proteins were centrifuged to avoid aggregates in the protein solution.

3.9.4 ATPase Activity Assay

A regenerative ATP system [Gosselin $\mathrm{et\ al.}$, 1994] was used for the characterisation of the ATPase activity of Hsp90 in the presence or the absence of its co-chaperones and modulators, respectively. In this assay, the ATPase driven hydrolysis of ATP to ADP results in the reaction of pyruvate kinase (PK) which converts phosphoenol pyruvate (PEP) to pyruvate. This reaction is coupled to the conversion of pyruvate to lactate by lactat dehydrogenase (LDH). This step requires NADH which is oxidised to NAD^+. NADH shows a strong absorption at 340 nm, whereas NAD^+ does not absorb at this wave-

length. Therefore, the ATPase activity of a protein can be followed by monitoring the decrease of NADH at 340 nm. One molecule of oxidised NADH corresponds thereby to the production of one molecule ADP by to ATPase.
The ATPase 2x premix contained the following components:

ATPase Premix (2x)	
100 mM PEP	240 µl
50 mM NADH	48 µl
PK	12 µl
LDH	44 µl
Assay Buffer	4328 µl

ATPase activity assays were measured in a final volume of 150 µl. 1x premix and 3 µM of Hsp90 was used. Measurements were performed in a Cary 50 with quartz class cuvettes at 30 °C for yeast proteins and 37 °C for human proteins, respectively. Hydrolysis rates were calculated with the following equation:

$$k_{cat} = -\frac{\Delta A}{\epsilon_{NADH} \cdot c_{ATPase} \cdot d} \tag{3.5}$$

k_{cat} = specific ATPase activity in min^{-1}
ΔA = decrease in absorption of NADH at 340 nm
ϵ_{NADH} = molar extinction coefficient of NADH (6200 M^{-1} cm^{-1})
c_{ATPase} = concentration of the ATPase (here: Hsp90) in M
d = path length of cuvette

Affinity titrations

Affinity titrations were performed with the ATPase assay setup to determine affinities of co-chaperones or nucleotides to Hsp90. The apparent affinity of ATP to Hsp90 was determined by titration of 0.2-3 mM ATP to Hsp90. Co-chaperone affinities were determined by titration of the respective co-chaperones to Hsp90 with constant ATP concentrations of 2 mM. Aha1 was titrated at concentrations of 1-30 µM in low salt assay buffer to 1 µM Hsp90. Cpr6 and Cpr7 were titrated with 2-20 µM to 2 µM Hsp90 in low salt buffer. Sti1 and Sba1 were titrated to 3 µM Hsp90 in standard assay buffer. The catalytical activities (k_{cat}) at different ATP and co-chaperone concentrations, respectively, were plotted against the respective concentrations. Data was fitted with non-linear regression in Origin 8G (OriginLab Corporation, Northhampton, USA). The apparent affinity (kD_{app})

and maximal catalytical activity can be determined using the Michaelis-Menten model as follows:

$$k_{cat} = V_{max} \cdot \frac{c}{c + kD_{app}} \tag{3.6}$$

V_{max} = maximal catalytical activity in min^{-1}
c = ATP/co-chaperone concentration in M
kD_{app} = apparent affinity in M

3.9.5 Malachite Green Assay

Malachite green reagent:	
Malachite green	0.034 % (w/v)
Ammonium molybdate	1.05 % (w/v)
HCl	1 M

The malachite green (MLG) assay [O'Toole $\mathrm{et\ al.}$, 2007] was applied in order to assess the ATPase activity of Hsp90 at higher temperatures. The commonly used regenerative ATPase assay contains an enzyme system which is not stable at higher temperatures; thus, the MLG assay was chosen since it does not contain unstable enzymes. The MLG assay was performed with 1 μg of protein in a volume of 25 μl which was preincubated at the respective temperature for 3-5 min. A final concentration of 2 mM of ATP was added the protein and the reaction was incubated for 10 min at the respective (high) temperature to allow ATP hydrolysis. The reaction was terminated by the addition of 800 μl MLG reagent. Colour development (caused by formation of the green molybdophosphoric acid complex) was allowed at room temperature and stopped by the addition of 100 μl citric acid (34 % (w/v)). 200 μl from the reaction mixture were taken out and measured in a spectrometer at 650 nm (max. absorption of malachite green). Values were calibrated against KH_2PO_4 standards (0-100 μM phosphate standards) and corrected for phosphate release in the absence of ATPases. ATP cleavage rates were calculated as nmoles phosphate per min per μl per μg protein.

3.10 Fluorescence spectroscopy

Fluorescence spectroscopy allows to measure for the intensity of photons emitted from a fluorescent sample after is has been excited. Excitation results in the molecule reach-

ing an excited, higher electronic state by absorbing a photon. Thereby, the molecule is excited from the ground state S_0 to a higher singlet, metastable state (S_n). From this energy state the S_1 state can be reached. As the molecule's energy decreases again to the ground state S_0, a photon is emitted in a time range of 10^{-9} - 10^{-7} s when fluorescence occurs. Alternative pathways to reach the ground state are phosphorescence or non-radiative relaxation [Jablonski, 1933, Lakowicz, 2006].

3.10.1 Fluorescence Resonance Energy Transfer (FRET)

Fluorescence or Förster Resonance Energy Transfer (FRET) describes a phenomenon where energy of an excited fluorophore (donor) is transmitted to a fluorophore (acceptor) in close proximity (1-10 nm) to the donor [Förster $\mathrm{et\ al.}$, 1939,Stryer, 1978]. This will yield in an increase of the acceptor fluorescence while the donor emission decreases. FRET can only occur when the two fluorophores have an overlap in the donor emission and acceptor excitation spectra. The efficiency of the energy transfer is thereby dependent on the quantum yield of the process [Stryer, 1978]. Furthermore, the FRET efficiency E is dependent on the distance between the fluorophores and can be calculated as follows:

$$E = \frac{{R_0}^6}{{R_0}^6 + r} \tag{3.7}$$

E = energie transfer
R_0 = Förster radius
r = distance between donor and acceptor fluorophore

The Förster radius R_0 between the molecules is the distance between the two fluorophores at which the FRET efficiency is 50 % and depends on the photophysical parameters of the FRET pair [Bastiaens and Pepperkok, 2000]. Due to the dependence of close proximity of the fluorophores, FRET is a useful tool for studying protein-protein interaction. In this work, previously estabilshed FRET systems, like an Hsp90 intramolecular FRET [Hessling $\mathrm{et\ al.}$, 2009] and an Hsp90-Aha1 FRET system [Li $\mathrm{et\ al.}$, 2013] were used to study further aspects of the Hsp90 chaperone system. To this end, the Hsp90 cysteine-engineered variants, 61C and 385C, were labelled with Atto fluorophores. Dependent of the type of the positions and domains of interest, Atto488 (donor) or Atto550 (acceptor) fluorophores were applied. For the Hsp90-Aha1 FRET system, Hsp90 385C was labelled with Atto550 while Aha1 was labelled over maleimide chemistry with Alexa488. The following table summarises the FRET pairs used in this work.

Table: FRET pairs

FRET System	Donor	Acceptor
Hsp90 N-N	61C*Atto488	61C*Atto550
Hsp90 N-M	61C*Atto488	385C*Atto550
Hsp90-Aha1	Aha1*Alexa488	385C*Atto550

Experiments with the Hsp90 intramolecular FRET system were performed as described by Hessling *et al.* (2009). Experiments with the Hsp90-Aha1 FRET system were performed as described by Li *et al.* (2013). Briefly, 400 nM of donor and 400 nM of acceptor were mixed in standard assay buffer, or, for measurements with Aha1, in low salt assay buffer. Measurements were performed in a total volume of 150 µl in a fluorescence quartz cuvette (Hellma Analytics, Müllheim, Germany). Kinetics and spectra were recorded in a Fluoromax-3 (Horiba Jobin Yvon, Munich, Germany) at 25-30 °C. For the spectrum measurements, the donor fluorophore was excited at 490 nm, whilst acceptor fluorescence was followed from 500 to 600 nm. Spectra were recorded in the absence and the presence of nucleotides. To analyse the different conformational states of Hsp90, ADP, ATPγS and AMP-PNP were used at final concentrations of 2 mM. For recording changes in the closing kinetics of Hsp90 with the Hsp90 intramolecular FRET system, 2 mM ATPγS served as a starter for monitoring the closing of Hsp90. Kinetic measurements in the Hsp90-Aha1 FRET system were started by the addition of 2 mM AMP-PNP. After addition of nucleotides, the decrease in donor and increase in acceptor fluorescence could be followed in both FRET systems at the respective wavelengths.

3.10.2 Screening for modulators of the Hsp90/Aha1 interaction

Screening Buffer: 40 mM HEPES, 20 mM KCl, 5 mM $MgCl_2$, pH 7.5

The previously established Hsp90/Aha1-FRET system [Li et al., 2013] was applied to screen for modulators of the Hsp90/Aha1 interaction. A library of 10,000 small molecules was screened in collaboration with Prof. Dr. Gunter Fischer at the Max-Planck Research Unit for Enzymology of Protein Folding (Halle/Saale, Germany). The FRET complex was made by adding 500 nM of Hsp90 385C labelled with Atto550 to 500 nM of labelled Aha1 (Alexa488) in a total volume of 70 µl. The complex was incubated on ice for 10 min. 50 µg/ml of each compound was added to the Hsp90/Aha1 FRET complex. Since the compounds were solubilised in DMSO, 1 % DMSO served as negative control. 100 µM of geldanamycin were used as positive control. After the addition of 1 mM AMP-PNP, fluorescence kinetics were recorded. Assays were performed in a 96-well plate at 20 °C in a Wallac EnVision Xcite Multilabel Reader (Perkin Elmer, Waltham, United States). Results were evaluated with the Wallac EnVision Manager Software 1.12. Compounds

that altered the kinetics of the Hsp90/Aha1 interaction were rescreened twice to exclude false positive hits.

3.11 Chaperone Assay

CS assay buffer: 40 mM HEPES, pH 7.5

To analyse for the chaperoning activity of a protein, a chaperone assay using citrate synthase (CS) as substrate was performed. CS catalyses the reaction of oxaloacidic acid (OAA) and acetyl-coenzyme A (Ac-CoA) to citrate and CoA. CS rapidly denatures and aggregates at temperatures over 37 °C in the absence of its substrates OAA and AcCoA. Therefore, it is suitable as a substrate for chaperone assays. The chaperone assays were performed in 40 mM HEPES buffer, pH 7.5 at 43.5 °C. Aggregation of 0.6 μM CS was followed at 350 nm. The chaperones were added in different ratios to the CS (CS: chaperone: 1:10, 1:5, 1:2). Curves were plotted and analysed with the Origin 8G software.

3.12 Isothermal calorimetry

ITC Buffer: 20 mM HEPES, 5 mM $MgCl_2$, pH 7.5

Isothermal calorimetry (ITC) is a highly sensitive method for the determination of thermodynamic parameters (affinity, enthalpy and stochiometry) of a binding reaction [Wiseman et al., 1989, Duff, Jr. et al., 2011]. Heat generation in the sample cell is measured upon titration of a ligand to its potential binding partner. The change in heat is upon the binding reaction is measured and referred to a reference cell which holds a constant temperature throughout the measurement. Fitting of the isotherm allows to determine the thermodynamic parameters of the reaction [Duff, Jr. et al., 2011]. ITC measurements were performed in a MicroCal VP-ITC device (Malvern Instruments Ltd., Malvern, UK) at 20 °C. All proteins were dialysed over night against ITC assay buffer. For nucleotide affinity measurements, 2 mM of AMP-PNP or ADP were titrated to 50 μM of full-length Hsp90. For the assessment of binding properties of Hsp90/Aha1-modulators, measurements were performed in a PEAQ-ITC (Malvern Instruments, Malvern, UK). 200 μM of inhibitor were titrated to 20 μM Hsp90 and 20 μM Aha1, respectively. A titration of DMSO to Hsp90 served as control. ITC binding curves were analysed with the ITC implemented Origin-based analysis software provided by the manufacturer (Malvern Instruments, Malvern, UK).

3.13 Surface Plasmon Resonance

Surface Plasmon Resonance (SPR) is a powerful tool for the investigation of protein interactions in real-time [Willander and Al-Hilli, 2009]. This label-free interaction analysis allows to monitor protein-protein interaction but also protein-small molecule interaction. In this work, a Biacore X100 system (GE Healthcare Life Sciences, Freiburg, Germany) was used to assess binding affinities of Hsp90 co-chaperones to Hsp90. Further, binding of an inhibitor of the Hsp90/Aha1 interaction was tested. Proteins were coupled to a CM5 Biacore chip. Immobilization via -NH_2 groups was chosen for all proteins. A pH scouting was performed to screen for the optimal pH for the coupling reaction. The pH scouting as well as the coupling reaction were performed according to the manufacturer's instructions. 500 response units (RU) of Hsp90 were coupled to the chip. 12.5 μg/ml of Hsp90 in 10 mM acetate buffer, pH 3.8 were coupled. The Hsp90 co-chaperones Sba1 and Sgt1 were coupled to the CM5 chip in order to test the binding affinity of fully closed Hsp90 (preincubated with 1 mM AMP-PNP for 30 min at 30 °C). For the interaction of the screened Hsp90/Aha1 modulators with this protein system, Aha1 was coupled to a CM5 chip. For the coupling of Hsp90 co-chaperones, 1000 RU of protein were coupled. Aha1 was coupled at a pH of 4.6, Sgt1 showed best coupling efficiencies at pH 4.4, Sba1 was coupled at a pH of 4.0. Affinity titrations were then performed in low salt assay buffer with the respective proteins at concentrations ranging from 0 to 5 μM. Regeneration of the chip between sample injections was carried out with 1.5 M KCl. This step removes bound analytes from the chip surface without damaging the coupled protein. The recorded Biacore sensorgrams were analysed with the Biacore X100 software (GE Healthcare Life Sciences, Freiburg, Germany). Interaction kinetics were analysed by fitting the interaction as a function of time over the range of applied analyte (ligand) concentrations. Association and dissociation constants were obtained. For the determination of binding affinities, steady state affinity was determined. The steady state reponse against concentration was derived from the recorded sensorgrams and then fitted with the Biacore software to obtain the kD.

3.14 *In vivo* Assays

3.14.1 Plasmid shuffling

To address effects of Hsp90 mutants *in vivo*, a plasmid shuffling system was applied [Nathan and Lindquist, 1995]. An ECU 82α yeast strain with a genomic deletion of both HSP82 genes, supplemented with a Hsp90-coding plasmid (mediating Ura auxotrophie) was used. A p423 GPD plasmid harbouring Hsp90 wt, Hsp90 F104W or Hsp90 F124W

was transformed into cells which were then plated onto -Leu -His medium. After allowing growth for 2-3 days at 30 °C, cells were transferred to 0.1 % 5-FOA (5-fluoroorotic acid) plates and incubated for another 2-3 days at 30 °C. In turn, the initially supplemented URA plasmid coding for Hsp90 is lost due to toxicity of 5-FOA (reaction with 5'-phosphate decarboxylase) [Boeke et al., 1987]. 5-FOA grown yeast cells thus only harbour the one Hsp90 variant which was shuffled in, using the p423 GPD vector background (auxotrophic for His). Yeast cells not growing harbour a non-functional Hsp90 variant or an empty vector which was used as a control. Subsequently, grown yeast cells were transferred to His selective media plates and glycerol stocks were prepared for long term storage.

3.14.2 β-Galactosidase Assay

Wild-type and ΔAha1 yeast strains were tested for their ability for client activation. The activities of human SHRs (MR and GR) were tested by making use of a β-Galactosidase reporter assay [Smale, 2010, Johnson and Craig, 2000, Louvion et al., 1996]. Yeast cells were transformed with the GR and MR expression vectors (p413-GPD-hGR and p413-GPD-hMR), respectively, and the reporter vector pUCΔSS26x. Singles clones were inoculated in 5 ml -Ura -His selective medium and incubated o/N at 30 °C. Compounds were then titrated with concentrations ranging from 0 to 1000 μM to a 10 μl overnight culture of yeasts and supplemented with 190 μl selection (-Ura -His) medium. Cells treated with DMSO in the respective concentrations served as negative controls. The GR- and MR-dependent transcription was induced with 10 mM 11-deoxycorticosterone (Sigma-Aldrich, St. Louis, USA) and aldosterone (Sigma-Aldrich, St. Louis, USA), respectively. Cultures were incubated over night at 30 °C. 50 μl of the yeast cultures were centrifuged and the pellet was lysed with 150 μl SDS buffer (82 mM Na_2HPO_4, 12 mM NaH_2PO_4, 0.1 % (w/v) SDS, pH 7.5) for 15 minutes on a shaker at room temperature. The β-Galactosidase activity was determined after the addition of 50 μl ONPG (4 mg/ml stock in SDS buffer) by measuring the absorption in a Tecan Sunrise Absorbance Reader (Tecan, Mainz, Germany) at 405 nm. Differences in cell amounts were corrected by the respective OD_{600}. Activities were normalised to the DMSO controls.

3.14.3 CFTR Degradation Assay

TCA sample buffer: 80 mM Tris-HCl, pH 8, 8 mM EDTA, 120 mM DTT, 3.5 % SDS, 5 % glycerol, 0.25 % Tris base, bromophenol blue

Yeast wild-type BY4741 cells were transformed with CFTR expression plasmids for CFTR

wt and CFTR $\triangle$F508, respectively. CFTR harbouring cells were grown to log phase in selective medium (-Ura) o/N at 30 °C. 50 µg/ml of cycloheximide were added to the cultures and 1 OD of cells was harvested after 5, 15, 25, and 40 min. The supernatant was removed and cell pellets were stored at 80 °C or immediately prepared for TCA extraction. For TCA extraction, pellets were resuspended in 1 ml of ddH_2O and 150 µl of a freshly prepared 2 M NaOH/1.12 M β-Mercaptoethanol was added. Cells were vortexed and incubated on ice for 15 min. 150 µl of 100 % TCA was added and cells were incubated on ice for 20 min. Cells were spun at 13,000 rpm for 5-10 min at 4°C. The TCA solution was carefully removed, pellets were respun and all further traces of TCA were removed. Pellets were resuspended in 100 µl TCA sample buffer and either stored at -20 °C or heated for 10-15 min at 37 °C before loading on a gradient gel (ServaGel™ TG PRIME™ 4-12 %, Serva, Heidelberg, Germany). Samples were run for 60 min at 35 mA and then transferred on a PVDF-membrane following the Western Blot standard protocol. CFTR was detected using an α-HA antibody. PGK was used a loading control. Antibodies against Hsp82, Aha1 and Ssa1 were used as controls to assess protein levels under cycloheximide influence. No increase in Ssa1 levels was detected, thus, no heat shock response was induced.

Bibliography

[Acerenza and Mizraji, 1997] Acerenza, L. and Mizraji, E. (1997). Cooperativity: A unified view.

[Agashe and Hartl, 2000] Agashe, V. R. and Hartl, F. U. (2000). Roles of molecular chaperones in cytoplasmic protein folding. Seminars in cell & developmental biology *11*, 15–25.

[Ahmad and Kumar, 2011] Ahmad, N. and Kumar, R. (2011). Steroid hormone receptors in cancer development: A target for cancer therapeutics. Cancer Letters *300*, 1–9.

[Aisner et al., 1999] Aisner, D. L., Holt, S. E., Baur, J., Tesmer, V. M., Dy, M., Ouellette, M., Trager, J. B., Morin, G. B., Toft, D. O., Shay, J. W., Wright, W. E. and White, M. A. (1999). Functional requirement of p23 and Hsp90 in telomerase complexes. Genes & development *13*, 817–26.

[Akner et al., 1992] Akner, G., Mossberg, K., Sundqvist, K. G., Gustafsson, J. A. and Wikström, A. C. (1992). Evidence for reversible, non-microtubule and non-microfilament-dependent nuclear translocation of hsp90 after heat shock in human fibroblasts. European journal of cell biology *58*, 356–64.

[Ali et al., 2006] Ali, M. M. U., Roe, S. M., Vaughan, C. K., Meyer, P., Panaretou, B., Piper, P. W., Prodromou, C. and Pearl, L. H. (2006). Crystal structure of an Hsp90-nucleotide-p23/Sba1 closed chaperone complex. Nature *440*, 1013–1017.

[Altschul et al., 1990] Altschul, S. F., Gish, W., Miller, W., Myers, E. W. and Lipman, D. J. (1990). Basic local alignment search tool. Journal of Molecular Biology *215*, 403–10.

[Amaral, 2006] Amaral, M. D. (2006). Therapy through chaperones: Sense or antisense? Cystic fibrosis as a model disease. Journal of Inherited Metabolic Disease *29*, 477–487.

[Amaral and Farinha, 2013] Amaral, M. D. and Farinha, C. M. (2013). Rescuing mutant CFTR: a multi-task approach to a better outcome in treating cystic fibrosis. Current pharmaceutical design *19*, 3497–508.

[Amlacher et al., 2011] Amlacher, S., Sarges, P., Flemming, D., Van Noort, V., Kunze, R., Devos, D. P., Arumugam, M., Bork, P. and Hurt, E. (2011). Insight into structure and assembly of the nuclear pore complex by utilizing the genome of a eukaryotic thermophile. Cell *146*, 277–289.

[An et al., 2000] An, W. G., Schulte, T. W. and Neckers, L. M. (2000). The heat shock protein 90 antagonist geldanamycin alters chaperone association with p210bcr-abl and v-src proteins before their degradation by the proteasome. Cell growth & differentiation : the molecular biology journal of the American Association for Cancer Research *11*, 355–360.

[Anckar and Sistonen, 2011] Anckar, J. and Sistonen, L. (2011). Regulation of HSF1 function in the heat stress response: implications in aging and disease. Annual review of biochemistry *80*, 1089–115.

[Arnold et al., 2006] Arnold, K., Bordoli, L., Kopp, J. and Schwede, T. (2006). The SWISS-MODEL workspace: A web-based environment for protein structure homology modelling. Bioinformatics *22*, 195–201.

[Arteaga et al., 2012] Arteaga, C. L., Sliwkowski, M. X., Osborne, C. K., Perez, E. a., Puglisi, F. and Gianni, L. (2012). Treatment of HER2-positive breast cancer: current status and future perspectives. Nature reviews. Clinical oncology *9*, 16–32.

[Ashburner and Bonner, 1979] Ashburner, M. and Bonner, J. (1979). The induction of gene activity in drosophila by heat shock. Cell *17*, 241–254.

[Azevedo et al., 2002] Azevedo, C., Sadanandom, A., Kitagawa, K., Freialdenhoven, A., Shirasu, K. and Schulze-Lefert, P. (2002). The RAR1 interactor SGT1, an essential component of R gene-triggered disease resistance. Science (New York, N.Y.) *295*, 2073–2076.

[Back et al., 2013] Back, R., Dominguez, C., Rothé, B., Bobo, C., Beaufils, C., Moréra, S., Meyer, P., Charpentier, B., Branlant, C., Allain, F. H.-T. and Manival, X. (2013). High-resolution structural analysis shows how Tah1 tethers Hsp90 to the R2TP complex. Structure (London, England : 1993) *21*, 1834–47.

[Bamberger et al., 1997] Bamberger, C. M., Wald, M., Bamberger, A. M. and Schulte, H. M. (1997). Inhibition of mineralocorticoid and glucocorticoid receptor function by the heat shock protein 90-binding agent geldanamycin. Molecular and Cellular Endocrinology *131*, 233–240.

[Bansal et al., 2004] Bansal, P. K., Abdulle, R. and Kitagawa, K. (2004). Sgt1 associates with Hsp90: an initial step of assembly of the core kinetochore complex. Molecular and cellular biology *24*, 8069–79.

[Bardwell and Craig, 1987] Bardwell, J. C. and Craig, E. A. (1987). Eukaryotic Mr 83,000 heat shock protein has a homologue in Escherichia coli. Proceedings of the National Academy of Sciences of the United States of America *84*, 5177–81.

[Bastiaens and Pepperkok, 2000] Bastiaens, P. I. H. and Pepperkok, R. (2000). Observing proteins in their natural habitat: The living cell.

[Beatrix et al., 2000] Beatrix, B., Sakai, H. and Wiedmann, M. (2000). The alpha and beta subunit of the nascent polypeptide-associated complex have distinct functions. Journal of Biological Chemistry *275*, 37838–37845.

[Becker et al., 1994] Becker, W., Kentrup, H., Klumpp, S., Schultz, J. E. and Joost, H. G. (1994). Molecular cloning of a protein serine/threonine phosphatase containing a putative regulatory tetratricopeptide repeat domain. The Journal of biological chemistry *269*, 22586–92.

[Berezovsky et al., 2005] Berezovsky, I. N., Shakhnovich, E. I. and Fersht, A. R. (2005). Physics and evolution of thermophilic adaptation. PNAS *102*, 12742–12747.

[Berg et al., 2012] Berg, J. M., Tymoczko, J. L. and Stryer, L. (2012). Biochemistry: International edition. Palgrave MacMillan.

[Bergerat et al., 1997] Bergerat, a., de Massy, B., Gadelle, D., Varoutas, P. C., Nicolas, a. and Forterre, P. (1997). An atypical topoisomerase II from Archaea with implications for meiotic recombination.

[Berman et al., 2000] Berman, H. M., Westbrook, J., Feng, Z., Gilliland, G., Bhat, T. N., Weissig, H., Shindyalov, I. N. and Bourne, P. E. (2000). The Protein Data Bank. Nucleic acids research *28*, 235–242.

[Biaoxue et al., 2012] Biaoxue, R., Xiling, J., Shuanying, Y., Wei, Z., Xiguang, C., Jinsui, W. and Min, Z. (2012). Upregulation of Hsp90-beta and annexin A1 correlates with poor survival and lymphatic metastasis in lung cancer patients. Journal of experimental & clinical cancer research : CR *31*, 70.

[Birnby et al., 2000] Birnby, D. A., Link, E. M., Vowels, J. J., Tian, H., Colacurcio, P. L. and Thomas, J. H. (2000). A transmembrane guanylyl cyclase (DAF-11) and Hsp90 (DAF-21) regulate a common set of chemosensory behaviors in Caenorhabditis elegans. Genetics *155*, 85–104.

[Bitton, 2002] Bitton, G. (2002). Encyclopedia of environmental microbiology. John Wiley {&} Sons, New York [etc.].

[Bock et al., 2014] Bock, T., Chen, W. H., Ori, A., Malik, N., Silva-Martin, N., Huerta-Cepas, J., Powell, S. T., Kastritis, P. L., Smyshlyaev, G., Vonkova, I., Kirkpatrick, J., Doerks, T., Nesme, L., Bassler, J., Kos, M., Hurt, E., Carlomagno, T., Gavin, A. C., Barabas, O., Mueller, C. W., Noort, V. V., Beck, M. and Bork, P. (2014). An integrated approach for genome annotation of the eukaryotic thermophile Chaetomium thermophilum. Nucleic Acids Research *42*, 13525–13533.

[Boczek et al., 2015] Boczek, E. E., Reefschläger, L. G., Dehling, M., Struller, T. J., Häusler, E., Seidl, A., Kaila, V. R. I. and Buchner, J. (2015). Conformational processing of oncogenic v-Src kinase by the molecular chaperone Hsp90. Proceedings of the National Academy of Sciences of the United States of America *112*, E3189–3198.

[Boeke et al., 1987] Boeke, J. D., Trueheart, J., Natsoulis, G. and Fink, G. R. (1987). 5-Fluoroorotic acid as a selective agent in yeast molecular genetics. Methods in Enzymology *154*, 164–175.

[Bohm et al., 1992] Bohm, G., Muhr, R. and Jaenicke, R. (1992). Quantitative analysis of protein far UV circular dichroism spectra by neural networks. Protein Eng *5*, 191–195.

[Borkovich et al., 1989] Borkovich, K. A., Farrelly, F. W., Finkelstein, D. B., Taulien, J. and Lindquist, S. (1989). Hsp82 is an essential protein that is required in higher concentrations for growth of cells at higher temperatures. Molecular and cellular biology *9*, 3919–30.

[Bose et al., 1996] Bose, S., Weikl, T., Bügl, H. and Buchner, J. (1996). Chaperone function of Hsp90-associated proteins. Science *274*, 1715–7.

[Boulon et al., 2010] Boulon, S., Pradet-Balade, B., Verheggen, C., Molle, D., Boireau, S., Georgieva, M., Azzag, K., Robert, M.-C., Ahmad, Y., Neel, H., Lamond, A. I. and Bertrand, E. (2010). HSP90 and its R2TP/Prefoldin-like cochaperone are involved in the cytoplasmic assembly of RNA polymerase II. Molecular cell *39*, 912–24.

[Brady and Attardi, 2010] Brady, C. A. and Attardi, L. D. (2010). p53 at a glance. Journal of Cell Science *123*, 2527–2532.

[Brough et al., 2008] Brough, P. a., Aherne, W., Barril, X., Borgognoni, J., Boxall, K., Cansfield, J. E., Cheung, K.-M. J., Collins, I., Davies, N. G. M., Drysdale, M. J., Dymock, B., Eccles, S. a., Finch, H., Fink, A., Hayes, A., Howes, R., Hubbard, R. E., James, K., Jordan, A. M., Lockie, A., Martins, V., Massey, A., Matthews, T. P., McDonald, E., Northfield, C. J., Pearl, L. H., Prodromou, C., Ray, S., Raynaud, F. I., Roughley, S. D., Sharp, S. Y., Surgenor, A., Walmsley, D. L., Webb, P., Wood, M., Workman, P. and Wrightt, L. (2008). 4,5-diarylisoxazole HSP90 chaperone inhibitors: Potential therapeutic agents for the treatment of cancer. Journal of Medicinal Chemistry *51*, 196–218.

[Brugge et al., 1981] Brugge, J. S., Erikson, E. and Erikson, R. (1981). The specific interaction of the Rous sarcoma virus transforming protein, pp60src, with two cellular proteins. Cell *25*, 363–372.

[Bukau et al., 2006] Bukau, B., Weissman, J. and Horwich, A. (2006). Molecular Chaperones and Protein Quality Control.

[Burlison and Blagg, 2006] Burlison, J. a. and Blagg, B. S. J. (2006). Synthesis and evaluation of coumermycin A1 analogues that inhibit the Hsp90 protein folding machinery. Organic Letters *8*, 4855–4858.

[Catlett and Kaplan, 2006] Catlett, M. G. and Kaplan, K. B. (2006). Sgt1p is a unique co-chaperone that acts as a client adaptor to link Hsp90 to Skp1p. Journal of Biological Chemistry *281*, 33739–33748.

[Chang et al., 1997] Chang, H. C., Nathan, D. F. and Lindquist, S. (1997). In vivo analysis of the Hsp90 cochaperone Sti1 (p60). Molecular and Cellular Biology *17*, 318–325.

[Chen et al., 2005] Chen, B., Piel, W. H., Gui, L., Bruford, E. and Monteiro, A. (2005). The HSP90 family of genes in the human genome: Insights into their divergence and evolution. Genomics *86*, 627–637.

[Chen et al., 1996] Chen, M. S., Silverstein, A. M., Pratt, W. B. and Chinkers, M. (1996). The tetratricopeptide repeat domain of protein phosphatase 5 mediates binding to glucocorticoid receptor heterocomplexes and acts as a dominant negative mutant. Journal of Biological Chemistry *271*, 32315–32320.

[Chen and Cohen, 1997] Chen, M. X. and Cohen, P. T. (1997). Activation of protein phosphatase 5 by limited proteolysis or the binding of polyunsaturated fatty acids to the TPR domain. FEBS Letters *400*, 136–140.

[Chen et al., 1994] Chen, M. X., McPartlin, a. E., Brown, L., Chen, Y. H., Barker, H. M. and Cohen, P. T. (1994). A novel human protein serine/threonine phosphatase, which possesses four tetratricopeptide repeat motifs and localizes to the nucleus. The EMBO journal *13*, 4278–4290.

[Chen et al., 2013] Chen, Y., Chen, J., Loo, A., Jaeger, S., Bagdasarian, L., Yu, J., Chung, F., Korn, J., Ruddy, D., Guo, R., McLaughlin, M. E., Feng, F., Zhu, P., Stegmeier, F., Pagliarini, R., Porter, D. and Zhou, W. (2013). Targeting HSF1 sensitizes cancer cells to HSP90 inhibition. Oncotarget *4*, 816–29.

[Cherry et al., 2012] Cherry, J. M., Hong, E. L., Amundsen, C., Balakrishnan, R., Binkley, G., Chan, E. T., Christie, K. R., Costanzo, M. C., Dwight, S. S., Engel, S. R., Fisk, D. G., Hirschman, J. E., Hitz, B. C., Karra, K., Krieger, C. J., Miyasato, S. R., Nash, R. S., Park, J., Skrzypek, M. S., Simison, M., Weng, S. and Wong, E. D. (2012). Saccharomyces Genome Database: The genomics resource of budding yeast. Nucleic Acids Research *40*.

[Chiosis et al., 2003] Chiosis, G., Huezo, H., Rosen, N., Mimnaugh, E., Whitesell, L. and Neckers, L. (2003). 17AAG: low target binding affinity and potent cell activity–finding an explanation. Molecular Cancer Therapeutics *2*, 123–129.

[Chiosis et al., 2002] Chiosis, G., Lucas, B., Shtil, A., Huezo, H. and Rosen, N. (2002). Development of a Purine-Scaffold Novel Class of Hsp90 Binders that Inhibit the Proliferation of Cancer Cells and Induce the Degradation of Her2 Tyrosine Kinase. Bioorganic & Medicinal Chemistry *10*, 3555–3564.

[Chiosis et al., 2001] Chiosis, G., Timaul, M. N., Lucas, B., Munster, P. N., Zheng, F. F., Sepp-Lorenzino, L. and Rosen, N. (2001). A small molecule designed to bind to the adenine nucleotide pocket of Hsp90 causes Her2 degradation and the growth arrest and differentiation of breast cancer cells. Chemistry and Biology *8*, 289–299.

[Consalvi et al., 2000] Consalvi, V., Chiaraluce, R., Giangiacomo, L., Scandurra, R., Christova, P., Karshikoff, a., Knapp, S. and Ladenstein, R. (2000). Thermal unfolding and conformational stability of the recombinant domain II of glutamate dehydrogenase from the hyperthermophile Thermotoga maritima. Protein engineering *13*, 501–507.

[Corradi, 2015] Corradi, N. (2015). Microsporidia: Eukaryotic Intracellular Parasites Shaped by Gene Loss and Horizontal Gene Transfers. Annual Review of Microbiology *69*, 150720190645000.

[Cox and Miller 3rd, 2004] Cox, M. B. and Miller 3rd, C. A. (2004). Cooperation of heat shock protein 90 and p23 in aryl hydrocarbon receptor signaling. Cell Stress Chaperones *9*, 4–20.

[Creighton, 1989] Creighton, T. (1989). Protein structure : a practical approach. IRL Press at Oxford University Press, Oxford ;;New York.

[Csermely et al., 1998] Csermely, P., Schnaider, T., Soti, C., Prohászka, Z. and Nardai, G. (1998). The 90-kDa molecular chaperone family: structure, function, and clinical applications. A comprehensive review. Pharmacology & therapeutics *79*, 129–68.

[Cunningham et al., 2012] Cunningham, C. N., Southworth, D. R., Krukenberg, K. a. and Agard, D. a. (2012). The conserved arginine 380 of Hsp90 is not a catalytic residue, but stabilizes the closed conformation required for ATP hydrolysis. Protein science : a publication of the Protein Society *21*, 1162–71.

[Dai et al., 1996] Dai, K., Kobayashi, R. and Beach, D. (1996). Physical interaction of mammalian CDC37 with CDK4. J Biol Chem *271*, 22030–22034.

[Daugaard et al., 2007] Daugaard, M., Rohde, M. and Jaattela, M. (2007). The heat shock protein 70 family: Highly homologous proteins with overlapping and distinct functions. FEBS Lett *581*, 3702–3710.

[Davies et al., 2002] Davies, H., Bignell, G., Cox, C. and Stephens, P. (2002). Mutations of the BRAF gene in human cancer. Nature *417*, 949–954.

[De Luca et al., 1978] De Luca, P., Taddei, R. and Varano, L. (1978). Cyanidioschyzon merolae: a new alga of thermal acidic environments.

[DeBoer et al., 1970] DeBoer, C., Meulman, P. A., Wnuk, R. J. and Peterson, D. H. (1970). Geldanamycin, a new antibiotic. The Journal of Antibiotics *23*, 442–447.

[Delmotte and Delmotte-Plaque, 1953] Delmotte, P. and Delmotte-Plaque, J. (1953). A new antifungal substance of fungal origin.

[Derichs, 2013] Derichs, N. (2013). Targeting a genetic defect: Cystic fibrosis transmembrane conductance regulator modulators in cystic fibrosis.

[Dey et al., 1996] Dey, B., Lightbody, J. J. and Boschelli, F. (1996). CDC37 is required for p60v-src activity in yeast. Molecular Biology of the Cell *7*, 1405–1417.

[Dhillon et al., 2007] Dhillon, A., Hagan, S., Rath, O. and Kolch, W. (2007). MAP kinase signalling pathways in cancer. Oncogene *26*, 3279–3290.

[Dolinski et al., 1998] Dolinski, K. J., Cardenas, M. E. and Heitman, J. (1998). CNS1 encodes an essential p60/Sti1 homolog in Saccharomyces cerevisiae that suppresses cyclophilin 40 mutations and interacts with Hsp90. Molecular and Cellular Biology *18*, 7344–52.

[Duerfeldt et al., 2009] Duerfeldt, A. S., Brandt, G. E. L. and Blagg, B. S. J. (2009). Design, synthesis, and biological evaluation of conformationally constrained cis-amide Hsp90 inhibitors. Organic letters *11*, 2353–6.

[Duff, Jr. et al., 2011] Duff, Jr., M. R., Grubbs, J. and Howell, E. E. (2011). Isothermal Titration Calorimetry for Measuring Macromolecule-Ligand Affinity. Journal of Visualized Experiments *1*, 5–8.

[Duina et al., 1996] Duina, A. A., Chang, H. C., Marsh, J. A., Lindquist, S. and Gaber, R. F. (1996). A cyclophilin function in Hsp90-dependent signal transduction. Science *274*, 1713–5.

[Duina et al., 1998] Duina, A. A., Kalton, H. M. and Gaber, R. F. (1998). Requirement for Hsp90 and a CyP-40-type Cyclophilin in Negative Regulation of the Heat Shock Response. Journal of Biological Chemistry *273*, 18974–18978.

[Dunn et al., 2015] Dunn, D. M., Woodford, M. R., Truman, A. W., Jensen, S. M., Schulman, J., Caza, T., Remillard, T. C., Loiselle, D., Wolfgeher, D., Blagg, B. S. J., Franco, L., Haystead, T. A., Daturpalli, S., Mayer, M. P., Trepel, J. B., Morgan, R. M. L., Prodromou, C., Kron, S. J., Panaretou, B., Stetler-Stevenson, W. G., Landas, S. K., Neckers, L., Bratslavsky, G., Bourboulia, D. and Mollapour, M. (2015). c-Abl Mediated Tyrosine Phosphorylation of Aha1 Activates Its Co-chaperone Function in Cancer Cells. Cell reports *12*, 1006–18.

[Dutta and Inouye, 2000] Dutta, R. and Inouye, M. (2000). GHKL , an emergent ATPase / kinase superfamily Rinku Dutta and. Trends in Biochemical Sciences *25*, 24–28.

[Eccles et al., 2008] Eccles, S. a., Massey, A., Raynaud, F. I., Sharp, S. Y., Box, G., Valenti, M., Patterson, L., de Haven Brandon, A., Gowan, S., Boxall, F., Aherne, W., Rowlands, M., Hayes, A., Martins, V., Urban, F., Boxall, K., Prodromou, C., Pearl, L., James, K., Matthews, T. P., Cheung, K.-M., Kalusa, A., Jones, K., McDonald, E., Barril, X., Brough, P. a., Cansfield, J. E., Dymock, B., Drysdale, M. J., Finch, H., Howes, R., Hubbard, R. E., Surgenor, A., Webb, P., Wood, M., Wright, L. and Workman, P. (2008). NVP-AUY922: a novel heat shock protein 90 inhibitor active against xenograft tumor growth, angiogenesis, and metastasis. Cancer research *68*, 2850–60.

[Echeverria and Picard, 2010] Echeverria, P. C. and Picard, D. (2010). Molecular chaperones, essential partners of steroid hormone receptors for activity and mobility. Biochimica et biophysica acta *1803*, 641–9.

[Echtenkamp et al., 2011] Echtenkamp, F. J., Zelin, E., Oxelmark, E., Woo, J. I., Andrews, B. J., Garabedian, M. and Freeman, B. C. (2011). Global functional map of the p23 molecular chaperone reveals an extensive cellular network. Molecular cell *43*, 229–41.

[Eckert et al., 2010] Eckert, K., Saliou, J.-M., Monlezun, L., Vigouroux, A., Atmane, N., Caillat, C., Quevillon-Chéruel, S., Madiona, K., Nicaise, M., Lazereg, S., Van Dorsselaer, A., Sanglier-Cianférani, S., Meyer, P. and Moréra, S. (2010). The Pih1-Tah1 cochaperone complex inhibits Hsp90 molecular chaperone ATPase activity. The Journal of biological chemistry *285*, 31304–12.

[Eckl et al., 2014] Eckl, J. M., Drazic, A., Rutz, D. A. and Richter, K. (2014). Nematode Sgt1-homologue D1054.3 binds open and closed conformations of Hsp90 via distinct binding sites. Biochemistry *53*, 2505–14.

[Edelhoch, 1967] Edelhoch, H. (1967). Spectroscopic determination of tryptophan and tyrosine in proteins. Biochemistry *6*, 1948–1954.

[Eichner and Radford, 2011] Eichner, T. and Radford, S. E. (2011). A Diversity of Assembly Mechanisms of a Generic Amyloid Fold.

[Ellis and Hemmingsen, 1989] Ellis, R. J. and Hemmingsen, S. M. (1989). Molecular chaperones: proteins essential for the biogenesis of some macromolecular structures. Trends in Biochemical Sciences *14*, 339–342.

[Ellmann et al., 2009] Ellmann, S., Sticht, H., Thiel, F., Beckmann, M. W., Strick, R. and Strissel, P. L. (2009). Estrogen and progesterone receptors: From molecular structures to clinical targets. Cellular and Molecular Life Sciences *66*, 2405–2426.

[Erkine et al., 1995] Erkine, A. M., Szent-Gyorgyi, C., Simmons, S. F. and Gross, D. S. (1995). The upstream sequences of the HSP82 and HSC82 genes of Saccharomyces cevevisiae: Regulatory elements and nucleosome positioning motifs. Yeast *11*, 573–580.

[Eskew et al., 2011] Eskew, J. D., Sadikot, T., Morales, P., Duren, A., Dunwiddie, I., Swink, M., Zhang, X., Hembruff, S., Donnelly, A., Rajewski, R. a., Blagg, B. S., Manjarrez, J. R., Matts, R. L., Holzbeierlein, J. M. and Vielhauer, G. a. (2011). Development and characterization of a novel C-terminal inhibitor of Hsp90 in androgen dependent and independent prostate cancer cells. BMC Cancer *11*, 468.

[Fairbanks et al., 1971] Fairbanks, G., Steck, T. L. and Wallach, D. F. (1971). Electrophoretic analysis of the major polypeptides of the human erythrocyte membrane. Biochemistry *10*, 2606–2617.

[Fanghänel and Fischer, 2004] Fanghänel, J. and Fischer, G. (2004). Insights into the catalytic mechanism of peptidyl prolyl cis/trans isomerases. Frontiers in bioscience *9*, 3453–3478.

[Farinha and Amaral, 2005] Farinha, C. M. and Amaral, M. D. (2005). Most F508del-CFTR is targeted to degradation at an early folding checkpoint and independently of calnexin. Molecular and cellular biology *25*, 5242–5252.

[Felts et al., 2000] Felts, S. J., Owen, B. a. L., Nguyen, P., Trepel, J., Donner, D. B. and Toft, D. O. (2000). The hsp90-related protein TRAP1 is a mitochondrial protein with distinct functional properties. Journal of Biological Chemistry *275*, 3305–3312.

[Flaherty et al., 1991] Flaherty, K. M., McKay, D. B., Kabsch, W. and Holmes, K. C. (1991). Similarity of the three-dimensional structures of actin and the ATPase fragment of a 70-kDa heat shock cognate protein. Proceedings of the National Academy of Sciences of the United States of America *88*, 5041–5045.

[Flandrin et al., 2008] Flandrin, P., Guyotat, D., Duval, A., Cornillon, J., Tavernier, E., Nadal, N. and Campos, L. (2008). Significance of heat-shock protein (HSP) 90 expression in acute myeloid leukemia cells. Cell stress & chaperones *13*, 357–64.

[Forafonov et al., 2008] Forafonov, F., Toogun, O. a., Grad, I., Suslova, E., Freeman, B. C. and Picard, D. (2008). p23/Sba1p protects against Hsp90 inhibitors independently of its intrinsic chaperone activity. Molecular and cellular biology *28*, 3446–3456.

[Förster et al., 1939] Förster, T., Energiewanderung, Z. and Von, F. (1939). Zwischenmolekulare Energiewanderung und Fluoreszenz. Annalen der Physik *248*, 55–75.

[Freeman et al., 2000] Freeman, B. C., Felts, S. J., Toft, D. O. and Yamamoto, K. R. (2000). The p23 molecular chaperones act at a late step in intracellular receptor action to differentially affect ligand efficacies. Genes and Development *14*, 422–434.

[Freeman et al., 1996] Freeman, B. C., Toft, D. O. and Morimoto, R. I. (1996). Molecular chaperone machines: chaperone activities of the cyclophilin Cyp-40 and the steroid aporeceptor-associated protein p23. Science (New York, N.Y.) *274*, 1718–1720.

[Frizzell and Hanrahan, 2012] Frizzell, R. A. and Hanrahan, J. W. (2012). Physiology of epithelial chloride and fluid secretion. Cold Spring Harbor Perspectives in Medicine *2*.

[Frydman et al., 1994] Frydman, J., Nimmesgern, E., Ohtsuka, K. and Hartl, F. (1994). Folding of nascent polypeptide chains in a high molecular mass assembly with molecular chaperones. Nature *370*, 111–117.

[Gadsby et al., 2006] Gadsby, D. C., Vergani, P. and Csanády, L. (2006). The ABC protein turned chloride channel whose failure causes cystic fibrosis. Nature *440*, 477–83.

[Gao et al., 2013] Gao, G., Kun, T., Sheng, Y., Qian, M., Kong, F., Liu, X., Yu, Z., Zhang, H., Zhang, Q., Gu, J. and Zhang, X. (2013). SGT1 regulates Akt signaling by promoting beta-TrCP-dependent PHLPP1 degradation in gastric cancer cells. Molecular biology reports *40*, 2947–53.

[Garcia-Ranea et al., 2002] Garcia-Ranea, J. a., Mirey, G., Camonis, J. and Valencia, A. (2002). p23 and HSP20/alpha-crystallin proteins define a conserved sequence domain present in other eukaryotic protein families. FEBS letters *529*, 162–7.

[Gething and Sambrook, 1992] Gething, M. J. and Sambrook, J. (1992). Protein folding in the cell. Nature *355*, 33–45.

[Ghatak et al., 2005] Ghatak, S., Misra, S. and Toole, B. P. (2005). Hyaluronan constitutively regulates ErbB2 phosphorylation and signaling complex formation in carcinoma cells. Journal of Biological Chemistry *280*, 8875–8883.

[Goldman and Melo, 2008] Goldman, J. M. and Melo, J. V. (2008). BCR-ABL in chronic myelogenous leukemia–how does it work? Acta haematologica *119*, 212–7.

[Gomes et al., 2010] Gomes, N. M. V., Shay, J. W. and Wright, W. E. (2010). Telomere biology in Metazoa. FEBS Letters *584*, 3741–3751.

[Gosselin et al., 1994] Gosselin, S., Alhussaini, M., Streiff, M. B., Takabayashi, K. and Palcic, M. M. (1994). A Continuous Spectrophotometric Assay for Glycosyltransferases. Analytical Biochemistry *220*, 92–97.

[Grad et al., 2006] Grad, I., McKee, T. a., Ludwig, S. M., Hoyle, G. W., Ruiz, P., Wurst, W., Floss, T., Miller, C. a. and Picard, D. (2006). The Hsp90 cochaperone p23 is essential for perinatal survival. Molecular and cellular biology *26*, 8976–83.

[Grammatikakis et al., 1999] Grammatikakis, N., Lin, J. H., Grammatikakis, a., Tsichlis, P. N. and Cochran, B. H. (1999). p50(cdc37) acting in concert with Hsp90 is required for Raf-1 function. Molecular and cellular biology *19*, 1661–1672.

[Gray et al., 2007] Gray, P. J., Stevenson, M. A. and Calderwood, S. K. (2007). Targeting Cdc37 inhibits multiple signaling pathways and induces growth arrest in prostate cancer cells. Cancer research *67*, 11942–50.

[Greenfield, 2007] Greenfield, N. (2007). Using circular dichroism spectra to estimate protein secondary structure. Nature Protocols *1*, 2876–2890.

[Grenert et al., 1999] Grenert, J. P., Johnson, B. D. and Toft, D. O. (1999). The Importance of ATP Binding and Hydrolysis by Hsp90 in Formation and Function of Protein Heterocomplexes. Journal of Biological Chemistry *274*, 17525–17533.

[Grenert et al., 1997] Grenert, J. P., Sullivan, W. P., Fadden, P., Haystead, T. a. J., Clark, J., Mimnaugh, E., Krutzsch, H., Ochel, H. J., Schulte, T. W., Sausville, E., Neckers, L. M. and Toft, D. O. (1997). The amino-terminal domain of heat shock protein 90 (hsp90) that binds geldanamycin is an ATP/ADP switch domain that regulates hsp90 conformation. Journal of Biological Chemistry *272*, 23843–23850.

[Hagn et al., 2011] Hagn, F., Lagleder, S., Retzlaff, M., Rohrberg, J., Demmer, O., Richter, K., Buchner, J. and Kessler, H. (2011). Structural analysis of the interaction between Hsp90 and the tumor suppressor protein p53. Nature Structural & Molecular Biology *18*, 1086–1093.

[Hainzl et al., 2009] Hainzl, O., Lapina, M. C., Buchner, J. and Richter, K. (2009). The charged linker region is an important regulator of Hsp90 function. Journal of Biological Chemistry *284*, 22559–22567.

[Hainzl et al., 2004] Hainzl, O., Wegele, H., Richter, K. and Buchner, J. (2004). Cns1 is an activator of the Ssa1 ATPase activity. The Journal of biological chemistry *279*, 23267–73.

[Hartl et al., 2011] Hartl, F. U., Bracher, A. and Hayer-Hartl, M. (2011). Molecular chaperones in protein folding and proteostasis. Nature *475*, 324–332.

[Haupt et al., 2012] Haupt, A., Joberty, G., Bantscheff, M., Frohlich, H., Stehr, H., Schweiger, M. R., Fischer, A., Kerick, M., Boerno, S. T., Dahl, A., Lappe, M., Lehrach, H., Gonzalez, C., Drewes, G. and Lange, B. M. (2012). Hsp90 inhibition differentially destabilises MAP kinase and TGF-beta signalling components in cancer cells revealed by kinase-targeted chemoproteomics. BMC Cancer *12*, 38.

[Hawkins et al., 2008] Hawkins, T. a., Haramis, A.-P., Etard, C., Prodromou, C., Vaughan, C. K., Ashworth, R., Ray, S., Behra, M., Holder, N., Talbot, W. S., Pearl, L. H., Strähle, U. and Wilson, S. W. (2008). The ATPase-dependent chaperoning activity of Hsp90a regulates thick filament formation and integration during skeletal muscle myofibrillogenesis. Development (Cambridge, England) *135*, 1147–1156.

[Hayes and Stafford, 2010] Hayes, D. B. and Stafford, W. F. (2010). SEDVIEW, real-time sedimentation analysis. Macromolecular Bioscience *10*, 731–735.

[He et al., 2006] He, H., Zatorska, D., Kim, J., Aguirre, J., Llauger, L., She, Y., Wu, N., Immormino, R. M., Gewirth, D. T. and Chiosis, G. (2006). Identification of potent water soluble purine-scaffold inhibitors of the heat shock protein 90. Journal of Medicinal Chemistry *49*, 381–390.

[Hendrick and Hartl, 1993] Hendrick, J. P. and Hartl, F. U. (1993). Molecular chaperone functions of heat-shock proteins. Annual review of biochemistry *62*, 349–384.

[Herrera and Sebolt-Leopold, 2002] Herrera, R. and Sebolt-Leopold, J. S. (2002). Unraveling the complexities of the Raf/MAP kinase pathway for pharmacological intervention. Trends in Molecular Medicine *8*, 27–31.

[Hessling et al., 2009] Hessling, M., Richter, K. and Buchner, J. (2009). Dissection of the ATP-induced conformational cycle of the molecular chaperone Hsp90. Nature structural & molecular biology *16*, 287–293.

[Hesterkamp et al., 1996] Hesterkamp, T., Hauser, S., Lütcke, H. and Bukau, B. (1996). Escherichia coli trigger factor is a prolyl isomerase that associates with nascent polypeptide chains. Proceedings of the National Academy of Sciences of the United States of America *93*, 4437–4441.

[Hoffmann et al., 2010] Hoffmann, A., Bukau, B. and Kramer, G. (2010). Structure and function of the molecular chaperone Trigger Factor. Biochim Biophys Acta *1803*, 650–661.

[Holmes et al., 2008] Holmes, J. L., Sharp, S. Y., Hobbs, S. and Workman, P. (2008). Silencing of HSP90 cochaperone AHA1 expression decreases client protein activation and increases cellular sensitivity to the HSP90 inhibitor 17-allylamino-17-demethoxygeldanamycin. Cancer Research *68*, 1188–1197.

[Horwitz, 2003] Horwitz, J. (2003). Alpha-crystallin. Experimental Eye Research *76*, 145–153.

[Huber et al., 1986] Huber, R., Langworthy, T. A., Konig, H., Thomm, M., Woese, C. R., Sleytr, U. B. and Stetter, K. O. (1986). Thermotoga maritima sp. nov. represents a new genus of unique extremely thermophilic eubacteria growing up to 90 °C. Archives of Microbiology *144*, 324–333.

[Imamura et al., 1998] Imamura, T., Haruta, T., Takata, Y., Usui, I., Iwata, M., Ishihara, H., Ishiki, M., Ishibashi, O., Ueno, E., Sasaoka, T. and Kobayashi, M. (1998). Involvement of heat shock protein 90 in the degradation of mutant insulin receptors by the proteasome. The Journal of biological chemistry *273*, 11183–8.

[Ito et al., 1983] Ito, H., Fukuda, Y., Murata, K. and Kimura, A. (1983). Transformation of intact yeast cells treated with alkali cations. Journal of Bacteriology *153*, 163–168.

[Iwatsuki et al., 2010] Iwatsuki, M., Mimori, K., Sato, T., Toh, H., Yokobori, T., Tanaka, F., Ishikawa, K., Baba, H. and Mori, M. (2010). Overexpression of SUGT1 in human colorectal cancer and its clinicopathological significance. International Journal of Oncology *36*, 569–575.

[Jablonski, 1933] Jablonski, A. (1933). Efficiency of Anti-Stokes Fluorescence in Dyes. Nature *131*, 839–840.

[Jackson, 2012] Jackson, S. E. (2012). Hsp90: Structure and Function. In Molecular Chaperones vol. 11, pp. 155–240. Springer Berlin Heidelberg.

[Jahn et al., 2014] Jahn, M., Rehn, A., Pelz, B., Hellenkamp, B., Richter, K., Rief, M., Buchner, J. and Hugel, T. (2014). The charged linker of the molecular chaperone Hsp90 modulates domain contacts and biological function. PNAS *111*, 17881–17886.

[Jakob et al., 1993] Jakob, U., Gaestel, M., Engel, K. and Buchner, J. (1993). Small heat shock proteins are molecular chaperones. The Journal of biological chemistry *268*, 1517–1520.

[Jakob et al., 1995] Jakob, U., Lilie, H., Meyer, I. and Buchner, J. (1995). Transient interaction of Hsp90 with early unfolding intermediates of citrate synthase: Implications for heat shock in vivo. Journal of Biological Chemistry *270*, 7288–7294.

[Jeong et al., 2012] Jeong, J. Y., Yim, H. S., Ryu, J. Y., Lee, H. S., Lee, J. H., Seen, D. S. and Kang, S. G. (2012). One-step sequence-and ligation-independent cloning as a rapid and versatile cloning method for functional genomics Studies. Applied and Environmental Microbiology *78*, 5440–5443.

[Jhaveri et al., 2014] Jhaveri, K., Ochiana, S. O., Dunphy, M. P., Gerecitano, J. F., Corben, A. D., Peter, R. I., Janjigian, Y. Y., Gomes-DaGama, E. M., Koren, J., Modi, S. and Chiosis, G. (2014). Heat shock protein 90 inhibitors in the treatment of cancer: current status and future directions. Expert opinion on investigational drugs *23*, 611–28.

[Jiménez et al., 2012] Jiménez, B., Ugwu, F., Zhao, R., Ortí, L., Makhnevych, T., Pineda-Lucena, A. and Houry, W. a. (2012). Structure of Minimal Tetratricopeptide Repeat Domain Protein Tah1 Reveals Mechanism of Its Interaction with Pih1 and Hsp90. Journal of Biological Chemistry *287*, 5698–5709.

[Johnson, 2012] Johnson, J. L. (2012). Evolution and function of diverse Hsp90 homologs and cochaperone proteins. Biochimica et Biophysica Acta - Molecular Cell Research *1823*, 607–613.

[Johnson et al., 1994] Johnson, J. L., Beito, T. G., Krco, C. J. and Toft, D. O. (1994). Characterization of a novel 23-kilodalton protein of unactive progesterone receptor complexes. Molecular and cellular biology *14*, 1956–63.

[Johnson and Craig, 2000] Johnson, J. L. and Craig, E. a. (2000). A role for the Hsp40 Ydj1 in repression of basal steroid receptor activity in yeast. Molecular and cellular biology *20*, 3027–3036.

[Johnson et al., 2007] Johnson, J. L., Halas, A. and Flom, G. (2007). Nucleotide-dependent interaction of Saccharomyces cerevisiae Hsp90 with the cochaperone proteins Sti1, Cpr6, and Sba1. Molecular and cellular biology *27*, 768–776.

[Johnson and Toft, 1994] Johnson, J. L. and Toft, D. O. (1994). A novel chaperone complex for steroid receptors involving heat shock proteins, immunophilins, and p23. Journal of Biological Chemistry *269*, 24989–24993.

[Johnson and Toft, 1995] Johnson, J. L. and Toft, D. O. (1995). Binding of p23 and hsp90 during assembly with the progesterone receptor. Molecular endocrinology (Baltimore, Md.) *9*, 670–8.

[Johnson et al., 2014] Johnson, J. L., Zuehlke, A. D., Tenge, V. R. and Langworthy, J. C. (2014). Mutation of essential Hsp90 co-chaperones SGT1 or CNS1 renders yeast hypersensitive to overexpression of other co-chaperones. Current Genetics *60*, 265–276.

[Kadota et al., 2008] Kadota, Y., Amigues, B., Ducassou, L., Madaoui, H., Ochsenbein, F., Guerois, R. and Shirasu, K. (2008). Structural and functional analysis of SGT1-HSP90 core complex required for innate immunity in plants. EMBO reports *9*, 1209–1215.

[Kamal et al., 2003] Kamal, A., Thao, L., Sensintaffar, J., Zhang, L., Boehm, M. F., Fritz, L. C. and Burrows, F. J. (2003). A high-affinity conformation of Hsp90 confers tumour selectivity on Hsp90 inhibitors. Nature *425*, 407–410.

[Kampinga and Craig, 2010] Kampinga, H. H. and Craig, E. A. (2010). The HSP70 chaperone machinery: J proteins as drivers of functional specificity. Nature reviews. Molecular cell biology *11*, 579–92.

[Karagoez et al., 2014] Karagoez, G. E., Duarte, A. M. S., Akoury, E., Ippel, H., Biernat, J., T, M. L., Radli, M., Didenko, T., Nordhues, B. A., Veprintsev, D. B., Dickey, C. A., Mandelkow, E., Zweckstetter, M., Boelens, R., Madl, T. and Ruediger, S. G. D. (2014). Hsp90-tau complex reveals molecular basis for specificity in chaperone action. Cell *156*, 963–974.

[Katinka et al., 2001] Katinka, M. D., Duprat, S., Cornillot, E., Méténier, G., Thomarat, F., Prensier, G., Barbe, V., Peyretaillade, E., Brottier, P., Wincker, P., Delbac, F., El Alaoui, H., Peyret, P., Saurin, W., Gouy, M., Weissenbach, J. and Vivarès, C. P. (2001). Genome sequence and gene compaction of the eukaryote parasite Encephalitozoon cuniculi. Nature *414*, 450–453.

[Keeling and Fast, 2002] Keeling, P. J. and Fast, N. M. (2002). Microsporidia: biology and evolution of highly reduced intracellular parasites. Annu.Rev.Microbiol. *56*, 93–116.

[Kelly et al., 2005] Kelly, S. M., Jess, T. J. and Price, N. C. (2005). How to study proteins by circular dichroism.

[Kim et al., 2013] Kim, Y. E., Hipp, M. S., Bracher, A., Hayer-Hartl, M. and Hartl, F. U. (2013). Molecular chaperone functions in protein folding and proteostasis. Annual review of biochemistry *82*, 323–55.

[King et al., 2008] King, N., Westbrook, M. J., Young, S. L., Kuo, A., Abedin, M., Chapman, J., Fairclough, S., Hellsten, U., Isogai, Y., Letunic, I., Marr, M., Pincus, D., Putnam, N., Rokas, A., Wright, K. J., Zuzow, R., Dirks, W., Good, M., Goodstein, D., Lemons, D., Li, W., Lyons, J. B., Morris, A., Nichols, S., Richter, D. J., Salamov, A., Sequencing, J., Bork, P., Lim, W. A., Manning, G., Miller, W. T., McGinnis, W., Shapiro, H., Tjian, R., Grigoriev, I. V. and Rokhsar, D. (2008). The genome of the choanoflagellate Monosiga brevicollis and the origin of metazoans. Nature *451*, 783–788.

[Kirschke et al., 2014] Kirschke, E., Goswami, D., Southworth, D., Griffin, P. R. and Agard, D. A. (2014). Glucocorticoid receptor function regulated by coordinated action of the Hsp90 and Hsp70 chaperone cycles. Cell *157*, 1685–97.

[Kitagawa et al., 1999] Kitagawa, K., Skowyra, D., Elledge, S. J., Harper, J. W. and Hieter, P. (1999). SGT1 encodes an essential component of the yeast kinetochore assembly pathway and a novel subunit of the SCF ubiquitin ligase complex. Molecular cell *4*, 21–33.

[Kosano et al., 1998] Kosano, H., Stensgard, B., Charlesworth, M. C., McMahon, N. and Toft, D. (1998). The assembly of progesterone receptor-hsp90 complexes using purified proteins. Journal of Biological Chemistry *273*, 32973–32979.

[Koulov et al., 2010] Koulov, A. V., LaPointe, P., Lu, B., Razvi, A., Coppinger, J., Dong, M.-Q., Matteson, J., Laister, R., Arrowsmith, C., Yates, J. R. and Balch, W. E. (2010). Biological and structural basis of Aha1 regulation of Hsp90 ATPase activity in maintaining proteostasis in the human disease cystic fibrosis. Molecular biology of the cell *21*, 871–884.

[Kumar et al., 2009] Kumar, A., Manimekalai, M. S. S., Balakrishna, A. M., Hunke, C., Weigelt, S., Sewald, N. and Graeber, G. (2009). Spectroscopic and crystallographic studies of the mutant R416W give insight into the nucleotide binding traits of subunit B of the A 1A O ATP synthase. Proteins: Structure, Function and Bioinformatics *75*, 807–819.

[Kurien and Scofield, 2006] Kurien, B. T. and Scofield, R. H. (2006). Western blotting.

[Lakowicz, 2006] Lakowicz, J. R. (2006). Principles of fluorescence spectroscopy. Springer US.

[Lamphere et al., 1997] Lamphere, L., Fiore, F., Xu, X., Brizuela, L., Keezer, S., Sardet, C., Draetta, G. F. and Gyuris, J. (1997). Interaction between Cdc37 and Cdk4 in human cells. Oncogene *14*, 1999–2004.

[Langer et al., 1992] Langer, T., Lu, C., Echols, H., Flanagan, J., Hayer, M. K. and Hartl, F. U. (1992). Successive action of DnaK, DnaJ and GroEL along the pathway of chaperone-mediated protein folding. Nature *356*, 683–689.

[Laskey et al., 1978] Laskey, R., Honda, B., Mills, A. and Finch, J. (1978). Nucleosomes are assembled by an acidic protein which binds histones and transfers them to DNA. Nature *275*, 416–420.

[Laue and Stafford, 1999] Laue, T. M. and Stafford, W. F. (1999). Modern applications of analytical ultracentrifugation. Annual review of biophysics and biomolecular structure *28*, 75–100.

[Layne, 1957] Layne, E. (1957). Spectrophotometric and turbidimetric methods for measuring proteins. Methods in Enzymology *3*, 447–454.

[Lee et al., 2004] Lee, Y.-T., Jacob, J., Michowski, W., Nowotny, M., Kuznicki, J. and Chazin, W. J. (2004). Human Sgt1 binds HSP90 through the CHORD-Sgt1 domain and not the tetratricopeptide repeat domain. The Journal of biological chemistry *279*, 16511–7.

[Lens et al., 2010] Lens, S. M. a., Voest, E. E. and Medema, R. H. (2010). Shared and separate functions of polo-like kinases and aurora kinases in cancer. Nature reviews. Cancer *10*, 825–841.

[Lewis et al., 2004] Lewis, H. A., Buchanan, S. G., Burley, S. K., Conners, K., Dickey, M., Dorwart, M., Fowler, R., Gao, X., Guggino, W. B., Hendrickson, W. A., Hunt, J. F., Kearins, M. C., Lorimer, D., Maloney, P. C., Post, K. W., Rajashankar, K. R., Rutter, M. E., Sauder, J. M., Shriver, S., Thibodeau, P. H., Thomas, P. J., Zhang, M., Zhao, X. and Emtage, S. (2004). Structure of nucleotide-binding domain 1 of the cystic fibrosis transmembrane conductance regulator. The EMBO Journal *23*, 282–293.

[Li and Buchner, 2012] Li, J. and Buchner, J. (2012). Structure, function and regulation of the hsp90 machinery. Biomedical journal *36*, 106–17.

[Li et al., 2011] Li, J., Richter, K. and Buchner, J. (2011). Mixed Hsp90-cochaperone complexes are important for the progression of the reaction cycle. Nature structural & molecular biology *18*, 61–66.

[Li et al., 2013] Li, J., Richter, K., Reinstein, J. and Buchner, J. (2013). Integration of the accelerator Aha1 in the Hsp90 co-chaperone cycle. Nature structural & molecular biology *20*, 326–31.

[Lin and Nagy, 2013] Lin, J.-Y. and Nagy, P. D. (2013). Identification of novel host factors via conserved domain search: Cns1 cochaperone is a novel restriction factor of tombusvirus replication in yeast. Journal of virology *87*, 12600–10.

[Lin et al., 2008] Lin, T. Y., Bear, M., Du, Z., Foley, K. P., Ying, W., Barsoum, J. and London, C. (2008). The novel HSP90 inhibitor STA-9090 exhibits activity against Kit-dependent and -independent malignant mast cell tumors. Experimental Hematology *36*, 1266–1277.

[Lorenz et al., 2014] Lorenz, O. R., Freiburger, L., Rutz, D. A., Krause, M., Zierer, B. K., Alvira, S., Cuéllar, J., Valpuesta, J., Madl, T., Sattler, M. and Buchner, J. (2014). Modulation of the Hsp90 chaperone cycle by a stringent client protein. Molecular Cell *53*, 941–953.

[Lotz et al., 2003] Lotz, G. P., Lin, H., Harst, A. and Obermann, W. M. J. (2003). Aha1 binds to the middle domain of Hsp90, contributes to client protein activation, and stimulates the ATPase activity of the molecular chaperone. Journal of Biological Chemistry *278*, 17228–17235.

[Louvion et al., 1996] Louvion, J. F., Warth, R. and Picard, D. (1996). Two eukaryote-specific regions of Hsp82 are dispensable for its viability and signal transduction functions in yeast. Proceedings of the National Academy of Sciences of the United States of America *93*, 13937–13942.

[Ma et al., 2002] Ma, T., Thiagarajah, J. R., Yang, H., Sonawane, N. D., Folli, C., Galietta, L. J. V. and Verkman, A. S. (2002). Thiazolidinone CFTR inhibitor identified by high-throughput screening blocks cholera toxin-induced intestinal fluid secretion. Journal of Clinical Investigation *110*, 1651–1658.

[MacDonald, 2001] MacDonald, P. N. (2001). Two-Hybrid Systems: Methods and Protocols. Springer Science & Business Media.

[MacLean and Picard, 2003] MacLean, M. and Picard, D. (2003). Cdc37 goes beyond Hsp90 and kinases. Cell stress & chaperones *8*, 114–119.

[Mandal et al., 2007] Mandal, A. K., Lee, P., Chen, J. A., Nillegoda, N., Heller, A., DiStasio, S., Oen, H., Victor, J., Nair, D. M., Brodsky, J. L. and Caplan, A. J. (2007). Cdc37 has distinct roles in protein kinase quality control that protect nascent chains from degradation and promote posttranslational maturation. Journal of Cell Biology *176*, 319–328.

[Manival et al., 2014] Manival, X., Jacquemin, C., Charpentier, B. and Quinternet, M. (2014). (1)H, (15)N and (13)C resonance assignments of the yeast Pih1 and Tah1 C-terminal domains complex. Biomolecular NMR assignments *9*, 71–73.

[Manning et al., 2008] Manning, G., Young, S. L., Miller, W. T. and Zhai, Y. (2008). The protist, Monosiga brevicollis, has a tyrosine kinase signaling network more elaborate and diverse than found in any known metazoan. Proceedings of the National Academy of Sciences of the United States of America *105*, 9674–9679.

[Martinez-Yamout et al., 2006] Martinez-Yamout, M. A., Venkitakrishnan, R. P., Preece, N. E., Kroon, G., Wright, P. E. and Dyson, H. J. (2006). Localization of Sites of Interaction between p23 and Hsp90 in Solution. Journal of Biological Chemistry *281*, 14457–14464.

[Matulis et al., 2005] Matulis, D., Kranz, J. K., Salemme, F. R. and Todd, M. J. (2005). Thermodynamic stability of carbonic anhydrase: Measurements of binding affinity and stoichiometry using thermofluor. Biochemistry *44*, 5258–5266.

[Mayer, 2013] Mayer, M. P. (2013). Hsp70 chaperone dynamics and molecular mechanism.

[Mayer and Bukau, 2005] Mayer, M. P. and Bukau, B. (2005). Hsp70 chaperones: Cellular functions and molecular mechanism.

[Mayer and Le Breton, 2015] Mayer, M. P. and Le Breton, L. (2015). Hsp90: breaking the symmetry. Molecular cell *58*, 8–20.

[Mayr et al., 2000] Mayr, C., Richter, K., Lilie, H. and Buchner, J. (2000). Cpr6 and Cpr7, two closely related Hsp90-associated immunophilins from Saccharomyces cerevisiae, differ in their functional properties. Journal of Biological Chemistry *275*, 34140–34146.

[McDowell et al., 2009] McDowell, C. L., Bryan Sutton, R. and Obermann, W. M. J. (2009). Expression of Hsp90 chaperone proteins in human tumor tissue. International journal of biological macromolecules *45*, 310–4.

[McLaughlin et al., 2002] McLaughlin, S. H., Smith, H. W. and Jackson, S. E. (2002). Stimulation of the weak ATPase activity of human hsp90 by a client protein. Journal of molecular biology *315*, 787–798.

[McLaughlin et al., 2006] McLaughlin, S. H., Sobott, F., Yao, Z. P., Zhang, W., Nielsen, P. R., Grossmann, J. G., Laue, E. D., Robinson, C. V. and Jackson, S. E. (2006). The co-chaperone p23 arrests the Hsp90 ATPase cycle to trap client proteins. Journal of Molecular Biology *356*, 746–758.

[Meyer et al., 2003] Meyer, P., Prodromou, C., Hu, B., Vaughan, C., Roe, S. M., Panaretou, B., Piper, P. W. and Pearl, L. H. (2003). Structural and functional analysis of the middle segment of Hsp90: Implications for ATP hydrolysis and client protein and cochaperone interactions. Molecular Cell *11*, 647–658.

[Meyer et al., 2004] Meyer, P., Prodromou, C., Liao, C., Hu, B., Roe, S. M., Vaughan, C. K., Vlasic, I., Panaretou, B., Piper, P. W. and Pearl, L. H. (2004). Structural basis for recruitment of the ATPase activator Aha1 to the Hsp90 chaperone machinery. The EMBO journal *23*, 1402–1410.

[Mickler et al., 2009] Mickler, M., Hessling, M., Ratzke, C., Buchner, J. and Hugel, T. (2009). The large conformational changes of Hsp90 are only weakly coupled to ATP hydrolysis. Nature structural & molecular biology *16*, 281–286.

[Millson et al., 2008] Millson, S. H., Vaughan, C. K., Zhai, C., Ali, M. M. U., Panaretou, B., Piper, P. W., Pearl, L. H. and Prodromou, C. (2008). Chaperone ligand-discrimination by the TPR-domain protein Tah1. The Biochemical journal *413*, 261–8.

[Mimnaugh et al., 1996] Mimnaugh, E. G., Chavany, C. and Neckers, L. (1996). Polyubiquitination and proteasomal degradation of the p185c-erbB-2 receptor protein-tyrosine kinase induced by geldanamycin. The Journal of biological chemistry *271*, 22796–22801.

[Minami et al., 1994] Minami, Y., Yahara, I., Kimura, Y., Kawasaki, H. and Suzuki, K. (1994). The carboxy-terminal region of mammalian HSP90 is required for its dimerization and function in vivo. Molecular and cellular biology *14*, 1459–64.

[Mishra and Bolon, 2014] Mishra, P. and Bolon, D. N. A. (2014). Designed Hsp90 Heterodimers Reveal an Asymmetric ATPase-Driven Mechanism In Vivo. Molecular Cell *53*, 344–350.

[Misumi et al., 2005] Misumi, O., Matsuzaki, M., Nozaki, H., Miyagishima, S.-y., Mori, T., Nishida, K., Yagisawa, F., Yoshida, Y., Kuroiwa, H. and Kuroiwa, T. (2005). Cyanidioschyzon merolae genome. A tool for facilitating comparable studies on organelle biogenesis in photosynthetic eukaryotes. Plant physiology *137*, 567–585.

[Miyata et al., 2013] Miyata, Y., Nakamoto, H. and Neckers, L. (2013). The therapeutic target Hsp90 and cancer hallmarks. Current pharmaceutical design *19*, 347–365.

[Modi et al., 2011a] Modi, S., Stopeck, A., Linden, H., Solit, D., Chandarlapaty, S., Rosen, N., D'Andrea, G., Dickler, M., Moynahan, M. E., Sugarman, S., Ma, W., Patil, S., Norton, L., Hannah, A. L. and Hudis, C. (2011a). HSP90 inhibition is effective in breast cancer: A phase II trial of tanespimycin (17-AAG) plus trastuzumab in patients with HER2-positive metastatic breast cancer progressing on trastuzumab. Clinical Cancer Research *17*, 5132–5139.

[Modi et al., 2011b] Modi, S., Stopeck, A., Linden, H., Solit, D., Chandarlapaty, S., Rosen, N., D'Andrea, G., Dickler, M., Moynahan, M. E., Sugarman, S., Ma, W., Patil, S., Norton, L., Hannah, A. L. and Hudis, C. (2011b). HSP90 inhibition is effective in breast cancer: A phase II trial of tanespimycin (17-AAG) plus trastuzumab in patients with HER2-positive metastatic breast cancer progressing on trastuzumab. Clinical Cancer Research *17*, 5132–5139.

[Modi et al., 2007] Modi, S., Stopeck, A. T., Gordon, M. S., Mendelson, D., Solit, D. B., Bagatell, R., Ma, W., Wheler, J., Rosen, N., Norton, L., Cropp, G. F., Johnson, R. G., Hannah, A. L. and Hudis, C. a. (2007). Combination of trastuzumab and tanespimycin (17-AAG, KOS-953) is safe and active in trastuzumab-refractory HER-2 overexpressing breast cancer: a phase I dose-escalation study. Journal of clinical oncology : official journal of the American Society of Clinical Oncology *25*, 5410–7.

[Mollapour et al., 2014] Mollapour, M., Bourboulia, D., Beebe, K., Woodford, M. R., Polier, S., Hoang, A., Chelluri, R., Li, Y., Guo, A., Lee, M.-J., Fotooh-Abadi, E., Khan, S., Prince, T., Miyajima, N., Yoshida, S., Tsutsumi, S., Xu, W., Panaretou, B., Stetler-Stevenson, W. G., Bratslavsky, G., Trepel, J. B., Prodromou, C. and Neckers, L. (2014). Asymmetric Hsp90 N domain SUMOylation recruits Aha1 and ATP-competitive inhibitors. Molecular cell *53*, 317–29.

[Mollapour et al., 2011] Mollapour, M., Tsutsumi, S., Truman, A. W., Xu, W., Vaughan, C. K., Beebe, K., Konstantinova, A., Vourganti, S., Panaretou, B., Piper, P. W., Trepel, J. B., Prodromou, C., Pearl, L. H. and Neckers, L. (2011). Threonine 22 Phosphorylation Attenuates Hsp90 Interaction with Cochaperones and Affects Its Chaperone Activity. Molecular Cell *41*, 672–681.

[Morishima et al., 2003] Morishima, Y., Kanelakis, K. C., Murphy, P. J. M., Lowe, E. R., Jenkins, G. J., Osawa, Y., Sunahara, R. K. and Pratt, W. B. (2003). The Hsp90 cochaperone p23 is the limiting component of the multiprotein Hsp90/Hsp70-based chaperone system in vivo where it acts to stabilize the client protein-Hsp90 complex. Journal of Biological Chemistry *278*, 48754–48763.

[Muanprasat et al., 2004] Muanprasat, C., Sonawane, N. D., Salinas, D., Taddei, A., Galietta, L. J. V. and Verkman, A. S. (2004). Discovery of glycine hydrazide pore-occluding CFTR inhibitors: mechanism, structure-activity analysis, and in vivo efficacy. The Journal of general physiology *124*, 125–37.

[Nakamura et al., 1997] Nakamura, T. M., Morin, G. B., Chapman, K. B., Weinrich, S. L., Andrews, W. H., Lingner, J., Harley, C. B. and Cech, T. R. (1997). Telomerase catalytic subunit homologs from fission yeast and human. Science (New York, N.Y.) *277*, 955–9.

[Nakashima et al., 2010] Nakashima, T., Ishii, T., Tagaya, H., Seike, T., Nakagawa, H., Kanda, Y., Akinaga, S., Soga, S. and Shiotsu, Y. (2010). New molecular and biological mechanism of antitumor activities of KW-2478, a novel nonansamycin heat shock protein 90 inhibitor, in multiple myeloma cells. Clinical cancer research : an official journal of the American Association for Cancer Research *16*, 2792–802.

[Nathan and Lindquist, 1995] Nathan, D. F. and Lindquist, S. (1995). Mutational analysis of Hsp90 function: interactions with a steroid receptor and a protein kinase. Molecular and cellular biology *15*, 3917–25.

[Nathan et al., 1997] Nathan, D. F., Vos, M. H. and Lindquist, S. (1997). In vivo functions of the Saccharomyces cerevisiae Hsp90 chaperone. Proceedings of the National Academy of Sciences of the United States of America *94*, 12949–12956.

[Nathan et al., 1999] Nathan, D. F., Vos, M. H. and Lindquist, S. (1999). Identification of SSF1, CNS1, and HCH1 as multicopy suppressors of a Saccharomyces cerevisiae Hsp90 loss-of-function mutation. Proceedings of the National Academy of Sciences of the United States of America *96*, 1409–14.

[Neckers, 2000] Neckers, L. (2000). Effects of geldanamycin and other naturally occurring small molecule antagonists of heat shock protein 90 on HER2 protein expression. Breast Dis. *11*, 49–59.

[Neckers and Workman, 2012] Neckers, L. and Workman, P. (2012). Hsp90 molecular chaperone inhibitors: Are we there yet? Clinical Cancer Research *18*, 64–76.

[Neudegger et al., 2016] Neudegger, T., Verghese, J., Hayer-Hartl, M., Hartl, F. U. and Bracher, A. (2016). Structure of human heat-shock transcription factor 1 in complex with DNA. Nature Structural & Molecular Biology *1*.

[Obermann et al., 1998] Obermann, W. M. J., Sondermann, H., Russo, A. a., Pavletich, N. P. and Hartl, F. U. (1998). In vivo function of Hsp90 is dependent on ATP binding and ATP hydrolysis. Journal of Cell Biology *143*, 901–910.

[Ogi et al., 2015] Ogi, H., Sakuraba, Y., Kitagawa, R., Xiao, L., Shen, C., Cynthia, M. A., Ohta, S., Arnold, M. A., Ramirez, N., Houghton, P. J. and Kitagawa, K. (2015). The oncogenic role of the cochaperone Sgt1. Oncogenesis *4*, e149.

[O'Toole et al., 2007] O'Toole, M., Lau, K. T., Shepherd, R., Slater, C. and Diamond, D. (2007). Determination of phosphate using a highly sensitive paired emitter-detector diode photometric flow detector. Analytica Chimica Acta *597*, 290–294.

[Ou et al., 2014] Ou, J.-R., Tan, M.-S., Xie, A.-M., Yu, J.-T. and Tan, L. (2014). Heat Shock Protein 90 in Alzheimer's Disease. BioMed Research International *2014*, 1–7.

[Oxelmark et al., 2003] Oxelmark, E., Knoblauch, R., Arnal, S., Su, L. F., Schapira, M. and Garabedian, M. J. (2003). Genetic dissection of p23, an Hsp90 cochaperone, reveals a distinct surface involved in estrogen receptor signaling. Journal of Biological Chemistry *278*, 36547–36555.

[Panaretou et al., 1998] Panaretou, B., Prodromou, C., Roe, S. M., O'Brien, R., Ladbury, J. E., Piper, P. W. and Pearl, L. H. (1998). ATP binding and hydrolysis are essential to the function of the Hsp90 molecular chaperone in vivo. EMBO Journal *17*, 4829–4836.

[Panaretou et al., 2002] Panaretou, B., Siligardi, G., Meyer, P., Maloney, A., Sullivan, J. K., Singh, S., Millson, S. H., Clarke, P. a., Naaby-Hansen, S., Stein, R., Cramer, R., Mollapour, M., Workman, P., Piper, P. W., Pearl, L. H. and Prodromou, C. (2002). Activation of the ATPase activity of Hsp90 by the stress-regulated cochaperone Aha1. Molecular Cell *10*, 1307–1318.

[Panavas et al., 2009] Panavas, T., Sanders, C. and Butt, T. R. (2009). SUMO fusion technology for enhanced protein production in prokaryotic and eukaryotic expression systems. Methods in Molecular Biology (Clifton, N.J.) *497*, 303–17.

[Park et al., 2011] Park, S. J., Borin, B. N., Martinez-Yamout, M. a. and Dyson, H. J. (2011). The client protein p53 adopts a molten globule-like state in the presence of Hsp90. Nature structural & molecular biology *18*, 537–541.

[Paul and Mahanta, 2014] Paul, S. and Mahanta, S. (2014). Association of heat-shock proteins in various neurodegenerative disorders: Is it a master key to open the therapeutic door? Molecular and Cellular Biochemistry *386*, 45–61.

[Pearl and Prodromou, 2006] Pearl, L. H. and Prodromou, C. (2006). Structure and mechanism of the Hsp90 molecular chaperone machinery. Annual review of biochemistry *75*, 271–294.

[Pelin et al., 2016] Pelin, A., Moteshareie, H., Sak, B., Selman, M., Naor, A., Eyahpaise, M.-È., Farinelli, L., Golshani, A., Kvac, M. and Corradi, N. (2016). The genome of an Encephalitozoon cuniculi type III strain reveals insights into the genetic diversity and mode of reproduction of a ubiquitous vertebrate pathogen. Heredity *116*, 458–65.

[Perl and Schmid, 2002] Perl, D. and Schmid, F. X. (2002). Some like it hot: The molecular determinants of protein thermostability.

[Pesenti et al., 2016] Pesenti, M. E., Weir, J. R. and Musacchio, A. (2016). Progress in the structural and functional characterization of kinetochores. Current Opinion in Structural Biology *37*, 152–163.

[Picard, 2006] Picard, D. (2006). Chaperoning steroid hormone action.

[Picciotto et al., 1992] Picciotto, M. R., Cohn, J. A., Bertuzzi, G., Greengard, P. and Nairn, A. C. (1992). Phosphorylation of the cystic fibrosis transmembrane conductance regulator. J Biol Chem *267*, 12742–12752.

[Pind et al., 1994] Pind, S., Riordan, J. R. and Williams, D. B. (1994). Participation of the endoplasmic reticulum chaperone calnexin (p88, IP90) in the biogenesis of the cystic fibrosis transmembrane conductance regulator. Journal of Biological Chemistry *269*, 12784–12788.

[Pratt et al., 2006] Pratt, W. B., Morishima, Y., Murphy, M. and Harrell, M. (2006). Chaperoning of glucocorticoid receptors. Handbook of Experimental Pharmacology *172*, 111–138.

[Pratt and Toft, 1997] Pratt, W. B. and Toft, D. O. (1997). Steroid receptor interactions with heat shock protein and immunophilin chaperones. Endocrine reviews *18*, 306–360.

[Prince and Neckers, 2011] Prince, T. and Neckers, L. (2011). A Network of Its Own: The Unique Interactome of the Hsp90 Cochaperone, Sba1/p23. Molecular Cell *43*, 159–160.

[Prodromou et al., 2000] Prodromou, C., Panaretou, B., Chohan, S., Siligardi, G., O'Brien, R., Ladbury, J. E., Roe, S. M., Piper, P. W. and Pearl, L. H. (2000). The ATPase cycle of Hsp90 drives a molecular 'clamp' via transient dimerization of the N-terminal domains. The EMBO journal *19*, 4383–4392.

[Prodromou et al., 1997] Prodromou, C., Roe, S. M., O'Brien, R., Ladbury, J. E., Piper, P. W. and Pearl, L. H. (1997). Identification and structural characterization of the ATP/ADP-binding site in the Hsp90 molecular chaperone. Cell *90*, 65–75.

[Prodromou et al., 1999] Prodromou, C., Siligardi, G., O'Brien, R., Woolfson, D. N., Regan, L., Panaretou, B., Ladbury, J. E., Piper, P. W. and Pearl, L. H. (1999). Regulation of Hsp90 ATPase activity by tetratricopeptide repeat (TPR)-domain co-chaperones. EMBO Journal *18*, 754–762.

[Qu et al., 1997] Qu, B. H., Strickland, E. H. and Thomas, P. J. (1997). Localization and suppression of a kinetic defect in cystic fibrosis transmembrane conductance regulator folding. Journal of Biological Chemistry *272*, 15739–15744.

[Quinternet et al., 2015] Quinternet, M., Rothé, B., Barbier, M., Bobo, C., Saliou, J.-M., Jacquemin, C., Back, R., Chagot, M.-E., Cianférani, S., Meyer, P., Branlant, C., Charpentier, B. and Manival, X. (2015). Structure/function analysis of protein-protein interactions developed by the yeast Pih1 platform protein and its partners in box C/D snoRNP assembly. Journal of molecular biology *427*, 2816–39.

[Quinton, 2007] Quinton, P. M. (2007). Cystic Fibrosis: Lessons from the Sweat Gland. Physiology *22*, 212–225.

[Quon and Rowe, 2000] Quon, B. S. and Rowe, S. M. (2000). New and emerging targeted therapies for cystic fibrosis. BMJ *352*, 1–14.

[Ramdhave et al., 2013] Ramdhave, A. S., Patel, D., Ramya, I., Nandave, M. and Kharkar, P. S. (2013). Targeting heat shock protein 90 for malaria. Mini Rev Med Chem *13*, 1903–1920.

[Rao et al., 2001] Rao, J., Lee, P., Benzeno, S., Cardozo, C., Albertus, J., Robins, D. M. and Caplan, a. J. (2001). Functional interaction of human Cdc37 with the androgen receptor but not with the glucocorticoid receptor. J. Biol. Chem. *276*, 5814–20.

[Ratzke et al., 2012a] Ratzke, C., Berkemeier, F. and Hugel, T. (2012a). Heat shock protein 90's mechanochemical cycle is dominated by thermal fluctuations. Proceedings of the National Academy of Sciences *109*, 161–166.

[Ratzke et al., 2012b] Ratzke, C., Nguyen, M. N. T., Mayer, M. P. and Hugel, T. (2012b). From a ratchet mechanism to random fluctuations evolution of Hsp90's mechanochemical cycle. Journal of Molecular Biology *423*, 462–471.

[Razvi and Scholtz, 2006] Razvi, A. and Scholtz, J. M. (2006). Lessons in stability from thermophilic proteins. Protein science : a publication of the Protein Society *15*, 1569–1578.

[Retzlaff et al., 2010] Retzlaff, M., Hagn, F., Mitschke, L., Hessling, M., Gugel, F., Kessler, H., Richter, K. and Buchner, J. (2010). Asymmetric Activation of the Hsp90 Dimer by Its Cochaperone Aha1. Molecular Cell *37*, 344–354.

[Richter and Buchner, 2001] Richter, K. and Buchner, J. (2001). Hsp90: Chaperoning signal transduction. Journal of Cellular Physiology *188*, 281–290.

[Richter et al., 2006] Richter, K., Moser, S., Hagn, F., Friedrich, R., Hainzl, O., Heller, M., Schlee, S., Kessler, H., Reinstein, J. and Buchner, J. (2006). Intrinsic inhibition of the Hsp90 ATPase activity. Journal of Biological Chemistry *281*, 11301–11311.

[Richter et al., 2001] Richter, K., Muschler, P., Hainzl, O. and Buchner, J. (2001). Coordinated ATP Hydrolysis by the Hsp90 Dimer. Journal of Biological Chemistry *276*, 33689–33696.

[Richter et al., 2003] Richter, K., Muschler, P., Hainzl, O., Reinstein, J. and Buchner, J. (2003). Sti1 is a non-competitive inhibitor of the Hsp90 ATPase. Binding prevents the N-terminal dimerization reaction during the atpase cycle. The Journal of biological chemistry *278*, 10328–33.

[Richter et al., 2002] Richter, K., Reinstein, J. and Buchner, J. (2002). N-terminal residues regulate the catalytic efficiency of the Hsp90 ATPase cycle. Journal of Biological Chemistry *277*, 44905–44910.

[Richter et al., 2004] Richter, K., Walter, S. and Buchner, J. (2004). The Co-chaperone Sba1 connects the ATPase reaction of Hsp90 to the progression of the chaperone cycle. Journal of molecular biology *342*, 1403–13.

[Riggs et al., 2007] Riggs, D. L., Cox, M. B., Tardif, H. L., Hessling, M., Buchner, J. and Smith, D. F. (2007). Noncatalytic role of the FKBP52 peptidyl-prolyl isomerase domain in the regulation of steroid hormone signaling. Molecular and cellular biology *27*, 8658–69.

[Riordan, 2005] Riordan, J. R. (2005). Assembly of functional CFTR chloride channels. Annual review of physiology *67*, 701–718.

[Riordan et al., 1989] Riordan, J. R., Rommens, J. M., Kerem, B., Alon, N., Rozmahel, R., Grzelczak, Z., Zielenski, J., Lok, S., Plavsic, N. and Chou, J. L. (1989). Identification of the cystic fibrosis gene: cloning and characterization of complementary DNA. Science (New York, N.Y.) *245*, 1066–73.

[Robinson-Rechavi et al., 2006] Robinson-Rechavi, M., Alibes, A. and Godzik, A. (2006). Contribution of electrostatic interactions, compactness and quaternary structure to protein thermostability: Lessons from structural genomics of Thermotoga maritima. Journal of Molecular Biology *356*, 547–557.

[Roe et al., 2004] Roe, S. M., Ali, M. M. U., Meyer, P., Vaughan, C. K., Panaretou, B., Piper, P. W., Prodromou, C. and Pearl, L. H. (2004). The Mechanism of Hsp90 Regulation by the Protein Kinase-Specific Cochaperone p50cdc37. Cell *116*, 87–98.

[Roe et al., 1999] Roe, S. M., Prodromou, C., O'Brien, R., Ladbury, J. E., Piper, P. W. and Pearl, L. H. (1999). Structural basis for inhibition of the Hsp90 molecular chaperone by the antitumor antibiotics radicicol and geldanamycin. Journal of Medicinal Chemistry *42*, 260–266.

[Roemer et al., 2006] Roemer, L., Klein, C., Dehner, A., Kessler, H. and Buchner, J. (2006). p53 - A natural cancer killer: Structural insights and therapeutic concepts.

[Röhl et al., 2013] Röhl, A., Rohrberg, J. and Buchner, J. (2013). The chaperone Hsp90: Changing partners for demanding clients.

[Rosenhagen et al., 2001] Rosenhagen, M. C., Young, J. C., Wochnik, G. M., Herr, A. S., Schmidt, U., Hartl, F. U., Holsboer, F. and Rein, T. (2001). Synergistic inhibition of the glucocorticoid receptor by radicicol and benzoquinone ansamycins. Biological Chemistry *382*, 499–504.

[Rowe et al., 2005] Rowe, S. M., Miller, S. and Sorscher, E. J. (2005). Cystic fibrosis. The New England journal of medicine *352*, 1992–2001.

[Rüdiger et al., 1997] Rüdiger, S., Buchberger, A. and Bukau, B. (1997). Interaction of Hsp70 chaperones with substrates. Nature structural biology *4*, 342–9.

[Rudiger et al., 2002] Rudiger, S., Freund, S. M. V., Veprintsev, D. B. and Fersht, A. R. (2002). CRINEPT-TROSY NMR reveals p53 core domain bound in an unfolded form to the chaperone Hsp90. Proceedings of the National Academy of Sciences of the United States of America *99*, 11085–11090.

[Ruiz-Sanz et al., 2004] Ruiz-Sanz, J., Filimonov, V. V., Christodoulou, E., Vorgias, C. E. and Mateo, P. L. (2004). Thermodynamic analysis of the unfolding and stability of the dimeric DNA-binding protein HU from the hyperthermophilic eubacterium Thermotoga maritima and its E34D mutant. European Journal of Biochemistry *271*, 1497–1507.

[Sakahira and Nagata, 2002] Sakahira, H. and Nagata, S. (2002). Co-translational folding of caspase-activated DNase with Hsp70, Hsp40, and inhibitor of caspase-activated DNase. Journal of Biological Chemistry *277*, 3364–3370.

[Sambrook et al., 1989] Sambrook, J., Fritsch, E. F. and Maniatis, T. (1989). Molecular Cloning: A Laboratory Manual. 2 edition, Cold Spring Harbor, New York: Cold Spring Harbor Laboratory Press.

[Scheufler et al., 2000] Scheufler, C., Brinker, A., Bourenkov, G., Pegoraro, S., Moroder, L., Bartunik, H., Hartl, F. U. and Moarefi, I. (2000). Structure of TPR domain-peptide complexes: Critical elements in the assembly of the Hsp70-Hsp90 multichaperone machine. Cell *101*, 199–210.

[Schmid et al., 2012] Schmid, A. B., Lagleder, S., Gräwert, M. A., Röhl, A., Hagn, F., Wandinger, S. K., Cox, M. B., Demmer, O., Richter, K., Groll, M., Kessler, H. and Buchner, J. (2012). The architecture of functional modules in the Hsp90 co-chaperone Sti1/Hop. The EMBO Journal *31*, 1506–1517.

[Schneider et al., 1996] Schneider, C., Sepp-Lorenzino, L., Nimmesgern, E., Ouerfelli, O., Danishefsky, S., Rosen, N. and Hartl, F. U. (1996). Pharmacologic shifting of a balance between protein refolding and degradation mediated by Hsp90. Proceedings of the National Academy of Sciences of the United States of America *93*, 14536–14541.

[Schulte et al., 1998] Schulte, T. W., Akinaga, S., Soga, S., Sullivan, W., Stensgard, B., Toft, D. and Neckers, L. M. (1998). Antibiotic radicicol binds to the N-terminal domain of Hsp90 and shares important biologic activities with geldanamycin.

[Sequist et al., 2010] Sequist, L. V., Gettinger, S., Senzer, N. N., Martins, R. G., Jänne, P. a., Lilenbaum, R., Gray, J. E., Iafrate, a. J., Katayama, R., Hafeez, N., Sweeney, J., Walker, J. R., Fritz, C., Ross, R. W., Grayzel, D., Engelman, J. a., Borger, D. R., Paez, G. and Natale, R. (2010). Activity of IPI-504, a novel heat-shock protein 90 inhibitor, in patients with molecularly defined non-small-cell lung cancer. Journal of Clinical Oncology *28*, 4953–4960.

[Sevier and Machamer, 2001] Sevier, C. S. and Machamer, C. E. (2001). p38: A novel protein that associates with the vesicular stomatitis virus glycoprotein. Biochemical and biophysical research communications *287*, 574–82.

[Shao et al., 2003] Shao, J., Irwin, A., Hartson, S. D. and Matts, R. L. (2003). Functional Dissection of Cdc37: Characterization of Domain Structure and Amino Acid Residues Critical for Protein Kinase Binding. Biochemistry *42*, 12577–12588.

[Sharma et al., 1998] Sharma, S. V., Agatsuma, T. and Nakano, H. (1998). Targeting of the protein chaperone, HSP90, by the transformation suppressing agent, radicicol. Oncogene *16*, 2639–2645.

[Shiau et al., 2006] Shiau, A. K., Harris, S. F., Southworth, D. R. and Agard, D. a. (2006). Structural Analysis of E. coli hsp90 Reveals Dramatic Nucleotide-Dependent Conformational Rearrangements. Cell *127*, 329–340.

[Sievers et al., 2011] Sievers, F., Wilm, A., Dineen, D., Gibson, T. J., Karplus, K., Li, W., Lopez, R., McWilliam, H., Remmert, M., Söding, J., Thompson, J. D. and Higgins, D. G. (2011). Fast, scalable generation of high-quality protein multiple sequence alignments using Clustal Omega. Molecular systems biology *7*, 539.

[Silverstein et al., 1998] Silverstein, a. M., Grammatikakis, N., Cochran, B. H., Chinkers, M. and Pratt, W. B. (1998). p50(cdc37) binds directly to the catalytic domain of Raf as well as to a site on hsp90 that is topologically adjacent to the tetratricopeptide repeat binding site. The Journal of biological chemistry *273*, 20090–5.

[Smale, 2010] Smale, S. T. (2010). Beta-galactosidase assay. Cold Spring Harbor protocols *2010*, pdb.prot5423.

[Smith et al., 1995] Smith, D. F., Whitesell, L., Nair, S. C., Chen, S., Prapapanich, V. and Rimerman, R. a. (1995). Progesterone receptor structure and function altered by geldanamycin, an hsp90-binding agent. Molecular and cellular biology *15*, 6804–12.

[Smith and Workman, 2007] Smith, J. R. and Workman, P. (2007). Targeting the cancer chaperone HSP90. Drug Discovery Today: Therapeutic Strategies *4*, 219–227.

[Smith and Workman, 2009] Smith, J. R. and Workman, P. (2009). Targeting CDC37: an alternative, kinase-directed strategy for disruption of oncogenic chaperoning. Cell cycle (Georgetown, Tex.) *8*, 362–72.

[Soga et al., 1999] Soga, S., Neckers, L. M., Schulte, T. W., Shiotsu, Y., Akasaka, K., Narumi, H., Agatsuma, T., Ikuina, Y., Murakata, C., Tamaoki, T. and Akinaga, S. (1999). KF25706, a novel oxime derivative of radicicol, exhibits in vivo antitumor activity via selective depletion of Hsp90 binding signaling molecules. Cancer research *59*, 2931–8.

[Sorger and Pelham, 1987] Sorger, P. K. and Pelham, H. R. (1987). The glucose-regulated protein grp94 is related to heat shock protein hsp90. Journal of Molecular Biology *194*, 341–344.

[Soroka et al., 2012] Soroka, J., Wandinger, S. K., Mäusbacher, N., Schreiber, T., Richter, K., Daub, H. and Buchner, J. (2012). Conformational Switching of the Molecular Chaperone Hsp90 via Regulated Phosphorylation. Molecular Cell *45*, 517–528.

[Southworth and Agard, 2008] Southworth, D. R. and Agard, D. a. (2008). Species-Dependent Ensembles of Conserved Conformational States Define the Hsp90 Chaperone ATPase Cycle. Molecular Cell *32*, 631–640.

[Southworth and Agard, 2011] Southworth, D. R. and Agard, D. a. (2011). Client-Loading Conformation of the Hsp90 Molecular Chaperone Revealed in the Cryo-EM Structure of the Human Hsp90:Hop Complex. Molecular Cell *42*, 771–781.

[Spassov et al., 1995] Spassov, V. Z., Karshikoff, A. D. and Ladenstein, R. (1995). The optimization of protein-solvent interactions: thermostability and the role of hydrophobic and electrostatic interactions. Protein science : a publication of the Protein Society *4*, 1516–27.

[Sreedhar et al., 2004] Sreedhar, A. S., Kalmár, É., Csermely, P. and Shen, Y. F. (2004). Hsp90 isoforms: Functions, expression and clinical importance. FEBS Letters *562*, 11–15.

[Sriprapundh et al., 2000] Sriprapundh, D., Vieille, C. and Zeikus, J. G. (2000). Molecular determinants of xylose isomerase thermal stability and activity: analysis of thermozymes by site-directed mutagenesis. Protein engineering *13*, 259–65.

[Stancato et al., 1993] Stancato, L. F., Chow, Y. H., Hutchison, K. a., Perdew, G. H., Jove, R. and Pratt, W. B. (1993). Raf exists in a native heterocomplex with hsp90 and p50 that can be reconstituted in a cell-free system. The Journal of biological chemistry *268*, 21711–6.

[Stancato et al., 1994] Stancato, L. F., Chow, Y. H., Owens-Grillo, J. K., Yem, A. W., Deibel Jr., M. R., Jove, R. and Pratt, W. B. (1994). The native v-Raf.hsp90.p50 heterocomplex contains a novel immunophilin of the FK506 binding class. The Journal of biological chemistry *269*, 22157–22161.

[Stebbins et al., 1997] Stebbins, C. E., Russo, a. a., Schneider, C., Rosen, N., Hartl, F. U. and Pavletich, N. P. (1997). Crystal structure of an Hsp90-geldanamycin complex: targeting of a protein chaperone by an antitumor agent. Cell *89*, 239–250.

[Steensgaard et al., 2004] Steensgaard, P., Garrè, M., Muradore, I., Transidico, P., Nigg, E. a., Kitagawa, K., Earnshaw, W. C., Faretta, M. and Musacchio, A. (2004). Sgt1 is required for human kinetochore assembly. EMBO reports *5*, 626–631.

[Stoscheck, 1990] Stoscheck, C. M. (1990). Quantitation of protein. Methods in Enzymology *182*, 50–68.

[Street et al., 2012] Street, T. O., Lavery, L. A., Verba, K. A., Lee, C. T., Mayer, M. P. and Agard, D. A. (2012). Cross-monomer substrate contacts reposition the Hsp90 N-terminal domain and prime the chaperone activity. Journal of Molecular Biology *415*, 3–15.

[Stryer, 1978] Stryer, L. (1978). Fluorescence Energy Transfer as a Spectroscopic Ruler. Ann. Rev. Biochem. *47*, 819–846.

[Sun et al., 2015] Sun, L., Hartson, S. D. and Matts, R. L. (2015). Identification of proteins associated with Aha1 in HeLa cells by quantitative proteomics. Biochimica et biophysica acta *1854*, 365–80.

[Sun et al., 2012] Sun, L., Prince, T., Manjarrez, J. R., Scroggins, B. T. and Matts, R. L. (2012). Characterization of the interaction of Aha1 with components of the Hsp90 chaperone machine and client proteins. Biochimica et Biophysica Acta (BBA) - Molecular Cell Research *1823*, 1092–1101.

[Supko et al., 1995] Supko, J. G., Hickman, R. L., Grever, M. R. and Malspeis, L. (1995). Preclinical pharmacologic evaluation of geldanamycin as an antitumor agent. Cancer Chemotherapy and Pharmacology *36*, 305–315.

[Synoradzki and Bieganowski, 2015] Synoradzki, K. and Bieganowski, P. (2015). Middle domain of human Hsp90 isoforms differentially binds Aha1 in human cells and alters Hsp90 activity in yeast. Biochimica et biophysica acta *1853*, 445–52.

[Taipale et al., 2010] Taipale, M., Jarosz, D. F. and Lindquist, S. (2010). HSP90 at the hub of protein homeostasis: emerging mechanistic insights. Nature Reviews Molecular Cell Biology *11*, 515–528.

[Taipale et al., 2012] Taipale, M., Krykbaeva, I., Koeva, M., Kayatekin, C., Westover, K. D., Karras, G. I. and Lindquist, S. (2012). Quantitative analysis of Hsp90-client interactions reveals principles of substrate recognition. Cell *150*, 987–1001.

[Tenge et al., 2015] Tenge, V. R., Zuehlke, A. D., Shrestha, N. and Johnson, J. L. (2015). The Hsp90 cochaperones Cpr6, Cpr7, and Cns1 interact with the intact ribosome. Eukaryotic cell *14*, 55–63.

[Tesic et al., 2003] Tesic, M., Marsh, J. a., Cullinan, S. B. and Gaber, R. F. (2003). Functional interactions between Hsp90 and the co-chaperones Cns1 and Cpr7 in Saccharomyces cerevisiae. Journal of Biological Chemistry *278*, 32692–32701.

[Trendowski, 2015] Trendowski, M. (2015). PU-H71: An improvement on nature's solutions to oncogenic Hsp90 addiction. Pharmacological research *99*, 202–16.

[Trepel et al., 2010] Trepel, J., Mollapour, M., Giaccone, G. and Neckers, L. (2010). Targeting the dynamic HSP90 complex in cancer. Nature reviews. Cancer *10*, 537–549.

[Tripathi et al., 2014] Tripathi, V., Darnauer, S., Hartwig, N. R. and Obermann, W. M. J. (2014). Aha1 Can Act as an Autonomous Chaperone to Prevent Aggregation of Stressed Proteins. Journal of Biological Chemistry *289*, 36220–36228.

[Tsutsumi et al., 2009] Tsutsumi, S., Mollapour, M., Graf, C., Lee, C.-T., Scroggins, B. T., Xu, W., Haslerova, L., Hessling, M., Konstantinova, A. a., Trepel, J. B., Panaretou, B., Buchner, J., Mayer, M. P., Prodromou, C. and Neckers, L. (2009). Hsp90 charged-linker truncation reverses the functional consequences of weakened hydrophobic contacts in the N domain. Nature Structural & Molecular Biology *16*, 1141–1147.

[Tsutsumi et al., 2012] Tsutsumi, S., Mollapour, M., Prodromou, C., Lee, C.-T., Panaretou, B., Yoshida, S., Mayer, M. P. and Neckers, L. M. (2012). Charged linker sequence modulates eukaryotic heat shock protein 90 (Hsp90) chaperone activity. PNAS *109*, 2937–2942.

[Tyedmers et al., 2010] Tyedmers, J., Mogk, A. and Bukau, B. (2010). Cellular strategies for controlling protein aggregation. Nature reviews. Molecular cell biology *11*, 777–788.

[Van Der Straten et al., 1997] Van Der Straten, A., Rommel, C., Dickson, B. and Hafen, E. (1997). The heat shock protein 83 (Hsp83) is required for Raf-mediated signalling in Drosophila. EMBO Journal *16*, 1961–1969.

[Van Goor et al., 2011] Van Goor, F., Hadida, S., Grootenhuis, P. D. J., Burton, B., Stack, J. H., Straley, K. S., Decker, C. J., Miller, M., McCartney, J., Olson, E. R., Wine, J. J., Frizzell, R. A., Ashlock, M. and Negulescu, P. A. (2011). Correction of the F508del-CFTR protein processing defect in vitro by the investigational drug VX-809. Proceedings of the National Academy of Sciences of the United States of America *108*, 18843–8.

[Vaughan et al., 2006] Vaughan, C. K., Gohlke, U., Sobott, F., Good, V. M., Ali, M. M. U., Prodromou, C., Robinson, C. V., Saibil, H. R. and Pearl, L. H. (2006). Structure of an Hsp90-Cdc37-Cdk4 Complex. Molecular Cell *23*, 697–707.

[Vaughan et al., 2008] Vaughan, C. K., Mollapour, M., Smith, J. R., Truman, A., Hu, B., Good, V. M., Panaretou, B., Neckers, L., Clarke, P. a., Workman, P., Piper, P. W., Prodromou, C. and Pearl, L. H. (2008). Hsp90-Dependent Activation of Protein Kinases Is Regulated by Chaperone-Targeted Dephosphorylation of Cdc37. Molecular Cell *31*, 886–895.

[Vávra and Lukeš, 2013] Vávra, J. and Lukeš, J. (2013). Microsporidia and 'the art of living together'.

[Venter et al., 2001] Venter, J. C., Adams, M. D., Myers, E. W., Li, P. W., Mural, R. J., Sutton, G. G., Smith, H. O., Yandell, M., Evans, C. A., Holt, R. A., Gocayne, J. D., Amanatides, P., Ballew, R. M., Huson, D. H., Wortman, J. R., Zhang, Q., Kodira, C. D., Zheng, X. H., Chen, L., Skupski, M., Subramanian, G., Thomas, P. D., Zhang, J., Gabor Miklos, G. L., Nelson, C., Broder, S., Clark, A. G., Nadeau, J., McKusick, V. A., Zinder, N., Levine, A. J., Roberts, R. J., Simon, M., Slayman, C., Hunkapiller, M., Bolanos, R., Delcher, A., Dew, I., Fasulo, D., Flanigan, M., Florea, L., Halpern, A., Hannenhalli, S., Kravitz, S., Levy, S., Mobarry, C., Reinert, K., Remington, K., Abu-Threideh, J., Beasley, E., Biddick, K., Bonazzi, V., Brandon, R., Cargill, M., Chandramouliswaran, I., Charlab, R., Chaturvedi, K., Deng, Z., Di Francesco, V., Dunn, P., Eilbeck, K., Evangelista, C., Gabrielian, A. E., Gan, W., Ge, W., Gong, F., Gu, Z., Guan, P., Heiman, T. J., Higgins, M. E., Ji, R. R., Ke, Z., Ketchum, K. A., Lai, Z., Lei, Y., Li, Z., Li, J., Liang, Y., Lin, X., Lu, F., Merkulov, G. V., Milshina, N., Moore, H. M., Naik, A. K., Narayan, V. A., Neelam, B., Nusskern, D., Rusch, D. B., Salzberg, S., Shao, W., Shue, B., Sun, J., Wang, Z., Wang, A., Wang, X., Wang, J., Wei, M., Wides, R., Xiao, C., Yan, C., Yao, A., Ye, J., Zhan, M., Zhang, W., Zhang, H., Zhao, Q., Zheng, L., Zhong, F., Zhong, W., Zhu, S., Zhao, S., Gilbert, D., Baumhueter, S., Spier, G., Carter, C., Cravchik, A., Woodage, T., Ali, F., An, H., Awe, A., Baldwin, D., Baden, H., Barnstead, M., Barrow, I., Beeson, K., Busam, D., Carver, A., Center, A., Cheng, M. L., Curry, L., Danaher, S., Davenport, L., Desilets, R., Dietz, S., Dodson, K., Doup, L., Ferriera, S., Garg, N., Gluecksmann, A., Hart, B., Haynes, J., Haynes, C., Heiner, C., Hladun, S., Hostin, D., Houck, J., Howland, T., Ibegwam, C., Johnson, J., Kalush, F., Kline, L., Koduru, S., Love, A., Mann, F., May, D., McCawley, S., McIntosh, T., McMullen, I., Moy, M., Moy, L., Murphy, B., Nelson, K., Pfannkoch, C., Pratts, E., Puri, V., Qureshi, H., Reardon, M., Rodriguez, R., Rogers, Y. H., Romblad, D., Ruhfel, B., Scott, R., Sitter, C., Smallwood, M., Stewart, E., Strong, R., Suh, E., Thomas, R., Tint, N. N., Tse, S., Vech, C., Wang, G., Wetter, J., Williams, S., Williams, M., Windsor, S., Winn-Deen, E., Wolfe, K., Zaveri, J., Zaveri, K., Abril, J. F., Guigó, R., Campbell, M. J., Sjolander, K. V., Karlak, B., Kejariwal, A., Mi, H., Lazareva, B., Hatton, T., Narechania, A., Diemer, K., Muruganujan, A., Guo, N., Sato, S., Bafna, V., Istrail, S., Lippert, R., Schwartz, R., Walenz, B., Yooseph, S., Allen, D., Basu, A., Baxendale, J., Blick, L., Caminha, M., Carnes-Stine, J., Caulk, P., Chiang, Y. H., Coyne, M., Dahlke, C., Mays, A., Dombroski, M., Donnelly, M., Ely, D., Esparham, S., Fosler, C., Gire, H., Glanowski, S., Glasser, K., Glodek, A., Gorokhov, M., Graham, K., Gropman, B., Harris, M., Heil, J., Henderson, S., Hoover, J., Jennings, D., Jordan, C., Jordan, J., Kasha, J., Kagan, L., Kraft, C., Levitsky, A., Lewis, M., Liu, X., Lopez, J., Ma, D., Majoros, W., McDaniel, J., Murphy, S., Newman, M., Nguyen, T., Nguyen, N., Nodell, M., Pan, S., Peck, J., Peterson, M., Rowe, W., Sanders, R., Scott, J., Simpson, M., Smith, T., Sprague, A., Stockwell, T., Turner, R., Venter, E., Wang, M., Wen, M., Wu, D., Wu, M., Xia, A., Zandieh, A. and Zhu, X. (2001). The sequence of the human genome. Science (New York, N.Y.) *291*, 1304–51.

[Versteeg et al., 1999] Versteeg, S., Mogk, a. and Schumann, W. (1999). The Bacillus subtilis htpG gene is not involved in thermal stress management. Molecular & general genetics : MGG *261*, 582–8.

[Vousden and Lane, 2007] Vousden, K. H. and Lane, D. P. (2007). P53 in Health and Disease. Nature reviews. Molecular cell biology *8*, 275–283.

[Walter and Buchner, 2002] Walter, S. and Buchner, J. (2002). Molecular Chaperones – Cellular Machines for Protein Folding. Angewandte Chemie International Edition *41*, 1098–1113.

[Walton-Diaz et al., 2013] Walton-Diaz, A., Khan, S., Bourboulia, D., Trepel, J. B., Neckers, L. and Mollapour, M. (2013). Contributions of co-chaperones and post-translational modifications towards Hsp90 drug sensitivity. Future medicinal chemistry *5*, 1059–1071.

[Wandinger et al., 2006] Wandinger, S. K., Suhre, M. H., Wegele, H. and Buchner, J. (2006). The phosphatase Ppt1 is a dedicated regulator of the molecular chaperone Hsp90. The EMBO journal *25*, 367–376.

[Wang et al., 2013] Wang, N., Li, Q., Feng, N.-H., Cheng, G., Guan, Z.-L., Wang, Y., Qin, C., Yin, C.-J., Hua, L.-X., Akerfelt, M., Morimoto, R. I. and Sistonen, L. (2013). Heat shock factors: integrators of cell stress, development and lifespan. Nature reviews. Molecular cell biology *11*, 735–41.

[Wang et al., 2002] Wang, X., Grammatikakis, N. and Hu, J. (2002). Role of p50/CDC37 in hepadnavirus assembly and replication. The Journal of biological chemistry *277*, 24361–7.

[Wang et al., 2004] Wang, X., Matteson, J., An, Y., Moyer, B., Yoo, J.-S., Bannykh, S., Wilson, I. A., Riordan, J. R. and Balch, W. E. (2004). COPII-dependent export of cystic fibrosis transmembrane conductance regulator from the ER uses a di-acidic exit code. The Journal of cell biology *167*, 65–74.

[Wang et al., 2006] Wang, X., Venable, J., LaPointe, P., Hutt, D. M., Koulov, A. V., Coppinger, J., Gurkan, C., Kellner, W., Matteson, J., Plutner, H., Riordan, J. R., Kelly, J. W., Yates, J. R. and Balch, W. E. (2006). Hsp90 Cochaperone Aha1 Downregulation Rescues Misfolding of CFTR in Cystic Fibrosis. Cell *127*, 803–815.

[Wayne and Bolon, 2007] Wayne, N. and Bolon, D. N. (2007). Dimerization of Hsp90 is required for in vivo function: Design and analysis of monomers and dimers. Journal of Biological Chemistry *282*, 35386–35395.

[Weber et al., 1994] Weber, J., Wilkemounts, S., Grell, E. and Senior, A. E. (1994). Tryptophan Fluorescence Provides a Direct Probe of Nucleotide-Binding in the Noncatalytic Sites of Escherichia-Coli F(1)-Atpase. Journal of Biological Chemistry *269*, 11261–11268.

[Weikl et al., 1999] Weikl, T., Abelmann, K. and Buchner, J. (1999). An unstructured C-terminal region of the Hsp90 co-chaperone p23 is important for its chaperone function. Journal of molecular biology *293*, 685–691.

[Weikl et al., 2000] Weikl, T., Muschler, P., Richter, K., Veit, T., Reinstein, J. and Buchner, J. (2000). C-terminal regions of Hsp90 are important for trapping the nucleotide during the ATPase cycle. Journal of molecular biology *303*, 583–592.

[Whitesell and Lindquist, 2005] Whitesell, L. and Lindquist, S. L. (2005). HSP90 and the chaperoning of cancer. Nature reviews. Cancer *5*, 761–72.

[Whitesell et al., 1994] Whitesell, L., Mimnaugh, E. G., De Costa, B., Myers, C. E. and Neckers, L. M. (1994). Inhibition of heat shock protein HSP90-pp60v-src heteroprotein complex formation by benzoquinone ansamycins: essential role for stress proteins in oncogenic transformation. Proceedings of the National Academy of Sciences of the United States of America *91*, 8324–8328.

[Willander and Al-Hilli, 2009] Willander, M. and Al-Hilli, S. (2009). Analysis of biomolecules using surface plasmons.

[Wiseman et al., 1989] Wiseman, T., Williston, S., Brandts, J. F. and Lin, L. N. (1989). Rapid measurement of binding constants and heats of binding using a new titration calorimeter. Analytical Biochemistry *179*, 131–137.

[Woodhead et al., 2010] Woodhead, A. J., Angove, H., Carr, M. G., Chessari, G., Congreve, M., Coyle, J. E., Cosme, J., Graham, B., Day, P. J., Downham, R., Fazal, L., Feltell, R., Figueroa, E., Frederickson, M., Lewis, J., McMenamin, R., Murray, C. W., O'Brien, M. A., Parra, L., Patel, S., Phillips, T., Rees, D. C., Rich, S., Smith, D.-M., Trewartha, G., Vinkovic, M., Williams, B. and Woolford, A. J.-a. (2010). Discovery of (2,4-dihydroxy-5-isopropylphenyl)-[5-(4-methylpiperazin-1-ylmethyl)-1,3-dihydroisoindol-2-yl]methanone (AT13387), a novel inhibitor of the molecular chaperone Hsp90 by fragment based drug design. Journal of medicinal chemistry *53*, 5956–5969.

[Wrighton et al., 2008] Wrighton, K. H., Lin, X. and Feng, X.-H. (2008). Critical regulation of TGFbeta signaling by Hsp90. Proceedings of the National Academy of Sciences of the United States of America *105*, 9244–9249.

[Xu et al., 2001] Xu, W., Mimnaugh, E., Rosser, M. F. N., Nicchitta, C., Marcu, M., Yarden, Y. and Neckers, L. (2001). Sensitivity of Mature ErbB2 to Geldanamycin Is Conferred by Its Kinase Domain and Is Mediated by the Chaperone Protein Hsp90. Journal of Biological Chemistry *276*, 3702–3708.

[Xu et al., 2012] Xu, W., Mollapour, M., Prodromou, C., Wang, S., Scroggins, B. T., Palchick, Z., Beebe, K., Siderius, M., Lee, M. J., Couvillon, A., Trepel, J. B., Miyata, Y., Matts, R. and Neckers, L. (2012). Dynamic Tyrosine Phosphorylation Modulates Cycling of the HSP90-P50 CDC37-AHA1 Chaperone Machine. Molecular Cell *47*, 434–443.

[Yang et al., 2005] Yang, J., Roe, S. M., Cliff, M. J., Williams, M. a., Ladbury, J. E., Cohen, P. T. W. and Barford, D. (2005). Molecular basis for TPR domain-mediated regulation of protein phosphatase 5. The EMBO journal *24*, 1–10.

[Yano et al., 1996] Yano, M., Naito, Z., Tanaka, S. and Asano, G. (1996). Expression and roles of heat shock proteins in human breast cancer. Jpn J Cancer Res *87*, 908–915.

[Yarden and Sliwkowski, 2001] Yarden, Y. and Sliwkowski, M. X. (2001). Untangling the ErbB signalling network. Nature reviews. Molecular cell biology *2*, 127–137.

[Yifrach and Horovitz, 1995] Yifrach, O. and Horovitz, A. (1995). Nested cooperativity in the ATPase activity of the oligomeric chaperonin GroEL. Biochemistry *34*, 5303–5308.

[Young et al., 1998] Young, J. C., Obermann, W. M. J. and Hartl, F. U. (1998). Specific binding of tetratricopeptide repeat proteins to the C-terminal 12-kDa domain of hsp90. Journal of Biological Chemistry *273*, 18007–18010.

[Yue et al., 1999] Yue, L., Karr, T. L., Nathan, D. F., Swift, H., Srinivasans, S. and Lindquist, S. (1999). Genetic analysis of viable Hsp90 alleles reveals a critical role in Drosophila spermatogenesis. Genetics *151*, 1065–1079.

[Zabka et al., 2008] Zabka, M., Leśniak, W., Prus, W., Kuźnicki, J. and Filipek, A. (2008). Sgt1 has co-chaperone properties and is up-regulated by heat shock. Biochemical and biophysical research communications *370*, 179–83.

[Zhang et al., 2008] Zhang, M., Botër, M., Li, K., Kadota, Y., Panaretou, B., Prodromou, C., Shirasu, K. and Pearl, L. H. (2008). Structural and functional coupling of Hsp90- and Sgt1-centred multi-protein complexes. The EMBO journal *27*, 2789–2798.

[Zhao et al., 2005] Zhao, R., Davey, M., Hsu, Y. C., Kaplanek, P., Tong, A., Parsons, A. B., Krogan, N., Cagney, G., Mai, D., Greenblatt, J., Boone, C., Emili, A. and Houry, W. a. (2005). Navigating the chaperone network: An integrative map of physical and genetic interactions mediated by the hsp90 chaperone. Cell *120*, 715–727.

[Zhao et al., 2008] Zhao, R., Kakihara, Y., Gribun, A., Huen, J., Yang, G., Khanna, M., Costanzo, M., Brost, R. L., Boone, C., Hughes, T. R., Yip, C. M. and Houry, W. a. (2008). Molecular chaperone Hsp90 stabilizes Pih1/Nop17 to maintain R2TP complex activity that regulates snoRNA accumulation. Journal of Cell Biology *180*, 563–578.

[Zhu et al., 2001] Zhu, W., Zhang, J. S. and Young, C. Y. (2001). Silymarin inhibits function of the androgen receptor by reducing nuclear localization of the receptor in the human prostate cancer cell line LNCaP. Carcinogenesis *22*, 1399–1403.

[Zierer et al., 2014] Zierer, B. K., Weiwad, M., Rübbelke, M., Freiburger, L., Fischer, G., Lorenz, O. R., Sattler, M., Richter, K. and Buchner, J. (2014). Artificial accelerators of the molecular chaperone Hsp90 facilitate rate-limiting conformational transitions. Angewandte Chemie (International ed. in English) *53*, 12257–12262.

[Zimmerman and Trach, 1991] Zimmerman, S. B. and Trach, S. O. (1991). Estimation of macromolecule concentrations and excluded volume effects for the cytoplasm of Escherichia coli. Journal of Molecular Biology *222*, 599–620.

[Zuehlke and Johnson, 2012] Zuehlke, A. D. and Johnson, J. L. (2012). Chaperoning the chaperone: a role for the co-chaperone Cpr7 in modulating Hsp90 function in Saccharomyces cerevisiae. Genetics *191*, 805–14.

[Zurawska et al., 2010] Zurawska, A., Urbanski, J., Matuliene, J., Baraniak, J., Klejman, M. P., Filipek, S., Matulis, D. and Bieganowski, P. (2010). Mutations that increase both Hsp90 ATPase activity in vitro and Hsp90 drug resistance in vivo. Biochimica et Biophysica Acta - Molecular Cell Research *1803*, 575–583.

Abbreviations

A_{280}	absorption at 280 nm
Aha1	activator of heat shock protein 90 ATPase
ATPase	ATP hydrolase
a.U.	arbitrary units
aUC	analytical ultracentrifugation
CD	circular dichroism
CTD	C-terminal domain
CL	charged linker
Da	Dalton
DNA	Deoxyribonucleic acid
DOC	desoxycorticosterone
	molar extinction coefficient
GA	geldanamycin
GR	glucocorticoid receptor
Hch1	high-copy heat shock protein 90 suppressor
MR	mineralcorticoid receptor
Hsp	heat shock protein
kDa	kilo Dalton
kD	dissociation constant
kD_{app}	apparent affinity
k_{max}	maximal ATP turnover
k_{on}	association constant
k_{off}	dissociation constant
λ	wavelength
MEEVD	Met-Glu-Glu-Val-Asp amino acid motif
MD	middle domain
mM	millimolar
nM	nanomolar
NMR	nuclear magnetic resonance
NTD	amino-terminal domain
OD	optical density
o/N	overnight
PAGE	polyacrylamide gel electrophoresis
PBS	phosphate buffered saline
PCR	polymerase chain reaction
P_i	phosphate
PLATE	PEG, lithium acetate, tris and EDTA
PGK	phosphoglycerate kinase
pH	potentia hydrogenii

PPIase	peptidylprolyl isomerase
RD	radicicol
RT	room temperature
rpm	rounds per minute
S	Svedberg
UV	ultraviolet
SHR	steroid hormone receptor
TPR domain	tetratricopeptide repeat domain
yHsp90	Hsp90 from *Saccharomyces cerevisiae*
v/v	volume per volume
wt	wild type
w/v	weight per volume

Acknowledgements

I would like to express my sincere gratitude to **Prof. Johannes Buchner** for giving me the great opportunity to perform my PhD thesis in his laboratory. I am deeply grateful for his continuous support, trust and allowing ample creative freedom to explore my own scientific ideas.

Further, I owe sincere thanks to my collaboration partners on the different projects I have worked on: **Jochen Reinstein** for excellent discussions and free lessons on enzyme kinetics, **Martin Rübbelke** for the NMR measurements and **Klaus, Christine** and **Daniel** for the aUC measurements.

Generous financial support was provided by a fellowship of the '**Studienstitung des deutschen Volkes**'. Their workshops as well as the courses from the **TUM Graduate School** helped me in broadening my knowledge beyond my PhD project.

I warmly thank the members of the 'Buchner chair' for the great atmosphere and the fruitful discussions. My earnest thanks are to my office mates **Priyanka, Alex** and **Frank**. I really enjoyed working with you and that you never got tired in finding solutions for any kind of problems. I also would like to thank **Anja Liebscher** and **Bettina Richter** for their great technical assistance and **Margot Rubinstein** for her kind help at questions on bureaucracy and general organisation.
Thank you **Katha, Patzi, Bene** and **Gordie** for sharing great laughs and always being up for a chat. **Hannah**, I thank you for the great discussions about our work and beyond. Further, I also would like to thank the 'old' ones, **Vroni, Christoph, Julia, Alina** and **Natalia** for making my start in the Buchner laboratory easy and for always having an open ear for me.

I wish to extend my warmest thanks to everyone who was helping and supporting me in any ways they could during the last years. In particular, I want to express a deep sense of gratitude to **my parents** and my loving sister **Nadine**. Without your love, continuous encouragement and everlasting support, this work would not have been possible. Thank you!